ISTANBUL TECHNICAL UNIVERSITY ★ GRADUATE SCHOOL OF SCIENCE ENGINEERING AND TECHNOLOGY

EFFECTS OF BUILDING COLLAPSE DIRECTION AND BRIDGE FUNCTIONALITY ON ROAD NETWORKS FOLLOWING AN EARTHQUAKE

Ph.D. THESIS

Betül ERGÜN KONUKCU

Geomatics Engineering Department

Geomatics Engineering Doctorate Program

MARCH 2016

ISTANBUL TECHNICAL UNIVERSITY ★ GRADUATE SCHOOL OF SCIENCE ENGINEERING AND TECHNOLOGY

EFFECTS OF BUILDING COLLAPSE DIRECTION AND BRIDGE FUNCTIONALITY ON ROAD NETWORKS FOLLOWING AN EARTHQUAKE

Ph.D. THESIS

Betül ERGÜN KONUKCU
(501062601)

Geomatics Engineering Department

Geomatics Engineering Doctorate Program

Thesis Advisor: Prof. Dr. Muhammed ŞAHİN
Co Advisor: Assoc. Prof. Dr. Himmet KARAMAN

MARCH 2016

İSTANBUL TEKNİK ÜNİVERSİTESİ ★ FEN BİLİMLERİ ENSTİTÜSÜ

BİNA YIKILMA YÖNLERİNİN VE KÖPRÜ HASARLARININ DEPREM SONRASINDA YOL AĞLARINA ETKİSİ

DOKTORA TEZİ

Betül ERGÜN KONUKCU
(501062601)

Geomatik Mühendisliği Anabilim Dalı

Geomatik Mühendisliği Doktora Programı

Tez Danışmanı: Prof. Dr. Muhammed ŞAHİN
Eş Danışman: Doç. Dr. Himmet KARAMAN

MART 2016

Betül ERGÜN KONUKCU, a Ph.D. student of Graduate School of Science Engineering and Technology, student ID 501062601, successfully defended the thesis entitled "EFFECTS OF BUILDING COLLAPSE DIRECTION AND BRIDGE FUNCTIONALITY ON ROAD NETWORKS FOLLOWING AN EARTHQUAKE", which she prepared after fulfilling the requirements specified in the associated legislations, before the jury whose signatures are below.

Thesis Advisor :	**Prof. Dr. Muhammed ŞAHİN** Istanbul Technical University	.....
Co-advisor :	**Assoc. Prof. Dr. Himmet KARAMAN** Istanbul Technical University	.....
Jury Members :	**Prof. Dr. Ergin TARI** Istanbul Technical University	.....
	Prof. Dr. Derin N. URAL Istanbul Technical University	.....
	Prof. Dr. Turgut UZEL Kültür University	.....
	Prof. Dr. Haluk ÖZENER Boğaziçi University	.....
	Asst. Prof. Dr. Onur PEKCAN Middle East Technical University	.....

Date of Submission : 28 January 2016
Date of Defense : 10 March 2016

To my mother Bedia ERGÜN and my son Umut Utku KONUKCU,

FOREWORD

Istanbul is expected to face a huge earthquake and it is estimated that the effects of this earthquake will be desructive due to improper building constructions and transportation structures. This thesis aims to reveal effects of building collapse and transportation functionality on road network in Istanbul following a the expected Istanbul Earthquake. This study represents important results for decision makers for the used in areas such as risk mitigation studies and urban transformation projects.

This thesis was written after a long study. At the end of this long journey, I would like to give my special thanks to the people who accompanied me on this trip.

I would like to express my deepest gratitude to one of my advisors Prof. Muhammed Şahin for giving me an opportunity to study with him. My dear advisor thanks for sharing your knowledge and suggestions since the beginning of my phd study.

I would like to express my deepest gratitude to my other advisor Assoc. Prof. Himmet Karaman for his immense help and encouragement. My dear advisor thanks for always being ready with an advice on any scientific questions, explaining me how to think and do research and many corrections to the things I wrote for my thesis and articles.

I would like to thank my thesis committee Prof. Dr. Ergin Tarı, Prof. Dr. Derin N. Ural and Prof Dr. Turgut Uzel. They have provided important guidance throughout this process.

I would like to thank to City Planner Ayşe Gökbayrak, M.Sc. Geophysics Engineer Mahmut Baş for all their support and Doç. Dr. Nurdan Apaydın, M.Sc. Geology Engineer Hamdi Çınal for all their help about data they provided.

Finally, I would like to express my deepest gratitude to my husband, my son, my mother, my father, my brother and my aunt. Thanks for everything. I am more powerful with you.

March 2016

Betül ERGÜN KONUKCU
(M.Sc.Geology Engineer)

TABLE OF CONTENTS

Page

FOREWORD ..... **ix**
TABLE OF CONTENTS ..... **xi**
ABBREVIATIONS ..... **xiii**
SYMBOLS ..... **xvii**
LIST OF TABLES ..... **xix**
LIST OF FIGURES ..... **xxiii**
SUMMARY ..... **xxvii**
ÖZET ..... **xxxi**
1. INTRODUCTION **1**
2. PURPOSE OF THESIS **9**
2.1 Purpose of Building Age Determination 9
2.1.1 Development of structure codes in the world 12
2.1.2 Development of structure codes in Turkey 13
2.2 Purpose of Building Damage Analysis in Istanbul 16
2.3 Purpose of Building Collapse Direction 17
2.4 Purpose of Transportation Structure Functionality 19
3. LITERATURE **21**
4. BUILDING AND BRIDGE DATA ACQUISITION FOR ISTANBUL AND GÖLCÜK **29**
4.1 Create Update Building Dataset in Istanbul 29
4.1.1 Building inventory as vector data in Istanbul 29
4.1.2 Remote sensing data for the building age determination 36
4.2 Building Dataset Generation for Gölcük 37
4.3 Bridge Dataset Generation in Istanbul 38
5. DETERMINATION OF BUILDING AGE **43**
5.1 Building Age Determination Methodology 43
5.2 Building Age Analysis and Results 48
5.2.1 Production of 1968 and pre 1968 building data (Code Level 1) 48
5.2.2 Production of building data between 1969 and 1982 (Code Level 2) 49
5.2.3 Production of building data between 1983 and 1996 (Code Level 3) 49
5.2.4 Production of building data between 1997 and 2004 (Code Level 3) 51
5.2.5 Production of building data between 2005 and 2007 (Code Level 4) 53
5.2.6 Production of building data between 2008 and 2013 (Code Level 4) 55
6. BUILDING DAMAGE ANALYSIS **71**
6.1 Method of Building Damage Analysis 71
6.1.1 Earthquake hazard 71
6.1.2 Structural fragility 74
6.1.3 Building inventory 76
6.2 Building Damage Analysis and Results 78
6.2.1 The complete and heavily damage buildings according to Sa 81

6.2.2 The complete and heavily damage buildings according to PGA 87
6.2.3 The mean damage buildings according to the Sa 94
7. BUILDING COLLAPSE DIRECTION 105
7.1 Method of Building Collapse Direction 105
7.1.1 Determination of existing and collapsed buildings in Gölcük 106
7.2 Building Collapse Direction Analysis in Istanbul 124
7.2.1 Building collapse direction classification method 124
7.2.2 Building collapse direction in Küçükçekmece 131
7.2.3 Building collapse direction in Fevzi Çakmak 135
7.2.4 Average spreading distance application to Istanbul 141
8. BRIDGE DAMAGE AND FUNCTIONALITY 149
8.1 Method of Bridge Functionality 149
8.1.1 Hazard analysis of bridges 149
8.1.2 Bridge inventory 151
8.1.3 Fragility curves 151
8.2 Transformation Structures (Bridge, Viaduct) Damage Analysis and Results 155
8.2.1 Results of bridge damage analysis 155
8.2.2 Results of the bridge functionality analysis 162
8.2.3 Results of the bridge retrofitted analysis 167
8.2.4 Results of the expected bridge retrofit cost 168
9. POTENTIAL ROAD BLOCKAGE IN ISTANBUL 171
10. VALIDATION WITH OTHER STUDIES 179
10.1 Validation of the Building Age Study 179
10.1.1 Validation with the Küçükçekmece study 179
10.1.2 Validation with the TUIK study 181
10.2 Validation of the Building Damage Analysis Results 182
11. DISCUSSION AND CONCLUSIONS 185
REFERENCES 191
APPENDICES 199
APPENDIX A: Tables 200
APPENDIX B: Maps 225
CURRICULUM VITAE 237

ABBREVIATIONS

ADNKS	**:** Address-Based Census Registration System
AGR1	**:** Building Occupancy Classes- Agriculture
ArcGIS	**:** ESRI product, Geographic Information System programme
ArcMap	**:** The central application used in ArcGIS
ATC3	**:** Tentative Provisional for the Development of Seismic Regulation for Buildings
BSLEO	**:** Building Standard Law Enforcement Order
BU-ARC	**:** Study of Earthquake Risk Assessment for the Istanbul Metropolitan Area
C1	**:** Structure Type Classification -Reinforced Concrete
C2	**:** Structure Type Classification -Tunnel Form
C3	**:** Structure Type Classification- Concrete Frame with Unreinforced Masonry Infill Walls
C1	**:** HAZUS Building Structural Type- Concrete Moment Frame
C2	**:** HAZUS Building Structural Type- Concrete Shear Walls
C3	**:** HAZUS Building Structural Type- Concrete Frame with Unreinforced Masonry Infill Walls
CLS1	**:** The collapsed building belonging to Class 1
CLS2	**:** The collapsed building belonging to Class 2
CLS3	**:** The collapsed building belonging to Class 3
CLS4	**:** The collapsed building belonging to Class 4
CLS5	**:** The collapsed building belonging to Class 5
CLS6	**:** The collapsed building belonging to Class 6
CLS7	**:** The collapsed building belonging to Class 7
CLS8	**:** The collapsed building belonging to Class 8
CLS9	**:** The collapsed building belonging to Class 9
CLS10	**:** The collapsed building belonging to Class 10
CLS11	**:** The collapsed building belonging to Class 11
COM1	**:** Building Occupancy- Commercial- Retail Trade
COM2	**:** Building Occupancy- Commercial- Wholesale Trade
COM3	**:** Building Occupancy- Commercial- Personal and Repair Services
COM4	**:** Building Occupancy- Commercial- Professional / Technical Services
COM5	**:** Building Occupancy- Commercial- Banks
COM6	**:** Building Occupancy- Commercial- Hospital
COM7	**:** Building Occupancy- Commercial- Medical Office / Clinic
COM8	**:** Building Occupancy- Commercial- Entertainment & Recreation
COM9	**:** Building Occupancy- Commercial- Theaters
COM10	**:** Building Occupancy- Commercial- Parking

CRM : Consequence-based Risk Management
CSM : Capacity Spectrum Method
DBELA : Displacement-Based Loss Assessment
DESA : Department of Economic and Social Affairs, Population Division, United Nations.
D01 : First Digitized Aerial or Satellite Image Year
D02 : Digitisation on the Ending Years' Image
ED50TM30 : European Datum 30 Transverse Mercator 30
EDU1 : Building Occupancy- Education- Grade Schools
EDU2 : Building Occupancy- Education- Colleges / Universities
EFEO : Emergency Response- Emergency Operation Center
EFHS : Medical Care Facilities- Small Hospital
EFFS : Emergency Response- Fire Station
EFHM : Medical Care Facilities Medium Hospital
EFHL : Medical Care Facilities Large Hospital
EFMC : Medical Care Facilities Medical Clinics
EFPS : Emergency Response- Police Station
EFS1 : Schools - Grade Schools
EFS2 : Schools – Colleges / Universities
ELER : Earthquake Loss Estimation Routine
ERGO : Multi-Hazard Assessment, Response, and Planning
FALSE : Except Critical Facilities
FEMA : Federal Emergency Management Agency
GIS : Geographic Information System
GOV1 : Building Occupancy- Government- General Services
GOV2 : Building Occupancy- Government- Emergency Response
H : Number of Building- Height Rise (8 +)
HAZTURK : Hazards Turkey
HAZUS : Hazards U.S.
HGK : General Command of Mapping
ICC : The International Code Council
IND1 : Building Occupancy- Industrial- Heavy
IND2 : Building Occupancy- Industrial- Light
IND3 : Building Occupancy- Industrial- Food / Drugs / Chemicals
IND4 : Building Occupancy- Industrial- Metals / Mineral Processing
IND5 : Building Occupancy- Industrial- High Technology
IND6 : Building Occupancy- Industrial- Construction (office)
IMM : Istanbul Metropolitan Municipality
IRS : Indian Remote Sensing
İTÜ : Istanbul Technical University
JICA : Japan International Cooperation Agency
KDMP : The Urban Transformation Project in Küçükçekmece
KOERI : Kandilli Observatory and Earthquake Research Institute
L : Number of Building- Low Rise (1 – 3)
LDM : Linear Directional Mean
LDM1 : Approximately North East
LDM2 : Approximately North West
LDM3 : Approximately South
LDM4 : Approximately South East
LDM5 : Approximately West

M : Number of Building- Mid Rise (4 – 7)
MAEviz : Mid-America Earthquake Visualization
MH : HAZUS Building Structural Type- Mobile Homes
mHARP : Multi-Hazard Assessment, Response
MSC : Multi-span continuous
MSC Concrete : Multi Span Continuous Concrete Girder
MSC Slab : Multi Span Continuous Slab
MSC Steel : Multi Span Continuous Steel Girder
MSSS : Multi Span Simply Supported
MSSS Concrete : Multi Span Simply Supported Concrete Girder
MSSS Concrete Box : Multi Span Simply Supported Concrete Box Girder
MSSS Steel : Multi Span Simply Supported Steel Girder
MSSS Slab : Multi Span Simply Supported Slab
Mw : Moment Magnitute
NIBS : National Institute for Building Science
No_stories : Number of Building Floor
Occ_type : Building Functionality Type
Par_id : Parcel Identification
PC : Structure Type Classification - Prefabricate
PC1 : HAZUS Building Structural Type- Precast Concrete Tilt-Up Walls
PC2 : HAZUS Building Structural Type- Precast Concrete Frames with Concrete Shear Walls
PFM : Parameterized Fragility Method
PGA : Peak Ground Acceleration
REL1 : Building Occupancy- Religion
RES1 : Building Occupancy- Residental- Single Family Dwelling
RES2 : Building Occupancy- Residental- Mobile Home
RES3 : Building Occupancy- Residental- Multi Family Dwelling
RES4 : Building Occupancy- Residental- Temporary Lodging
RES5 : Building Occupancy- Residental- Institutiona
RES6 : Building Occupancy- Residental- Nursing Home
RM1 : Structure Type Classification - Reinforced Masonry Bearing Walls with Wood or Metal Deck
RM2 : Structure Type Classification - Reinforced Masonry Bearing Walls with Precast Concrete
RM1 : HAZUS Building Structural Type- Reinforced Masonry Bearing Walls with Wood or Metal Deck
RM2 : HAZUS Building Structural Type- Reinforced Masonry Bearing Walls with Precast Concrete
S : Structure Type Classification - Steel Construction
S1 : HAZUS Building Structural Type- Steel Moment Frame
S2 : HAZUS Building Structural Type- Steel Braced Frame
S3 : HAZUS Building Structural Type- Steel Light Frame
S4 : HAZUS Building Structural Type- Steel Frame with Cast-in-Place Concrete Shear Walls
S5 : HAZUS Building Structural Type- Steel Frame with Unreinforced Masonry Infill Walls
Sa : Spectral Acceleration
SELENA : Seismic Loss Estimation using a Logic Tree Approach

SRA : Seismic Risk Analysis
SS : Simply Supported
SS Concrete : Simply Supported Concrete Girder
Str_type : General Structural Type
Str_type2 : HAZUS Structural Category
TUIK : Turkish Statistical Institute
URM : Structure Type Classification - Unreinforced Masonry
URM : HAZUS Building Structural Type- Unreinforced Masonry Bearing Walls
USGS : U.S. Geological Survey
W1 : Structure Type Classification - Wooden
W1 : HAZUS Building Structural Type- Wood, Light Frame
W2 : HAZUS Building Structural Type- Wood, Commercial and Industrial
WGS84 : World Geodetic System 1984
Year_built : Building Construction Type

SYMBOLS

N_1 **:** Collapse direction (near angle between the collapsed building point and the debris spreading point)
S_S **:** Collapse distance (near distance between the collapsed building point and the debris spreading point)
N_2 **:** Fault direction (near angle between the collapsed building point and 1999 fault epicenter point)
S_F **:** Fault distance (near distance between the collapsed building point and 1999 fault epicenter point)
T_{1t} **:** Azimuth of collapse direction
T_{2t} **:** Azimuth of fault direction
α **:** ArcGIS Near angle value
t **:** Azimuth angle value

LIST OF TABLES

Page

Table 1.1 : TUIK population census between 1980-2014 (TUIK, 2014). **2**
Table 2.1 : History of Ministry of Environment and Urban Planning. **14**
Table 2.2 : Building codes in Turkey. **14**
Table 2.3 : Code level regarding to building codes in Turkey. **15**
Table 4.1 : Deleted structure data in building dataset. **30**
Table 4.2 : Building occupancy classes at HAZUS (FEMA 2003). **33**
Table 4.3 : Occupancy class distribution of buildings in Istanbul w/o Residential (FEMA, 2003). **34**
Table 4.4 : Critical facilities classificaiton (FEMA 2003). **35**
Table 4.5 : Structure type classification (FEMA 2003). **35**
Table 4.6 : HAZUS building structural type (FEMA 2003). **36**
Table 4.7 : Number of bridge distribution at districts based in Istanbul. **38**
Table 4.8 : Number of bridge category in Istanbul. **38**
Table 4.9 : Sample of bridge inventory card. **39**
Table 4.10 : HAZTURK attributes of bridge. **39**
Table 4.11 : Bridge classification mapping to NBI Terminology (Nilsson, 2008). **40**
Table 5.1 : Building code and building age classification. **45**
Table 5.2 : Number of building age distribution in Istanbul until 2013. ..... **59**
Table 5.3 : The number of occupancy classes distributionfor buildings in Istanbul w/o residential house. **60**
Table 5.4 : Number of buildings at districts based in Istanbul from 1968 to 2013. ..... **65**
Table 6.1 : HAZTURK building inventory attributes and explanations. **76**
Table 6.2 : The number of building age distribution in Istanbul. **77**
Table 6.3 : The number of building distribution according to HAZUS building structural type (FEMA 2003). **77**
Table 6.4 : The distribution of damage ratio of Istanbul buildings. **78**
Table 6.5 : Distribution of damage ratio of STR_TYP2 according to Sa. **79**
Table 6.6 : Distribution of damage ratio of building age according to Sa. **80**
Table 6.7 : Distribution of damage ratio of STR_TYP2 according PGA. **80**
Table 6.8 : Distribution of damage ratio of building age according to PGA. **81**
Table 6.9 : Number of buildings distribution that have the possibility of heavy & complete damage more than 40% based on 0.2 sec Sa in districts. **85**
Table 6.10 : Number of buildings distribution that have the possibility of heavy & complete damage more than 40% based on 0.2 sec Sa in sub-districts. **86**
Table 6.11 : Distribution of building number that have the possibility of heavy & complete damage more than 40% based on 0.2 sec Sa according to occupation type. **86**

Table 6.12 : Distribution of building number that have the possibility of heavy & complete damage more than 40% based on 0.2 sec Sa according to construction type. **87**
Table 6.13 : Number of buildings distribution that have the possibility of heavy & complete damage more than 40% based on PGA in districts. **92**
Table 6.14 : Number of buildings distribution that have the possibility of heavy & complete damage more than 40% based on PGA in sub-districts..... **93**
Table 6.15 : Distribution of building number that have the possibility of heavy & complete damage more than 40% based on PGA according to occupation type. **94**
Table 6.16 : Distribution of building number that have the possibility of heavy & complete damage more than 40% based on PGA according to construction type. **94**
Table 6.17 : Number of buildings distribution that have the possibility of mean damage more than 50 % based on 0.2 sec Sa in districts. **97**
Table 6.18 : Number of buildings distribution that have the possibility of mean damage more than 50 % based on 0.2 sec Sa in sub districts. **98**
Table 6.19 : Distribution of building number that have the possibility of mean damage more than 50 % based on 0.2 sec Sa according to occupation type. **98**
Table 6.20 : Distribution of building number that have the possibility of mean damage more than 50% based on 0.2 sec Sa according to construction type. **99**
Table 6.21 : Building damage situation of some sub-districts. **103**
Table 7.1 : Sample of near analysis results. **112**
Table 7.2 : Pearson correlation coefficient explanation. **113**
Table 7.3 : Correlation analysis results. **113**
Table 7.4 : Classification of near analysis results of collapsed building in Gölcük based on T_2t azimuth directions. **116**
Table 7.5 : The average N_1 and S_S according to classification of spreading direction of the collapsed building in Gölcük. **120**
Table 8.1 : Distribution of bridge classes within study area. **151**
Table 8.2: Distribution of average damage state of transportation structures based on bridge class. **155**
Table 8.3 : Distribution of construction type of bridges counts by step functionality in day 0. ..... **163**
Table 8.4 : Distribution of construction type of bridges counts by step functionality in day 3. ..... **164**
Table 8.5 : Distribution of construction type of bridges counts by step functionality in day 7. ..... **164**
Table 8.6 : Name of Retrofitting Bridges in Istanbul , Apaydin (2005). **167**
Table 8.7 : Bridge damage distribution without retrofitting process for retrofitted bridges. **168**
Table 8.8 : Bridge damage distribution after elastrometric retrofitting process retrofitted bridges. **168**
Table 8.9 : Bridge damage distribution after steel jacket retrofitting process for retrofitted bridges. **168**
Table 8.10 : Statistical Costing data per Bridge classification according to Elastrometric Bearing Method. **169**

Table 8.11 : Statistical Costing data per Bridge classification according to Steel Jacket Method. **169**
Table 10.1 : Comparison of building age classification between KDMP and this study. **180**
Table 10.2 : Correlation of KDMP and this study. **180**
Table 10.3 : Result of TUIK building census of 1984 and 2000 (TUIK, 2014). **181**
Table 10.4 : Comparison of Istanbul building damage estimation results based on Mw 7.5 earthquake scenario. **183**
Table A.1 : Classification of building collapse direction, distance and angle in Gölcük according to near and LDM analysis results - CLS01. ..... **200**
Table A.2 : Classification of building collapse direction, distance and angle in Gölcük according to near and LDM analysis results – CLS02. ..... **201**
Table A.3 : Classification of building collapse direction, distance and angle in Gölcük according to near and LDM analysis results – CLS03. ..... **201**
Table A.4 : Classification of building collapse direction, distance and angle in Gölcük according to near and LDM analysis results – CLS04. ..... **202**
Table A.5 : Classification of building collapse direction, distance and angle in Gölcük according to near and LDM analysis results – CLS05. ..... **202**
Table A.6 : Classification of building collapse direction, distance and angle in Gölcük according to near and LDM analysis results – CLS06. ..... **203**
Table A.7 : Classification of building collapse direction, distance and angle in Gölcük according to near and LDM analysis results – CLS07. ..... **203**
Table A.8 : Classification of building collapse direction, distance and angle in Gölcük according to near and LDM analysis results – CLS08. ..... **204**
Table A.9 : Classification of building collapse direction, distance and angle in Gölcük according to near and LDM analysis results – CLS09. ..... **205**
Table A.10 : Classification of building collapse direction, distance and angle in Gölcük according to near and LDM analysis results – CLS10. ..... **206**
Table A.11 : Classification of building collapse direction, distance and angle in Gölcük according to near and LDM analysis results – CLS11. ..... **207**
Table A.12 : Damage state distribution of MSC Conc Box bridges. **208**
Table A.13 : Damage state distribution of MSC Concrete bridges. **209**
Table A.14 : Damage state distribution of MSC Slab bridges. **214**
Table A.15 : Damage state distribution of MSC Steel bridges. **216**
Table A.16 : Damage state distribution of SS Concrete bridges. **217**
Table A.17 : Damage state distribution of Tunnel /Culvert bridges. **218**
Table A.18 : Damage distribution of retrofitted bridge in Istanbul according to bridge classification. **222**
Table A.19 : Damage distribution of retrofitted bridge by using elastrometric bear method in Istanbul according to bridge classification. **223**
Table A.20 : Damage distribution of retrofitted bridge by using steel jacket method in Istanbul according to bridge classification. **224**

LIST OF FIGURES

Page

Figure 1.1 : Global seismic hazard map and location of the study area (Giardini et al. 2003; Karaman and Erden 2014). **1**
Figure 1.2 : Historical earthquakes of Marmara Region, (Ambraseys&Finkel, 1991). **3**
Figure 1.3 : Marmara fault model according to Le Pichon et. al, (2003). **4**
Figure 1.4 : Marmara fault model according to Armijo et. al, (2005). **4**
Figure 1.5 : Marmara fault focal mechanism visualization, (Karaman&Erden, 2014). **5**
Figure 1.6 : Steps of determination road blockage in this study. **7**
Figure 2.1 : The study area of JICA project. **10**
Figure 2.2 : The study area of BU-ARC project. **11**
Figure 2.3 : Road blockage due to the building collapse from 1995 Kobe Earthquake (2015) **18**
Figure 2.4 : Collapsed buildings photo from Gölcük. **18**
Figure 2.5 : Study area in Gölcük. **19**
Figure 4.1 : Buildings distribution in Istanbul. **31**
Figure 4.2 : Building occupancy classes in Istanbul. **32**
Figure 4.3 : Distribution of bridge classification in Istanbul **41**
Figure 5.1 : Building samples from Fatih District of Istanbul. **44**
Figure 5.2 : Digitized buildings in Sarıyer district by using 1966 Aerial image. 46
Figure 5.3 : Digitized buildings in Sarıyer district by using 1982 Aerial Image. **47**
Figure 5.4 : 1966 aerial image of Istanbul. **48**
Figure 5.5 : 1982 aerial image of Istanbul. **49**
Figure 5.6 : 1996, Ortho-Photo mosaic of Istanbul. **50**
Figure 5.7 : 2004, 1m resolution IKONOS satellite image of Istanbul. **52**
Figure 5.8 : 2007, 1m resolution IKONOS satellite image of Istanbul. **54**
Figure 5.9 : 2013, 50 cm resolution Ortho-Photo mosaic of Istanbul. **56**
Figure 5.10 : Building number distribution in Istanbul with respect to districts for 2013. ..... **58**
Figure 5.11 : Number of building age distributions at European Side of Istanbul. .. **61**
Figure 5.12 : Number of building age distributions at Asian Side of Istanbul. **63**
Figure 5.13 : Changes in Istanbul building numbers at district level between 1982 and 2013. ..... **67**
Figure 5.14 : Building counts of the districts of Istanbul. **68**
Figure 5.15 : Building counts of the sub-districts of Istanbul. **69**
Figure 6.1 : The necessary data for building damage. **71**

Figure 6.2 : Istanbul Earthquake Hazard Map according to Boore & Atkinson (2008) PGA. **72**
Figure 6.3 : Istanbul Earthquake Hazard Map according to Boore & Atkinson (2008) 0.2 second Sa. **73**
Figure 6.4 : Model A according to JICA and IMM (2002) study. **74**
Figure 6.5 : Fragility curve for concrete frame with unreinforced masonry infill walls according to 0.2 Sa. **75**
Figure 6.6 : Fragility curve for concrete frame with unreinforced masonry infill walls according to PGA. **76**
Figure 6.7 : Complete damage possibility distribution of Istanbul buildings according to 0.2 Sa. **82**
Figure 6.8 : Heavy damage possibility distribution of Istanbul buildings according to 0.2 Sa. **83**
Figure 6.9 : Buildings in Istanbul that have the complete and heavy damage possibility more than 40% based on 0.2 Sa. **84**
Figure 6.10 : Complete damage possibility distribution of Istanbul buildings according to PGA. **88**
Figure 6.11 : Heavy damage possibility distribution of Istanbul buildings according to PGA. **89**
Figure 6.12 : Buildings in Istanbul that have the complete and heavy damage possibility more than 30% based on PGA. **91**
Figure 6.13 : Mean damage possibility distribution of Istanbul buildings according to 0.2 Sa. **95**
Figure 6.14 : More than 50% mean damage possibility distribution of Istanbul buildings based on 0.2 Sa. **96**
Figure 6.15 : More than 40% Complete and heavy building damage possibility distribution of Istanbul districts based on 0.2 Sa. **101**
Figure 6.16 : More than 40% Complete and heavy building damage possibility distribution of Istanbuls' first 50 sub-districts based on 0.2 Sa. **102**
Figure 7.1 : Workflow and the order of the analysis for detecting road functionality based on building collapse direction. **105**
Figure 7.2 : Gölcük aerial photos taken in 1994 and 1999. ..... **106**
Figure 7.3 : The buildings that were built before 1994 in Gölcük. **106**
Figure 7.4 : Collapsed buildings in Gölcük during the 1999 Kocaeli Earthquake. **107**
Figure 7.5 : To define the remotest debris spreading point. **108**
Figure 7.6 : Debris database from 1999 Gölcük aerial photo. **109**
Figure 7.7 : Near analysis illustration on ArcGIS (ArcGIS Help File). **109**
Figure 7.8 : Model builder for near analysis. **110**
Figure 7.9 : The second model builder for near analysis. **111**
Figure 7.10 : How to obtain azimuth angle value from near analysis angle value. **112**
Figure 7.11 : LDM analysis illustration on ArcGIS (ArcGIS Help File). **114**
Figure 7.12 : LDM analysis (field case: empty). **114**
Figure 7.13 : LDM analysis (field case: $T_{1\text{-}A}$). **115**
Figure 7.14 : The formula between N_2 and N_1 obtained from collapsed buildings in Gölcük. **121**
Figure 7.15 : The formula between N_2 and T_{1t} obtained from collapsed buildings in Gölcük. **121**
Figure 7.16 : The formula between N_2 and N_1 obtained from building classes in Gölcük. **122**

Figure 7.17 : The formula between N_2 and T_{1t} obtained from building classes in Gölcük. **122**
Figure 7.18 : Debris spreading vectors around the collapsed buildings in Gölcük. **123**
Figure 7.19 : Determination of average collapsed building spreading. **124**
Figure 7.20 : The buildings in Istanbul that have the mean damage possibility more than 30% **125**
Figure 7.21 : The buildings in Istanbul that their near angles are between 31.2700 – 55.8160. ..... **127**
Figure 7.22 : The distribution of collapse direction classification in Istanbul..... **129**
Figure 7.23 : Road blockage in Istanbul because of the building collapse direction. **130**
Figure 7.24 : Buildings in Küçükçekmece. **131**
Figure 7.25 : Buildings in Küçükçekmece with more than 30% mean damage possibility..... **132**
Figure 7.26 : Classification of spreading direction of collapsed buildings in Küçükçekmece..... **133**
Figure 7.27 : Road blockage in Küçükçekçemece because of the building collapse direction. **134**
Figure 7.28 : Location of Fevzi Çakmak sub district of Küçükçekmece district.... **135**
Figure 7.29 : Buildings in Fevzi Çakmak sub district..... 136
Figure 7.30 : Buildings in Fevzi Çakmak sub district that mean damage possibility more than 30%. **137**
Figure 7.31 : Classification of spreading direction of collapsed buildings in Fevzi Çakmak. **138**
Figure 7.32 : Buffer analysis according to the average debris spreading of LDM2 classification in Fevzi Çakmak sub district. **139**
Figure 7.33 : Road blockage in Fevzi Çakmak because of the building collapse direction. 140
Figure 7.34 : Accessibility of critical facilities around Fevzi Çakmak sub district. **141**
Figure 7.35 : Buildings that have the complete possibility more than 30%. **142**
Figure 7.36 : Model builder for defining road blockage in Istanbul by using average debris value (17.45 m). **144**
Figure 7.37 : Road blockage in Istanbul. **145**
Figure 7.38 : Accessibility of fire stations in Istanbul **147**
Figure 8.1 : Methodology of bridge functionality..... **149**
Figure 8.2 : Distribution of bridge locations on Istanbul Earthquake Hazard Map according to Boore & Atkinson (2008) PGA..... **150**
Figure 8.3 : Fragility curves for the continuous bridge classes: MSC_Conc Box.. **152**
Figure 8.4 : Fragility curves for the continuous bridge classes: MSC_Concrete. .. **153**
Figure 8.5 : Fragility curves for the continuous bridge classes: MSC_Slab..... **153**
Figure 8.6 : Fragility curves for the single span simply supported bridge classes: SS Steel..... **154**
Figure 8.7 : Distribution of complete damage possibility of bridges in Istanbul. .. **156**
Figure 8.8 : Distribution of mean damage possibility of bridges in Istanbul..... **157**
Figure 8.9 : Non functional roads and bridge damage distribution in Istanbul. **159**
Figure 8.10 : Large scale representation of non functional roads and bridge damage distribution in Europian Side..... **160**
Figure 8.11 : Large scale representation of non functional roads and bridge damage distribution in Küçükçekmece and Avcılar Districts..... **161**
Figure 8.12 : Continuous functionality analysis for bridge in Istanbul. **162**

Figure 8.13 : Step functionality analysis for bridge in Istanbul. **163**
Figure 8.14 : Functional and non functional bridge distribution in Istanbul following potential Istanbul Earthquake (Step Functionality). **165**
Figure 8.15 : Functional and non functional bridge distribution in Istanbul after 3 days from potential Istanbul Earthquake (Step Functionality). **166**
Figure 8.16 : Distribution of Retrofitted bridges in Istanbul. **167**
Figure 9.1 : Road blockage in Istanbul immediately after a potential earthquake.. **172**
Figure 9.2 : Road blockage in Istanbul immediately after 3 days a potential earthquake. **173**
Figure 9.3 : Large scale representation of road blockage for day 0. ..... **174**
Figure 9.4 : Large scale representation of road blockage for day 3. ..... **174**
Figure 9.5 : Representation of road blockage in Istanbul with population distribution based on sub district. **176**
Figure 9.6 : Large scale representation of road blockage in Istanbul with population distribution based on sub district. **177**
Figure 10.1 : Change of buildings at Küçükçekmece district between 2004 and 2013. ..... **179**
Figure 10.2 : Building age comparison of KDMP and this study in Küçükçekmece district. **180**
Figure 10.3 : Building age comparison of TUIK 2000 and this study. **182**
Figure A.1 : Complete damage possibility distribution of Küçükçekmece district according to PGA. **225**
Figure A.2 : Heavy damage possibility distribution of Küçükçekmece district according to PGA. **226**
Figure A. 3 : Mean damage possibility distribution of Küçükçekmece district according to PGA. **227**
Figure A.4 : Complete damage possibility distribution of Fevzi Çakmak sub district according to PGA. **228**
Figure A. 5 : Heavy damage possibility distribution of Fevzi Çakmak sub district according to PGA. **229**
Figure A. 6 : Mean damage possibility distribution of Fevzi Çakmak sub district according to PGA. **230**
Figure A.7 : Complete damage possibility distribution of Küçükçekmece district according to PGA. **231**
Figure A. 8 : Heavy damage possibility distribution of Küçükçekmece district according to Sa. **232**
Figure A.9 : Mean damage possibility distribution of Küçükçekmece district according to Sa. **233**
Figure A.10 : Complete damage possibility distribution of Fevzi Çakmak sub district according to Sa. **234**
Figure A. 11 : Heavy damage possibility distribution of Fevzi Çakmak sub district according to Sa. **235**
Figure A.12 : Complete damage possibility distribution of Fevzi Çakmak sub district according to Sa. **236**

EFFECTS OF BUILDING COLLAPSE DIRECTION AND BRIDGE FUNCTIONALITY ON ROAD NETWORKS FOLLOWING AN EARTHQUAKE

SUMMARY

Istanbul is one the most important megacities in the world with a population approaching 15 million in the world. Migration from all over Turkey to Istanbul is still ongoing because, Istanbul is the industrial, commercial, cultural and educational centre of Turkey. However, those migrations caused unplanned construction and these led to the formation of vulnerable and undocumented building stock in Istanbul. Besides this, Istanbul is located in one of the most active seismic zones in the world. Many scientific studies estimate that Istanbul is expecting a major earthquake and the possible damage to the structures will be extensive.

The occurrence of earthquakes cannot be prevented by human efforts. If an earthquake were to occur in a populated area, especially one covered with vulnerable building stock such as the city of Istanbul, it could cause a serious impact on human life. Besides this, if the road's functionality decreases due to damage to the transportation structures, the level of damage gets even higher and earthquake impacts may not be managed properly. Therefore, road network also plays an important role in activities of search and rescue, evacuation, firefighting operations and medical services after an earthquake.

This study aims to estimate road functionality in Istanbul following the potential Istanbul Earthquake by taking into account the direction of the collapsed buildings and damaged transporation structures.

One of the major disadvantages of Istanbul case is the lack of knowledge about the absolute number of buildings and the ages of those buildings. The various instances of earthquake loss asssessment software require the age, the construction type and the height of the buildings to estimate the possible damage of a scenario earthquake. The accuracy of such an estimation also depends on the reliability of the input data. To make a reliable earthquake damage estimation, a building database containing at least the; building age, construction type, and number of floors is required in most of the earthquake loss assessment software. For this reason, the first part of this study aims to create a recent and accurate building data of Istanbul including the occupacy classes, construction types, the number of floors and the most important one of all, their age.

Firstly, in order to create the recent building dataset of Istanbul, the structure data and the building data were separated from each other. The building dataset was then classified but this data set did not include the building age. This is why the building age data was determined for every single building in Istanbul, according to structural codes for the earthquake zones by using aerial and satellite images of Istanbul. The classification should be based on the regulations in order to minimise the age classes and maximise their accuracy. First, building regulations in Turkey came into force in

1940 in order to determine the essential conditions for the realisation of functional, safe and disaster-resistant building design in Turkey.

The last updated building code regulations in Turkey came into force in 2007. It was also important to investigate the proper building detection method for the aim of this study and it was determined as the manual digitisation. In this study, the buildings of Istanbul and their age are determined for every single building, by digitising the selected aerial photos (1966, 1982), orthophoto mosaics (1996, 2013) and satellite images (2004, 2007) of Istanbul based on the official structural codes in Turkey. Thus, first the exact number and location of buildings in Istanbul, rather than the structures and the age of every single building were determined and the recent building data consisted of occupacy classes, construction types, the number of floors and building age were produced in GIS. The results were also validated with two separate studies of Istanbul for different periods of times. In this way, the earthquake damage analysis for the Istanbul buildings can be run for the real building data of Istanbul with any earthquake loss assessment software.

The second part of this study presents a building damage analysis for every single building in Istanbul, based on updated building data. The building damage analysis was made using the scenario based deterministic earthquake hazard maps of PGA and 0,2 second Sa demand types by using HAZTURK software. Results from the damage analysis for Istanbul were also presented for districts and sub-districts, in order to compare with other studies.

The third part of this study is to determine the building collapse direction and the debris area radius in order to reveal road blockages in Istanbul. The building collapse direction estimation method generated is based on the collapsed buildings data during the 1999 Kocaeli Earthquake by using 1994 and 1999 Gölcük aerial photos, before and after the earthquake. Based on the method developed, if roadside buildings collapsed during the earthquake, then the scattered parts of the buildings could cause roads to lose their functionality. After the determination of the collapse directions of the buildings, the roads still functioning were also revealed during emergency operations. Defining the collapse direction of buildings has helped us to define which roads would be open after an earthquake. Routes are important for defining evacuation or escape roads, while emergency transportation roads, and roads are urgently needed for emergency use. This is hence the first study on this subject both in the national and international literature.

It is not only collapsed buildings but also transportation structures that damage that effect the functionality of the road network. For this reason, in the fourth part of this study, we will estimate transportation structures' (bridge, viaducts, tunnels, overpasses, etc.) damage analysis according to PGA demand type by using HAZTURK software. Functionalities are then determined for a certain time period. It is also very important to reveal the functionality of transportation structures based on potential Istanbul earthquake, because they have critical importance during the post-earthquake response and long-term recovery phases of the disaster management. A complete understanding of the earthquake impact on the transportation structures with damage possibility, post-earthquake functionality and retrofitted damage possibility analysis, is a very important input for the decision makers in order to mitigate, prepare for, respond to, and recover from the potential impact on the potential Istanbul earthquake.

At the end of the study, we have estimated building collapse directions, building debris areas, and transportation structures' damages and then performedan overall evaluation to reveal road functionality in Istanbul following an earthquake scenario.

The results and the proposed methods in this study represent very important contributions that could be used as base data for decision makers to develop important strategies for risk reduction. That is, they could be used to prevent a hazard from becoming a disaster, to mitigate possible risks and to transform urban areas based on the earthquake risk.

BİNA YIKILMA YÖNLERİNİN VE KÖPRÜ HASARLARININ DEPREM SONRASINDA YOL AĞLARINA ETKİSİ

ÖZET

Asırlar boyu farklı uygarlık ve kültürlere ev sahipliği yapmış olan İstanbul, 15 milyona yaklaşan nüfusu ile dünyanın en önemli mega şehirlerinden biridir. Kültür, sanayi, ticaret ve eğitim merkezi olan bu kentte yaşayan insan sayısı her geçen gün artmaktadır. Türkiye İstatistik Kurumu tarafından yayınlanan "İllerin aldığı, verdiği göç, net göç ve net göç hızı, 1980, 2013" tablosu incelendiğinde, Istanbul'un en çok göçü 1985 – 1990 yılları arasında aldığı görülmektedir. Nüfus bu yıllar arasında 656677 kişi artmıştır. İstanbul göç almaya devam etmektedir. 2013-2014 yılları arasında İstanbul'a net göç 14336 kişidir. Göç karşısında bina talebini karşılamak adına oluşan plansız, sağlıksız ve ilgili yönetmeliklerden uzak yapılaşma, İstanbul için kentsel yerleşim alanlarında afete karşı dayanıksız, projesiz, kayıtsız yerleşim çevreleri ve yapı stoğunun oluşmasına sebebiyet vermiştir.

Tarihi boyunca deprem nedeniyle büyük yıkımlar yaşayan İstanbul, en son 1999 Kocaeli depreminden etkilenmiş ve özelikle Avcılar ve Büyükçekmece ilçelerinde ciddi hasar meydana gelmiştir. 1999 depremleri (Kocaeli ve Düzce depremleri) büyük bir farkındalık yaratmış, İstanbul için ulusal ve uluslarası ölçekte afet risk yönetimi odaklı, birçok önemli bilimsel çalışmalar yapılmıştır ve yapılmaya devam etmektedir. Bu çalışmalar göstermektedir ki İstanbul büyük bir deprem tehlikesi ile karşı karşıyadır. Bunula birlikte olası depremin; Istanbul'un mevcut yapı stoğu, altyapısı ve sahip olduğu kaynakları ile baş edemeyeceği sonuçlar yaratması beklenmektir.

Tektonik hareketler sonucunda oluşan deprem, bir doğa olayıdır. Bugünkü koşullar ile deprem engellenemeyeceği gibi, depremin kontrol edilmesi imkansız, tahmin edilmesi ise oldukça zordur. Bu durumda yapılması gereken tek şey depreme dayanıklı ve hazırlıklı şehirler oluşturmaktır.

İstanbul binaları ve altyapısı ile depreme hazır bir şehir değildir. İstanbul ile ilgili bazı çalışmalar, bina hasarlarına bağlı olarak deprem sonrasında olası can kayıpları ve yaralanmalar ile ilgili tahminlerde bulunmuştur.

2009 yılında İstanbul Büyükşehir Belediyesi ve Boğaziçi Üniversitesi Kandilli Rasathanesi ve Deprem Araştırma Enstitüsü tarafından yapılan "İstanbul'un Olası Deprem Kayıpları Tahminleri Güncellenmesi İşi" sonucunda yayınlanan rapora gore; İstanbul'da potansiyel depremin gerçekleşmesi durumunda; 10,000 – 30,000 arası kişinin hayatını kaybedeceği, 20,000 – 60,000 arası kişinin hastanede tedavi göreceği, 50,000 -140,000 arası kişinin ise hafif yaralanacağı tahmin edilmektedir.

Hasarlı binalar sadece sebep olduğu can kayıplarından dolayı değil, aynı zamanda oluşturduğu enkaz ile binayı çevreleyen yolları kapatmasından dolayı da deprem karşısında önemli bir risk unsuru oluşturmaktadır. Yolların kullanılabilirliği etkileyen diğer bir unsurda ulaşım yapılarında oluşabilecek hasardır. Yolların deprem

sonrasında kullanılamaması afet bölgesine veya bölgelerine erişimi engelleyerek, kayıpların sayısının artmasına sebep olabilir.

Bu çalışmanın amacı; olası İstanbul Depremi'nin gerçekleşmesi durumunda, hasar alması muhtemel binaların yıkılma yönlerini ve ulaşım yapılarındaki hasarı tahmin etmek böylece İstanbul'un mevcut yollarının deprem sonrası kullanılabilirliğini ortaya koymaktır. Çünkü yol ağları deprem sonrasında arama kurtarma ve tahliye çalışmalarında, yangın söndürme operasyonlarında, ilk yardım ve medikal ulaştırma işlemlerinde en önemli rollerden birini üstlenmektedir. Bina yıkılma yönlerinin belirlenmesi için öncelikle İstanbul için güncel bina veri seti oluşturulmuş, bu bina veri seti kullanılarak bina hasar analizleri gerçekleştirilmiş ve hasar alması muhtemel binaların yıkılma yönleri tahmin edilmiştir. Ulaşım yapılarındaki hasarın hesaplanması için ana yol üzerinde bulunan köprülerin hasarı sonrasında bu hasara bağlı kullanılabilirliği ortaya konmuştur. Bu iki veri daha sonra ArcGIS programında entegre edilmiş İstanbul'daki yolların deprem sonrasında kullanılabilirliği tahmin edilmeye çalışılmıştır.

Çalışmanın birinci bölümünde amaçlanan, güncel ve doğru verilerle İstanbul için bina veri setinin oluşturulmasıdır. İstanbul'un, hasar tahmin çalışmaları için en büyük dezavantajı gerçek bina sayılarının ve bu binalarının yaşlarının bilinmemesinden kaynaklanmaktadır. Bir diğer dezavantaj ise Istanbul için var olan bina veri setlerinin bina dışında yapı verisinide içeriyor olmasıdır. Bu çalışma kapsamında Istanbul bina veri seti oluşturulurken öncelikle bina ve yapı verisi birbirinden ayrılmıştır. Istanbul Büyükşehir Belediyesi'nden bu çalışma kapsamında kullanılmak için temin edilen yapı veri seti, 1,439,981 adet yapı verisini içermekteydi. Yapılan çalışma ile bina ve yapı verisi 3194 sayılı İmar Kanunu'nda geçen bina ve yapı tanımlasına gore ayrılmıştır. Buna gore İstanbul'daki bina sayısı 2013 yılı itibari ile 990,584 adettir.

Birçok hasar tahmin çalışması olası deprem senaryosu karşısında, analizi gerçekleştirebilmek için binanın yaş, yapım cinsi ve binanın yükseklik bilgisine ihtiyaç duyar. Bu tür hasar tahmin çalışmalarının sonuçlarının doğruluğu, girdi olarak kullanılan bilgilerin güvenirliğine bağlıdır. Güvelinir hasar tahmin çalışması yapabilmek için, bina veri setinin en azından bina yaşı, yapım türü ve kat bilgisini içermesi gerekmektedir. Çalışma kapsamında oluşturulan veri setinin binanın kullanım tipini, yapım türünü, kat bilgisini ve en önemli olarak bina yaş bilgisini bina bazında kapsaması sağlanmıştır. Bu çalışma sonuçlarına göre İstanbul'daki binaların %80 i konut olarak kullanılmaktadır ve bu şehirde yaklaşık 5000 adet eğitim tesisi ve 1500 adet sağlık tesisi bulunmaktadır.

İstanbul'daki binaların her biri için bina yaş bilgisi, Türkiye'de yürürlüğe girmiş bina yönetmeliklerinin tarihleri baz alınıp, sayısal olarak üretilmiştir. Türkiye'de ilk deprem yönetmeliği yürürlüğe 1940 yılında girmiştir, en son yürürlüğe giren deprem yönetmeliğinin tarihi ise 2007'dir. Mevcut yönetmeliğin günün şartlarına ve ihtiyaçlarına göre güncellenmesi çalışmaları, Başbakanlık Afet ve Acil Durum Yönetimi Başkanlığı (AFAD) tarafından devam ettirilmektedir. Yönetmelik tarihleri ile uyumlu hava fotoğrafı, ortofoto mozaik ve uydu görüntüleri kullanılarak sayısal ortamda üretilecek bina yaş bilgisi için 1966 ve 1982 yıllarına ait hava fotoğrafları, 1996 ve 2013 yıllarına air ortofoto mozaik haritalar ve 2004 ve 2007 yıllarına ait uydu görüntüleri kullanılmıştır. Böylece İstanbul'daki yapıların değil binaların kesin sayıları ve lokasyonları ve her bir binanın yaş bilgisi tanımlanmış olacak ve CBS ortamında üretilmiştir. Bu da yapılacak deprem hasar analiz çalışmasının gerçek veriler ile yapılmasını sağlamıştır. Bu çalışmaya gore İstanbul'da 1996 yılından once

inşa edilen 794,325 adet bina bulunmaktadır. Bina stoğu 1996 ve 2013 yılları arasında %24.71 oranda artmıştır. 1982 ve 2013 tarihleri arasında bina stoğu en fazla yükselen ilçe 33,688 adet bina ile Silivri ilçesi olup, en az yükselen ise 2,914 bina ile Bakırköy İlçesidir.

Çalışmanın ikinci bölümünde güncellenmiş bina verileri ile Istanbul için olası deprem senaryosu ışığında bina hasar analizleri gerçekleştirilmiştir. Bina hasar analizleri HAZTURK programı ile senaryo bazlı PGA ve Sa deterministik deprem haritaları kullanılarak yapılmıştır. Sonuç bölümünde bina bazlı hasar tahmin sayılarının yanında diğer çalışmalar ile karşılaştırılabilmesi için sonuçlar ilçe ve mahalle bazlı olmak koşulu ile de paylaşılmıştır. Hasar analizi Sa deterministik deprem haritası kulllanılarak yapıldığında; İstanbul'daki binaların %21.52 sinin hafif hasar, %35.55 nin orta hasar, %28.21 nin ağır hasar alması % 14.68 inin yıkılması, %35.23 nün ise ortalama hasar görmesi beklenmektedir. Hasar analizi PGA deterministik deprem haritası kulllanılarak yapıldığında ise; İstanbul'daki binaların % 50.37 sinin hafif hasar, % 31.85 nin orta hasar, % 13.99 nin ağır hasar alması % 3.80 inin yıkılması, %15.6 sının ise ortalama hasar görmesi beklenmektedir.

Çalışmanın üçüncü bölümünde hasar görme potansiyeli taşıyan binaların; bina yıkılma yönleri ve oluşturdukları enkazların çapları tanımlanmıştır. Bu bilgi ile Istanbul'daki yolların kapanma olasılıkları ortaya konmuştur. Bina yıkılma yönü tahmininde kullanılan method , 1994 ve 1999 yıllarına ait Gölcük hava fotoğraflarının sayısal olarak analizi ile üretilen 1999 Kocaeli Depremi'nde Gölcük'te yıkılan binalardan üretilmiştir. Geliştirilen metoda göre, yol kenarında bulunan binaların deprem esnasında yıkılmasıyla, etrafa saçılan enkaza ait parçalar, etrafta bulunan yolların kullanılabilirliklerin düşmesine sebeb olmaktadır. Binaların yıkılma yönlerinin tanımlanması; acil durum operasyonları sırasında kullanılabilirliği devam edecek yollar hakkında önemli bilgiler verecektir. Bina yıkılma yıkılma yönlerinin tanımlanması deprem sonrasında hangi yolların açık hangi yolların kapalı olacağı hakkında bilgi verecektir. Rotalar, tahliye ve kaçış yollarının tanımlanmasında, acil durum yollarının belirlenmesinde çok önemlidir. Bu çalışma ulusal ve uluslarası literatürde bu konuda yapılan ilk çalışmadır.

Çalışmanın dördüncü bölümünde, ulaşım yapılarında deprem tehlikesi karşısında oluşabilecek olası hasar analizleri yapılmıştır. Çünkü sadece yıkılan binaların oluşturdukları enkaz değil, ulaşım yapılarında oluşabilecek hasar da yol ağlarının kullanılabilirliğini azaltmaktadır. Bu bölümde köprü (üstgeçit, altgeçit) ve viyadüklerde deprem nedeni ile oluşabilecek hasar, HAZTURK program ile senaryo bazlı PGA deterministik deprem haritası kullanılarak hesaplanmıştır. Bu çalışmada ana yollar üzerinde bulunan 247 adet köprü çalışılmıştır. Hasar analizini takiben ulaşım yapılarının deprem sonrası kullanılabilirlikleri belli zaman periyotları için paylaşılmıştır. Buna göre 194 adet köprü olası depremin hemen sonrasında kullanılabilir değildir. Deprem gününden 3 gün sonra ise 33 köprünün kullanılamaz olduğu tahmin edilmektedir.

Çalışmanın son bölümünün İstanbul için önemli olmasının sebebi yolların deprem sonrası müdahele ve uzun dönem için iyileştirme çalışmalarında kritik derecede önemli olmasından kaynaklanmaktadır. Çalışmanın sonucunda bina yıkılma yönleri, enkaz alanları ve ulaşım yapılarındaki hasar birlikte değerlendirilmiş ve İstanbul'daki mevcut yol ağlarının kullanılabilirlikleri, olası Istanbul depremi sonrası için ortaya konmuştur. Çalışma çıktılarına gore yaklaşık 3500 km lik yol ağı deprem sonrasında kullanılamaz olduğu tahmin edilmektedir.

Bu çalışmanın sonuçları karar vericiler için risk azaltma, hazırlıklı olma, müdahele ve iyileştirme çalışmalarında kullanılacabilecek önemli bir veritabanını içermektedir. Sonuçlar ve önerilen metodlar; karar vericilere, risk azaltma stratejilerini geliştirirken, olası tehlikelerin baş edilemeyecek afetleri dönüşmesini engellerken, olası risklerin azaltırken ve deprem odaklı kentsel dönüşüm çalışmalarında; temel ve dayanak bilgi olarak kullanabilecekleri önemli katkılar sunmaktadır.

1. INTRODUCTION

Istanbul has hosted many civilizations and cultures for centuries. Today the city is Turkey's cultural, industrial, commercial and educational centre and one of the highest populated cities in the world (DESA, 2014). According to the 2014 Address Based Census System Registration (ADNKS) of Turkey Statistical Institute (TUIK, 2014), 14,377,18 people live in Istanbul, which has the highest population of all the Turkish cities. Unfortunately, it is also located in one of the most active seismic zones in Turkey and the world (Karaman & Erden, 2014) as can be easily been seen in Figure 1.1.

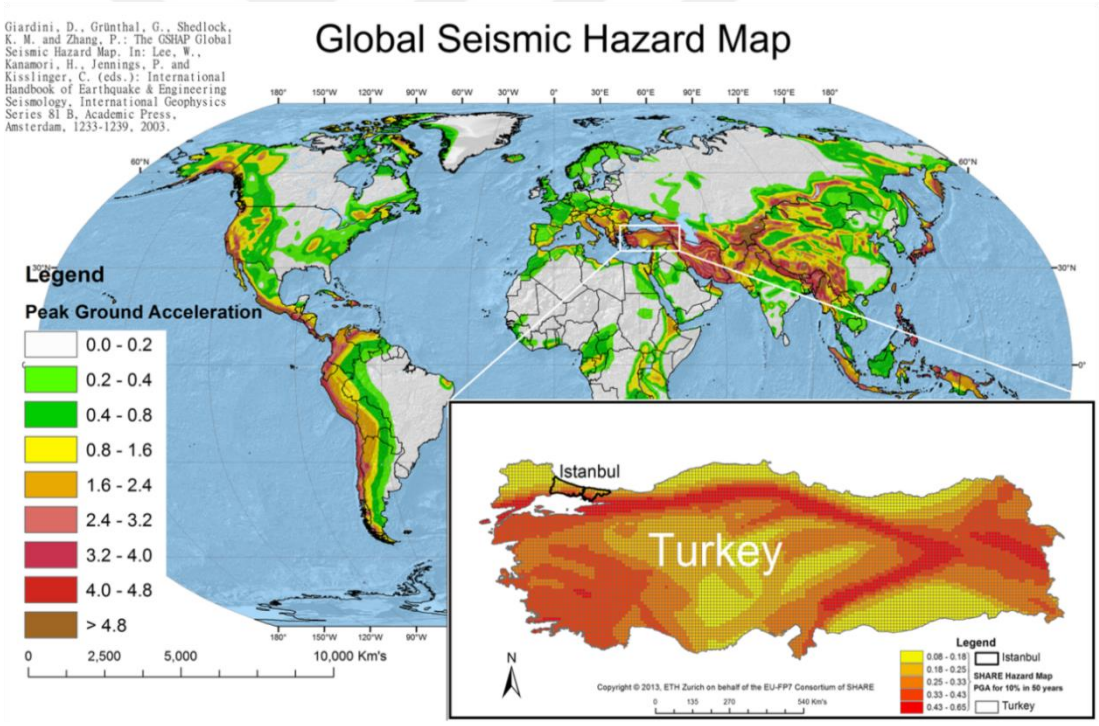


Figure 1.1 : Global seismic hazard map and location of the study area (Giardini et al. 2003; Karaman and Erden 2014).

The risk of earthquakes depends on the number of assets that will be exposed to the hazard. Therefore, earthquake risk increases according to the increase in population and the number of buildings in the region of interest. This is why, at least, in the most hazardous regions, the number of physical assets should be reduced to mitigate the risk. Since the 1999 Kocaeli and Duzce earthquakes, it is accepted that Istanbul is

waiting for a large scale earthquake; in fact, there is a 29–66% probability of a M ≥ 7 earthquake rupturing beneath the Sea of Marmara to the south of Istanbul in the next 30 years (Parsons, 2004).

However, migration to Istanbul is continuing from other cities. The rate of net migration between 1980 and 2014 can be seen in Table 1.1, published by TUIK (2014). The highest amount of migration to Istanbul took place between 1985 and 1990 with 656,677 people arriving. The sheer quantity of migration has caused unplanned and unregistered construction, and this has created the vulnerable habitats and building stocks in Istanbul by increasing the earthquake risk.

Table 1.1 : TUIK population census between 1980-2014 (TUIK, 2014).

Census Type	*Period*	*Total population*	*In-migration*	*Out-migration*	*Net migration*	*Rate of net migration (‰)*
Address Based Population Registration System	2013-2014	14 377 018	438 998	424 662	14 336	1.0
	2012-2013	14 160 467	437 922	371 601	66 321	4.7
	2011-2012	13 854 740	384 535	354 074	30 461	2.2
	2010-2011	13 624 240	450 445	328 663	121 782	9.0
	2009-2010	13 255 685	439 515	336 932	102 583	7.8
	2008-2009	12 915 158	388 467	348 986	39 481	3.1
	2007-2008	12 697 164	374 868	348 193	26 675	2.1
General Population Censuses	1995-2000	9 044 859	920 955	513 507	407 448	46.1
	1985-1990	6 433 569	995 717	339 040	656 677	107.6
	1980-1985	4 074 806	557 082	268 429	288 653	73.4

Istanbul has been affected by earthquakes throughout its history. Based on worldwide historical earthquake catalogues, Istanbul has suffered repeated damage due to earthquakes (Utsu, 1990). When the historical earthquake data of Istanbul is analysed, we see that the city has been affected by a moderate intensity earthquake every fifty years and a high intensity earthquake every 300 year (Ambraseys & Finkel, 1991) (Figure 1.2).

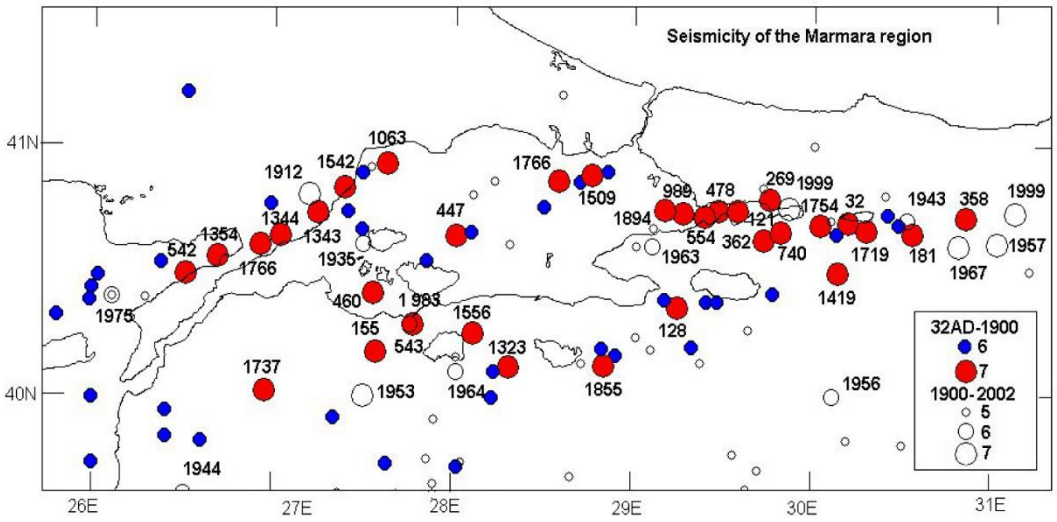


Figure 1.2 : Historical earthquakes of Marmara Region, (Ambraseys&Finkel, 1991).

The most recent earthquake to shake Istanbul was on August 17 1999, along the North Anatolian Fault, 12 km southeast of the Izmit Province, with a magnitude of 7.4. During this earthquake, the most damage, occurred in Izmit, Sakarya and Yalova. Despite being far away from the epicenter, there was damage in Istanbul, Bolu, Bilecik, Bursa and Eskişehir. This earthquake resulted in heavy damage of 66,441 houses and 10,901 workplaces, in moderate damage to 67,242 houses and 9,927 workplaces and with, insignificant damage of 80,160 houses and 9,712 workplaces in these cities (Özmen, 2000). According to Bibbee, Gönenç, Jacobs, Konvitz, and Price (2000), the total cost of damage from the 1999 earthquake is estimated at between $9 and $13 billion.

In 1999, the Kocaeli earthquake occurred approximately 117 km from Istanbul but the Avcılar and Buyukcekmece districts of Istanbul, which were the districts furthest to the epicentre, had the highest amount of damage. Due to this earthquake, 3,073 buildings suffered extensive damage, 11,339 buildings had moderate damage, and 12,455 buildings had insignificant damage in Istanbul. Unfortunately, 454 people died and 1880 people injured (Özmen, 2000).

Following the 1999 Izmit earthquakes, the earthquake risk in Istanbul started to draw attention and leading researchers to estimate the hazard and risks of possible earthquake scenarios in Istanbul.

After the 1999 Kocaeli Earthquake, many scientific studies were conducted on the potential earthquake risk in Istanbul. Based on these studies, predictions are that

Istanbul is going to face a major earthquake in the near future and this will cause severe damage to the built environment. Some of these studies have been made to determine the characteristics of the Marmara Fault. According to the works of Le Pichon, Chamot-Rooke, Rangin, and Sengör (2003); Rangin et al. (2001), the North Anatolian fault has been determined as a right-lateral fault which lengthens to the northern side of Marmara Sea (Figure 1.3).

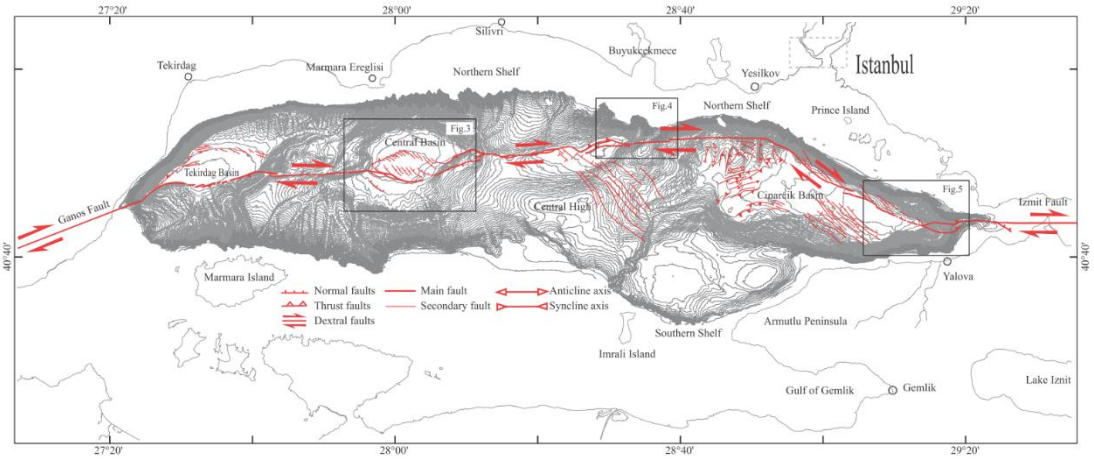


Figure 1.3 : Marmara fault model according to Le Pichon et. al, (2003).

Regarding to another study made by Armijo, Meyer, Navarro, King, and Barka (2002); (2005), the Marmara Fault is considered as a complex structure including the Ganos pull-apart system and the Izmit lateral slip with normal faulting in the Cinarcik trench (Figure 1.4).

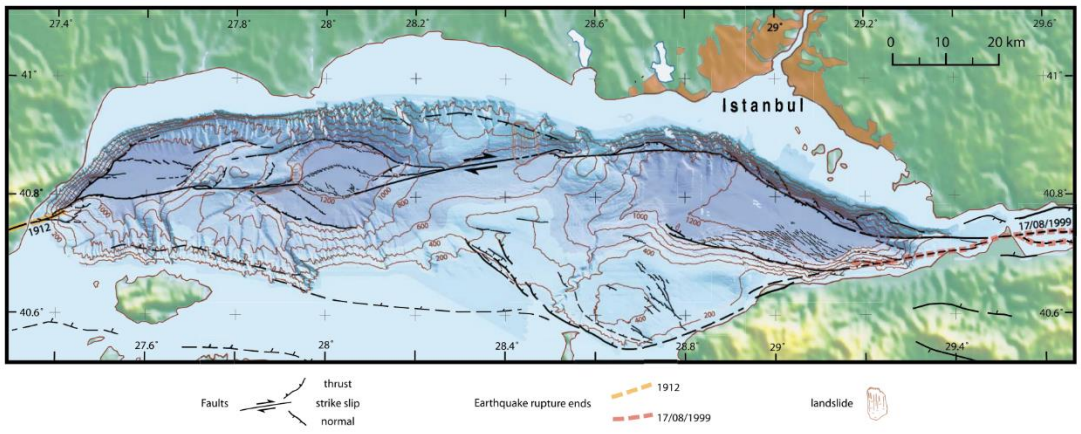


Figure 1.4 : Marmara fault model according to Armijo et. al, (2005).

According to the study of Parsons, Toda, Stein, Barka, and Dieterich (2000), the probability of a devastating earthquake occurrence in the Marmara Sea in the following 30 years is 60% (with a 50 year return period). The study conducted by Ambraseys

(2002) concludes that the region of Marmara Sea has been shaken by an earthquake of more than Mw 6.7 in the last 2000 years which caused serious devastation. According to Parsons (2004), the probability is between 29% and 66% of a Marmara earthquake with a magnitude of more than 7.0 occurring in the following 30 years. A study conducted by Karaman and Erden (2014) has combined all these studies about the fault mechanism for the Sea of Marmara (Figure 1.5) and combined all the separate fault mechanism results in one Marmara fault line map.

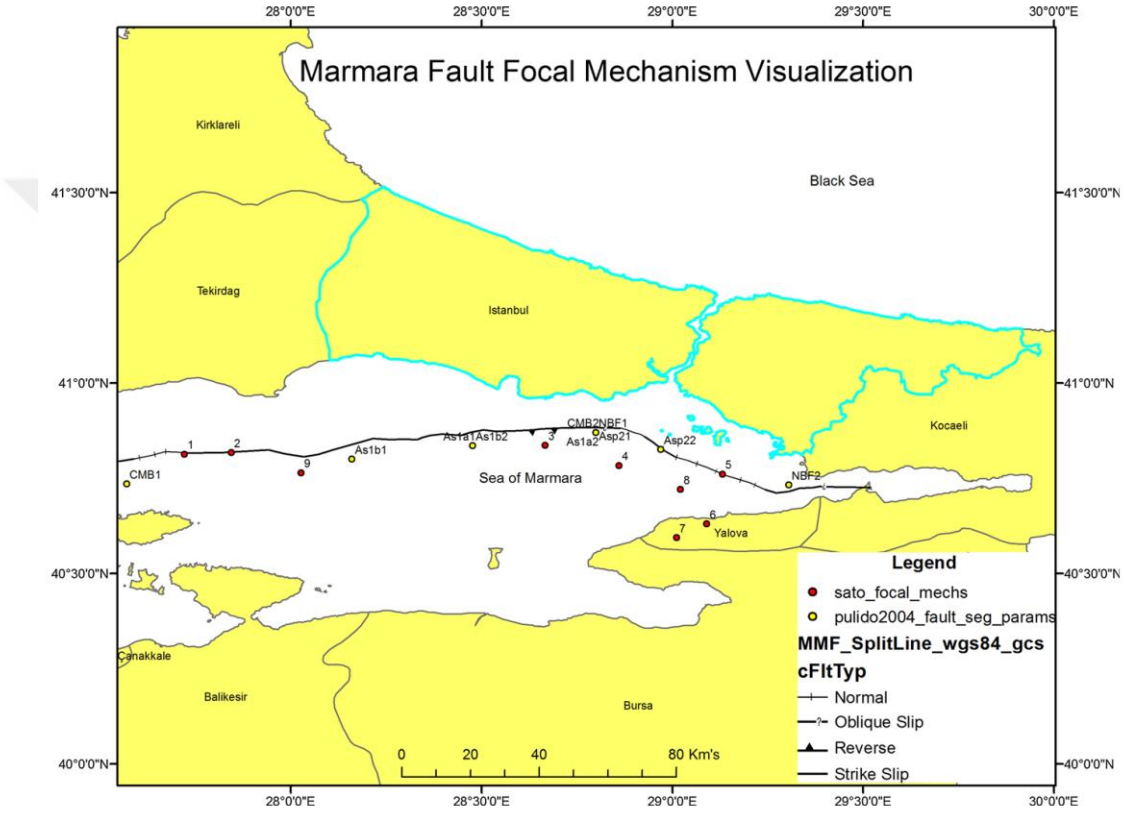


Figure 1.5 : Marmara fault focal mechanism visualization, (Karaman&Erden, 2014).

Following the studies on fault mechanism and earthquake scenario generation, the damage possibilities were taken into consideration. The first large scale study for Istanbul against the earthquake hazard is "The Study on A Disaster Prevention / Mitigation Basic Plan in Istanbul including Seismic Microzonation in the Republic of Turkey" (JICA). This study was conducted with The Japan International Cooperation Agency and The Istanbul Metropolitan Municipality in 2002 (JICA & IMM, 2002). The second study on earthquake risk, one that consists of the building data "Earthquake Risk Assessment for Istanbul Metropolitan Area", was conducted by Kandilli Observatory and Earthquake Research Institute (KOERI) in 2002 (BU-ARC, 2002).

A third study was conducted for both Zeytinburnu District (Karaman, Sahin, Elnashai, & Pineda, 2008) and the city of Istanbul (HAZTURK, 2007). In order to calculate damage, HAZTURK software was used in this study and building damages were estimated for every single building for the first time in the city of Istanbul (H. Karaman et al., 2008). The latest work for Istanbul "Updating of Probable Earthquake Losses for Istanbul" was conducted by IMM and Kandilli in 2009 (IMM, 2009).

The latest building damage analysis was completed seven years ago. During this period, the building stock increased and some buildings were demolished due to urban transformation. Within this period, the earthquake risk in Istanbul is increasing rapidly. In order to take necessary precautions, earthquake risk analysis for Istanbul are hence going to be repeated with the recent data and the results of this analysis should be used for risk mitigation studies in Istanbul.

Roads are important for human life both under normal circumstances and during a natural disaster, where they have crititical roles for response and recovery activities. If roads lose their functionality immediately, following an earthquake, some activities such as search and rescue, firefighting and accessibility to shelters area can be impracticable during the recovery time, while this situation could cause an increase in the number of deaths and injuries.

One of the most important reasons for road blockage during the disaster time is building collapse. Currently, no international nor national studies exist of building collapse direction. The determination of the building collapse direction supply the important data such as open roads for recovery time. Open roads data supplies important and necessary data for decision makers to divert the traffic during the disaster time for recovery. Not only building damage but also transportation damage analysis is necessary to use risk mitigation studies and decisions, being that experiences showed that the functionality of transportation structure effects post-earthquake emergency response and recovery operation seriously. Up until now, only a JICA study has evaluated Istanbul bridges from the point of earthquake risk analysis before 14 years ago. Since then, some bridges in Istanbul have been retrofitted and loss assessment programs such as Maeviz and HAZTURK have been developed to calculate building and bridge damage.

This study aims to reveal a method for road functionality in Istanbul following a potential Istanbul Earthquake by using building collapse direction and bridge damage. Hence two steps are needed to determine the road blockage in Istanbul. One is to determine road blockage due to building collapse direction. Firstly a recent, accurate building dataset in Istanbul has been created, but this dataset did not include the building age data for every single building in Istanbul. Building age data is necessary for making building damage analysis in order to be assigned to every single building in Istanbul. Thus, building damage analysis were made for every single building in Istanbul.

In order to determine building collapse direction in Istanbul a collapsed building in Gölcük during the 1999 Kocaeli earthquake was studied. According to this study, two methods for studying buildings collapse direction have been obtained and these two methods have been applied to the buildings in Istanbul that have damage possibility. In regard to the direction and distances of buildings collapse, we are going to determine the potential road blockage in Istanbul. The second step will then be to determine the bridge damage and functionality after an earthquake because, following an earthquake, non-functional bridges have cause roads to lose their accessibility. Firstly, recent bridge data was created from the paper data and then by using this update bridge data, bridge damage and functionality analysis were made. By combining these two data sets, the potential road blockage in Istanbul has been revealed (Figure 1.6).

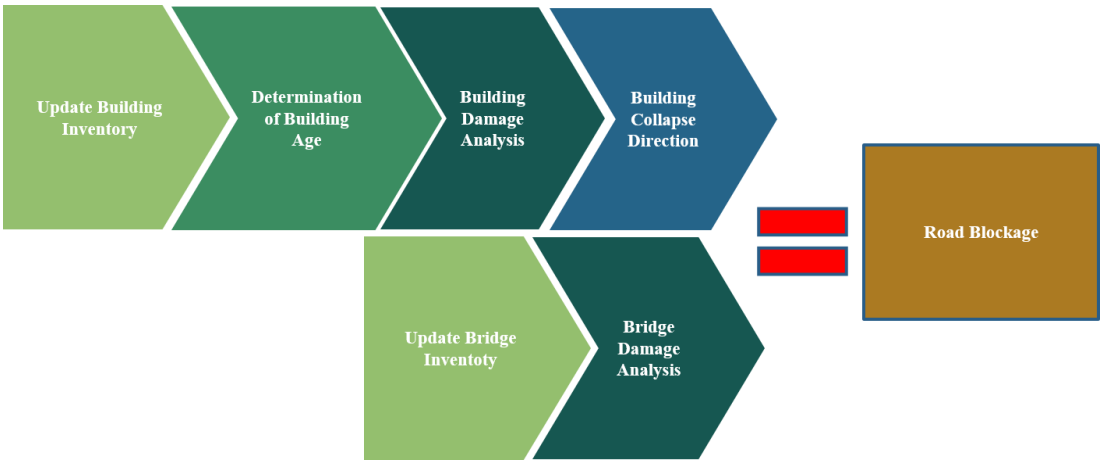


Figure 1.6 : Steps of determination road blockage in this study.

The analysis and their results of them have taken a long period of time following the data creation, involving almost 5 years of research and study. In particular, studies involving the creation of current and recent building and bridge database and the

determination of the age of building have taken approximately four years owing to some limitations.

The first building database was taken from IMM, under the understanding that structure and building data were used together in this database. In order to separate them from each other, a long study was made. Moreover, for defining a building age for every single building in Istanbul, six remote sensing image were studied manually. In view of the fact, no remote sensing software currently exists for use throughout all of Istanbul. In addition to this, the raw bridge data was not GIS based. For this reason, all the bridges studied in this study were digitised using ArcGIS.

The limitations in this study are given below.

- In order to achieve reliable building damage analysis, the building data set should not consist of structure data. Instead, the building data obtained from IMM consisted of structure data. For this reason, we had to eliminate structure from building data.
- In order to determine the age for every single building in Istanbul, a remote sensing programme that works all Istanbul successfully should be developed. Being that it is given at literature part, the current programme is useful for buildings with similar colour and shape in small area.
- In order to use bridge damage analysis, all the bridge data was digitized manually. This took a long time.
- Some bridges were retrofitted in Istanbul, but we could not realise the methods that were used for retrofitting bridge. For this reason, the damage analysis was repeated twice using different retrofitting types.

2. PURPOSE OF THESIS

As stated previously within the Introduction section, Istanbul is expecting a major earthquake. It is impossible to prevent an occurrence of the earthquake as a common knowledge. In that case, the only way to go is to take necessary precautions for earthquakes in the light of related risk analysis results.

The aim of this thesis is to research earthquake effects on buildings and transportation structures in order to use risk mitigation strategies and studies by decision makers. Within the context of this aim, building age determination, building damage, building collapse direction and transportation structures damage and functionality were studied as a part of study.

2.1 Purpose of Building Age Determination

A major disadvantage of Istanbul case is the lack of knowledge for the absolute number of buildings and the ages of those buildings in GIS system. To make a correct or reliable earthquake damage estimation, a building database that contains at least, building age, construction type and the number of floors is required in most of the earthquake loss assessment software.

Any building database for Istanbul does not consist of a building age for every single building at GIS based. Previously making studies about earthquake risk analysis use the building age after classification them.

In JICA and IMM (2002) study, the total number of buildings are determined as 724609 according to the 2000 Building Census by State Institute of Statistics. Building data consisted of construction type, construction year and number of stories of each building, and these items were necessary to carry out the damage estimation. In this study construction year, data was aggregated into six categories: 1949 and before, 1950-1959, 1960-1969, 1970-1979, 1980-1989, and 1990 and after. JICA database consists of building attribute information such as district or sub-district based in GIS

(Figure 2.1) (JICA & IMM, 2002). For this reason, it is impossible to obtain building age from JICA database based on every single building. In addition, this data was produced before 2000.

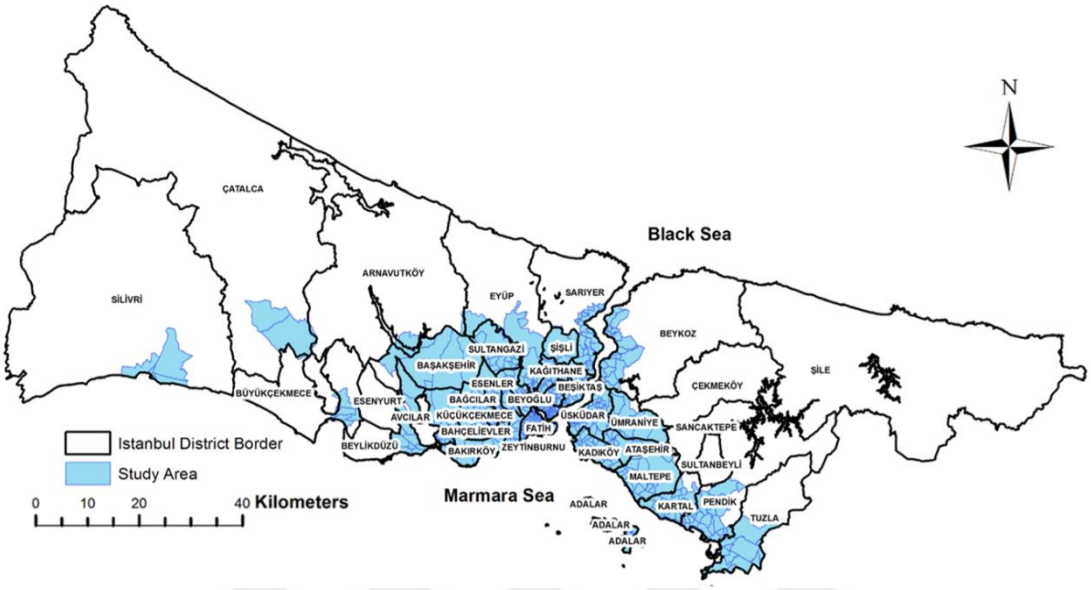


Figure 2.1 : The study area of JICA project.

Building inventory of BU-ARC (2002) study was created by using aerial photographs from 1995 and 1999 (Figure 2.2) (BU-ARC, 2002). However, this data producing from aerial photographs does not contain building attributes information. For this reason, TUIK 2000 data (TUIK, 2014) (construction type, number of floors, construction year) was assigned to building inventory data by using a geocoding method in this study. Construction year data is divided into two classes: pre 1979; and post 1980. The study area divided into grids of approximately 400m x 600m (BU-ARC, 2002). Building age data cannot be acquired for every single building using the BU-ARC (2002) study. For this reason, it is impossible to obtain a building age from a BU-ARC (2002) study database based on every single building. In addition, this data was produced before 2000.

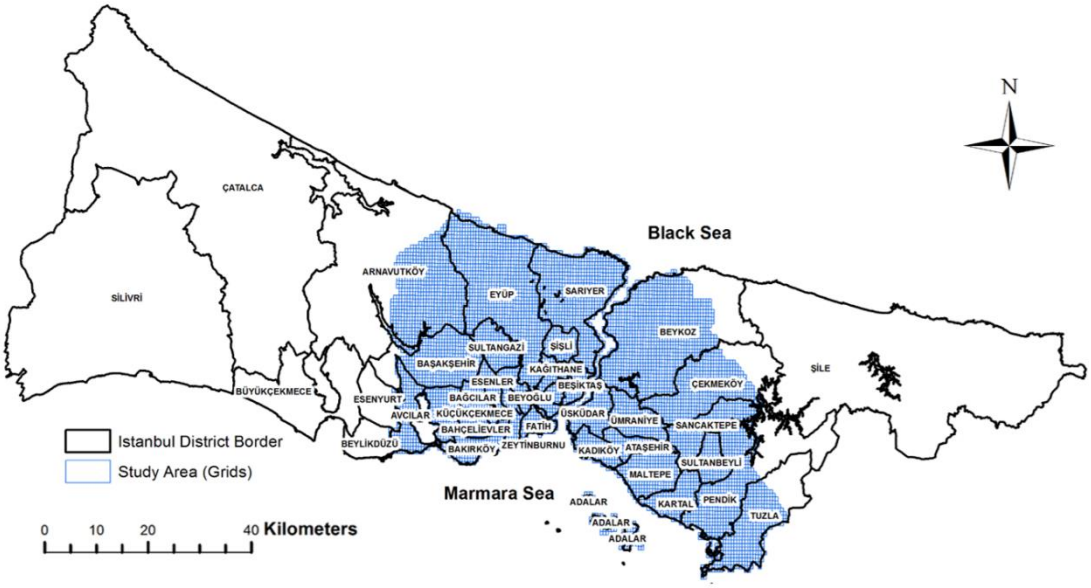


Figure 2.2 : The study area of BU-ARC project.

The required building age data for the Zeytinburnu study was obtained from tax accrual database and construction permits (Karaman et al., 2008). The zonal age classification of BU-ARC (2002) study was used to add age information to every single building (HAZTURK, 2007). A building inventory of this study is covered only by the Zeytinburnu district. This data prove not to be adequate for Istanbul. For this reason, it was not used.

The results of the IMM (2009) study were given as grids of approximately 400m x 600m. In order to create a building inventory, a TUIK 2000 Building Census Work, JICA Dataset, 2008 base map were used. The study used three building age classifications: pre 1970; between 1980 and 2000; and after 2000 as a grid system and it is impossible to take building age data for every single building (IMM, 2009). Because of the availability of this data, the building dataset of this study was not used.

In order to make reliable and acceptable building damage analysis, the first step of study focused on the creation of the Istanbul building inventory, not for a region average or a grid average, but, for every single building of the city. The base data for the study purchased as the "Istanbul Structure Data" from IMM. The first investigations of the inventory revealed that, the data does not contain the building construction year (building age). Building age is a necessary factor along with construction type and number of floors of a building to estimate the earthquake damage on a building (Karaman & Erden, 2014). Another important result of the first step is

the exploration of the truth that no agency or institution had information about building ages on GIS. The necessity of recording a building age for every building of Istanbul in GIS thus became obvious.

The building construction year (building age) in building risk analysis gives information about the construction standards for building codes. The reason for the creation of building code is to determine essential conditions for the realisation of a functional, safety and earthquake resistant building design. Regarding the "Specification for Buildings to be Built in Seismic Zone" published by the Official Gazette in 2007 in Turkey, the general principle of earthquake resistant design is to prevent structural and non-structural elements of buildings from any damage in low-intensity earthquakes. Hence, the following objectives hold: to limit the damage in structural and non-structural elements to repairable levels in medium-intensity earthquakes; and to prevent the overall or partial collapse of buildings in high-intensity earthquakes in order to avoid the loss of life.

When the building age is provided in GIS, it is possible to classify the buildings with respect to the structural codes and map them with the appropriate fragility curves. This study took the official structural codes of Turkey for the building age classification in order to place every single building into the appropriate age classification for the damage estimation process based on the fragility curves of the Istanbul building inventory.

2.1.1 Development of structure codes in the world

Earthquakes are uncontrollable mechanisms, yet earthquakes themselves are not the cause of loss of life; the cause is inadequately constructed buildings. At this point, it is necessary to ensure that buildings get built according to structural codes.

The first comprehensive building code was enforced in London by the government after a devastating fire in London in 1666 (Holmes, Kircher, Petak, & Youssef, 2008). The government control of design and construction gradually spread throughout the world largely based on the London precedent. However, each country has its own, often unique, history and legal authorisation for building code development and implementation (Meacham, Bowen, Traw, & Moore, 2005).

Another study looked at the development of seismic codes that came into force after the 1755 Lisbon earthquake. Prescriptive rules for the construction of the most

common building types (gaiola construction) were promulgated here, added to this the 1911 Messina and 1923 Kanto Tokyo Earthquakes, which resulted in the development of more technical guidelines, including the design of buildings (Holmes et al., 2008).

The studies about structural codes studied in Japan, started after the 1923 Big Kanto Earthquake. The Seismic Coefficient Method was used in its first applications in 1926. Two regulations, "Building Standard Law Enforcement Order" (BSLEO) and "Standards for Seismic Civil Engineering Construction in Japan" were put into place by the Japanese Ministry of Public Works (Catal, Yazıcı, & Tüzün, 1999).

Building code studies in America started after the 1906 San Francisco earthquake. The 1933 Long Beach earthquake resulted in strict seismic design being supplied for schools in California and the implementation of mandatory seismic design for all buildings in California. A major effort to update seismic design concepts and make them more applicable on a national level was funded by the federal government in the 1970s. The resulting document, Tentative Provisional for the Development of Seismic Regulation for Buildings (commonly known as ATC 3) expanded and clarified the premise that seismic buildings codes should not be expected to produce a zero-risk environment (Holmes et al., 2008). A performance code was also developed by The International Code Council (ICC), developers of the International Building Code, alongside The International Code Council Performance Code for Buildings and Facilities, an effort initiated in 1996 and culminating with the first edition in 2001 (Holmes et al., 2008).

2.1.2 Development of structure codes in Turkey

Following the foundation of the Turkish Republic, many different rules were tried for building construction and have since been revealed as disaster regulation. The responsibility of these regulations has been passed to various Ministries throughout the history of Turkey (Table 2.1). Nowadays, the Ministry of Environment and Urban Planning is responsible for making regulations about building codes.

Table 2.1 : History of Ministry of Environment and Urban Planning.

The ministries responsible for buildings construction	*Year Intervals*
Ministry of Public Works in Ottoman Empire	1848 -1920
Ministry of Public Works	1920 - 1928
Ministry of Public Works	1928 -1983
Ministry of Reconstruction and Housing	1958 -1983
The Ministry of Public Works and Settlement	1983 - 2011
Ministry of Environment and Urban Planning	2011

The Ministry of Environment and Urban Planning has published ten building codes since its inception. The ministry is still involved in the update process of structural codes for buildings (Table 2.2).

Table 2.2 : Building codes in Turkey.

Year	***Building Code Name***
1940	Italian Structural Code for the Earthquake Zone Constructions
1944	Temporal Structure Code for the Earthquake Zone Constructions
1949	Structure Regulation for Turkey Earthquake Zones
1953	Regulation for the Structures that are going to be Constructed within the Earthquake Zones
1962	Specification for Buildings to be Built in Seismic Zones
1968	Specification for Buildings to be Built in Seismic Zones
1975	Specification for Buildings to be Built in Seismic Zones
1997	Specification for Buildings to be Built in Seismic Zones
2007	Specification for Buildings to be Built in Seismic Zones
2015	Preparation phase of the New Building Code

The most recent comparison of the official structural codes in Turkey was conducted by Alyamac and Erdogan (2005). As they indicated, the changes within each code raise new aspects of how to deal with the earthquake resistant design of the structures. The first official code was named as the Italian Structural Code for the Earthquake Zone Constructions and came into force in 1940. It focused mostly on architectural issues. During this period, the major building stock was masonry buildings.

The Temporal Structure Code for the Earthquake Zone Constructions came into force in 1944 and enforced punitive articles requiring the constructor companies to get a licence for new constructions. The most important difference from the previous regulations was to mention the soil properties of the construction areas. The third official code was named as Structure Regulation for Turkey Earthquake Zones and punitive articles were removed as a consequence. The 1st and 2nd degree earthquake zones have been created superficially. An equation was given for the first time in order to calculate the seismic forces with this regulation.

However, the following codes added independent aspects: the Structural Code of 1962 introduced a separate section for the structures in the earthquake zones, as well as

construction foundations, and slab girders (Alyamac & Erdogan, 2005). However, most of them were applied following the introduction of the 1968 Specification for Buildings to be Built in Seismic Zones Structural Code. This why the 1962 Code has been a turning point in Turkish earthquake resistant building construction.

Most of the buildings in Istanbul constructed were under the enforcement of the structural code of 1975, going under the name of Specification for Buildings to be built in Seismic Zones. Turkey is divided into 4 earthquake zone in this regulation (Table 2.3). The site effects were taken into account for earthquake calculations. Calculation of the earthquake forces were mentioned in more detail, while lots of missing specifications detected from the previous codes and added in this regulation. The acceleration of spectrum coefficients were also determined here according to Alyamac and Erdogan (2005).

Table 2.3 : Code level regarding to building codes in Turkey.

Building Code Name	***Building Code Year***	***Code Level***
Italian Structure Regulations	1940	Code Level 1
Temporal Structure Code for the Earthquake Zone Constructions	1944	Code Level 1
Structure Regulation for Turkey Earthquake Zones	1949	Code Level 1
Regulation for the Structures that are going to be Constructed within the Earthquake Zones	1953	Code Level 1
Specification for Buildings to be Built in Seismic Zones	1962	Code Level 1
Specification for Buildings to be Built in Seismic Zones	1968	Code Level 1
Specification for Buildings to be Built in Seismic Zones	1975	Code Level 2
Specification for Buildings to be Built in Seismic Zones	1997	Code Level 3
Specification for Buildings to be Built in Seismic Zones	2007	Code Level 4

The most recent regulation aimed at earthquakes for Turkey was introduced in 2007. This building code was the revised version of the American Earthquake Regulation (IBC) and then adapted for Turkey. Currently, a new building code being created with plans to introduce it in 2016 on the part of The Republic of Turkey's Disaster and Emergency Management Presidency.

It is important to be aware of the structural codes that force the constructers for specific designs to create an adequate building inventory for the purpose of earthquake loss assessment. In this study, the structural codes dates that have come into force in Turkey

from 1940 to 2007 were taken as a reference in order to determine building age classification for Turkey and especially for Istanbul. Aerial photos, satellite images and ortho-photo mosaics were obtained for the detection of the buildings constructed before and after the related structural codes. After determination of building age data for every single building in Istanbul, the next step is to define a building damage state for every single building in Istanbul.

2.2 Purpose of Building Damage Analysis in Istanbul

Studies of earthquake risk analysis based on building damage have been conducted since 2002 for Istanbul (BU-ARC, 2002; IMM, 2009; JICA & IMM, 2002; H. Karaman et al., 2008). In regard to these studies, building-based losses have been very high. In addition, previous studies have shown that the highest cause of deaths and heavy injuries was building collapse during the earthquakes.

The estimation of possible building damage constitutes very useful data to conduct risk reduction studies. Several loss assessment tools currently exist worldwide to estimate building damage. However, most of them are proprietary, closed code, region-specific, or all of the above (H. Karaman et al., 2008).

Several scientific studies have proven that the possibility of Istanbul facing a major earthquake in the near future is high (NN Ambraseys & Finkel, 1991; Le Pichon et al., 2003; Parsons et al., 2000). It is estimated that the damage caused by the anticipated earthquake will be extensive as a consequence of Istanbul's low quality building stock of Istanbul (Karaman, 2009). One of the most effective ways to mitigate earthquake risks in Istanbul is to design earthquake resistant buildings. The other approach is to determine which buildings have an inadequate seismic performance; these buildings should be either reinforced or rebuilt. In order to determine a building's risk, it is important to determine the vulnerability of the buildings against potential earthquake scenarios. To reduce losses in an earthquake, it is necessary to start a risk mitigation study as soon as possible in accordance with the damage estimation analysis conducted in a city where the number of buildings is too much to handle one by one.

The latest damage estimation study for building damage in Istanbul was completed seven years ago (IMM, 2009). It is of vital importance to undertake diligently a realistic approach to collecting accurate and current data for making building damage

analysis. It is therefore necessary to update building damage analysis with current building data. In this study, the updated building inventory was used based on structural building codes and remote sensing images. The most important feature of this data set is its inclusion of the building age for every single building in Istanbul for the first time in the GIS medium. HAZTURK loss assessment software was used to estimate the building damage in this study.

The buildings that have the possibility of being damaged cause debris around them. If roadside buildings collapsed during the earthquake, the scattered parts of the buildings could cause roads to lose their functionality. However, if the direction of collapse of the buildings can be determined, then functioning roads during emergency operations will be revealed. At a later stage, the aim is to determine the direction of building collapse and the possible debris around it.

2.3 Purpose of Building Collapse Direction

Building damage is one of the highest causes of death and injures during earthquakes. Besides this, the collapsed buildings can create debris around the buildings and this debris may cause road blockages in the vicinity of the damaged buildings, especially in narrow roads (Figure 2.3). Road blockages decrease road functionality during a disaster. The inability to use roads makes it difficult and impossible for some activities during the response and recovery time; such as search and rescue, firefighting and accessibility to temporary shelter areas. This situation could cause an increase in the number of deaths and injuries. For this reason, it is important to define the direction of building collapse during the earthquake.



Figure 2.3 : Road blockage due to the building collapse from 1995 Kobe Earthquake, (2015).

In this part of the study, we have estimated the building collapse direction and debris spreading distance (debris area radius of buildings) of collapsed buildings for the buildings in Istanbul, which have the possibility of damage during the potential Istanbul earthquake. One of the basic methods for determining “building collapse direction” is to reveal the road blockages and then road functionality after an earthquake in order to identify open roads and suitable response routes. This method of definition building collapse direction was developed for Gölcük based on the investigations of collapsed buildings after the 1999 Kocaeli earthquake. It used the 1994 and 1999 aerial images of Gölcük, where the highest amount of buildings collapsed in various directions (Figure 2.4).



Figure 2.4 : Collapsed buildings photo from Gölcük.

Gölcük has been choosen as a study area for this developing method. According to Özmen (2000), 35.7 % of buildings in Gölcük were heavily damaged, while 5,025 people died in Gölcük because of the 1999 Izmit Earthquake. The study area in Gölcük is located to the northeast of the Gölcük district of the Kocaeli province (Figure 2.5).

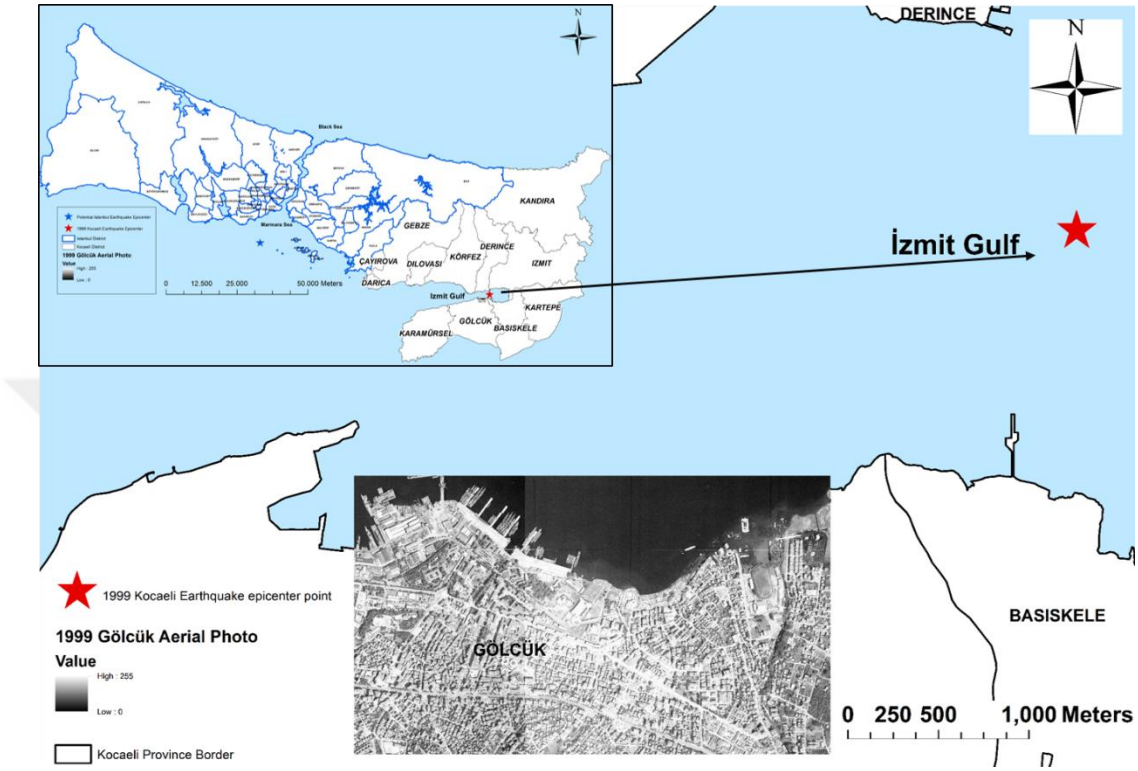


Figure 2.5 : Study area in Gölcük.

Not only has the building collapsed, but transportation structure damage has also caused the roads to lose its functionality. For this reason, transportation structure damage will be analysed in the next part of this study.

2.4 Purpose of Transportation Structure Functionality

Highway transportation systems play a significant role in the overall impact that a seismic event has upon a region because it interconnects with other infrastructure in the region. According to Chang and Nojima (1998) and Kameda (2000) studies, the highway system is configured into a network which consist of a large number of links and nodes. The disruption of any of these links, such as a road, or nodes such as a bridge, can disrupt a section of the network, the impact of which is dependent on the redundancy in the system (Rojahn, Scawthorn, & Khater, 1992).

In order to estimate the performance of bridge functionality during an earthquake, it is necessary to make a seismic risk assessment, by calculating damage possibility and revealing a loss of functionality. Risk assessment studies allow necessary precautions to be taken, along with the planning of repair works and defining emergency transportation routes for search and rescue activities, and firefighting during the response process and, finally recovery time. Moreover, surveying post-earthquake functionality of transportation structures will provide the grounds for making the right decision for appropriate retrofitting study and proper routes during recovery time.

This study aims to reveal functionality of transportation structures in Istanbul against an anticipated Istanbul earthquake. This is very imporatant because, during the post-earthquake response and long-term recovery time, transportation structure (bridge, viaducts) functionality is of critical importance to increase disaster response capacity and the use of evacuation routes.

The results of the study also provide an important data to the decision makers of city to prioritise bridge retrofit strategies that are both cost-effective and efficient in their application.

At the end of the study, building collapse direction and bridge functionality results are assessed together. Finally, the road functionality in Istanbul against a potential Istanbul Earthquake are going to be revealed as GIS based.

3. LITERATURE

The accuracy of the earthquake damage estimations is based strictly on the quality of the data that were used for the analysis undertaken. Being that no institution or agencies in Turkey have the accurate dates of the constructions for the buildings in Istanbul, it is important to acquire the ages of every single building with an appropriate method of high accuracy, in order to increase the accuracy of the earthquake damage estimation.

The building age data is used to map the building's construction to an official structural code, while and this code is used for the fragility match to estimate the damage possibilities. The best method for the determination of the building ages for the use of damage estimation is to attain every single building in a structural code. That's why the most important reference is the official structural codes, if those buildings were constructed between the interval of separate codes. Based on this information, it would be easy to determine the compulsory structural codes at the time of the construction for every single building.

Detection of the buildings for an interval of time, based on the official structural codes in Turkey, only depends solely on the aerial images taken either from planes or from satellites. The building detection and extraction from the aerial images started in the 1980s. Huertas and Nevatia (1988) have described the technique by rectangular components and shadows of the buildings. In the 1990s the detection techniques evolved from 2D building edges to 3D building shapes as is seen in the research of Roux and McKeown (1994) and Lin and Nevatia (1998). With the development of image processing techniques and the increase in satellite image resolution after 2000, the accuracy of building detection started to increase in both detecting the building and detection of the edges (Fraser, Baltsavias, & Gruen, 2002; Lee, Shan, & Bethel, 2003; Sohn & Dowman, 2001) from approximately 64% to 74% (Sirmacek & Unsalan, 2009).

Following the 2010s, building detection accuracy increased through the addition of the airborne laser scanner data up to 85% (Matikainen, Hyyppä, Ahokas, Markelin, & Kaartinen, 2010) only with aerial and satellite images raised up to approximately 76% with probabilistic methods (Sirmacek & Unsalan, 2011) to approximately 80% with the merging of high resolution panchromatic and low resolution multispectral images (Aytekin, Erener, Ulusoy, & Düzgün, 2012) and approximately to 77% with multi-temporal marked point processes on remotely sensed image pairs (Benedek, Descombes, & Zerubia, 2012). The highest precision in building detection from aerial images was acquired recently by Ok, Senaras, and Yuksel (2013) with 85.7%, by Hron and Halounova (2015) with 82% in city centres and by Manno-Kovacs and Sziranyi (2015) with approximately 88% in several European cities.

The recent approach is to integrate laser scanner or lidar data to aerial images to increase the building detection accuracy up to 93% and 96% respectively, as presented by Awrangjeb (2015) and Niemeyer, Rottensteiner, and Soergel (2014).

Another area of usage of aerial photographs in building detection from, satellite images and ortho-photo mosaics is for the detection of the collapsed buildings. Gupta, Saraf, Saxena, and Chander (1994) and Saraf, Sinvhal, Sinvhal, Ghosh, and Sarma (2002) who have investigated buildings which collapsed during the Uttarkashi and Kutch earthquakes by using IRS remote sensing data. M Turker and San (2003); (2004), and Kaya, Curran, and Llewellyn (2005) have studied collapsed building detection by using respectively SPOT HRV, aerial-photographs, SPOT HRVIR XI, SPOT HRVIR Panchromatic and governmental statistics for the Kocaeli, Golcuk and Adapazari regions. The highest accuracy was provided by studies of aerial –photographs with 92.50% by M Turker and San (2004). The literature review of studies shows that aerial photographs and satellite images were used in lots of national and international publications in order to detect collapsed buildings. These achieved over an 80% success rate for detecting collapsed buildings at local sites.

However, the study aim is not the detection or change of current buildings or the collapse building detection following an earthquake. The main goal of this study is to determine the ages of the current building inventory of the city of Istanbul by the use of oldest aerial and satellite images in order to assign even the oldest non-historical building of an age attribute. This is why the use of laser or lidar data was not possible for this study.

Another important criterion was the differences in the size and the complexity of the study regions of previous studies. Most of the studies worked best in the regions where the complexity was low and the size or the number of buildings to be detected low, but when the size and complexity became larger most of the methods fail to reach their highest accuracy. When the studies of this region are taken into consideration in both complexity and the amount of buildings to be detected, we see that in the sample of a small area of Istanbul none of the methods provide the desired results. Hence, the manual building digitisation method chosen for the highest accuracy.

Building damage analysis is generally made with loss estimation tools, programs and software. The pioneer and the leader of these tools are HAZUS, which was developed by National Institute for Building Science (NIBS) and Federal Emergency Management Agency (FEMA) (Karaman, 2009). KOERILoss software was developed by the KOERI at Boğaziçi University. This tool gives the results as a grid system which can be applied to a minimum defined region BU-ARC (2002). SELENA (Seismic Loss Estimation using a logic tree Approach) is a software package, developed at NORSAR, for earthquake building damage assessment (Molina & Lindholm, 2005). ESCENARIS is the software tool developed for Catalonia from Spain. The losses are based on the building stock and classes of social impact (Strasser et al., 2008). SIGE, developed by Italian National Seismic service of the Civil Protection Department, is used for rapid approximate estimate of the damage (Di Pasquale et al., 2004). DBELA (Displacement-Based Loss Assessment) is an earthquake loss estimation tool currently being developed by ROSE School/EU-Centre in Pavia (Crowley, Pinho, & Bommer, 2004).

ELER (Earthquake Loss Estimation Routine) is a methodology and software for rapid estimation of earthquake damages and causalities throughout the Euro-Med Region (Erdik et al., 2008; IMM, 2009). MAEViz was developed in the Mid-America Earthquake Center in University of Illinois, integrating spatial information, data, and visual information to perform seismic risk assessment and analysis (Karaman, Şahin, & Elnashai, 2008). HAZTURK is the software that visualises the earthquake risk and its possible damage to structures and people, considering all the aspects of a seismic risk assessment process and offering options for decision makers in one tool (Elnashai et al., 2008). It is defined as the internationalization of the MAEviz system.

There have then been to apply the MAEviz system to several other countries or studies as Multi-Hazard Assessment, Response (mHARP) system and the system recently named and delivered as ERGO as a seismic risk assessment tool, based on Consequence-based Risk Management (CRM) (ERGO, 2015). The advantages and disadvantages of all those systems are compared by Karaman (2009) and it has been shown that the only building based loss assessment system was HAZTURK. For this reason, we have decided to use HAZTURK loss assessment software for damage analysis.

There is no published literature about building collapse direction because of earthquakes on a national and international scale. However, there are many articles determining the state of both existing and collapsed buildings during earthquakes by using aerial photographs and remote sensing images.

Fraser et al. (2002) have tried to define buildings by using IKONOS Satellite Image in their study (Fraser et al., 2002). Moreover, Sohn et al. have suggested methods to obtain buildings' polygons from the building corners analysis from IKONOS images in their study of 2001 (Sohn & Dowman, 2001). Lee et al. have also suggested a building classification method to obtain buildings from IKONOS images in their 2003 study.

Gupta et al. have studied collapsed buildings at Uttarkashi during the Uttarkashi Earthquake in their 1994 study. Remote Sensing data was used to determine changes caused by earthquakes in their studies (Gupta et al., 1994). Saraf et al. have used IRS satellite images in order to reveal collapsed building caused by the earthquake and the areas affected, due to liquefaction after the Kutch earthquake (Saraf et al., 2002). Turker et al. have used SPOT HRV images to detect earthquake-induced changes in the 1999 Kocaeli earthquake in 2003. They determine the collapsed buildings by using satellite images. However, vertically collapsed buildings were not detected because their roofs had no damage (M Turker & San, 2003). In another study by Turker et al. post-earthquake aerial photographs were digitally processed and analysed to detect collapsed buildings in the Gölcük area caused by the 1999 Kocaeli in their 2004 study. This analysis relies on the idea that if a building has collapsed then it will not have corresponding shadows. In this study, of the 80 collapsed buildings, 74 were detected correctly, providing 92.5% accuracy (M Turker & San, 2004).

Furthermore, Kaya et al. used three different data sources to estimate the proportion of Adapazarı that contained collapsed buildings in their study of 2005. One of them is SPOT HRVIR XI image, the other one is SPOT HRVIR Panchromatic image, while the last one is government statistics (Kaya et al., 2005). In 2008, Turker et al. used aerial photographs to detect the damage buildings due to earthquakes using watershed segmentation in their study. Of the 284 buildings processed and analysed, 229 were correctly labeled as damaged and undamaged, providing an overall accuracy of 80.63% (Mustafa Turker & Sumer, 2008).

The literature reviews show that aerial photos and satellite images were used by many national and international publications in order to detect collapsed buildings. These images have obtained a rate of over 80% success for detecting collapsed building at local base. However, they provide no information to detect building collapsed direction. Hence, the building collapse directions have been revealed by using manual digitisation, analysis and process on ArcGIS.

Basoz and Kiremidjian (1996) have developed a risk assessment methodology for highway transportation system used against to earthquake hazard. With this system, the methodology is based on vulnerability. Moreover, many case studies were made for Palo Alto and Northridge, California areas using this method (Başöz & Kiremidjian, 1996).

Werner, Taylor, Moore, and Walton (1999) have considered transportation network systems subjected to earthquake events. In this study, the risk to the transportation system is calculated from the direct damage.

Werner and Taylor (2000) have described the risk-based methodology in their paper. This methodology estimates how earthquake damage to highway systems can affect post-earthquake traffic flows and travel times.

In a JICA and IMM (2002) study, information about 480 bridges was collected while the vulnerability of bridges was analysed statistically based on Katayama's methodology. As a result of the analysis, 24 bridges were calculated as having a higher possibility of collapse, while two bridges constructed as viaduct structures were calculated as having a higher vulnerability to a Model C earthquake (JICA & IMM, 2002).

Werner et al. (2004) have developed a seismic risk analysis (SRA) of highway system. This methodology consists of earthquakes scenarios and analysis of, seismic hazards, bridge fragility, and transportation network. This system has been applied to the Shelby County, Tennessee highway system in USA. In this paper, it was mentioned that this system is now being programmed into a publicdomain software package named REDARS 2 (Werner et al., 2004)

Kiremidjian et al (2002) has also presented seismic risk assessment methodologies for transportation structures (Kiremidjian et al., 2002).

Karim and Yamazaki (2003) have also presented an analytical approach that was adopted to develop the fragility curves for highway bridges based on numerical simulation (Karim & Yamazaki, 2003). Meanwhile, Nielson (2005) has presented to use analytical methods to generate fragility curves for nine bridges classes in his PhD thesis (Nielson, 2005). Meanwhile;

Padgett and DesRoches (2007) have aimed to reveal the need for data to relate the effects of bridge component damage to the functionality of bridge, expressed as allowable traffic carrying capacity in their study (Padgett & DesRoches, 2007).

Nielson and DesRoches (2007a) have developed seismic fragility curves for nine classes of bridges common to the central and southeastern United States in their study (Nielson & DesRoches, 2007a).

Nielson and DesRoches (2007b) have presented a metholodology about the generation of analytical fragility curves for highway bridges (Nielson & DesRoches, 2007b). Meanwhile;

Reginald DesRoches, Padgett, and Nilsson (2008) have presented seismic risk assessment of transportation in network in Charleston at South California. In this study, approximately 375 bridges were studied. As a result of this study, the distribution of potential bridge damage and functionality for several scenarios have been shared (Reginald DesRoches et al., 2008).

Nilsson (2008) has presented an evaluation of the performance of the transportation infrastructure in Charleston, SC against earthquakes with a focus on bridge and network performance (Nilsson, 2008)

Apaydın (2010) has presented the performance Istanbul's of two suspension bridges (the Bosporus and Fatih Sultan Mehmet Bridges) in relation to earthquakes and their retrofit investigations (Apaydın, 2010).

Dönmez, Cilingir, and Özer (2014) have explained that the required structural repair and seismic retrofit measure of Istanbul Yeşilköy Demiryolu Caddesi Overpass Bridge in their study (Dönmez et al., 2014). Furthermore,

Namlı, Yıldız, Erinçer, and Özer (2014) have presented the evaluation and retrofit work implemented on Uskudar Haydarpaşa Overpass Bridge in their study (Namlı et al., 2014). Finally, in her study,

Apaydin (2014) has presented the seismic retrofit and structural strengthening campaign for large scale bridges in Istanbul (Apaydin, 2014).

4. BUILDING AND BRIDGE DATA ACQUISITION FOR ISTANBUL AND GÖLCÜK

The reliability of the earthquake loss assessment analysis results depends strictly on the input data. Using recent, enough and correct data improves the accuracy of the estimation results (Crowley, Bommer, Pinho, & Bird, 2005). During the study process, two basic vector data were used for analysis. One of them is building data and the other one is bridge data. The raw building data was obtained from IMM and the bridge data was obtained from General Directorate of Highways – 17th. As it is explained herebelow section these data were classified according to HAZTURK data type for being suitable for analysis. Except from the vector data sets, a series of raster data were also used in order to determine the ages of the buildings in Istanbul. To determine the ages of buildings, aerial photos taken between 1966 – 1982, ortho photo mosaic of 1996 and 2013 were obtained from Istanbul Metropolitan Municipality and the satellite images of 2004 and 2007 were obtained from Istanbul Technical University. Another set of air photos of 1994 and 1999 for Gölcük district of Kocaeli were also obtained from General Command of Mapping (HGK) to determine the building collapse direction method.

4.1 Create Update Building Dataset in Istanbul

4.1.1 Building inventory as vector data in Istanbul

Building data is one of our basic data for this study. The building data of this study is acquired from the IMM in 2011 which was created by the Address-based Census Registration System (ADNKS) and the data was updated in 2013. The updated ADNKS data show that, the number of structures in Istanbul is 1,439,981 and this data was used as the building data for Istanbul earthquake loss assessment studies after 2013.

Regarding to Turkish Zoning Law 3194 (1985); the term structure means any fixed or mobile facilities including constructions on land or in water, temporary or permanent,

public or private, under or over the ground, and additions, modifications and repairs thereof. On contrary, the term building means any covered, individually usable structure which can be entered into and is used for people to live in work, entertain and rest or worship, or used to keep animals and things. According to the definitions given above, structures that do not match the building definition were also deleted from the Istanbul Structure Data (Table 4.1).

Table 4.1 : Deleted structure data in building dataset.

Name of the Deleted Structure Type						
Volleyball court	Swimming pool	Camping Site	GSM antenna	Historic fountain	Basketball court	Train station
Park – Free space	Children park	Minibuses stop	Subway stop	Ancient monument	Metro bus stop	Barn – Coop
Picnic area	Telephone box	Historic walls	Force main	Historic pillar	Heliport	Water tank
Astroturf	Fun Fair	Cesspit	Forest	Toilet	Tunnel	Pool
Racecourse	Junction	Hayloft	Porch	Shrine	Cable car	Shed
Tram stop	Beach	Greenhouse	Buffet	Cemetery	Harbor	Altar
Transformer	Junkyard	Camellia	Towers	Water pump	Marina	Box office
Trailer truck park	Coalbunker	Field	Boiler room	Tee house	Cistern	Tea garden
Stadium	Pier	Zoo	Attic	Security	Land	Atm

Up to now all of the building damage estimations for Istanbul used that structure data instead of the building data. This study used the building data generated from the structure data of ADNKS. Thus, the number of buildings in Istanbul determined as 990,584 for the year of 2013. This data set consists of location, construction type, number of floors and building usage. These data was also used to determine the building age as a 2013 data (Figure 4.1).

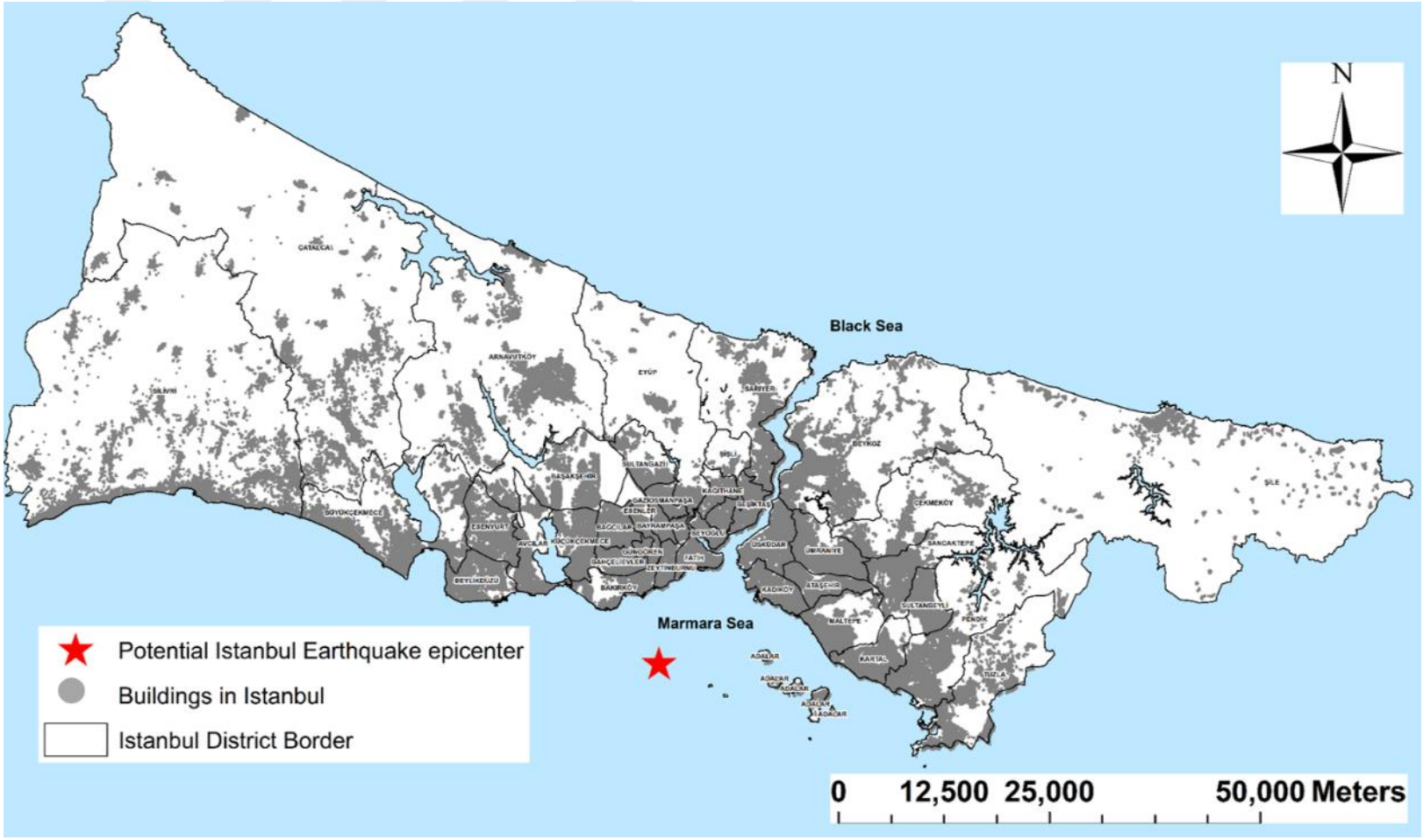


Figure 4.1 : Buildings distribution in Istanbul.

An important parameter to estimate the damages of a building after an earthquake is the age of it. Most of the studies on building damage estimation for Istanbul was also conducted without the knowledge of the real ages of each single building. Determination of building age for every single building in Istanbul were revealed next chapter.

This database field names were reclassified in order to be suiatable for damage analysis with HAZTURK. When the buildings in Istanbul were examined with regard to usage types, more than 80% of the buildings are used as residential buildings (Figure 4.2).

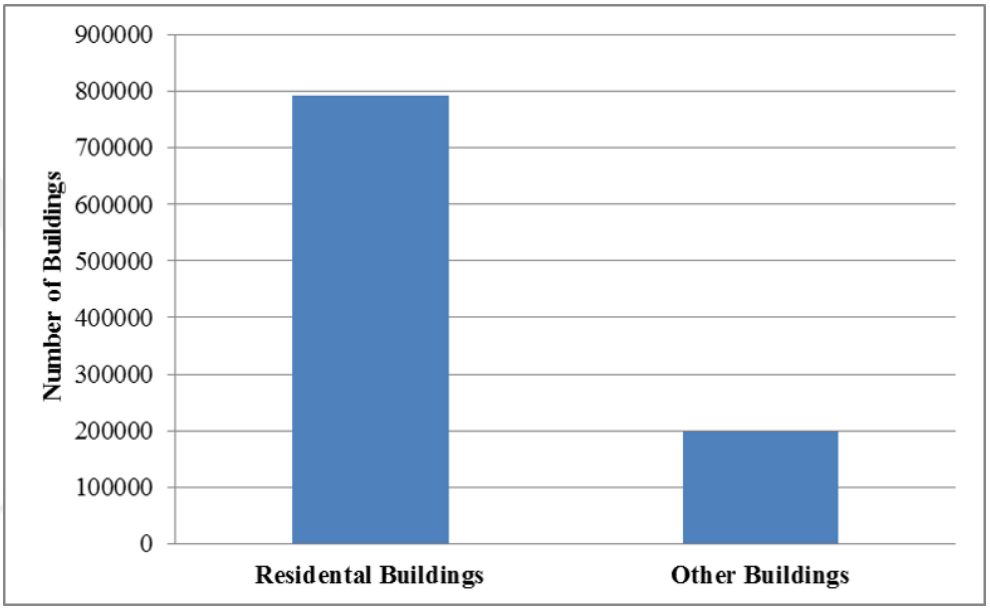


Figure 4.2 : Building occupancy classes in Istanbul.

Except residential buildings in Istanbul were reclassified regarding to its usage according to the Building Occupancy Class at HAZUS (Table 4.2) (FEMA, 2003).

Table 4.2 : Building occupancy classes at HAZUS (FEMA 2003).

Label	***Occupancy Class***		***Example Descriptions***
RES1	Residential	Single Family Dwelling	House
RES2		Mobile Home	Mobile Home
RES3		Multi Family Dwelling	Apartment
RES4		Temporary Lodging	Hotel / Motel
RES5		Institutional Dormitory	Group Housing, Jails
RES6		Nursing Home	
COM1	Commercial	Retail Trade	Store
COM2		Wholesale Trade	Warehouse
COM3		Personal and Repair Services	Service Station / Shop
COM4		Professional / Technical Services	Offices
COM5		Banks	
COM6		Hospital	
COM7		Medical Office / Clinic	
COM8		Entertainment & Recreation	Restaurants / Bars
COM9		Theaters	Theaters
COM10		Parking	Garages
IND1	Industrial	Heavy	Factory
IND2		Light	Factory
IND3		Food / Drugs / Chemicals	Factory
IND4		Metals / Mineral Processing	Factory
IND5		High Technology	Factory
IND6		Construction	Office
AGR1	Agriculture	Agriculture	
REL1	Religion	Church / Mosque	
GOV1	Government	General Services	Office
GOV2		Emergency Response	Police / Fire Station
EDU1	Education	Grade Schools	
EDU2		Colleges / Universities	

Regardings this occupancy classification, the number of buildings regarding to their occupancy is given at Table 4.3. According to this table, approximately 1500 buildings occupied for health facilities and 5000 buildings for education in Istanbul.

Table 4.3 : Occupancy class distribution of buildings in Istanbul w/o Residential (FEMA, 2003).

Label	***Occupancy Class***	***Building Number***
COM1	Retail Trade	136167
COM2	Wholesale Trade	4863
COM3	Personal / Repair Services	1381
COM4	Professional / Technical Services	21736
COM5	Banks	543
COM6	Hospital	721
COM7	Medical Office / Clinic	825
COM8	Entertainment & Recreation	2825
COM9	Theaters, Cinema etc.	798
EDU1	Grade Schools	3115
EDU2	Colleges / Universities	1783
GOV1	General Services	2788
GOV2	Emergency Response	229
IND1	Heavy Industrial	1259
IND2	Light Industrial	6796
IND3	Foods / Drugs / Chemicals	597
IND4	Metals /Mineral Processing	1770
IND5	High Technology	211
IND6	Construction	489
REL1	Mosque, church etc	2176
RES4	Temporary Lodging (Hotel etc)	1235
RES5	Institutional Dormitory	1869
RES6	Nursing Home	112

The building data has also been reclassified according to whether it is a critical facility or not. It is accepted that educational facilities, health facilities, fire stations, police stations and emergency operation centers are critical facilities (Table 4.4). In this table the buildings were classified as False except medical care facilities, buildings using for emergency response and schools based on FEMA (2003) Technical Manual.

Table 4.4 : Critical facilities classificaiton (FEMA 2003).

Label	*Occupancy Class*		*Description*
EFHS	Medical Care Facilities	Small Hospital	Hospital with less than 50 Beds
EFHM		Medium Hospital	Hospital with beds between 50 & 150
EFHL		Large Hospital	Hospital with greater than 150 Beds
EFMC		Medical Clinics	
EFFS	Emergency Response	Fire Station	
EFPS		Police Station	
EFEO		Emergency Operation Center	
EFS1	Schools	Grade Schools	Primary / High Schools
EFS2		Colleges / Universities	
FALSE			

One of the necessary data for building is the construction type of buildings. The construction types of buildings were classified according to the HAZUS Handbook (Table 4.5). Regarding to this table, the most common construction type of Istanbul buildings is Concrete Frame with Unreinforced Masonry Infill Walls (C3).

Table 4.5 : Structure type classification (FEMA 2003).

Construction Type	*Construction Code*	*Explanation*	*Building #*
Wooden	W1	House	3410
	W2	Commercial, Industry	429
Reinforced Concrete		C1	205233
Tunnel Form		C2	117298
Concrete Frame with Unreinforced Masonry Infill Walls		C3	618457
Prefabricate	PC1	Constructed before 2007	305
	PC2	Constructed after 2007	836
Steel Construction	S1	Commercial building Number of floor 1 - 4	31
	S3	Commercial building Number of floor > 4	358
Reinforced Masonry Bearing Walls with Wood or Metal Deck	RM1	Number of floor < 4	10298
Reinforced Masonry Bearing Walls with Precast Concrete	RM2	Number of floor ≥ 4	1252
Unreinforced Masonry	URM		32679

Buildings construction type were reclassified according to number of floor in order to determine STR_TYPE2 class, which is a category of HAZUS structural type (FEMA, 2003) (Table 4.6).

Table 4.6 : HAZUS building structural type (FEMA 2003).

Description	*Label*	*Height*	*Stories*
Wood, Light Frame	W1		1 – 2
Wood, Commercial and Industrial	W2		All
Steel Moment Frame	S1L	Low-Rise	1 – 3
	S1M	Mid-Rise	4 – 7
	S1H	High-Rise	8 +
Steel Braced Frame	S2L	Low-Rise	1 – 3
	S2M	Mid-Rise	4 – 7
	S2H	High-Rise	8 +
Steel Light Frame	S3		All
Steel Frame with Cast-in-Place Concrete Shear Walls	S4L	Low-Rise	1 – 3
	S4M	Mid-Rise	4 – 7
	S4H	High-Rise	8 +
Steel Frame with Unreinforced Masonry Infill Walls	S5L	Low-Rise	1 – 3
	S5M	Mid-Rise	4 – 7
	S5H	High-Rise	8 +
Concrete Moment Frame	C1L	Low-Rise	1 – 3
	C1M	Mid-Rise	4 – 7
	C1H	High-Rise	8 +
Concrete Shear Walls	C2L	Low-Rise	1 – 3
	C2M	Mid-Rise	4 – 7
	C2H	High-Rise	8 +
Concrete Frame with Unreinforced Masonry Infill Walls	C3L	Low-Rise	1 – 3
	C3M	Mid-Rise	4 – 7
	C3H	High-Rise	8 +
Precast Concrete Tilt-Up Walls	PC1		All
Precast Concrete Frames with Concrete Shear Walls	PC2L	Low-Rise	1 – 3
	PC2M	Mid-Rise	4 – 7
	PC2H	High-Rise	8 +
Reinforced Masonry Bearing Walls with Wood or Metal Deck	RM1L	Low-Rise	1 – 3
	RM1M	Mid-Rise	8 +
Reinforced Masonry Bearing Walls with Precast Concrete	RM2L	Low-Rise	1 – 3
	RM2M	Mid-Rise	4 – 7
	RM2H	High-Rise	8 +
Unreinforced Masonry Bearing Walls	URML	Low-Rise	1 – 3
	URMM	Mid-Rise	4 – 7
Mobile Homes	MH		All

The buildings data can be operationalized to use HAZTURK with this classification.

4.1.2 Remote sensing data for the building age determination

To determine the ages of buildings in Istanbul, aerial photos of 1966 – 1982, ortho photo mosaic of 1996 and 2013 were obtained from Istanbul Metropolitan Municipality and the satellite images of 2004 and 2007 were obtained from Istanbul Technical University.

1966 air photo covers only 415km^2 of Istanbul. 1983 air photo covers only 3200 km^2 of Istanbul. Other ortophoto mosaics and satellite images cover all Istanbul.

4.2 Building Dataset Generation for Gölcük

Witihin the context of study, the buildings in Gölcük that were constructed before and after 1999 Kocaeli Earthquake were not obtained from anywhere at GIS based. First of all, SPOT HRVIR Images data dated June 25, 1999 and October 4, 1999 obtained from Istanbul Technical University were used to determine existing and collapsed building in Gölcük during the 1999 Kocaeli Earthquake. However, it was seen that the resolution of images was not enough for a building based analysis. For this reason, satellite images were not used for this analysis.

In order to determine the collapsed buildings during the earthquake in Gölcük, both the 1999 aerial image with ED50TM30 coordinate system taken on September 1999 and 1994 the aerial image with no coordinate were obtained from General Command of Mapping (HGK). The reason of choosen 1994 and 1999 years is that the necessary of determination of the existing buildings in Gölcük before the earthquakes. For this reason, not only the aerial image taken after the 1999 earthquake but also the aerial image taken before the 1999 earthquake are necessary for this study.

In order to use both aerial photos in the same analysis, they must have the same coordinate system. Because of this reason, the1994 aerial photo must be transported to the same spatial with 1999 aerial photo by using “Spatial Adjustment” on ArcGIS. For this, 32 points as control points were determined between the 1994 and 1999 aerial photos then the 1994 aerial photo was carried with the same spatial as the 1999 aerial photo by using Georeferencing Tool on ArcGIS. Georeferencing is the process of scaling, rotating, translating and deskewing the image to match a particular size and position. The 1994 aerial photo was moved to where it should be based on 32 control points with a georeferencing tool. Thus, these two aerial photos are made ready for necessary analysis.

4.3 Bridge Dataset Generation in Istanbul

The last raw data acquired for this study was the for the transportation structures (bridges, overpass, underpass, viaducts) in Istanbul. The bridge data (including their location, construction year, girder type, bearing type, height of abutment, structure) were obtained from the General Directorate of Highways – 17 th Division by Excel format and all were transferred to GIS. The number of transportation structure are 247 and the distribution of bridge according to districts is given herebelow Table 4.7.

Table 4.7 : Number of bridge distribution at districts based in Istanbul.

Districts	Quantity	Districts	Quantity
Istanbul Bosphorus	2	Gaziosmanpaşa	1
Çekmeköy	3	Güngören	1
Arnavutköy	2	Kağıthane	14
Ataşehir	9	Kadiköy	7
Avcılar	3	Küçükçekmece	3
Başakşehir	9	Pendik	0
Bağcılar	8	Silivri	27
Bahçelievler	3	Sancaktepe	2
Bakırköy	3	Sarıyer	3
Bayrampaşa	10	Şile	2
Beşiktaş	11	Şişli	15
Beykoz	6	Sultanbeyli	2
Beyoğlu	4	Sultangazi	3
Büyükçekmece	14	Tuzla	2
Çatalca	1	Ümraniye	24
Esenler	11	Üsküdar	11
Esenyurt	10	Zeytinburnu	6
Eyüp	15		

Category of 247 transportation structures (overpass, underpass, bridge, suspension bridge, tunnel and viaducts) is given Table 4.8.

Table 4.8 : Number of bridge category in Istanbul.

Transportation Structure	Number
Underpass	88
Overpass	125
Bridge	8
Suspension Bridge	2
Tunnel	1
Viaduct	23

Every single transportation structure that were listed in Table 4.8 had the attributes in Table 4.9.

Table 4.9 : Sample of bridge inventory card.

Bridge Inventory Card (Basic Information)	
Bridge name or number	K-305 Overpass Bridge
Province	Istanbul
Carried road name	Mecidiyeköy –Levent
Construction date	1974
Km	(0+232,299 - 0+394,567);1+076 (B.C.)
Span (m)	(26,50+33,20+2X35,40+28,30)
Length (m)	158,80
Width (m)	(1,25+8,00+3,25)=12,50 m
Skew angle	0º
Construction type	Post-tensioned-prestressed beton-box girder
Structure statics	Continuous beam
Abutment (middle)	Ø 150 Cm. Circular reinforced concretete column
Abutment	Concrete wall
Foundation system	Planar concrete foundation

This database field names were reclassified in order to match the required classifications for the damage analysis of HAZTURK software. The transportation structures were classified with the methodology used by Nielson (2005) (Table 4.10). And bridge classification distribution in Istanbul is given at Figure 4.2.

Transportation data must include these fields that were given at Table 4.10 in order to make damage analysis with HAZTURK software.

Table 4.10 : HAZTURK attributes of bridge.

Field Name	Field Description	Field Type
id	Bridge identifier	Integer
class	Bridge classification	String
spans	Number of bridge spans	String
str_lng	Structure length	String
dckwidth	Deck width out to out	String

Every bridge has been classified according to Bridge classification given in Table 4.11 by using their attributes. This classifications describes the bridges according to their span configuration – simply supported (SS), multi-span simply supported (MSSS), multi-span continuous (MSC) – and their girder material type – concrete or steel. The distribution of bridge classification in Istanbul is given in Figure 4.3.

Table 4.11 : Bridge classification mapping to NBI Terminology (Nilsson, 2008).

Name	Abbreviation	Material	Type	Spans
Multi-Span Continuous Concrete Girderı	MSC Concrete	Concrete Continuous Prestressed Concrete Continuous	Stringer Tee-Beam Floor Girder Channel Beam	>1
Multi-Span Continuous Steel Girder	MSC Steel	Continuous Steel	Stringer Tee-Beam Floor Girder Channel Beam	>1
Multi-Span Continuous Slab	MSC Slab	Concrete Continuous Prestressed Concrete Continuous	Slab	>1
Multi- Span Simply Supported Concrete Girder	MSSS Concrete	Concrete Continuous Prestressed Concrete Continuous	Stringer Tee-Beam Floor Girder Channel Beam	>1
Multi- Span Simply Supported Steel Girder	MSSS Steel	Steel	Stringer Tee-Beam Floor Girder Channel Beam	>1
Multi-Span Simply Supprted Slab	MSSS Slab	Concrete Prestressed Concrete	Slab	>1
Multi-Span Simply Supprted Concrete Box Girder	MSSS Concrete-Box	Concrete Prestressed Concrete	Box Beam - Multiple	>1
Single – Span Concrete Girder	SS_Concrete	Concrete Prestressed Concrete Concrete Continuous Presteressed Concrete Continuous	Stringer Tee-Beam Floor Girder Channel Beam Slab Box-Beam - Multiple	<2
Single – Span Steel Girder	SS Steel	Steel Steel Continuous	Stringer Tee-Beam Floor Girder Channel Beam Slab Box-Beam - Multiple	<2

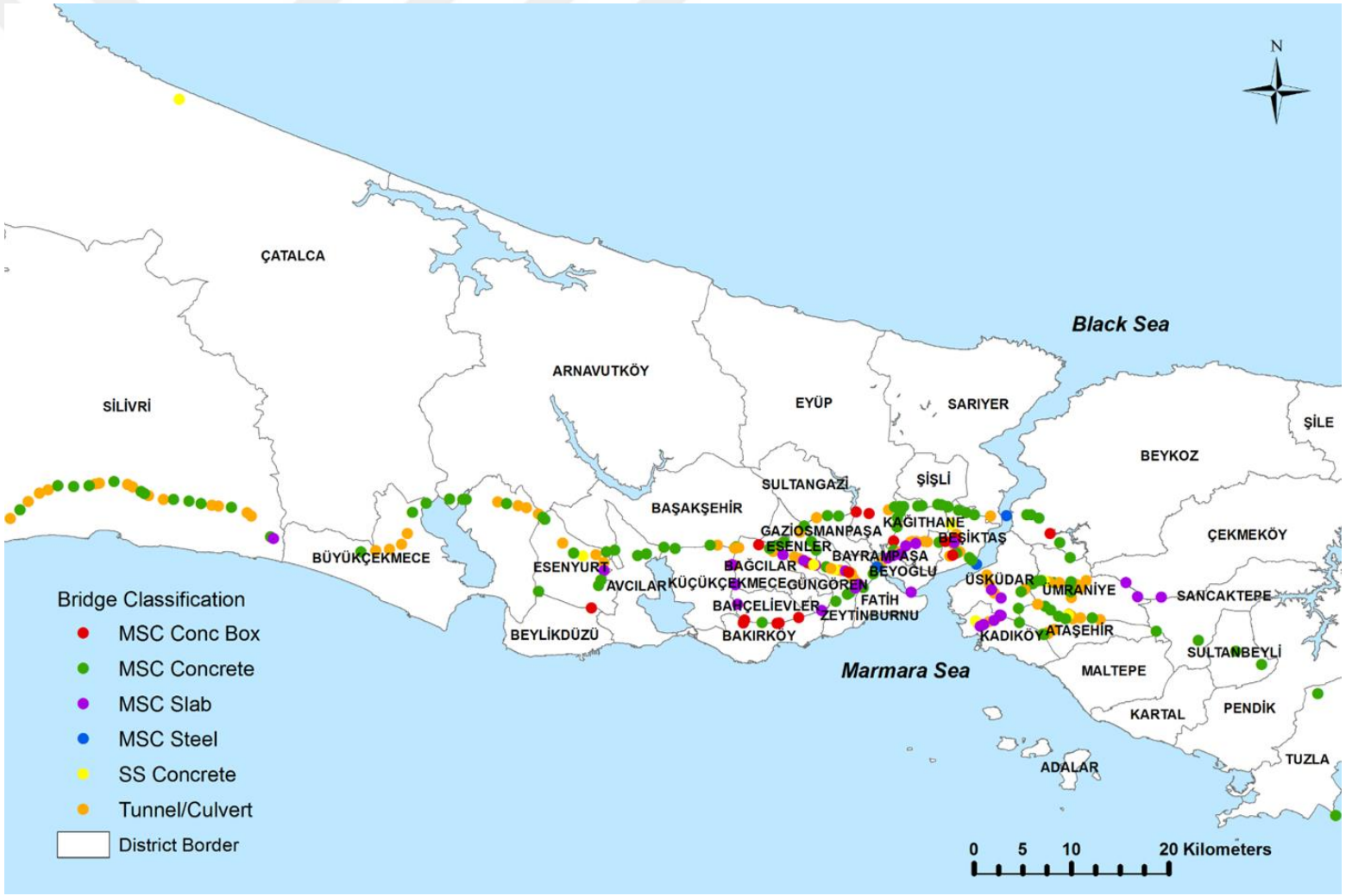


Figure 4.3 : Distribution of bridge classification in Istanbul .

After preparing related data for the analysis in order to reveal road functionality in Istanbul following in Istanbul potential Earthquake, the next step is to describe to methodology using in this study.

5. DETERMINATION OF BUILDING AGE

5.1 Building Age Determination Methodology

In this section, methodology of determination building age was revealed for every single building in Istanbul.

In order to determine buildings automatically from aerial photos, ortho photo mosaics and satellite images, remote sensing and photogrammetric software were examined firstly; however, desired outcome could not be obtained. The reason for the failure was those methods and software perform best with a standardized colors and shapes of roofs, area and distribution of buildings. However, the buildings in Istanbul are far from meeting the construction standards in both shape, size and colors. In addition, most of the buildings in Istanbul are attached buildings, and some buildings do not have a roof or there are some gaps in the central parts of building roofs. Another disadvantage of the study area was the complex distribution of the buildings with respect to aforementioned methods (Figure 5.1). For this reason, it is decided to produce buildings from aerial photos, ortho photo mosaics and satellite images by digitisation on ArcGIS.



Figure 5.1 : Building samples from Fatih District of Istanbul.

Another important reason for the selection of digitizing the buildings manually was, the highest accuracy methods including the airborne laser or lidar techniques with the addition of digital elevation models of the study area (Awrangjeb, 2015; Matikainen et al., 2010; Niemeyer et al., 2014).

In this part of the study, it is interested on the determination of the building ages of the old buildings where the recent technologies were not existed. For example, in order to determine the age of the buildings that were constructed between 1966 and 1982, the only available data was aerial photographs of 1966 flights'. The available data for this study were; 1966 and 1982 aerial images, 1996 and 2013 ortho-photo mosaics, 2004 and 2007 satellite images and all of them purchased from IMM with the funding. The available were used in combination with effective date of structural codes at the time of building's existence. Structural codes that came into force in Turkey and the buildings age classification that were made according to effective date of code are given at Table 5.1. This classification constructed the basis of this study section.

Table 5.1 : Building code and building age classification.

Building Code Name	*Building Code Year*	*Code Level*	*Building Age Classification*	*Data Source*
Italian Structure Regulations	1940	1	Pre 1969	1966 Air Photo
Temporal Structure Code for the Earthquake Zone Constructions	1944			
Structure Regulation for Turkey Earthquake Zones	1949			
Regulation for the Structures that are going to be Constructed within the Earthquake Zones	1953			
Specification for Buildings to be Built in Seismic Zones	1962			
Specification for Buildings to be Built in Seismic Zones	1968			
Specification for Buildings to be Built in Seismic Zones	1975	2	1969 - 1982	1982 Air Photo
Specification for Buildings to be Built in Seismic Zones	1997	3	1983 - 1996	1996 Ortho Photo Mosaic
			1997 – 2004	2004 Satellite Image
Specification for Buildings to be Built in Seismic Zones	2007	4	2005 – 2007	2007 Satellite Image
			2008 - 2013	2013 Ortho Photo Mosaic

It is also important to decide the datum and coordinate system of the input and outputs of a GIS based study. World Geodetic System 1984 (WGS84) Geographic Coordinate System (gcs) was chosen as datum and coordinate system for the data set, since, it is currently a commonly used system for many mobile practices as navigation, GPS measurements in disaster management.

First step of the methodology was to transform the input data into WGS84 gcs, then the buildings of the aerial or satellite images for the beginning and ending years of the assigned code levels were digitized manually, so as not to let errors on automatic building detection and detection of structures that seems like but not buildings. If the digitized building at the ending year of the code level is existing at the digitisation of the beginning year of the code level, it means that, that building was constructed before the respective code level, if not it means that, the building has to be constructed based on the respective structural code of the code level. First step of the manual digitisation process was to create a database on ArcCatalog. Shape file format was chosen as the

data format and data type was selected as point. The first digitized aerial or satellite image year was named as D01 (Figure 5.2).



Figure 5.2 : Digitized buildings in Sarıyer district by using 1966 Aerial image.

Then the ending years' image has been digitized based on the previous steps and named as D02. Following the digitisation of two end of an assigned code level, the D02 was used as a base map to compare the beginning and the ending years' images building data. D01 and D02 building data were compared using the spatial join tool to bind two different version of same data according to spatial characteristics on ArcMap software (Figure 5.3).

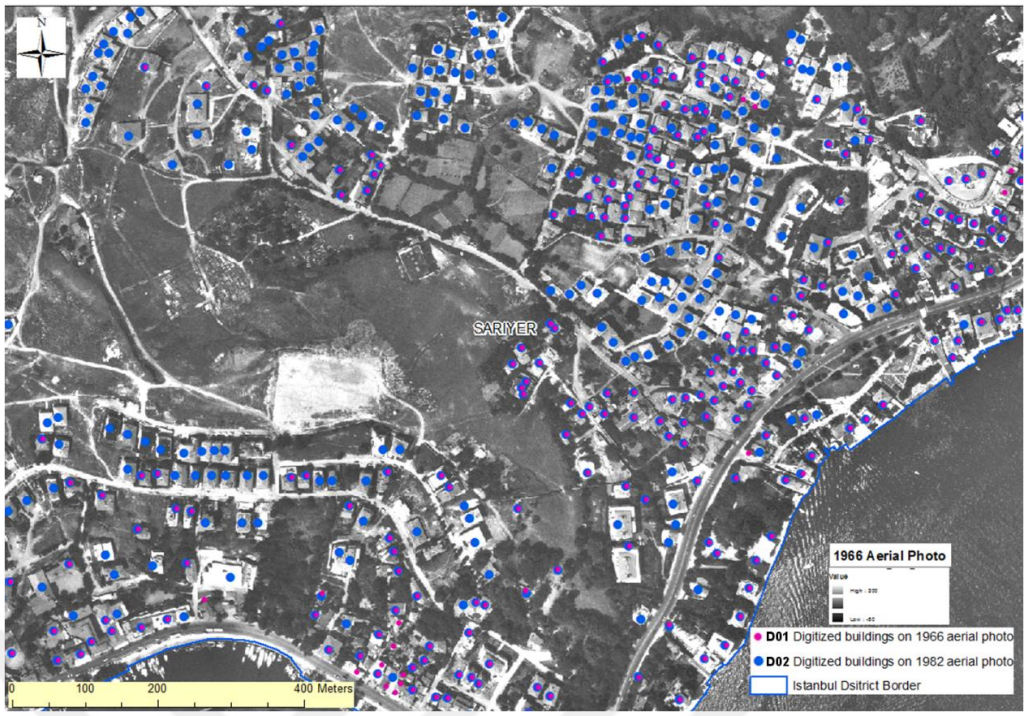


Figure 5.3 : Digitized buildings in Sarıyer district by using 1982 Aerial Image.

After the spatial join, 1 was assigned to spatially overlapping buildings and 0 was assigned to spatially non overlapping buildings, where 1 defines buildings that were constructed before the beginning year and 0 defines the buildings that were constructed after the beginning year. Same process followed starting from aerial images of 1966 to 1982, aerial image of 1982 to ortho-photo mosaic of 1996, ortho-photo mosaic of 1996 to satellite image of 2004, satellite images of 2004 to 2007, and satellite images of 2007 to ortho-photo mosaic of 2013 respectively. Except the others only for ortho-photo mosaic of 2013 building data were not produced by digitisation. The buildings data obtained from IMM is accepted as 2013 building data. By this way, every single structure in Istanbul has been assigned a construction year interval based on the official structural codes that were came into force in Turkish Republic.

5.2 Building Age Analysis and Results

5.2.1 Production of 1968 and pre 1968 building data (Code Level 1)

1966 Aerial Photograph covers Fatih, Kadıköy, Üsküdar, Beşiktaş, Şişli, Sarıyer, Zeytinburnu districts and some parts of the Bakırköy, Güngören, Bayrampaşa, Gaziosmanpaşa, Eyüp, Kağıthane, Beykoz ve Ataşehir districts (Figure 5.4). By digitisation of the 1966 aerial image, the total number buildings within the 415 km2 urban area determined as 98239 and assumed as built prior to 1968.

In order to increase the accuracy of building data that were constructed before 1968, buildings in Küçükçekmce districts that were construted before 1968 obtained from the IMM project of The Urban Transformation Project in Küçükçekmece (KDMP) were added this buildings dataset. 417 buildings from Küçükçekmece were integrated this database. After this process there are 98656 buildings in Istanbul that were constructed before 1968.

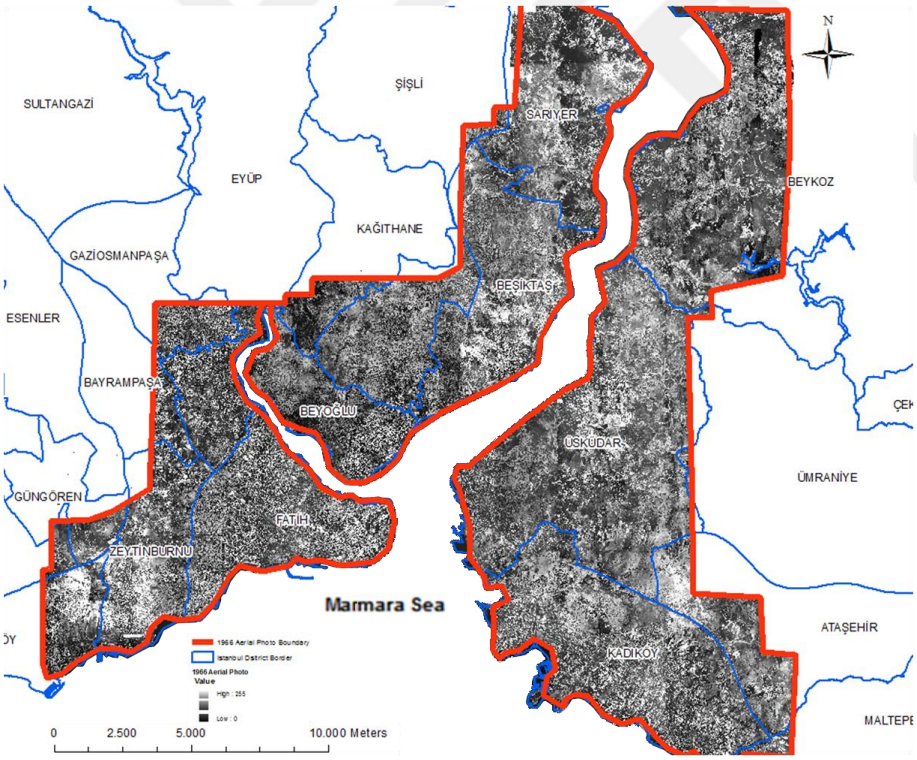


Figure 5.4 : 1966 aerial image of Istanbul.

5.2.2 Production of building data between 1969 and 1982 (Code Level 2)

1982 Aerial image was digitized to determine the buildings constructed between 1969 and 1982. The 3200 km2 urban area of the Istanbul for the year of 1982 contains all the current districts except for the Şile, Arnavutköy, Çatalca, Silivri, Büyükçekmece ve Beylikdüzü districts (Figure 5.5). According to the digitisation results, the total number buildings within the study area was determined as 432150. However, this number contains the buildings constructed before 1968. Following the spatial join method described in section 5.1, the number of buildings that were constructed between 1969 and 1982 has been determined as 333494.

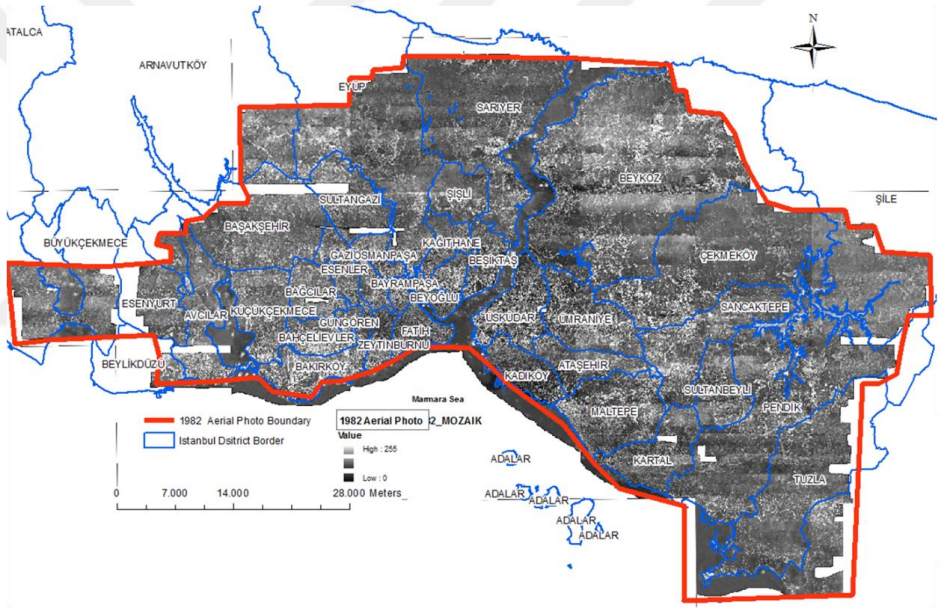


Figure 5.5 : 1982 aerial image of Istanbul.

5.2.3 Production of building data between 1983 and 1996 (Code Level 3)

In order to detect the buildings that were constructed between 1983 and 1996, 2 m resolution 1996 ortho-photo mosaic which covers the whole Istanbul area was digitized (Figure 5.6). The total number of structures that were detected from 1996 ortho-photo was 839288. After the elimination of the previously constructed structures by using the spatial join analysis, the number of buildings that were constructed between 1983 and 1996 determined as 407138.



Figure 5.6 : 1996, Ortho-Photo mosaic of Istanbul.

5.2.4 Production of building data between 1997 and 2004 (Code Level 3)

To detect the structures that were constructed before 2004, the buildings that were constructed between 1997 and 2004 were identified by using a 2004 satellite image from IKONOS with 1 m resolution (Figure 5.7). Total number of 196259 buildings were detected after the digitisation of 2004 IKONOS satellite image. Following the spatial join process of digitized 1996 orto-photo structure data 114480 structures that were built between 1997 and 2004 are determined.

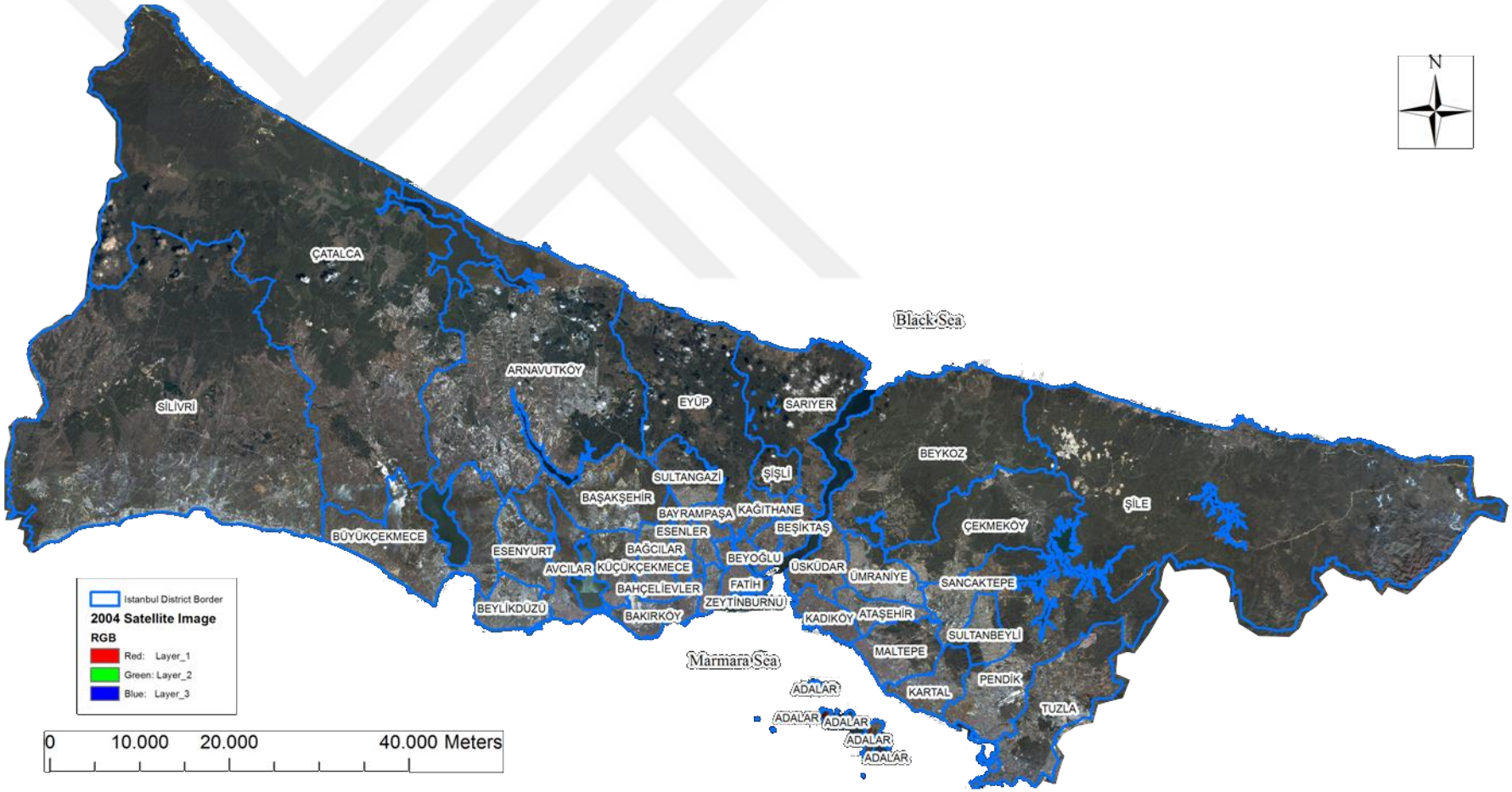


Figure 5.7 : 2004, 1m resolution IKONOS satellite image of Istanbul.

5.2.5 Production of building data between 2005 and 2007 (Code Level 4)

The structures that were built between 2005 and 2007 were detected by the use of 1 m resolution 2007 IKONOS Satellite Image (Figure 5.8). The digitisation and spatial join processes detected total number of 46336 structures that were constructed between 2005 and 2007.

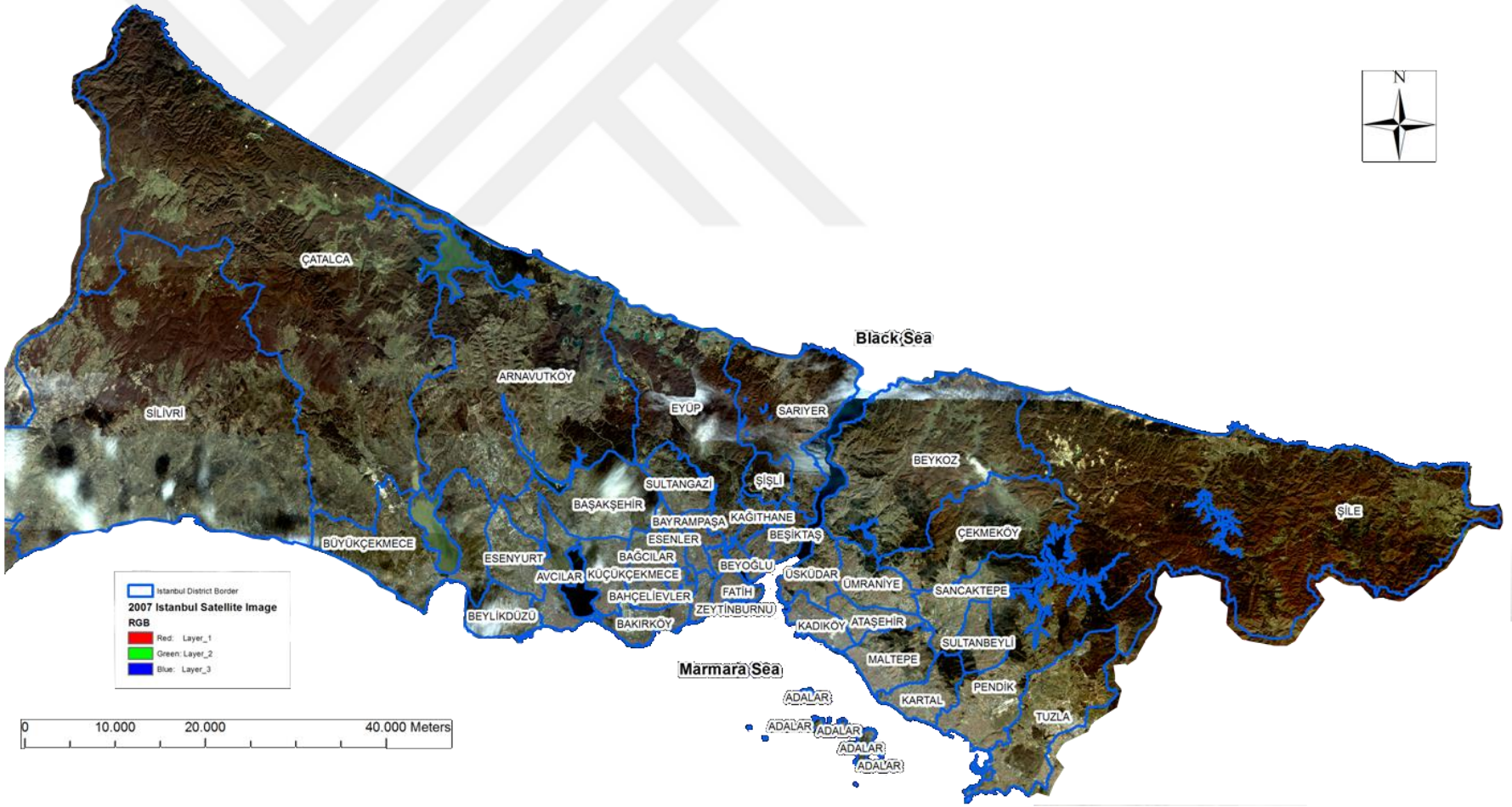


Figure 5.8 : 2007, 1m resolution IKONOS satellite image of Istanbul.

5.2.6 Production of building data between 2008 and 2013 (Code Level 4)

The detection of the structures that were constructed between the year of 2008 and 2013 constituted by digitizing the ortho-photo mosaic of 2013 (Figure 5.9) with cm resolution. 35443 structures were detected by spatially joining the digitized 2007 satellite image structures.

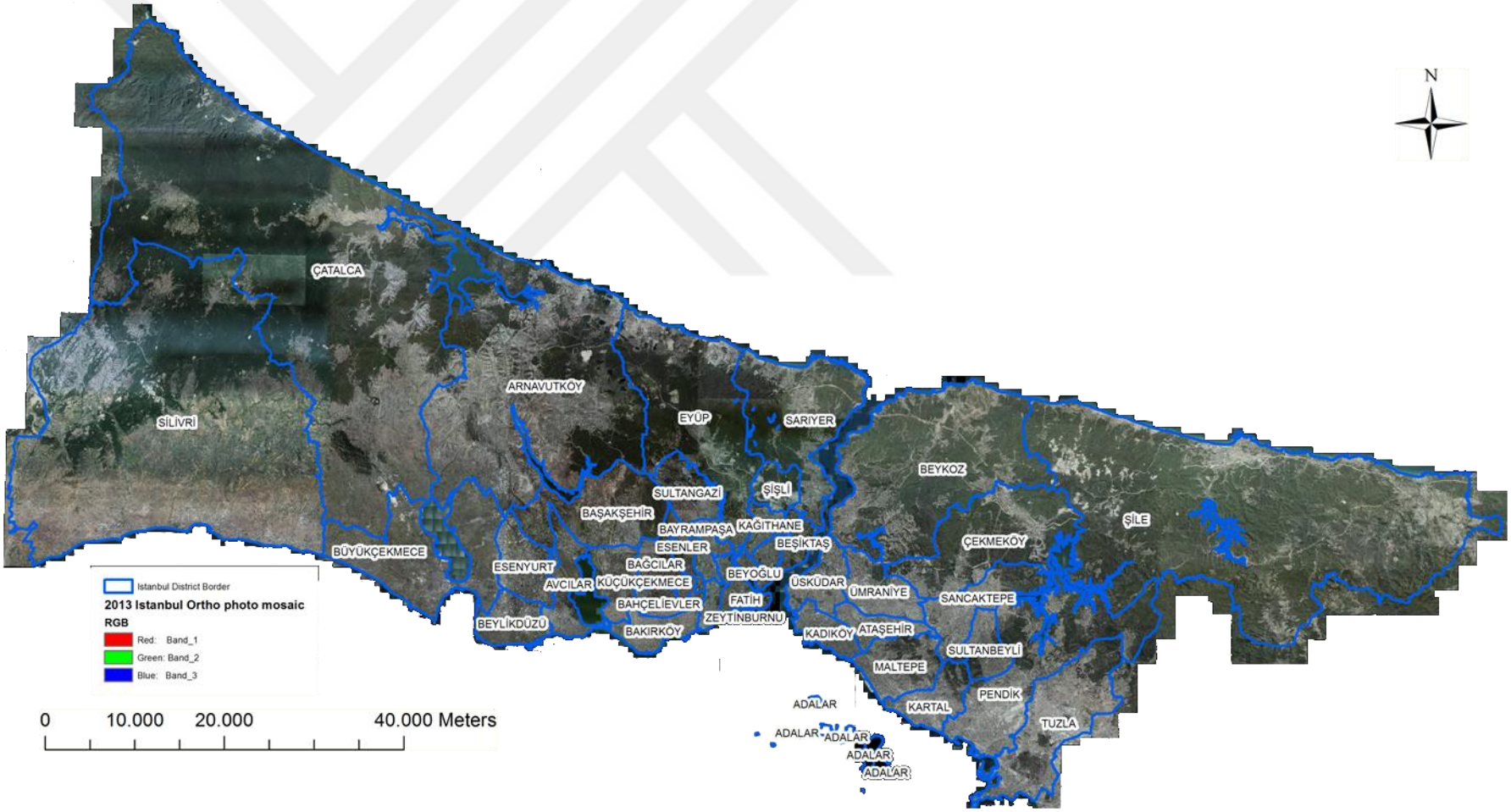


Figure 5.9 : 2013, 50 cm resolution Ortho-Photo mosaic of Istanbul.

Another step was the the detection of the collapsed or rebuilt buildings, the structures were controlled by using 1982 aerial photo, 1996 ortho-photo, 2004, 2007 satellite images and 2013 ortho photo mosaic if they were collapsed between those years. By comparing the shapes and the sizes of the structures, it was understood that 44963 buildings were demolished between 2004 – 2013 years.

As it was mentioned in section 4, some of the structures of the 2013 ADNKS shapefile formatted Istanbul Structure Data contains 1439981 structures and this data includes the attributes of location, construction type, number of floors and occupancy types of buildings; however, does not contain building ages. This polygon shaped vector building data intersected with the created structure data and the structures that has the attributes which does not meets the building definition were eliminated from the dataset. Hereunder, the number of buildings in Istanbul was determined as 990584 for the year of 2013 (Figure 5.10).

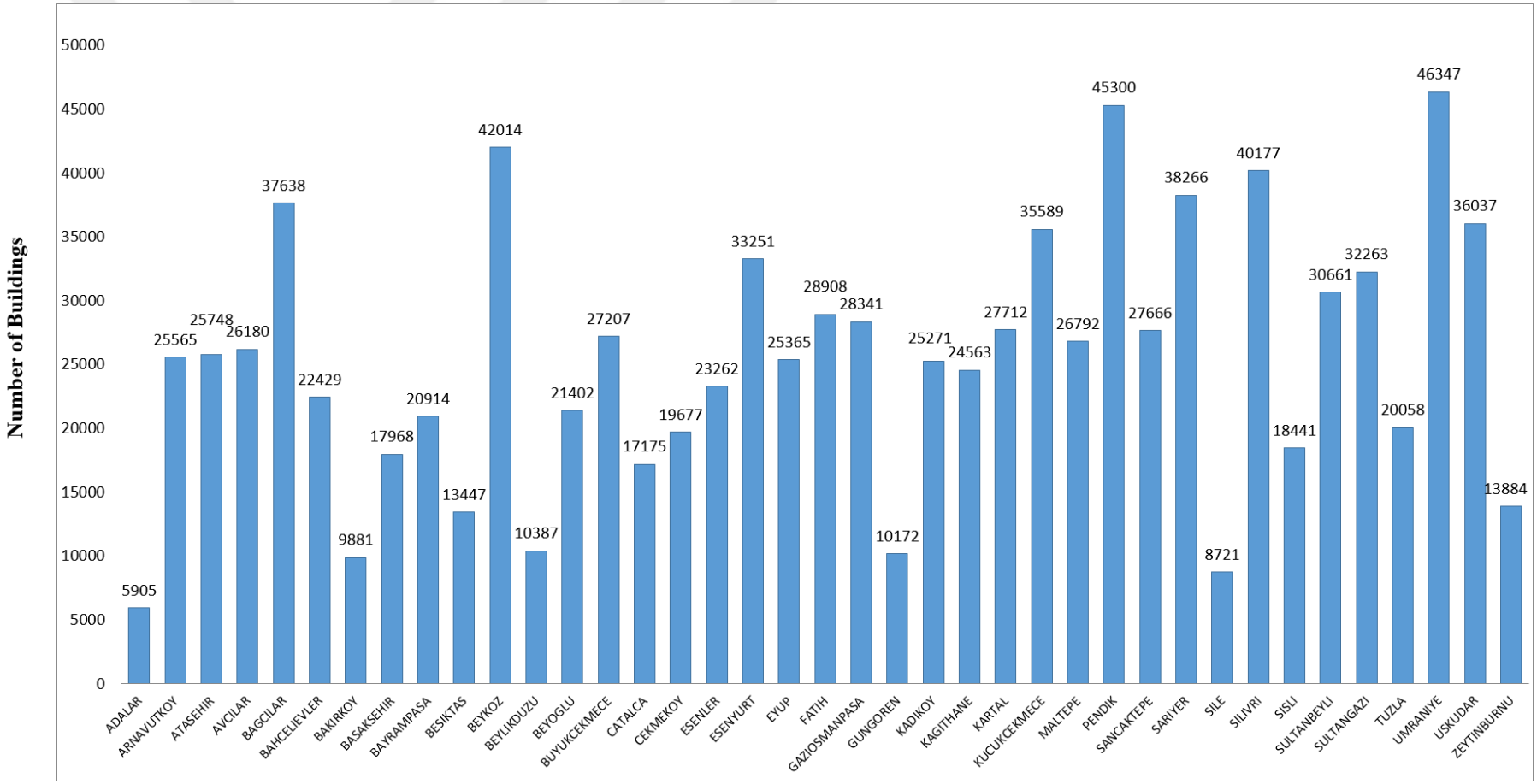


Figure 5.10 : Building number distribution in Istanbul with respect to districts for 2013.

The distribution of building age in Istanbul was given in Table 5.2. According to the results, the building stock of Istanbul have been increased 1095% from 98656 to 990584 buildings between 1968 and 2013.

Table 5.2 : Number of building age distribution in Istanbul until 2013.

The year of Air Photo, Ortho photo mosaic, satellite image	***Digitizing buildings on Air Photo – Ortho photo mosaic***	***Construction date range***	***The current number of building by year 2013***
1966	98656	Pre 1968	82828 (8.4%)
1982	432150	Between 1969 - 1982	330489 (33.4%)
1996	839288	Between 1983 - 1996	381008(38.5%)
2004		Between 1997- 2004	114480(11.5%)
2007		Between 2005 - 2007	46336(4.7%)
2013		Between 2008 - 2013	35443(3.5%)

It was determined that 794325 buildings were constructed before 1996 in Istanbul. The increase of the building stock between 1996 and 2013 determined as 24.71% from 794325 to 990584 buildings. This value presents a very important information due to the alarming earthquakes of 1999 in Kocaeli and Düzce. Because, since 1999 the earthquake hazard is known in Istanbul and with a rough estimation this data shows that the earthquake risk has been increased at least 20% since 1996 due to the increase in building stocks.

When the buildings in Istanbul were analyzed according to occupancy, it emerges that, 80% of the buildings are occupied as Multi Family Dwellings. The occupancy distribution of buildings in Istanbul, except for multi-family dwellings, can be seen in Table 5.3.

Table 5.3 : The number of occupancy classes distributionfor buildings in Istanbul w/o residential house.

Label	Occupancy Class	Building Count (number)
COM1	Retail Trade	136167 (13.7 %)
COM2	Wholesale Trade	4863
COM3	Personal / Repair Services	1381
COM4	Professional / Technical Services	21736 (21.9%)
COM5	Banks	543
COM6	Hospital	721
COM7	Medical Office / Clinic	825
COM8	Entertainment & Recreation	2825
COM9	Theaters, Cinema etc.	798
EDU1	Grade Schools	3115
EDU2	Colleges / Universities	1783
GOV1	General Services	2788
GOV2	Emergency Response	229
IND1	Heavy Industrial	1259
IND2	Light Industrial	6796
IND3	Foods / Drugs / Chemicals	597
IND4	Metals /Mineral Processing	1770
IND5	High Technology	211
IND6	Construction	489
REL1	Mosque, church etc	2176
RES4	Temporary Lodging (Hotel etc)	1235
RES5	Institutional Dormitory	1869
RES6	Nursing Home	112

The city of Istanbul divided into two parts by the Bosporus Strait. Western part of the city was named as European Side and the eastern part was the Asian or Anatolian Side and the total number of districts are today 39 within the city while 25 districts were occupied in European side. The oldest buildings were located in the Fatih district of the European side. The increase in the number of buildings between 1969 and 1982 was seen mostly in the Sarıyer, Kağıthane, Gaziosmanpaşa, Bayrampaşa and Bağcılar districts. Between 1983 and 1996 the Silivri, Sultangazi, Bağcılar, Avcılar and Esenyurt distircts have had the highest increases in the number of buildings. Districts with the highest increase rate from 1997 to 2004 were Esenyurt, Silivri, Büyükçekmece, Avcılar and Başakşehir. The highest increase rate occurred in Büyükçekmece, Esenyurt, Arnavutköy, Avcılar and Silivri between 2005 and 2007, while Esenyurt, Büyükçekmece, Arnavutköy, Sarıyer and Zeytinburnu districts increase rate maximized between 2008 and 2013 (Figure 5.11).

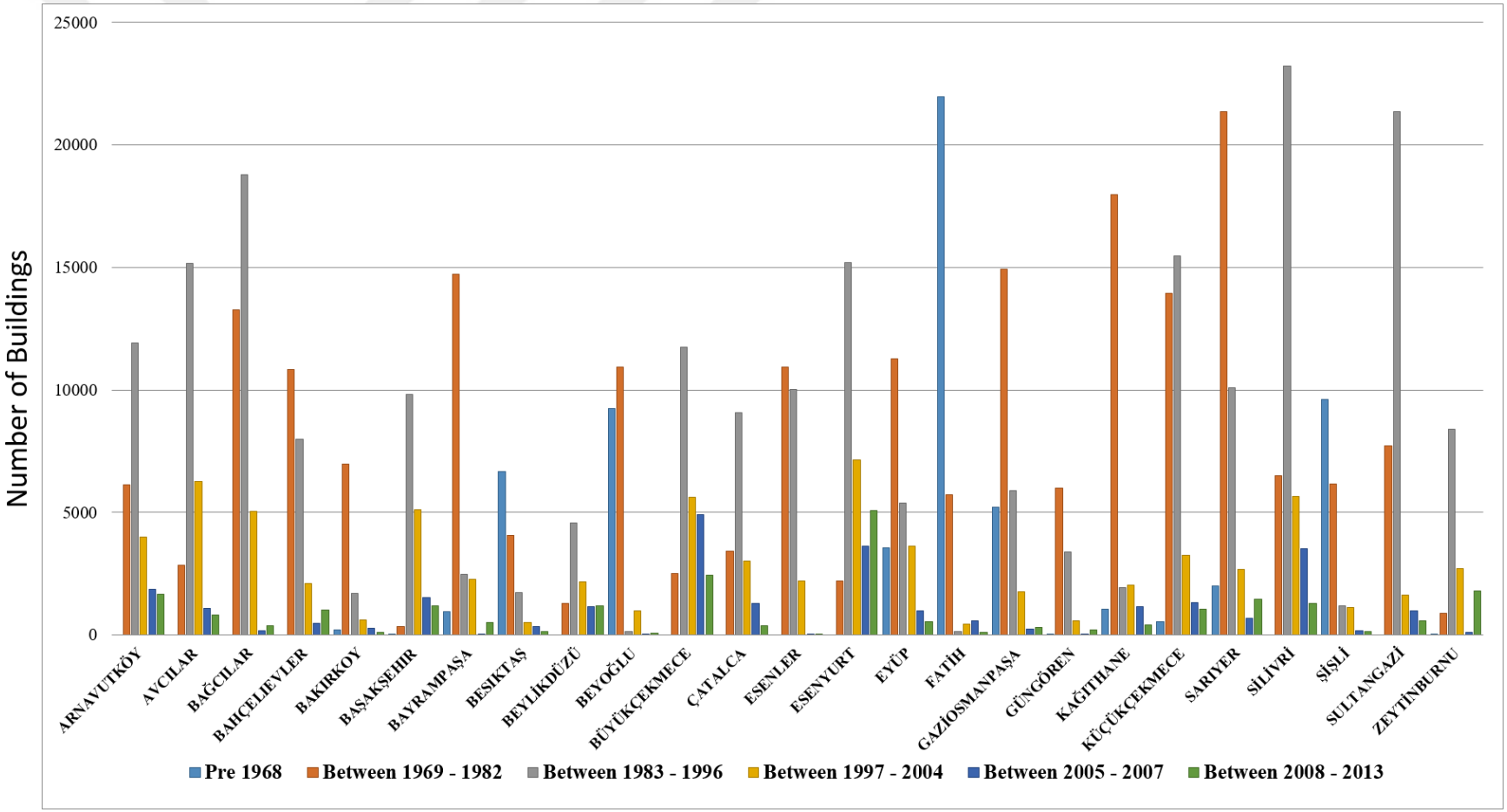


Figure 5.11 : Number of building age distributions at European Side of Istanbul.

Asian side hosts 14 districts were most of the buildings that were constructed before 1969 mostly located in Kadiköy and Üsküdar districts. Between 1969 and 1982, the number of buildings were mostly increased in Üsküdar, Beykoz, Ümraniye, Kartal and Maltepe districts. Pendik, Sultanbeyli, Ümraniye, Sancaktepe ve Beykoz were the top five districts where the increase rates are the most between the years of 1983 and 1996. Between 1997 and 2004, the Beykoz, Ataşehir, Ümraniye, Pendik, Çekmeköy districts saw the highest increase. The increase in the number of buildings between 2005 and 2007 occurred mostly in Çekmeköy, Ümraniye, Sancaktepe, Pendik and Maltepe. Between 2008 and 2013, the Tuzla, Sancaktepe, Pendik, Ataşehir ve Çekmeköy saw the highest increase in buildings (Figure 5.12).

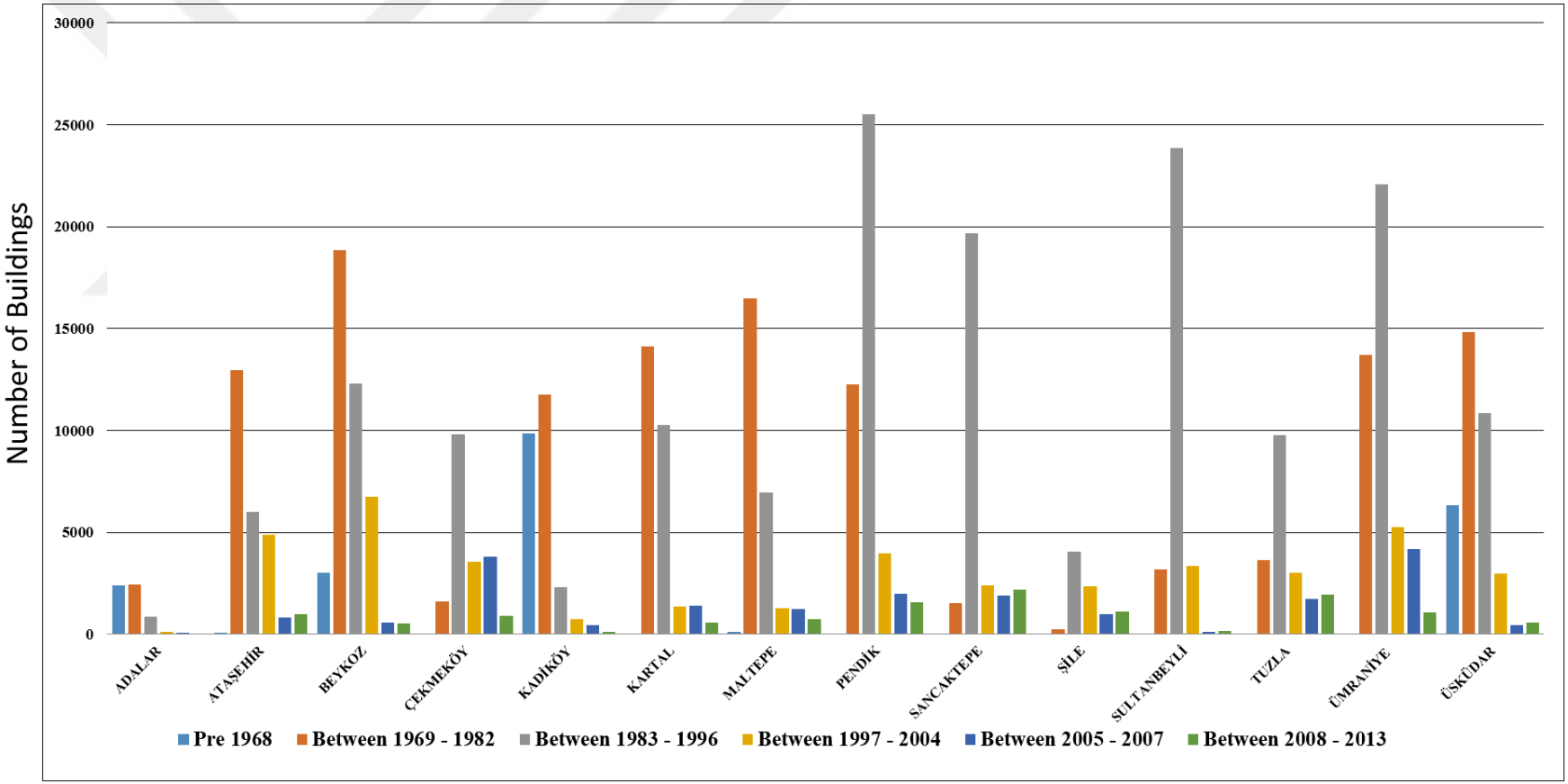


Figure 5.12 : Number of building age distributions at Asian Side of Istanbul.

.

The number of buildings in the districts of Istanbul has increased drastically starting from 1968 to 2013. The increase rate of the buildings through the years in districts of Istanbul can be seen in Table 12 where, some districts of Istanbul had no buildings before 1968. The reason for this was the lack of coverage of the 1966 aerial image for the whole Istanbul. If there were any other data to complete the pre-1968 buildings, it could be the next step of this study. When the increases in the number of buildings were analyzed between 1982 and 2013 on a district basis, the highest increase in the number of buildings was seen in the Silivri district with 33688 buildings. This was closely followed by the districts of Pendik, Ümraniye, Esenyurt and Sancaktepe. The lowest increase rate was observed in Bakırköy district with 2914 buildings (Table 5.4).

Table 5.4 : Number of buildings at districts based in Istanbul from 1968 to 2013.

Districts	*Pre 1968 Building Count*	*Building Count Between 1969 - 1982*	*Total Number of Building 2013*	*The change between 1982 - 2013*
Adalar	2381	2437	5905	3468
Arnavutköy	0	6123	25565	19442
Ataşehir	83	12983	25748	12765
Avcılar	0	2848	26180	23332
Bağcılar	0	13265	37638	24373
Bahçelievler	0	10839	22429	11590
Bakırköy	221	6967	9881	2914
Başakşehir	9	327	17968	17641
Bayrampaşa	935	14714	20914	6200
Beşiktaş	6654	4078	13447	9369
Beykoz	3011	18826	42014	23188
Beylikdüzü	0	1282	10387	9105
Beyoğlu	9254	10943	21402	10459
Büyükçekmece	0	2515	27207	24692
Çatalca	0	3410	17175	13765
Çekmeköy	0	1626	19677	18051
Esenler	0	10935	23262	12327
Esenyurt	0	2205	33251	31046
Eyüp	3565	11257	25365	14108
Fatih	21959	5706	28908	23202
Gaziosmanpaşa	5196	14940	28341	13401
Güngören	2	6003	10172	4169
Kadıköy	9846	11756	25271	13515
Kağıthane	1052	17972	24563	6591
Kartal	0	14103	27712	13609
Küçükçekmece	533	13955	35589	21634
Maltepe	125	16480	26792	10312
Pendik	0	12270	45300	33030
Sancaktepe	0	1510	27666	26156
Sarıyer	2013	21345	38266	16921
Şile	0	231	8721	8490
Silivri	0	6489	40177	33688
Şişli	9616	6166	18441	12275
Sultanbeyli	0	3197	30661	27464
Sultangazi	0	7730	32263	24533
Tuzla	0	3631	20058	16427
Ümraniye	13	13718	46347	32629
Üsküdar	6333	14838	36037	21199
Zeytinburnu	27	869	13884	13015
Total	82828	330489	990584	

With 46347 buildings, the highest number of buildings, were located in the Ümraniye district at the Asian side of the city, while the smallest number of buildings were respectively located in Adalar with 5905 buildings. 196529 buildings were constructed in Istanbul between years of 1997 and 2013. Esenyurt, Büyükçekmece, and Ümraniye respectively, are the top three districts where the most buildings were constructed. Büyükçekmece, Esenyurt, and Küçükçekmece are the districts where the newest buildings were located, while the oldest buildings are located in Fatih, Beyoğlu, and Beşiktaş. Nowadays, the numbering project for the buildings is ongoing for Istanbul and this means that, the new buildings constructed after 2013 can be added to this dataset directly as a GIS building data. It is also available today to use most recent building detection techniques for the recently constructed buildings. It can be easily seen at Figure 5.13, that, the city of Istanbul is expanding both in area and in the number of buildings against the earthquake risk. As a result of this part of this study, Figure 5.14 shows the number of buildings in Istanbul according to distribution of based on district. In addition to this, the distribution of based on sub-district is given at Figure 5.15.

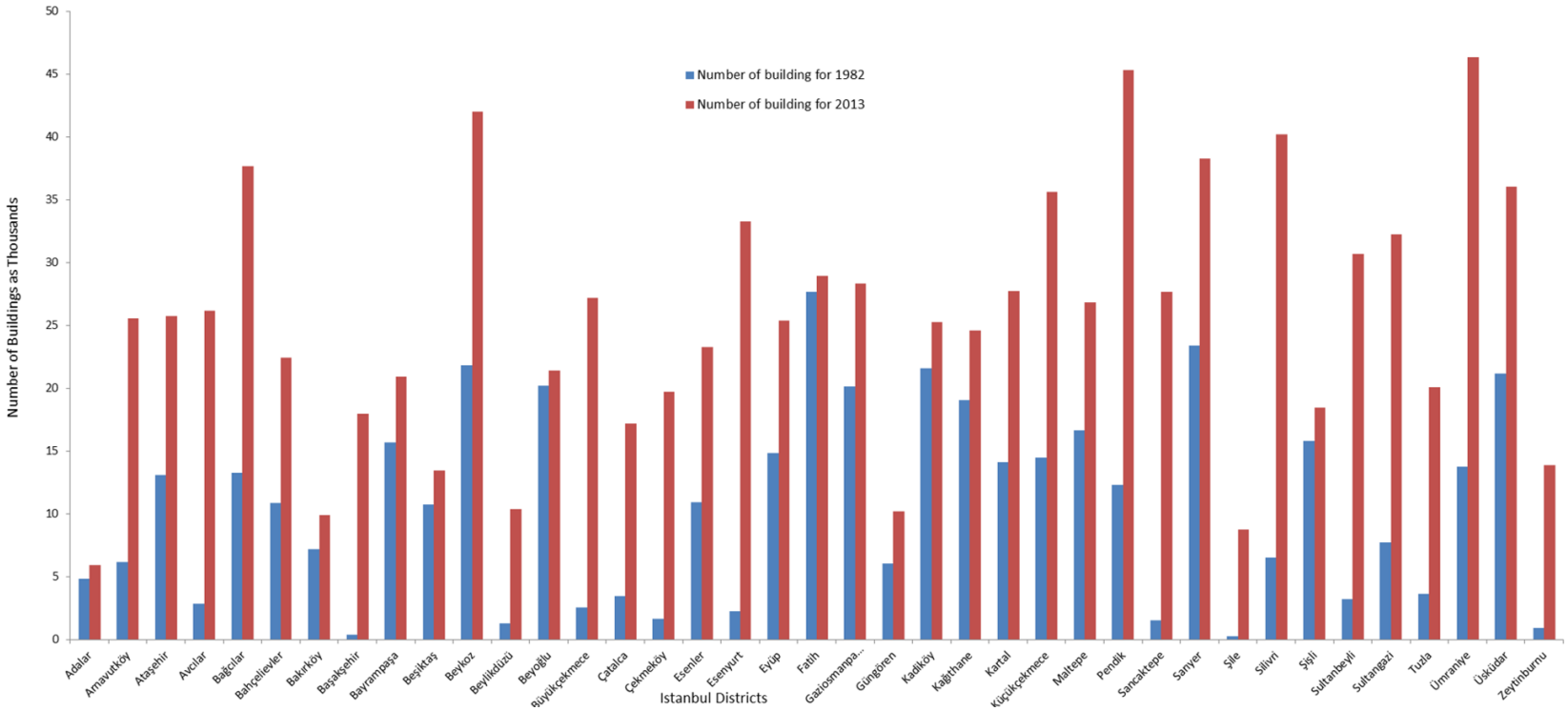


Figure 5.13 : Changes in Istanbul building numbers at district level between 1982 and 2013.

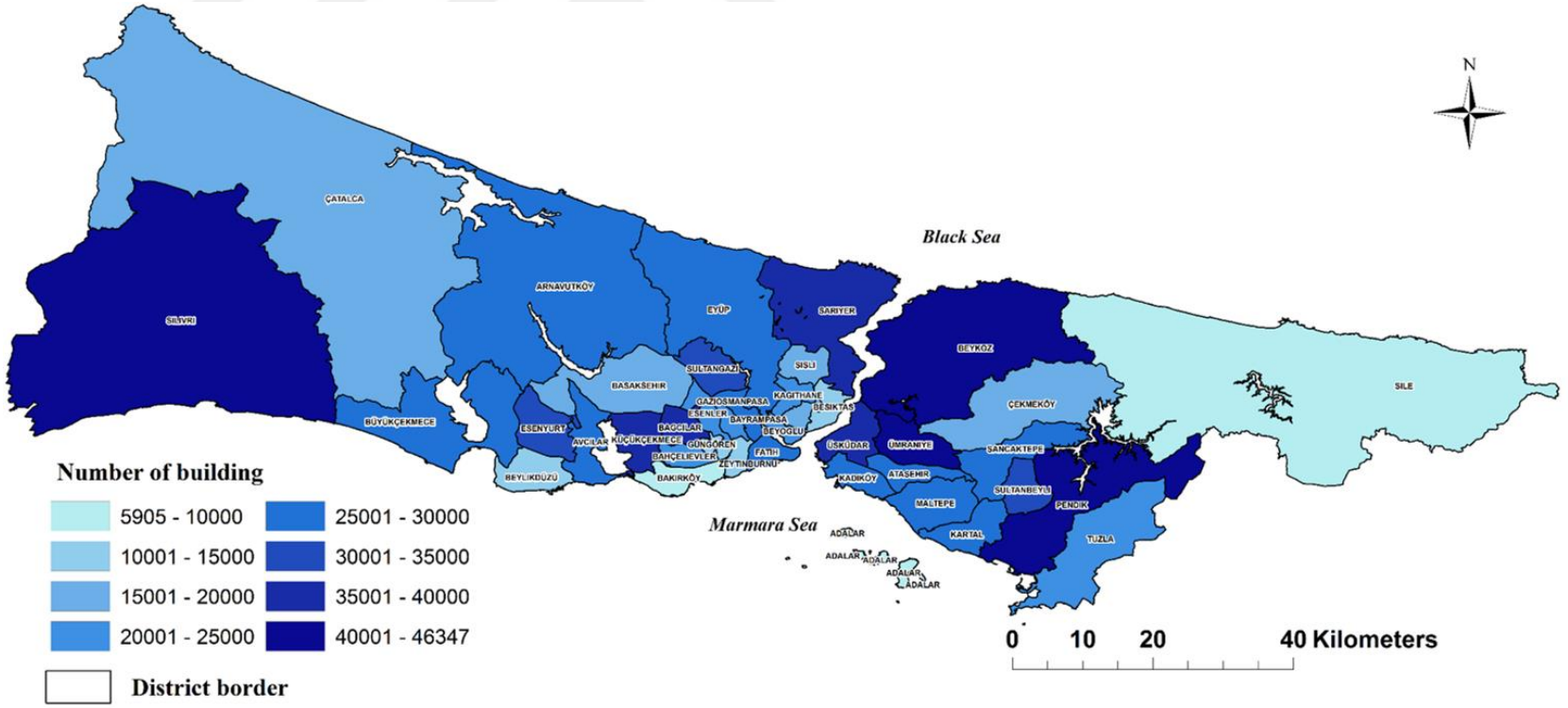


Figure 5.14 : Building counts of the districts of Istanbul.

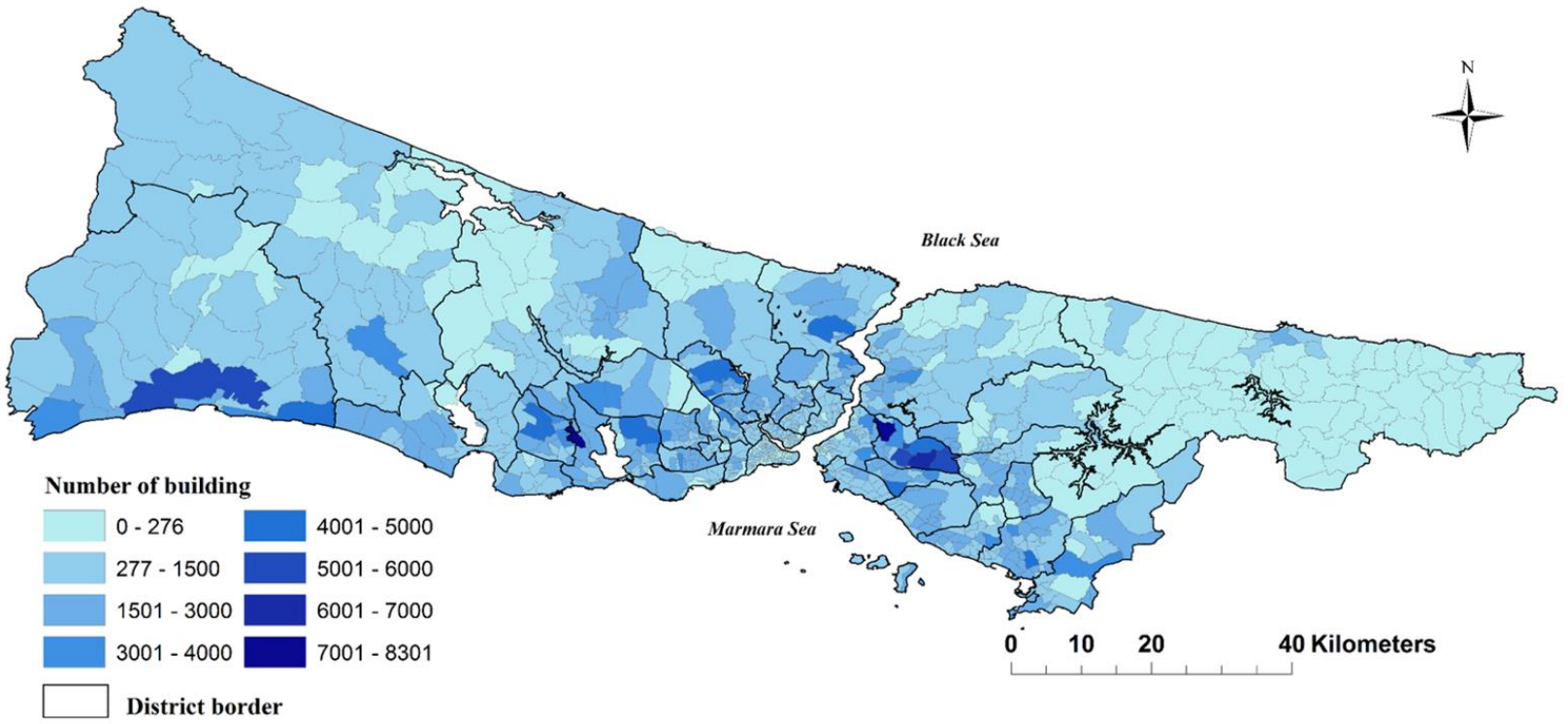


Figure 5.15 : Building counts of the sub-districts of Istanbul.

6. BUILDING DAMAGE ANALYSIS

6.1 Method of Building Damage Analysis

Building damage analysis computes the structural damage to buildings based on a particular hazard. It quantifies probabilities of physical damage states as well as an estimation of the overall expected damage level of buildings in the study region (Himmet Karaman et al., 2008).Within the context of this study, building damage analysis were calculated for every single 990584 buildings in Istanbul. The necessary data for this analysis is given in Figure 6.1.

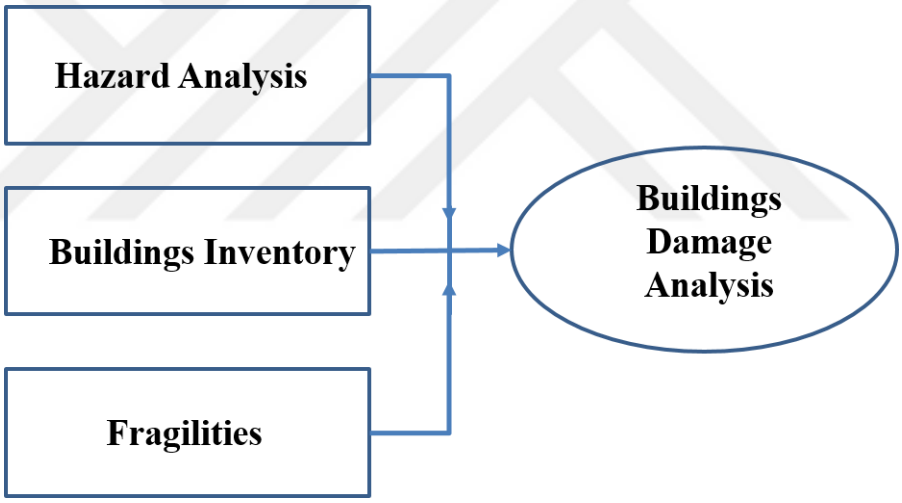


Figure 6.1 : The necessary data for building damage.

6.1.1 Earthquake hazard

Hazard is described as an input ground motion parameter or a spectral response value (Himmet Karaman et al., 2008). The magnitude of acceleration in a specific site is associated with earthquake magnitude, depth of focus, type of fault, distance of fault, soil class, average shear wave velocity, the morphology and several related criteria. In this study, Boore and Atkinson (2008) ground motion estimation equation has been used to simulate the earthquake hazard map for Istanbul with PGA (Figure 6.2) and Sa (T=0.2s) demands (Figure 6.3).

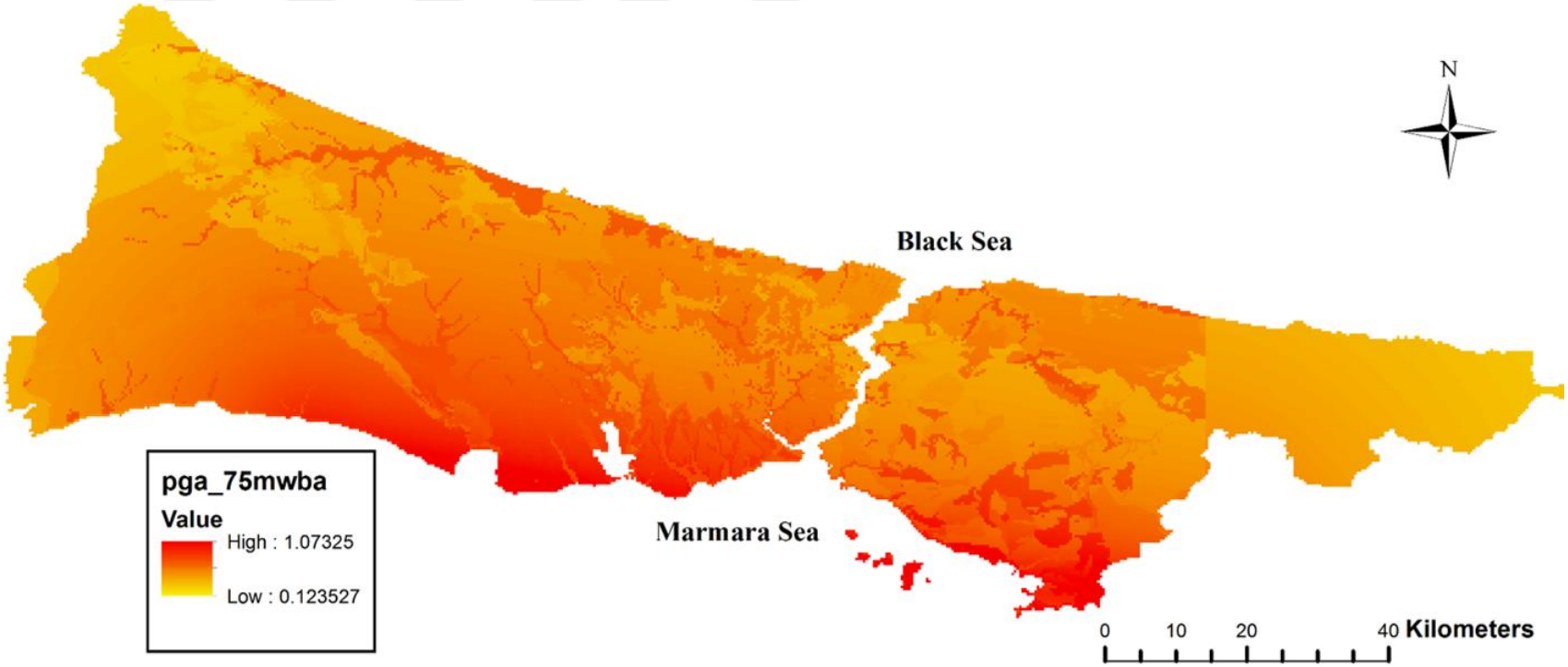


Figure 6.2 : Istanbul Earthquake Hazard Map according to Boore & Atkinson (2008) PGA.

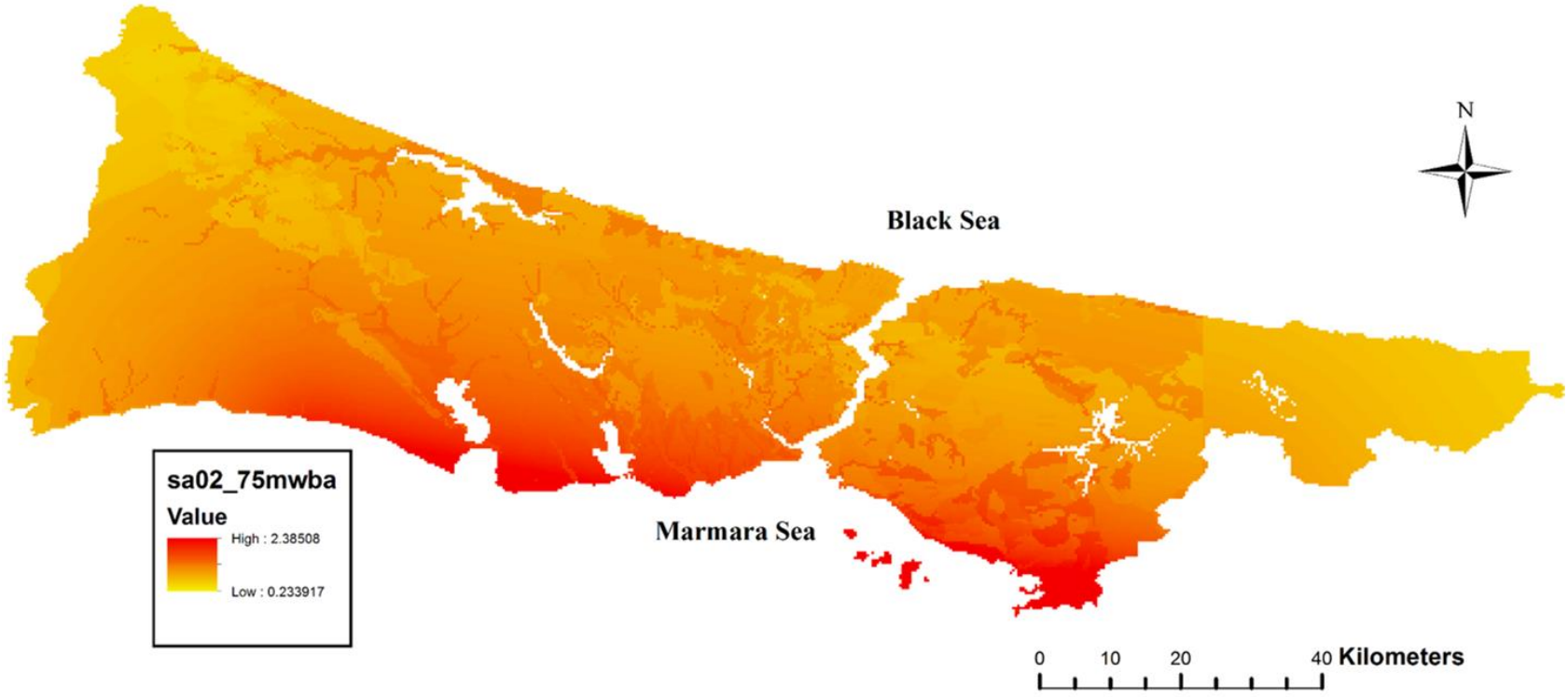


Figure 6.3 : Istanbul Earthquake Hazard Map according to Boore & Atkinson (2008) 0.2 second Sa.

In this study; Model A produced by JICA and IMM (2002) study was used as a scenario earthquake (Figure 6.4). Model A is defined as a fracture in the eastern part of the fault line and is the most anticipated model. The magnitude of this scenario earthquake was assumed as Mw 7.5 (JICA & IMM, 2002).

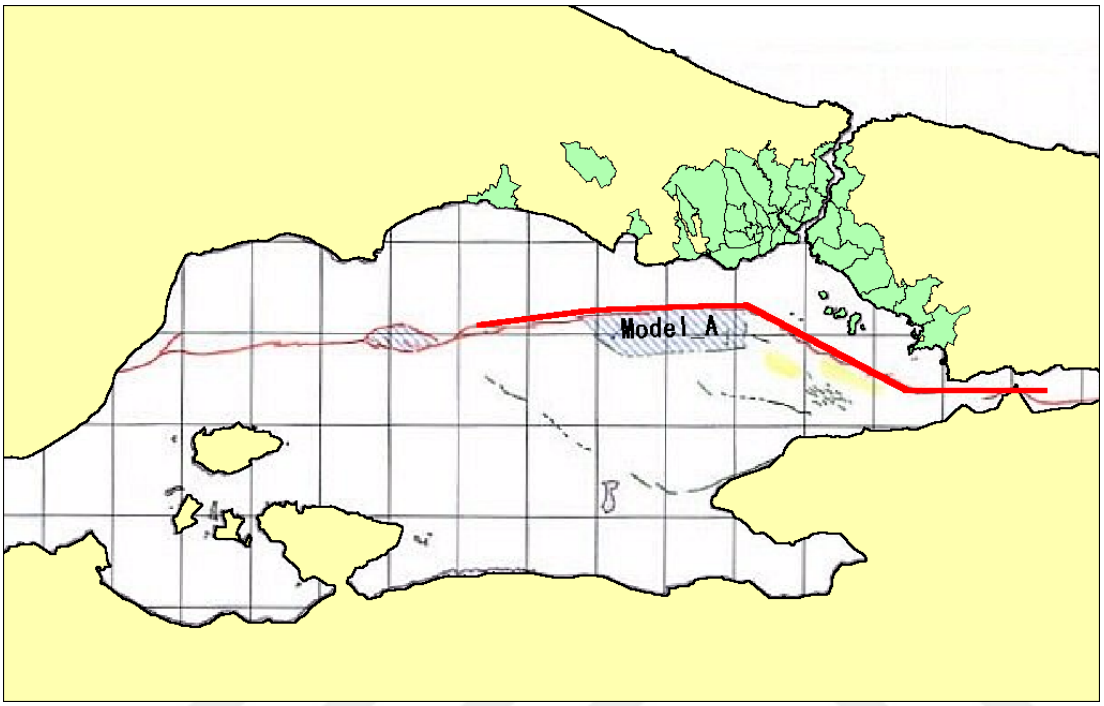


Figure 6.4 : Model A according to JICA and IMM (2002) study.

6.1.2 Structural fragility

In this study, fragility curves for buildings of Istanbul were already embedded inside the HAZTURK software and they were developed by using the Parameterized Fragility Method (PFM) of Jeong and Elnashai (2006). The probability of the damage to buildings is estimated by matching every building in the dataset to a fragility curve in the database by using the number of stories, construction year, construction type, and hazard values at the building location. HAZTURK calculates the probability of earthquake damage on a building in four limit states based on PGA, 0.2 sec Sa and Sd demands (Himmet Karaman et al., 2008).

The probability of damage is obtained from the probability of exceeding each limit state. The damage states used by HAZTURK are: Insignificant, Moderate, Heavy, and Complete. To get mean and standard derivation of damage, the damage probabilities are weighted (Himmet Karaman et al., 2008).

In this study, fragility curves for both spectral acceleration and peak ground acceleration were used. The fragility curves for Istanbul buildings in HAZTURK software are shown in Figure 6.5 and Figure 6.6 respectively for 0.2 sec Sa and PGA demands for concrete frame with unreinforced masonry infill wall structures.

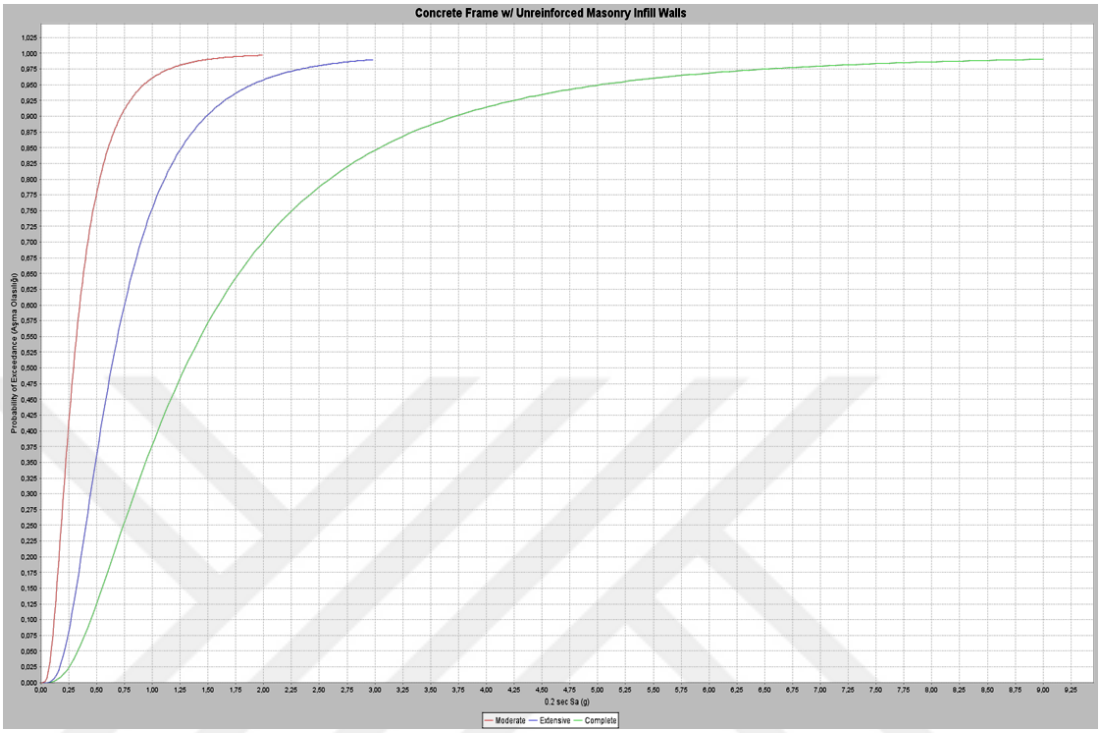


Figure 6.5 : Fragility curve for concrete frame with unreinforced masonry infill walls according to 0.2 Sa.

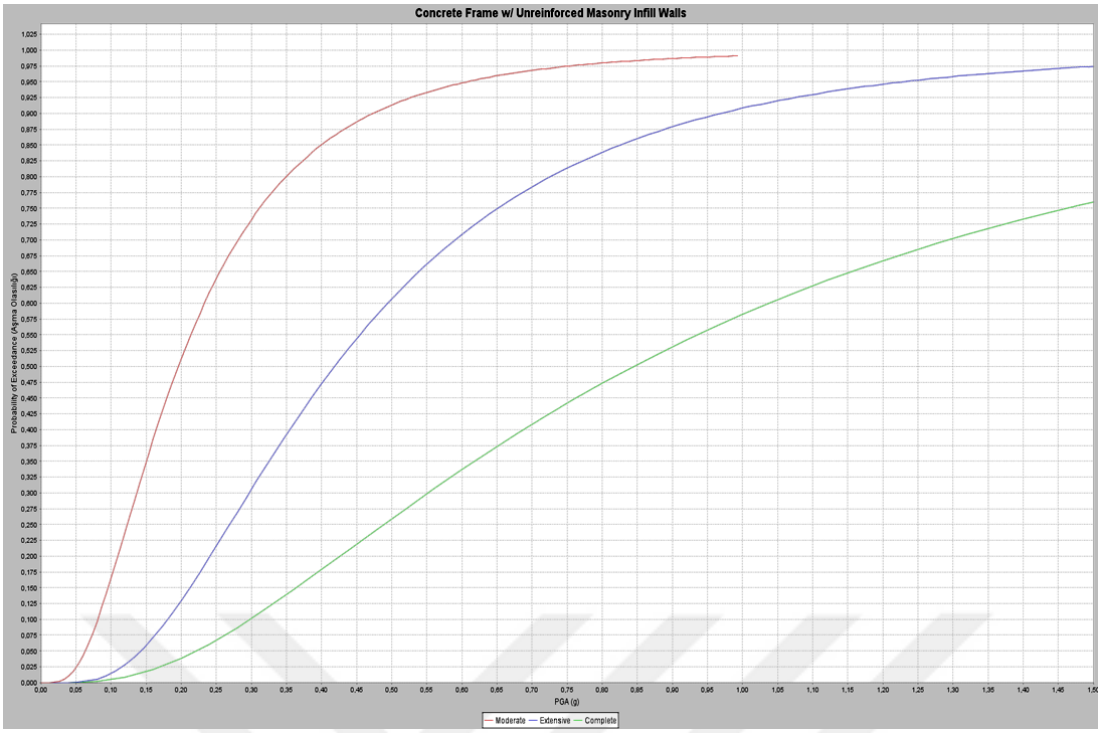


Figure 6.6 : Fragility curve for concrete frame with unreinforced masonry infill walls according to PGA.

6.1.3 Building inventory

The HAZTURK software requires point vector data format for the building input data. For this reason, the polygon vector formatted building data was converted point data format first. Then, the data was projected from ITRF96 to WGS84 geographic coordinate system due to HAZTURK needs.

In order to use building type data in the HAZTURK software, the necessary reclassification and standardization process were done. HAZTURK building inventory attributes and explanations are shown in Table 6.1.

Table 6.1 : HAZTURK building inventory attributes and explanations.

Attribute ID	***Attribute Explanation***
Par_id	Parcel Identification
Str_type	General Structural Type
Year_built	Building Construction Year
Occ_type	Building Functionality Type
Efacility	Critical Services
No_stories	Number of Building Story
Str_type_2	HAZUS Structural Category

The distribution of the buildings based on the building age are shown inTable 6.2. According to Table 6.2 most of the buildings in Istanbul were constructed before 1999 Kocaeli Earthquake.

Table 6.2 : The number of building age distribution in Istanbul.

Building age	***Building #***
Pre 1968	82828
Between 1969 - 1982	330489
Between 1983 - 1996	381008
Between 1997- 2004	114480
Between 2005 - 2007	46336
Between 2008 - 2013	35443

The number of buildings that were classified according to HAZUS buildings structural type is given at Table 6.3.

Table 6.3 : The number of building distribution according to HAZUS building structural type (FEMA 2003).

Description	***Label***	***Height***	***Stories***	***Number***
Wood, Light Frame	W1		1 – 2	3368
Wood, Commercial and Industrial	W2		All	471
Steel Moment Frame	S1M	Mid-Rise	4 – 7	26
	S1H	High-Rise	8 +	5
Steel Light Frame	S3		All	358
Concrete Moment Frame	C1L	Low-Rise	1 – 3	3839
	C1M	Mid-Rise	4 – 7	76647
	C1H	High-Rise	8 +	3839
Concrete Shear Walls	C2L	Low-Rise	1 – 3	63426
	C2M	Mid-Rise	4 – 7	43559
	C2H	High-Rise	8 +	10323
Concrete Frame with Unreinforced Masonry Infill Walls	C3L	Low-Rise	1 – 3	312869
	C3M	Mid-Rise	4 – 7	293384
	C3H	High-Rise	8 +	12203
Precast Concrete Tilt-Up Walls	PC1		All	305
Precast Concrete Frames with Concrete Shear Walls	PC2L	Low-Rise	1 – 3	820
	PC2M	Mid-Rise	4 – 7	12
	PC2H	High-Rise	8 +	4
Reinforced Masonry Bearing Walls with Wood or Metal Deck	RM1L	Low-Rise	1 – 3	10298
Reinforced Masonry Bearing Walls with Precast Concrete	RM2L	Low-Rise	1 – 3	1
	RM2M	Mid-Rise	4 – 7	1246
	RM2H	High-Rise	8 +	5
Unreinforced Masonry Bearing Walls	URML	Low-Rise	1 – 3	21561
	URMM	Mid-Rise	4 – 7	11118

6.2 Building Damage Analysis and Results

In this study, building damage estimation were made for 990584 building in Istanbul. According to estimation results of Istanbul, the damage ration of Istanbul buildings are given at Table 6.4. The contribution of this study to the previous HAZTURK building damage analyses, is to update the fragility curve mappings for the URM and PC1 construction types in the HAZTURK software and the use of the most current real building data with the real age information of them.

Table 6.4 : The distribution of damage ratio of Istanbul buildings.

HAZTURK in 2015	***Insignificant (%)***	***Moderate (%)***	***Heavy (%)***	***Complete (%)***	***Mean Damage (%)***
Boore and Atkinson (2008) Sa	21.52	35.55	28.21	14.68	35.23
Boore and Atkinson (2008) PGA	50.37	31.85	13.99	3.80	15.6

URML, URMM and C3L are the STR_TYP2 classification that have the highest complete damage risk when the damage analysis were calculated according to Sa. These buildings are more than 4 floors and were constructed with unreinforced masonary bearing walls and concrete frame with unreinforced masonary infill walls. URMM, RM1L and RM2M type of buildings have the highest heavy damage. These type of buildings were constructed wit reinforced masonary bearing walls with wood, metal deck and precast concrete (Table 6.5).

Table 6.5 : Distribution of damage ratio of STR_TYP2 according to Sa.

STR_TYP2	*Insignificant (%)*	*Moderate (%)*	*Heavy (%)*	*Complete (%)*	*Mean Damage (%)*
C1H	22.7	48.1	21.7	7.4	26.2
C1L	22.8	37.2	27.4	12.4	32.1
C1M	22.0	49.0	21.3	7.5	26.2
C2H	26.7	50.4	17.9	4.8	22.1
C2L	35.6	35.7	22.3	6.2	23.6
C2M	32.5	43.8	17.2	6.4	22.2
C3H	15.1	40.3	28.4	16.0	36.3
C3L	19.0	28.8	31.5	20.6	40.4
C3M	17.2	37.8	27.8	17.1	36.6
PC1	18.9	35.1	31.0	14.8	35.9
PC2H	21.5	46.1	25.5	6.7	27.3
PC2L	21.4	31.9	32.4	14.1	35.6
PC2M	16.3	37.8	31.5	14.2	36.1
RM1L	23.6	31.8	32.6	11.8	33.6
RM2H	11.5	39.8	34.5	14.0	37.8
RM2M	21.3	59.7	17.8	1.0	20.1
S1H	34.3	41.0	19.4	5.1	21.8
S1M	20.0	37.4	28.8	13.6	34.0
S3	9.8	28.6	37.8	23.6	46.5
URML	12.7	23.1	27.6	36.4	51.6
URMM	11.5	26.2	33.4	28.7	48.4
W1	25.9	39.6	23.1	11.1	29.0
W2	32.8	44.1	17.2	6.2	22.1

The buildings that have the highest complete possibility aacordign to Sa were built before 1968 years. The buildings that were built between 1969 and 1996 have the highest heavy damage (Table 6.6).

Table 6.6 : Distribution of damage ratio of building age according to Sa.

YEAR BUILT	*Insignificant (%)*	*Moderate (%)*	*Heavy (%)*	*Complete (%)*	*Mean Damage (%)*
Before 1968	14.1	31.8	31.7	22.2	42.4
Between 1969 – 1982	19.1	34.4	28.9	17.4	37.0
Between 1983 – 1996	18.9	33.4	29.3	18.2	37.8
Between 1997 – 2004	27.0	39.9	23.7	9.8	27.7
Between 2005 – 2007	36.4	45.0	15.3	3.2	18.4
Between 2008 - 2013	30.1	51.30	15.7	2.8	19.2

Results are obtained from the building damage analysis based on STR_TYP2 distribution according to PGA are given at Table 6.7.

Table 6.7 : Distribution of damage ratio of STR_TYP2 according PGA.

STR_TYP2	*Insignificant (%)*	*Moderate (%)*	*Heavy (%)*	*Complete (%)*	*Mean Damage (%)*
C1H	59.7	31.5	7.0	1.6	10.5
C1L	55.2	32.2	9.9	2.5	13.0
C1M	58.4	33.7	6.2	1.6	10.3
C2H	63.3	30.7	4.9	0.09	8.6
C2L	65.7	24.4	8.67	1.09	9.8
C2M	67.2	27.1	4.3	1.26	8.0
C3H	48.1	34.6	13.0	4.1	16.5
C3L	47.1	29.5	18.9	4.3	19.1
C3M	48.4	36.5	10.5	4.4	15.6
PC1	46.0	32.8	17.6	3.3	18.1
PC2H	59.7	31.8	7.3	1.0	10.1
PC2L	50.1	30.8	16.0	2.8	16.4
PC2M	46.0	35.8	14.2	3.8	17.1
RM1L	52.0	29.0	16.8	2.0	15.8
RM2H	38.4	40.6	17.1	3.7	19.3
RM2M	45.5	38.6	12.9	2.9	15.9
S1H	74.6	19.9	4.6	0.7	6.7
S1M	52.3	31.5	12.1	3.9	15.4
S3	32.2	36.0	25.51	6.1	25.3
URML	32.5	29.5	22.5	15.3	30.9
URMM	34.0	35.1	22.0	8.7	25.6
W1	53.7	32.7	10.7	2.8	13.7
W2	65.0	29.2	4.6	1.0	8.3

Damage distribution according to PGA is given at Table 6.8 were classified by using year built.

Table 6.8 : Distribution of damage ratio of building age according to PGA.

YEAR BUILT	*Insignificant (%)*	*Moderate (%)*	*Heavy (%)*	*Complete (%)*	*Mean Damage (%)*
Before 1968	41.6	34.8	17.8	5.6	20.5
Between 1969 – 1982	32.7	50.0	13.1	4.0	16.1
Between 1983 – 1996	48.6	32.4	14.4	4.4	17.2
Between 1997 – 2004	59.0	29.8	9.16	1.9	11.72
Between 2005 – 2007	69.8	25.3	4.2	0.05	4.7
Between 2008 - 2013	66.4	29.6	3.4	0.03	7.1

6.2.1 The complete and heavily damage buildings according to Sa

Complete damage distribution of the Istanbul buildings are based on 0.2 sec Sa is represented in Figure 6.7, while the heavy damage distribution according to Sa is shown in Figure 6.8.

There are 19,679 buildings in Istanbul that may have complete and heavy damage with a possibility greater than 40% according to 0.2 sec Sa. As it is shown in Figure 6.9, most of those buildings are located at the southern shore lines of Istanbul.

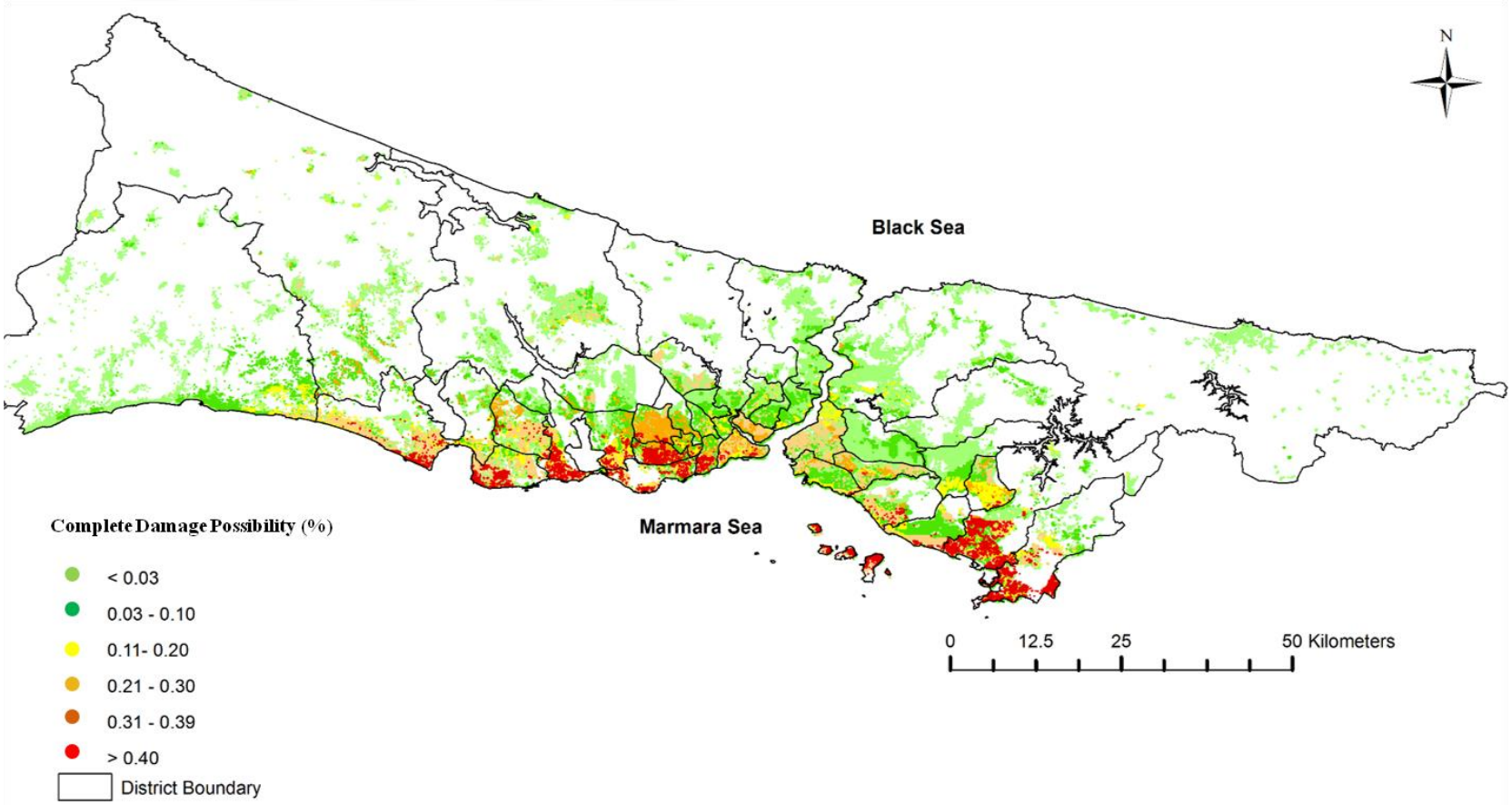


Figure 6.7 : Complete damage possibility distribution of Istanbul buildings according to 0.2 Sa.

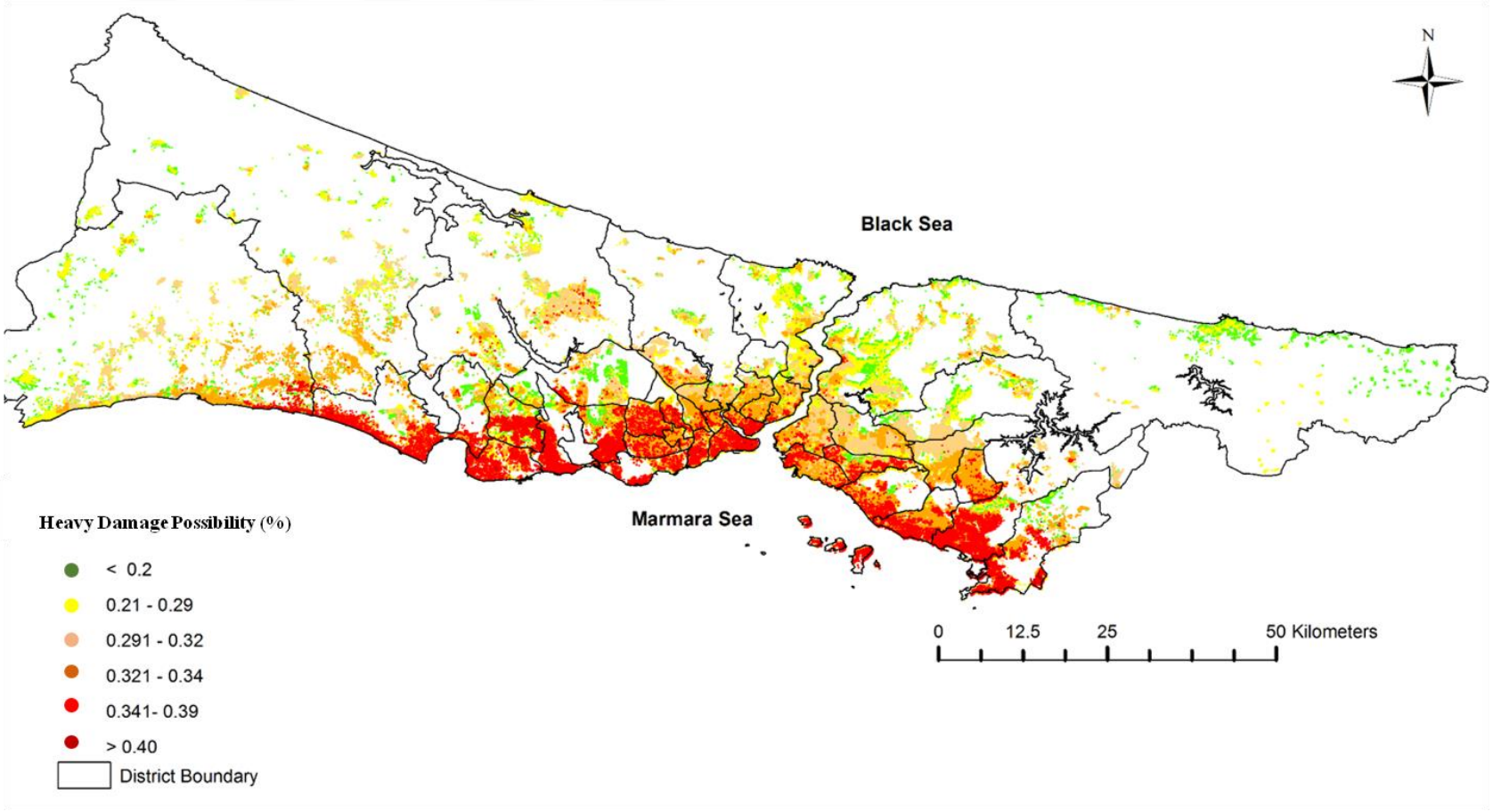


Figure 6.8 : Heavy damage possibility distribution of Istanbul buildings according to 0.2 Sa.

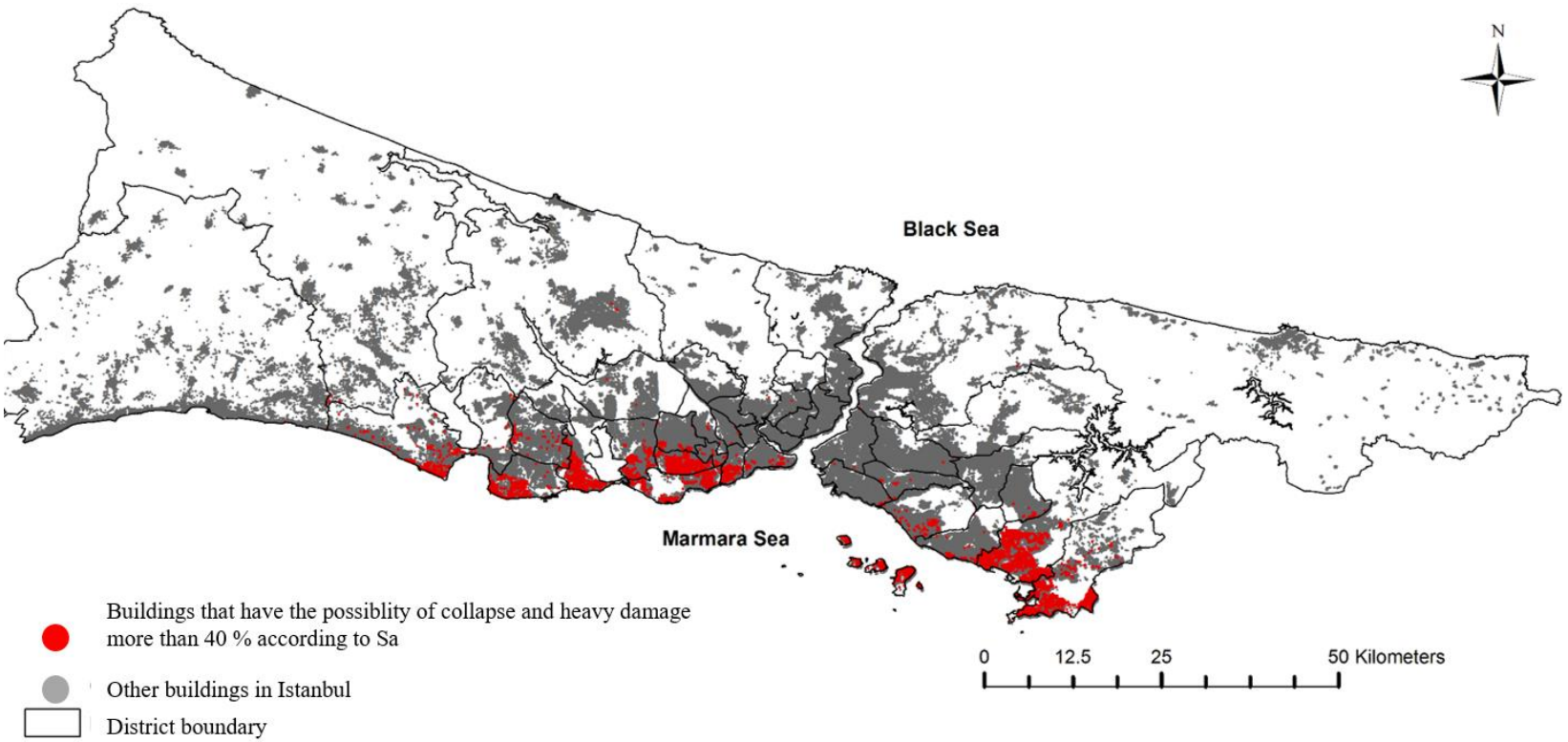


Figure 6.9 : Buildings in Istanbul that have the complete and heavy damage possibility more than 40% based on 0.2 Sa.

The distribution of the buildings that have the complete and heavy damage possibility more than 40% according to 0.2 Sa can be seen based on districts in Table 6.9. According to Table 6.9, Tuzla and Pendik districts have the buildings with the highest possibility of heavy and complete damage at the Anatolian side of Istanbul.

Table 6.9 : Number of buildings distribution that have the possibility of heavy & complete damage more than 40% based on 0.2 sec Sa in districts.

No	*District*	*Building #*	*No*	*District*	*Building #*	*No*	*District*	*Building #*
1	Tuzla	5459	14	Bagcılar	90	27	Basaksehır	2
2	Pendık	5238	15	Esenyurt	66	28	Eyüp	1
3	Adalar	2846	16	Sultanbeylı	53	29	Kagıthane	1
4	Beylıkdüzü	1454	17	Güngören	28	30	Sılıvrı	1
5	Büyükçekmece	1279	18	Kadıköy	14	31	Besıktas	0
6	Bahçelıevler	840	19	Atasehır	13	32	Beyoglu	0
7	Avcılar	756	20	Çatalca	7	33	Gazıosmanpasa	0
8	Zeytınburnu	403	21	Esenler	6	34	Sarıyer	0
9	Bakırköy	396	22	Arnavutköy	5	35	Sıslı	0
10	Küçükçekmece	344	23	Bayrampasa	3	36	Sıle	0
11	Kartal	141	24	Ümranıye	3	37	Çekmeköy	0
12	Maltepe	131	25	Beykoz	2	38	Sultangazı	0
13	Fatıh	95	26	Üsküdar	2	39	Sancaktepe	0

The comparison of the sub-districts in Istanbul according to damage possibilities based on heavy damage and complete damage limit states, shows that Mimar Sinan and Ertugrul Gazi sub-districts located in Tuzla and Pendik have the highest number of buildings to have heavy and complete damage with a possibility exceeding 40% (Table 6.10).

Table 6.10 : Number of buildings distribution that have the possibility of heavy & complete damage more than 40% based on 0.2 sec Sa in sub-districts.

No	*Sub-district*	*District*	*Building #*	*No*	*Sub-district*	*District*	*Building #*
1	Mımar Sınan	Tuzla	1482	26	Fatıh	Pendik	189
2	Ertugrul Gazı	Pendik	1119	27	Sahıl	Beylıkdüzü	183
3	Sıfa	Tuzla	1101	28	Evlıya Çelebı	Tuzla	177
4	Postane	Tuzla	1009	29	Sapan Bagları	Pendik	167
5	Nızam	Adalar	784	30	Esenler	Pendik	163
6	Maden	Adalar	731	31	Mustafa K.Pasa	Avcılar	141
7	Heybelıada	Adalar	672	32	Kurtköy	Pendik	139
8	Dereagzı	Beylıkdüzü	669	33	Zafer	Bahçelıevler	139
9	Güzelce	Büyükçekmece	580	34	Cıhangır	Avcılar	137
10	Velıbaba	Pendik	495	35	Yenı Mahalle	Pendik	136
11	Batıköy	Büyükçekmece	495	36	Orta	Pendik	134
12	Yayla	Tuzla	488	37	Kavakpınar	Pendik	123
13	Içmeler	Tuzla	470	38	Kanarya	Küçükçekmece	113
14	Esenyalı	Pendik	406	39	Camı	Tuzla	111
15	Sülüntepe	Pendik	401	40	Hürrıyet	Bahçelıevler	109
16	Burgazada	Adalar	365	41	Çobançesme	Bahçelıevler	107
17	Kavaklı	Beylikdüzü	344	42	Kaynarca	Pendik	106
18	Güzelyalı	Pendik	307	43	Orhangazı	Pendik	104
19	Aydıntepe	Tuzla	295	44	Telsız	Zeytinburnu	103
20	Kınalıada	Adalar	294	45	Bestelsız	Zeytinburnu	102
21	Dumlupınar	Pendik	258	46	Ramazanoglu	Pendik	98
22	Istasyon	Tuzla	240	47	Fıruzköy	Avcılar	98
23	Merkez	Beylıkdüzü	201	48	Bahçelıevler	Büyükçekmece	93
24	Çınardere	Pendik	195	49	Bahçelıevler	Bahçelievler	92
25	Yayalar	Pendik	195	50	Ünıversıte	Avcılar	91

The comparison of the heavy to complete damaged buildings more than 40% possibility exceedance based on the occupancy classes shows that, according to 0.2 sec Sa; 17,241 of the buildings are occupied as residential, while lodging and dormitories have 59 buildings in that category (Table 6.11).

Table 6.11 : Distribution of building number that have the possibility of heavy & complete damage more than 40% based on 0.2 sec Sa according to occupation type.

Occupation types	*Building #s*
Residence	17241
Lodging, Dormitory	59
Commercial Facilities	1881
Industrial Facilities	251
Governmental Facilities	98
Religious Facilities	76
Educational Facilities	73

Most of the buildings that have the possibility of complete and heavy damage possibilities more than 40% according to 0.2 sec Sa were constructed between 1983 and 1996. The number of buildings that were constructed between 1969 and 1982 is in the second line with 5,699 buildings. This result shows that the construction quality and controls should be less between those years.

The most vulnerable construction type in Istanbul, according to the analysis results appeared as Concrete Framed structures with Unreinforced Masonry Infill Walls with 11,273 buildings with more than 40% heavy and complete damage possibilities based on 0.2 second Sa demand, as it shown in Table 6.12.

Table 6.12 : Distribution of building number that have the possibility of heavy & complete damage more than 40% based on 0.2 sec Sa according to construction type.

Construction Type	***Building #***
C1	323
C3	11273
PC1	7
PC2	17
RM1	7
S3	154
URM	7896

6.2.2 The complete and heavily damage buildings according to PGA

PGA based complete damage distribution of the Istanbul buildings illustrated in Figure 6.10. The heavy damage distribution of the same inventory is also represented in Figure 6.11 based on PGA.

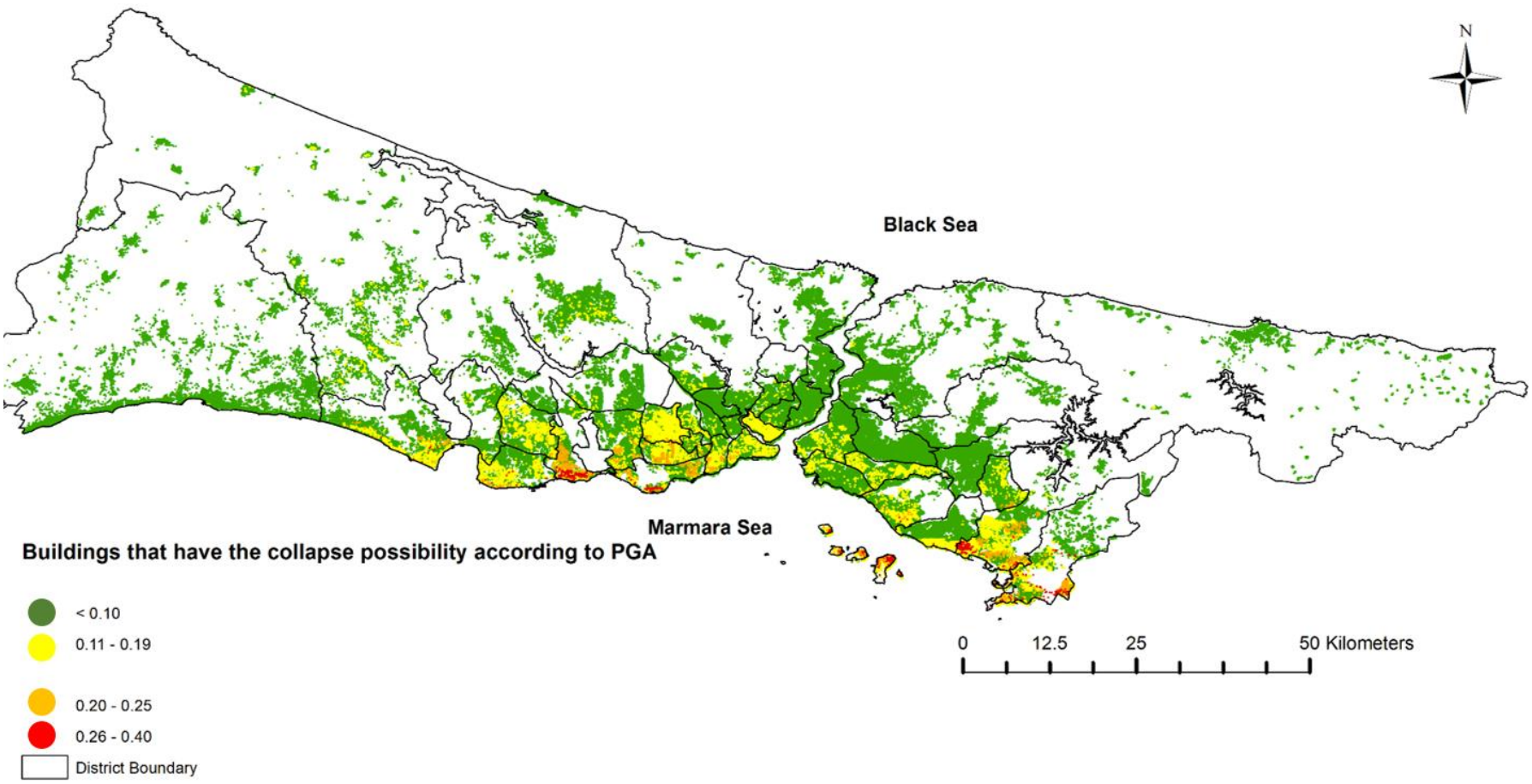


Figure 6.10 : Complete damage possibility distribution of Istanbul buildings according to PGA.

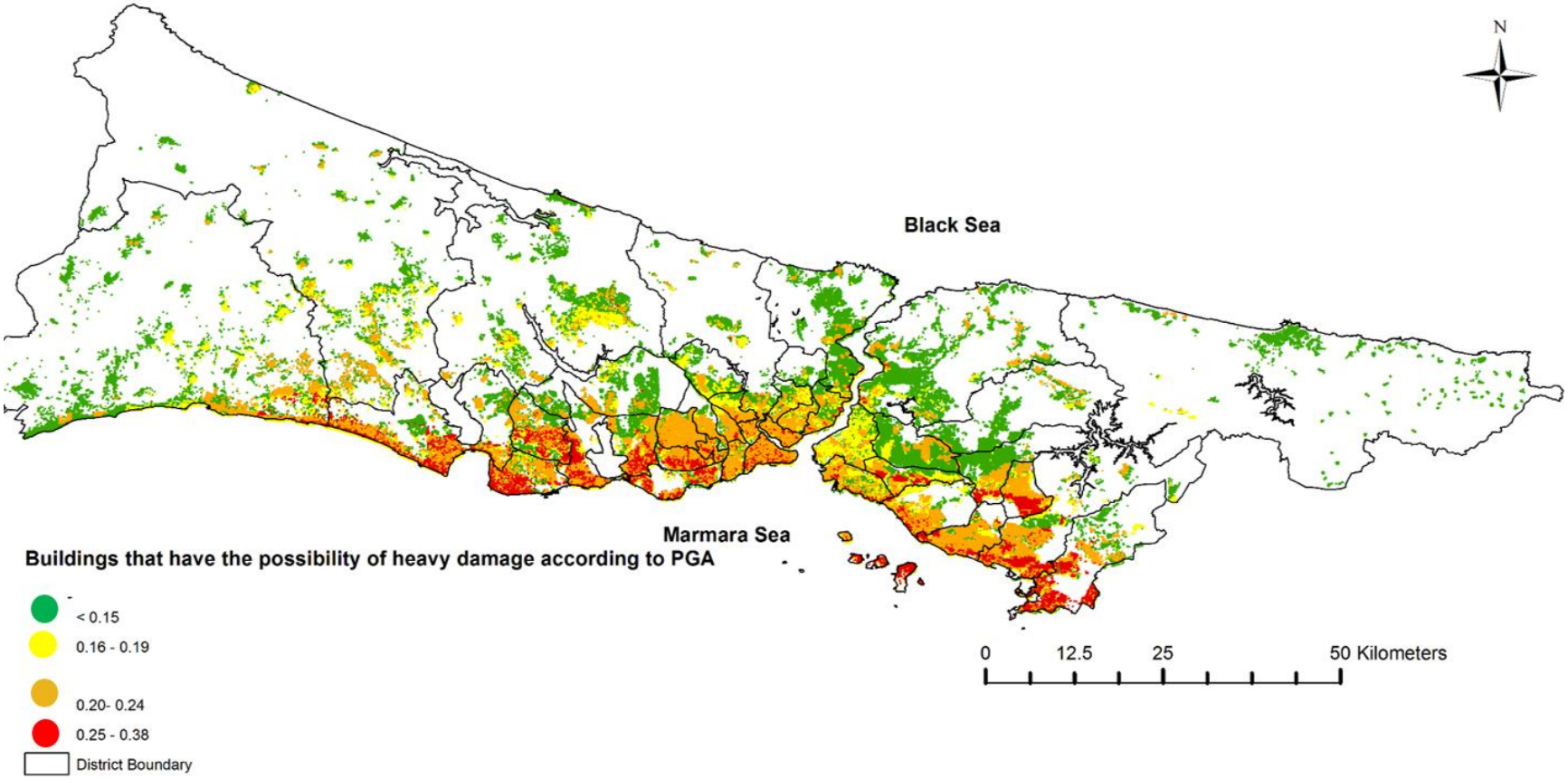


Figure 6.11 : Heavy damage possibility distribution of Istanbul buildings according to PGA.

The damage possibilities of the Istanbul buildings based on PGA are less than the 0.2 sec Sa. While there were 19,679 buildings to have heavy and complete damage with a possibility more than 40%, there are 14,066 buildings that have the possibility of complete and heavy damage more than 30% due to PGA (Figure 6.12).

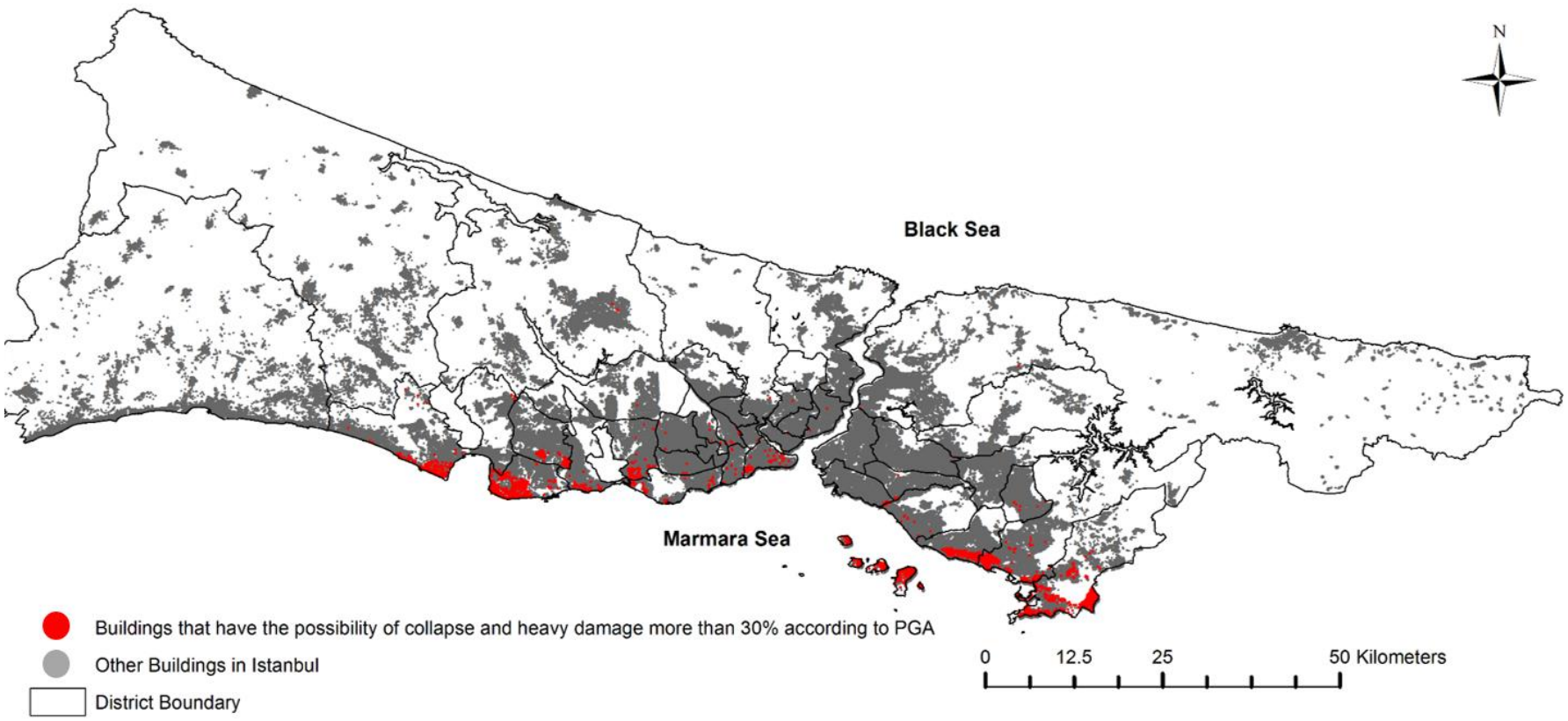


Figure 6.12 : Buildings in Istanbul that have the complete and heavy damage possibility more than 30% based on PGA.

According to the aforementioned analysis results based on PGA, it is estimated that Tuzla district will have the highest heavy and complete damage ratio in Istanbul just like 0.2 second Sa analysis results (Table 6.13).

Table 6.13 : Number of buildings distribution that have the possibility of heavy & complete damage more than 40% based on PGA in districts.

No	*District*	*Building #*	*No*	*District*	*Building #*	*No*	*District*	*Building #*
1	Tuzla	4680	14	Zeytınburnu	11	27	Ümranıye	1
2	Adalar	2559	15	Bayrampasa	9	28	Basaksehır	1
3	Pendık	1813	16	Sultanbeylı	7	29	Gazıosmanpasa	0
4	Beylıkdüzü	1791	17	Arnavutköy	5	30	Güngören	0
5	Büyükçekmece	1331	18	Esenler	4	31	Sarıyer	0
6	Kartal	1112	19	Bagcılar	3	32	Sıslı	0
7	Esenyurt	175	20	Bahçelıevler	3	33	Üsküdar	0
8	Küçükçekmece	141	21	Kadıköy	3	34	Sıle	0
9	Avcılar	126	22	Besıktas	2	35	Sılıvrı	0
10	Bakırköy	124	23	Beykoz	2	36	Çatalca	0
11	Fatıh	116	24	Eyüp	2	37	Çekmeköy	0
12	Maltepe	24	25	Beyoglu	1	38	Sultangazı	0
13	Atasehır	19	26	Kagıthane	1	39	Sancaktepe	0

While the district with the highest risk of building damage remaining the same as Tuzla in Sa and PGA analysis, the European side sub-districts' heavy and complete damage possibilities increased in the damage distribution. Şifa, Mimar Sinan, Dereağzı, Nizam and Maden sub-districts, respectively from Tuzla, for first two, Beylikduzu and Adalar for the last two enlisted at the top of the list in Istanbul (Table 6.14).

Table 6.14 : Number of buildings distribution that have the possibility of heavy & complete damage more than 40% based on PGA in sub-districts.

No	*District*	*Sub-district*	*Building #*	*No*	*District*	*Sub-district*	*Building #*
1	Tuzla	Sıfa	1665	26	Kartal	Petrol ıs	119
2	Tuzla	Mımar Sinan	1583	27	Kartal	Yukarı	112
3	Beylıkdüzü	Dereagzı	853	28	Tuzla	Içmeler	111
4	Adalar	Nızam	720	29	Tuzla	Camı	107
5	Adalar	Maden	719	30	Esenyurt	Mehter çesme	79
6	Tuzla	Postane	702	31	Avcılar	Ambarlı	73
7	Büyükçekmece	Güzelce	618	32	Beylıkdüzü	Adnan kahvecı	73
8	Büyükçekmece	Batıköy	535	33	Tuzla	Evlıya çelebı	72
9	Adalar	Heybelıada	519	34	Pendık	Batı	64
10	Pendık	Yenı mahalle	493	35	Tuzla	Istasyon	63
11	Pendık	Sapan bagları	460	36	Esenyurt	Saadet dere	62
12	Kartal	Yunus	441	37	Bakırköy	Senlık	57
13	Adalar	Burgazada	378	38	Pendık	Dogu	53
14	Beylıkdüzü	Kavaklı	359	39	Küçükçekmece	Yenı mahalle	48
15	Pendık	Esenyalı	304	40	Avcılar	Denız köskler	43
16	Beylıkdüzü	Merkez	266	41	Kartal	Topselvı	40
17	Pendık	Bahçelıevler	252	42	Fatıh	Hacı evhaddın	39
18	Kartal	Çavusoglu	249	43	Fatıh	Abdı çelebı	35
19	Adalar	Kınalıada	223	44	Büyükçekmece	Pınartepe	34
20	Tuzla	Yayla	219	45	Esenyurt	Namık kemal	32
21	Beylıkdüzü	Sahıl	210	46	Bakırköy	Yesılköy	29
22	Pendık	Güzelyalı	147	47	Küçükçekmece	Yesılova	27
23	Tuzla	Aydınlı	133	48	Bakırköy	Basınköy	26
24	Kartal	Karlıktepe	128	49	Küçükçekmece	Cennet	24
25	Büyükçekmece	Bahçelıevler	125	50	Tuzla	Aydıntepe	21

Damage distribution based on occupancy shows that, 11,900 buildings have the more than 30% possibility of complete and heavy damage according to PGA demand type were used as residential buildings (Table 6.15), while the educational facilities have 2 buildings that may exceed the limit states of complete and heavy damage.

Table 6.15 : Distribution of building number that have the possibility of heavy & complete damage more than 40% based on PGA according to occupation type.

Occupation types	*Building #*
Residence	11900
Commercial Facilities	1958
Industrial Facilities	110
Governmental Facilities	52
Religious Facilities	44
Educational Facilities	2

The analysis results highlight the buildings that were constructed between 1983 and 1996 have the highest possibility to exceed the heavy and complete damage limit states with a number of 7,187 buildings. The Concrete Frame structures with Unreinforced Masonry Infill Walls are determined to be the buildings with the highest possibility of complete and heavy damage based on PGA demand as it was shown in Table 6.16.

Table 6.16 : Distribution of building number that have the possibility of heavy & complete damage more than 40% based on PGA according to construction type.

Construction Type	*Building #*
C1	426
C2	88
C3	12426
PC1	44
PC2	32
RM1	145
S3	141
URM	564

6.2.3 The mean damage buildings according to the Sa

If the specific limit states are not taken into account and only the mean damage situation of all buildings considered, the mean damage possibility distribution of buildings in Istanbul according to 0.2 second Sa earthquake hazard map is determined as in Figure 6.13.

Based on the mean damage analysis, the number of buildings which have more than 50% mean damage possibility based on Sa demand type with 0.2 sec period is determined as 68,389 and represented in (Figure 6.14).

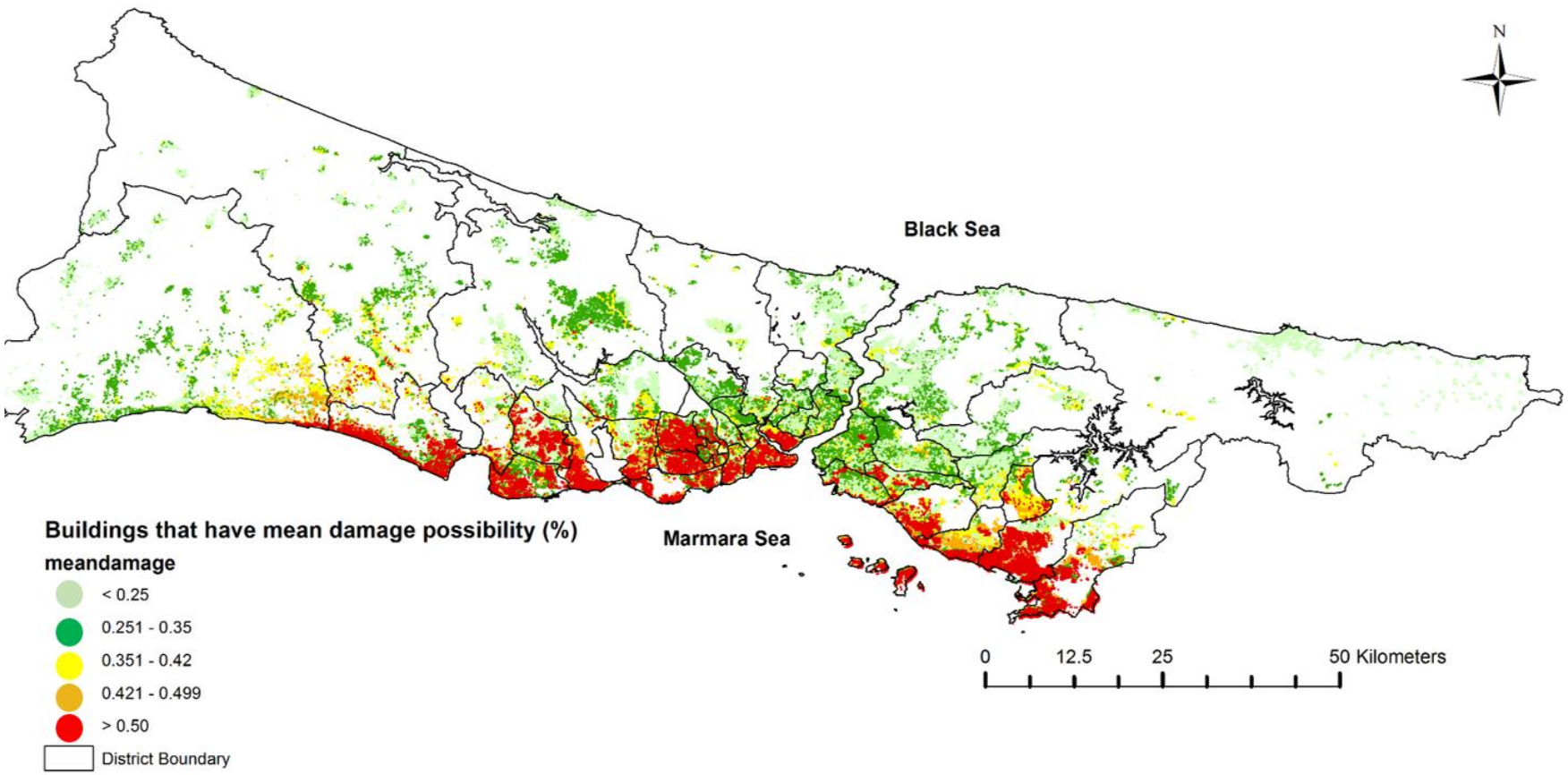


Figure 6.13 : Mean damage possibility distribution of Istanbul buildings according to 0.2 Sa.

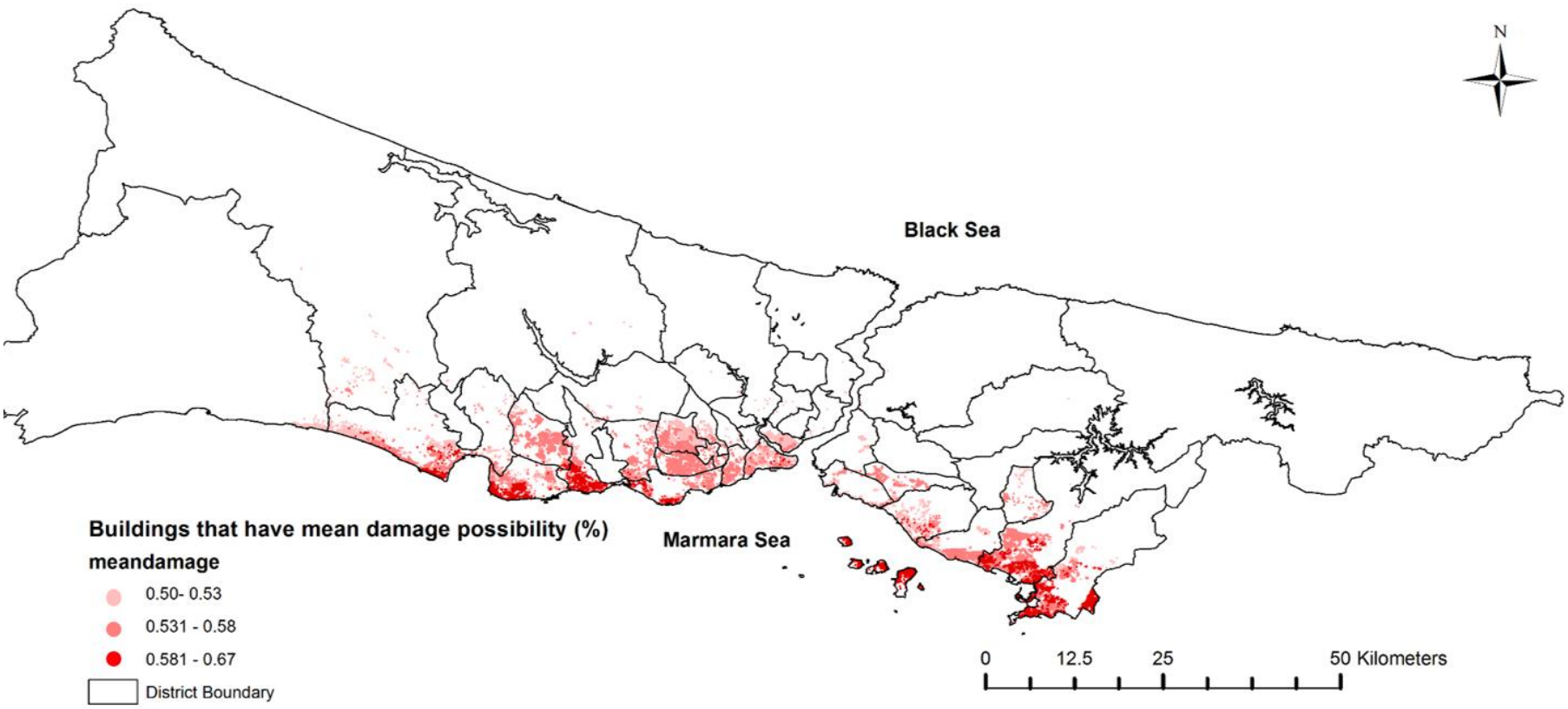


Figure 6.14 : More than 50% mean damage possibility distribution of Istanbul buildings based on 0.2 Sa.

Most of the buildings that have the possibility of mean damage more than 50% according to 0.2 sec Sa were located in Pendik district at the Asian side of Istanbul as it can be seen from Table 6.17.

Table 6.17 : Number of buildings distribution that have the possibility of mean damage more than 50 % based on 0.2 sec Sa in districts.

No	*District*	*Building #*	*No*	*District*	*Building #*	*No*	*District*	*Building #*
1	Pendık	17698	14	Küçükçekmece	1354	27	Eyüp	43
2	Tuzla	10844	15	Bahçelıevler	1115	28	Arnavutköy	27
3	Büyükçekmece	5697	16	Zeytınburnu	924	29	Besıktas	9
4	Adalar	4808	17	Sılıvrı	710	30	Sultangazı	8
5	Kartal	4305	18	Atasehır	627	31	Kagıthane	7
6	Beylıkdüzü	3402	19	Kadıköy	355	32	Beykoz	5
7	Avcılar	2755	20	Sultanbeylı	242	33	Sarıyer	3
8	Beyoglu	2599	21	Esenler	162	34	Sıslı	1
9	Maltepe	2465	22	Çatalca	148	35	Ümranıye	1
10	Fatıh	2300	23	Güngören	136	36	Çekmeköy	1
11	Bakırköy	2034	24	Üsküdar	91	37	Gazıosmanpasa	0
12	Esenyurt	1940	25	Basaksehır	74	38	Sıle	0
13	Bagcılar	1438	26	Bayrampasa	61	39	Sancaktepe	0

Kavakpınar sub-district of Pendik has the highest mean damage ratio in the Table 6.18 based on mean damage distribution of the sub-districts.

Table 6.18 : Number of buildings distribution that have the possibility of mean damage more than 50 % based on 0.2 sec Sa in sub districts.

No	*District*	*Sub-district*	*Building #*	*No*	*District*	*Sub-district*	*Building #*
1	Pendık	Kavakpınar	1864	26	Pendık	Yenı mahalle	766
2	Tuzla	Sıfa	1844	27	Pendık	Sapan bagları	732
3	Tuzla	Mımar sınan	1801	28	Adalar	Kınalıada	731
4	Tuzla	Postane	1694	29	Sılıvrı	Merkez	710
5	Tuzla	Aydınlı	1479	30	Kartal	Orhantepe	659
6	Pendık	Ertugrul gazı	1437	31	Pendık	Batı	652
7	Adalar	Maden	1304	32	Pendık	Çamçesme	642
8	Beylıkdüzü	Dereagzı	1249	33	Pendık	Velıbaba	599
9	Adalar	Nızam	1207	34	Pendık	Fevzı çakmak	592
10	Büyükçekmece	Celalıye	1149	35	Beylıkdüzü	Kavaklı	559
11	Pendık	Orhangazı	1105	36	Avcılar	Cıhangır	558
12	Pendık	Ahmet yesevı	1036	37	Adalar	Burgazada	555
13	Adalar	Heybelıada	1011	38	Bakırköy	Yesılköy	551
14	Pendık	Güzelyalı	983	39	Kartal	Çavusoglu	550
15	Pendık	Fatıh	919	40	Pendık	Sülüntepe	545
16	Tuzla	Yayla	906	41	Beylıkdüzü	Gürpınar merkez	538
17	Büyükçekmece	Batıköy	899	42	Maltepe	Baglarbası	534
18	Tuzla	Içmeler	877	43	Pendık	Bahçelıevler	509
19	Pendık	Kaynarca	865	44	Maltepe	Cevızlı	498
20	Tuzla	Aydıntepe	861	45	Kartal	Karlıktepe	486
21	Bakırköy	Senlık	821	46	Tuzla	Evlıya çelebı	481
22	Pendık	Dumlupınar	808	47	Pendık	Esenler	467
23	Büyükçekmece	Güzelce	791	48	Tuzla	Istasyon	458
24	Kartal	Yunus	777	49	Pendık	Dogu	455
25	Pendık	Esenyalı	769	50	Büyükçekmece	Hürrıyet	447

Approximately 80% of the buildings that have more than 50% possibility to have mean damage according to 0.2 second Sa are occupied as residential buildings as it can be seen from Table 6.19.

Table 6.19 : Distribution of building number that have the possibility of mean damage more than 50 % based on 0.2 sec Sa according to occupation type.

Occupation type of Building	*Building #*
Residence	54834
Commercial Facilities	13825
Industrial Facilities	924
Governmental Facilities	252
Religious Facilities	276
Educational Facilities	236

34,799 of 68,389 buildings that have more than 50% possibility of mean damage, were constructed between 1983 and 1996. The second line of the list is filled with the buildings that were constructed between 1969 and 1982 with 23,565 buildings.

The most vulnerable construction type in Istanbul, according to the mean damage ratio shown as Concrete Framed structures with Unreinforced Masonry Infill Walls with 45,029 of 68,389 buildings according to 0.2 second Sa (Table 6.20).

Table 6.20 : Distribution of building number that have the possibility of mean damage more than 50% based on 0.2 sec Sa according to construction type.

Construction Type	*Building #*
C1	5022
C2	754
C3	45029
PC1	38
PC2	70
RM1	98
S3	141
URM	17231

As a result of this study the real building number of Istanbul were determined as 990,586 for 2013. As a contribution to previous earthquake loss assessment studies of Istanbul, this study provides the actual building data in earthquake damage estimation. Another contribution of this study is to estimate the building damages based on currently added and classified building age data based on remote sensing image and ortho-photomaps of Istanbul. By this way, the real risk of earthquake on buildings have been assessed. This study represents the results of 7.5 Mw deterministic earthquake scenario on the Main Marmara Fault based on 0.2 second period spectral acceleration and peak ground acceleration based earthquake hazard maps of Boore and Atkinson (2008). The results have been classified based on the demand and the possibility to exceed the damage states of heavy and complete damages. Based on the more than 40% exceedance possibility of collapse and heavily damage due to 0.2 sec Sa, 19,679 buildings in Istanbul are exposed to risk. The following results are deducted from these buildings and those buildings are mostly located at the southern shoreline of Istanbul where the Main Marmara Fault is closer to the city. 17,241 of those buildings are occupied as residential buildings and 16,874 of them are between 1 to 3 floors while, 768 of them are between 4 to 7 floors.

The occupation classes of the exposed buildings in Istanbul distributed as 1881 commercial, 251 industrial, 91 governmental, 76 religious, 73 educational facilities. Based on the distribution on heavy and complete damage possibilities to occupancies, the damage that may occur in the commercial and industrial facilities could lead to a secondary disaster such as fire and chemical waste. According to the estimation results, approximately 2200 commercial and industrial buildings may have heavy and complete damage and they have the possibility to trigger secondary disasters that often cause far more damage and problems and increase the impact. If the earthquake occurs during the time of religious observance, it may also pose a major threat to the people gathered in the temples to perform their religious duties. Regarding to the results of this study, it is estimated that 76 worship and 73 educational facilities may have damage during the potential earthquake and this could affect very high number of people within the schools and religious communities.

Another deduction from the estimation results is the damage distribution based on building age classification. 59% of the buildings, which have more than 40% exceedance possibility of collapse and heavily damage due to 0.2 sec Sa, were constructed between 1983 and 1996, while 29% of them were constructed between 1969 and 1982. 9% of the buildings were built pre 1968, while 3% of them were built after 2003.

The construction type which has the highest possibility to have heavy or complete damage was determined as concrete frame with unreinforced masonry infill walls with 11,273 buildings. The second construction type with the highest damage possibility was unreinforced masonry with 7,896 buildings, and the third was concrete moment frame with 323 buildings.

There are 39 districts and 936 sub-districts in Istanbul. According to the number of buildings that have possibility of complete and heavy damage more than 40% according to Sa, the earthquake damage for the buildings based on districts is shown in Figure 6.15. The 10 districts that have the highest heavy and complete damage risk are Tuzla, Pendik, Adalar, Beylikduzu, Bahcelievler, Avcilar, Zeytinburnu, Bakirkoy and Kucukcekmece respectively.If the sub-districts are taken into account for the highest heavy and complete damage risk the distribution of the districts are changed as followed Tuzla, Adalar, Pendik, Beylikduzu, Buyukcekmece, Bahcelievler, Avcilar, Kucukcekmece, Zeytinburnu, Kartal and Bakirkoy respectively (Figure 6.16).

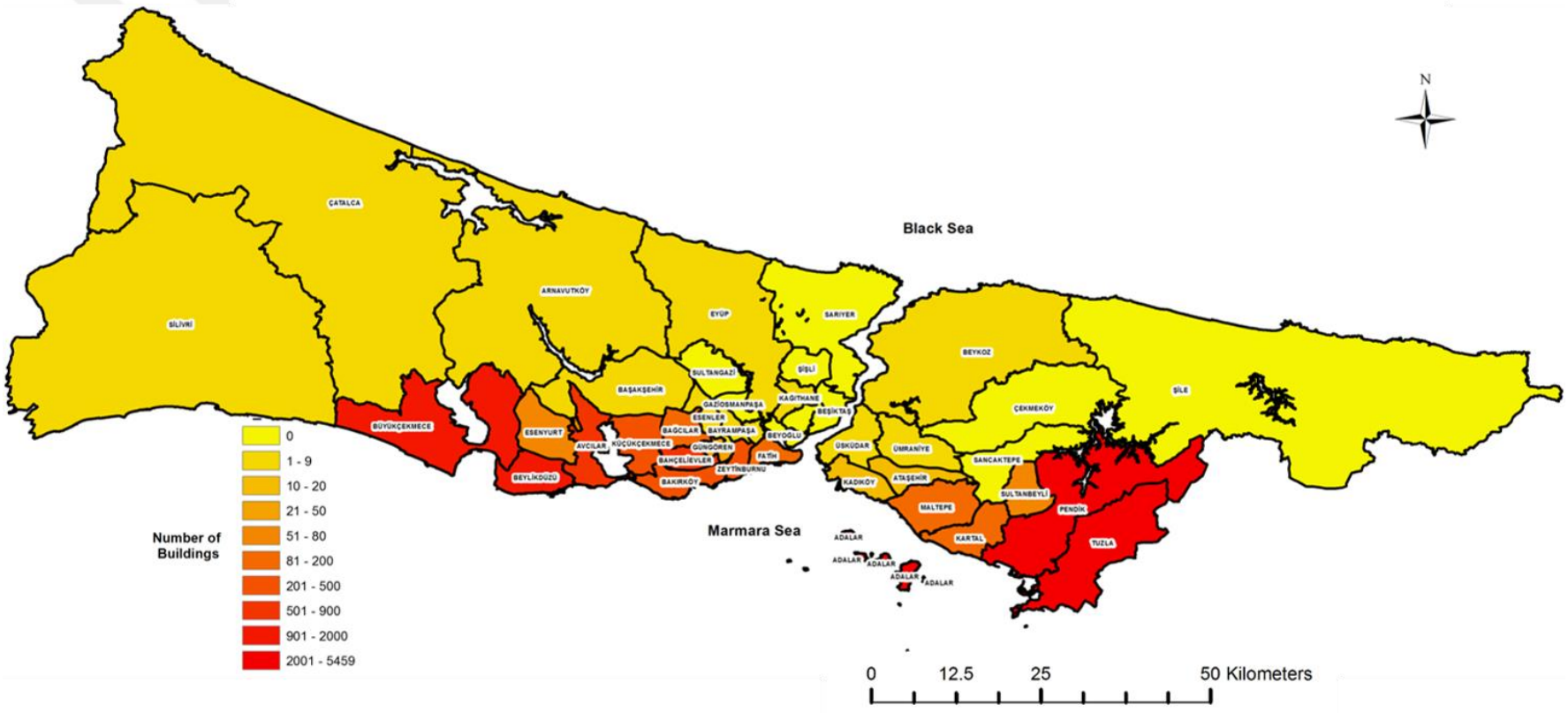


Figure 6.15 : More than 40% Complete and heavy building damage possibility distribution of Istanbul districts based on 0.2 Sa.

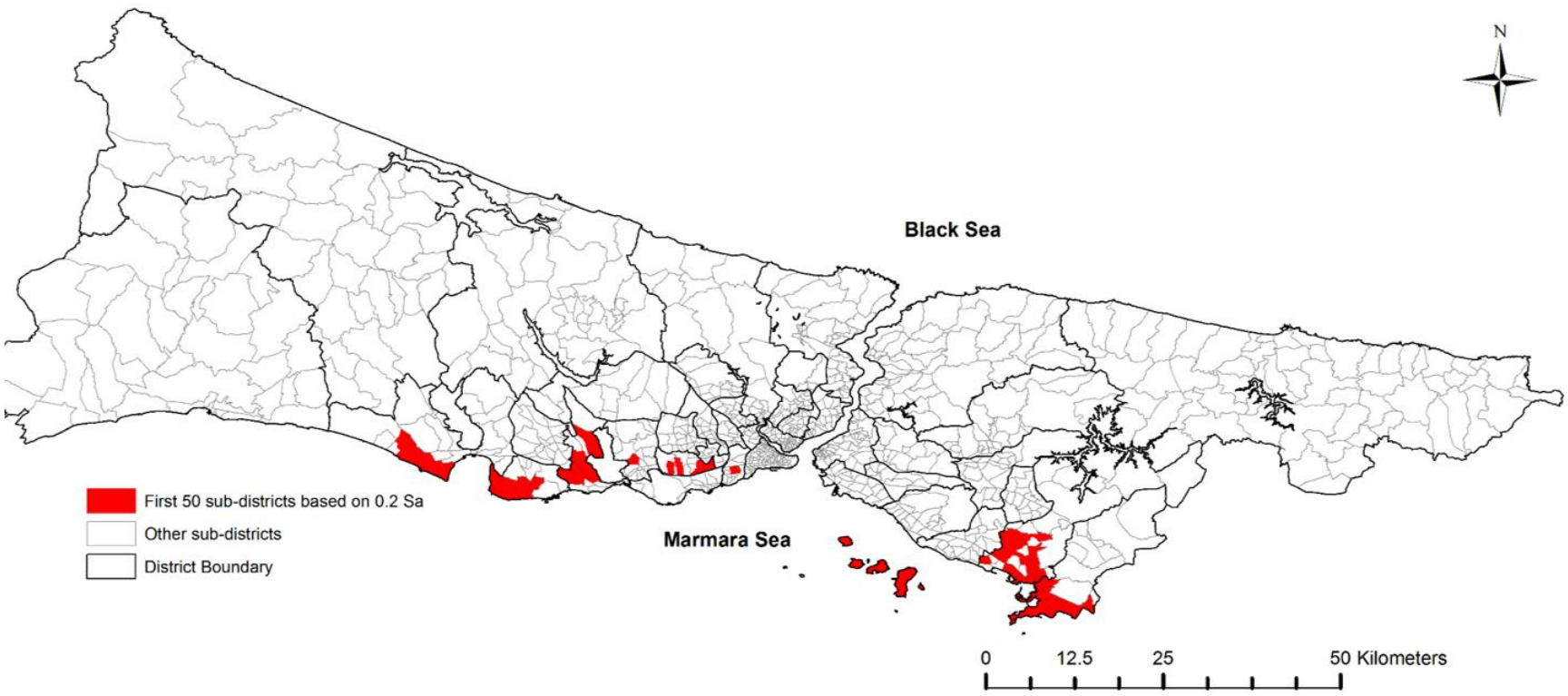


Figure 6.16 : More than 40% Complete and heavy building damage possibility distribution of Istanbuls' first 50 sub-districts based on 0.2 Sa.

There are 2003 buildings in the Mimar Sinan Sub-district, which has the highest damage possibility, and there are 21,874 people living in that sub-district. According to this study's estimations, 1482 buildings in Mimar Sinan sub-district have more than 40% possibility of complete and heavily damage. This means that the damage could occur to more than 75% of buildings. In this case, approximately 15,000 people will be severely affected. The estimation numbers for the other sub-districts are also given at Table 6.21.

Table 6.21 : Building damage situation of some sub-districts.

Sub-District Name	***District Name***	***Population 2014***	***Building # 2013***	***# of Buildings with Complete + Heavy damage possibility > %40***
Mimar Sinan	Tuzla	21874	2003	1482
Ertuğrul Gazi	Pendik	15204	3082	1101
Beştelsiz	Zeytinburnu	25198	1572	102
Bahçelievler	Bahçelievler	63388	1843	92
Yeni Mahalle	Bakırköy	7031	418	16
Muhsine Hatun	Fatih	2414	402	12

7. BUILDING COLLAPSE DIRECTION

7.1 Method of Building Collapse Direction

The collapse direction, distance and debris area estimation method of buildings in Istanbul is based on a potential Istanbul earthquake was obtained from collapsed building data in Gölcük, developed by using near and LDM (Linear Direction Mean) analysis on ArcGIS software. The conceptual workflow and the order of the analysis can be seen in Figure 7.1.

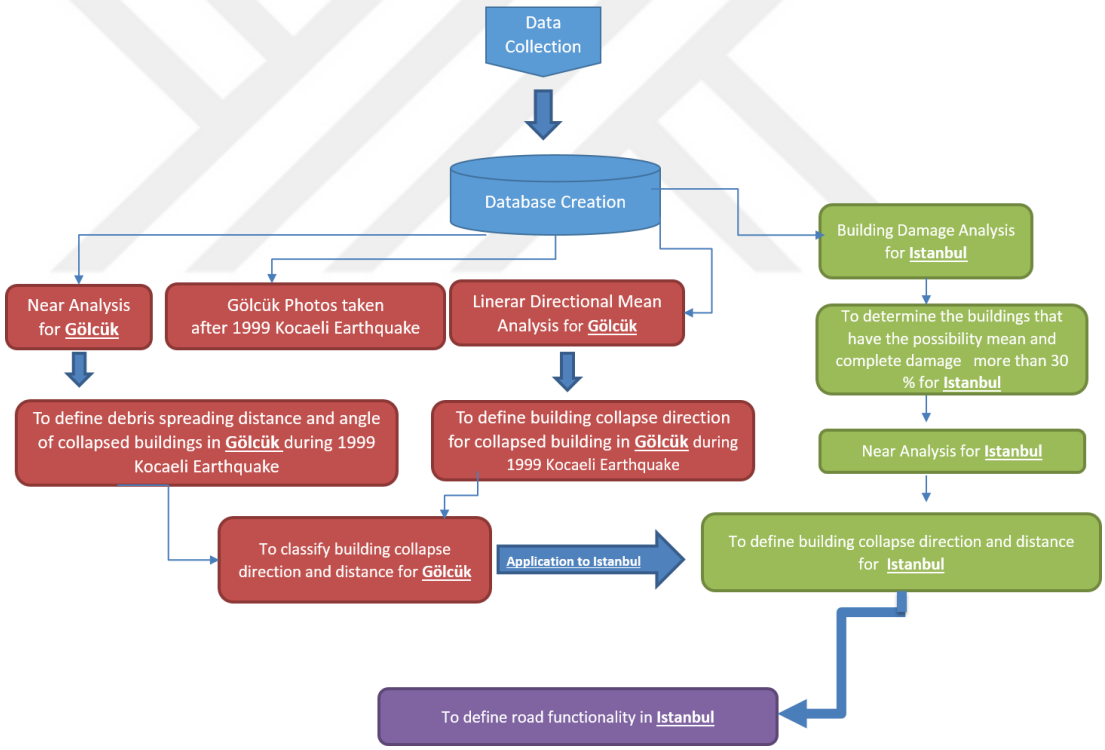


Figure 7.1 : Workflow and the order of the analysis for detecting road functionality based on building collapse direction.

The fist step of this study was to collect the data. Within the scope of this step, the Gölcük aerial photos taken before and after the 1999 Kocaeli Earthquake (in 1994 and September) were obtained from the General Command of Mapping (Figure 7.2).

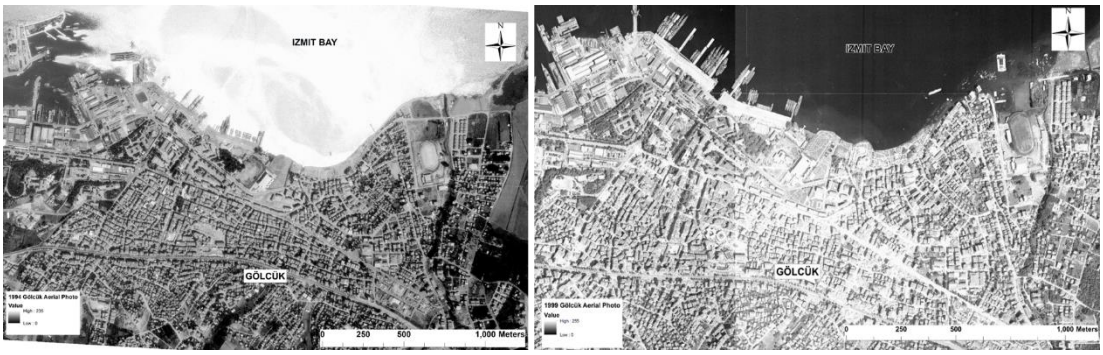


Figure 7.2 : Gölcük aerial photos taken in 1994 and 1999.

Then the polygon shaped building data were created for the 1994 and 1999 Gölcük aerial photos in ArcGIS. The debris spreading distance, angle and direction data were also obtained after making a Near and LDM Analysis. A classification table was created with the data. Then by using these classifications, the values were applied to the buildings in Istanbul, which may have possible damage in an earthquake.

7.1.1 Determination of existing and collapsed buildings in Gölcük

By using the 1994 aerial photo, 2157 building polygons were digitized for definition of the existing buildings in Gölcük before the 1999 earthquakes (Figure 7.3).



Figure 7.3 : The buildings that were built before 1994 in Gölcük.

In order to define the collapsed buildings in Gölcük during the 1999 earthquake, the existing buildings in Gölcük in 1994 were added to on the 1999 aerial photo by using ArcGIS software. The buildings were checked one by one then the collapsed buildings were determined. Therefore, we can conclude that 254 buildings collapsed due to the 1999 earthquake in the study area (Figure 7.4).

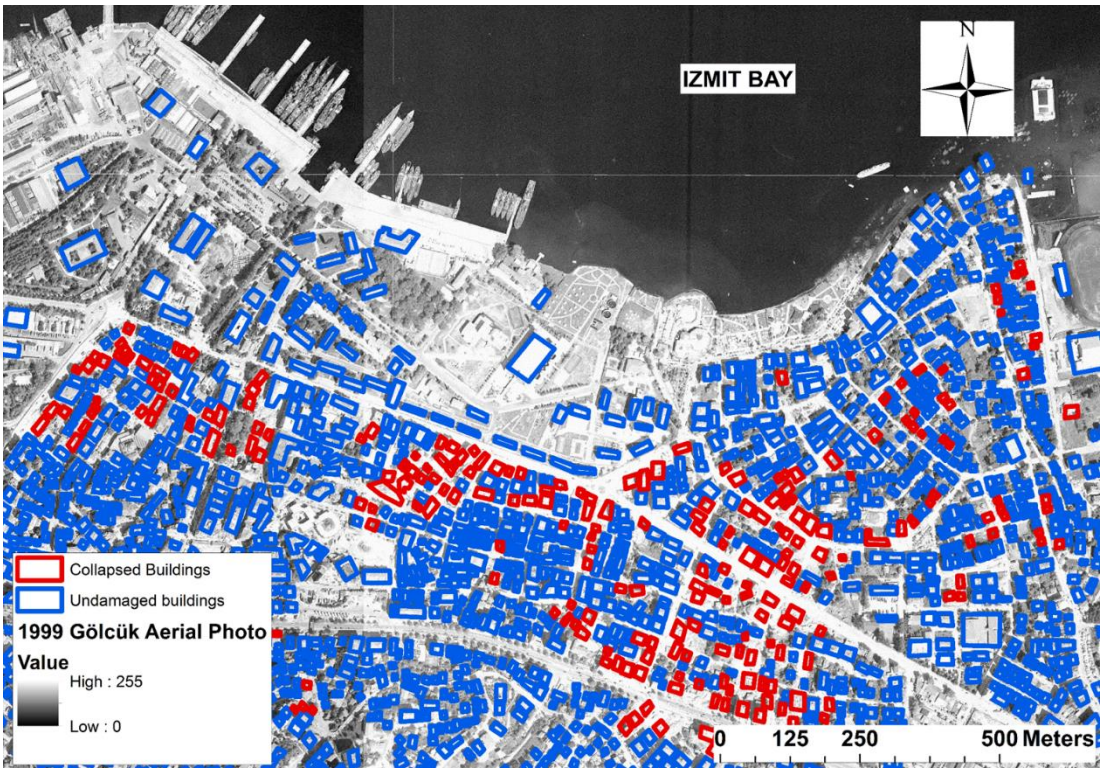


Figure 7.4 : Collapsed buildings in Gölcük during the 1999 Kocaeli Earthquake.

Collapsed buildings cause debris around them; this was seen easily in the1999 aerial photo due to the fact that it had a high resolution (Figure 7.12).

7.1.2 Determination of debris information in Gölcük

To define debris spreading, "building debris spreading polygon data" was produced for every collapsed building.

In order to define the remotest building debris spreading point that has the maximum distance from the collapsed building point, the points were created at different locations on the building debris spreading polygon data. These points were measured one by one from the centre of the collapsed buildings. Then the point that had the remotest distance from collapsed building was defined (Figure 7.5).

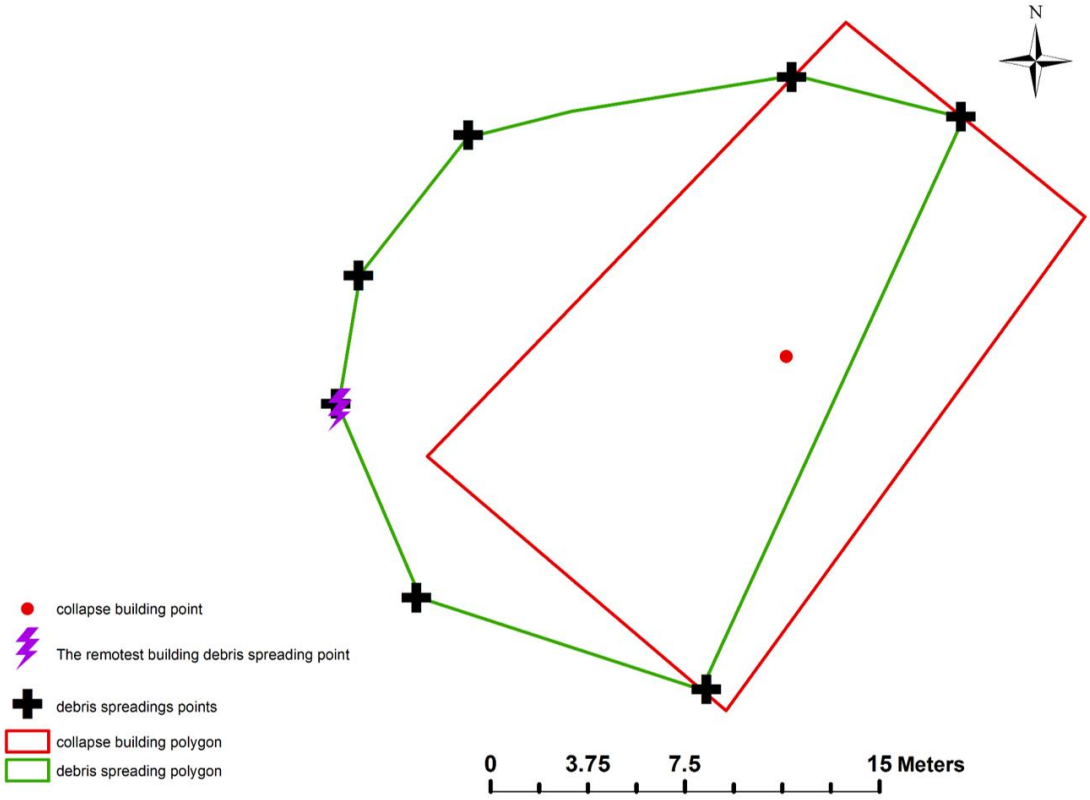


Figure 7.5 : To define the remotest debris spreading point.

Thus “the remotest building debris spreading point data” was generated for every collapsed building on the building debris spreading polygon data according to the remotest point on the polygon circumference from the collapsed building point. Hereinafter it is referred to as a “debris spreading point”. Then “the remotest building debris spreading line data” was generated by crossing a line between the debris spreading data and the collapsed building point for every collapsed building. Hereinafter it is referred to as a “collapse direction” (Figure 7.6).

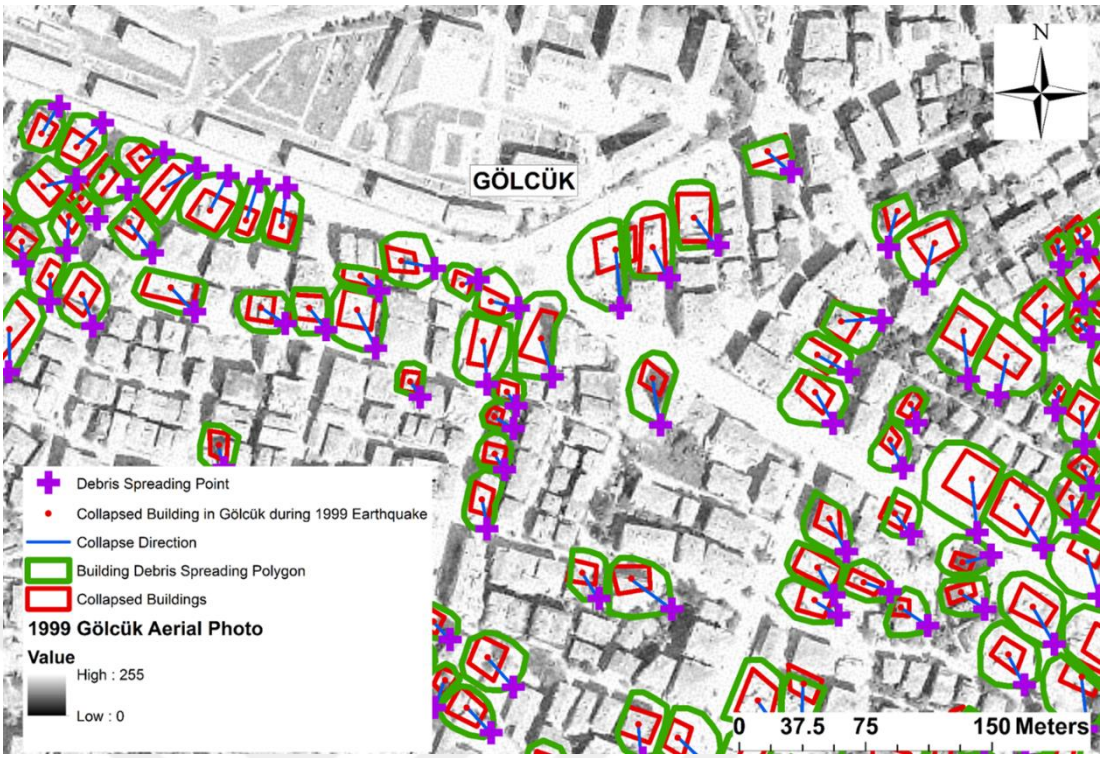


Figure 7.6 : Debris database from 1999 Gölcük aerial photo.

Near analysis on ArcGIS was used to find out the digital connection between the collapsed building location, debris spreading point and fault location (Figure 7.7). This analysis was repeated twice and the results were merged based on the building id number.

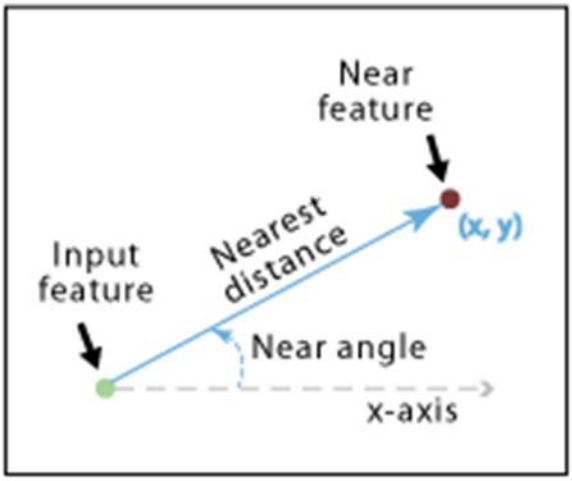


Figure 7.7 : Near analysis illustration on ArcGIS (ArcGIS Help File).

For the first Near analysis, collapsed building points were used as Input features and debris spreading pointS were used as Near future (Figure 7.7). Near analysis needs another point in that its location should be farther than the debris spreading point from the collapsed building centre to calculate the near angle and distance. For this reason,

another point was digitized manually far from the debris spreading point in order to make a near analysis with the debris spreading point. This process was repeated for every 254 collapsed buildings. To decrease the process time, the model builder was created on ArcGIS. The Near analysis was repeated for every collapsed building in Gölcük individually by using this model builder. When running the model, the angle and distance between the collapsed building point and debris spreading point were obtained (Figure 7.8). After finishing the analysis the result tables were merged.

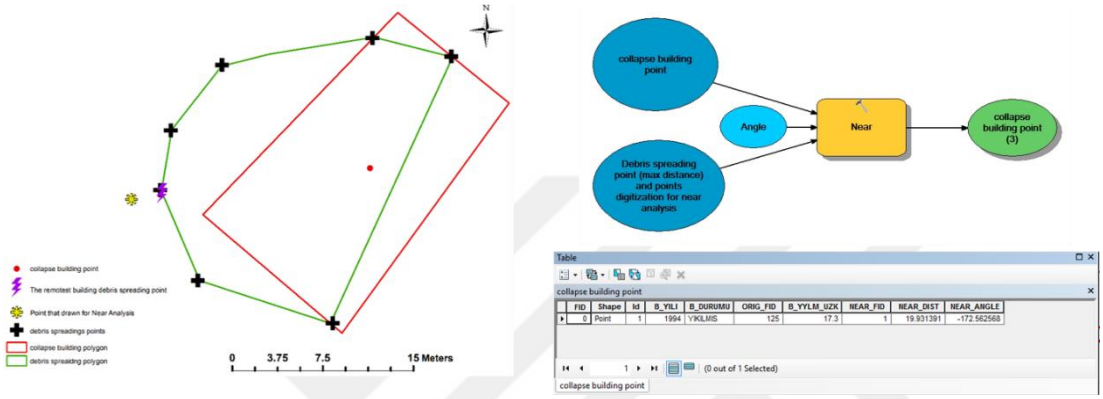


Figure 7.8 : Model builder for near analysis.

In the second Near analysis, collapsed building points were used as Input features and 1999 fault epicentre point were used as Near future. “A 1999 fault epicentre point” was digitized, according to the coordinates of the 1999 the Kocaeli Earthquake Epicentre (40.74 N., 29.86 E.), obtained from USGS (2015).

Model builder was created on ArcGIS and this model was run for every collapsed building individually (Figure 7.9). After finishing the analysis the result tables were merged.

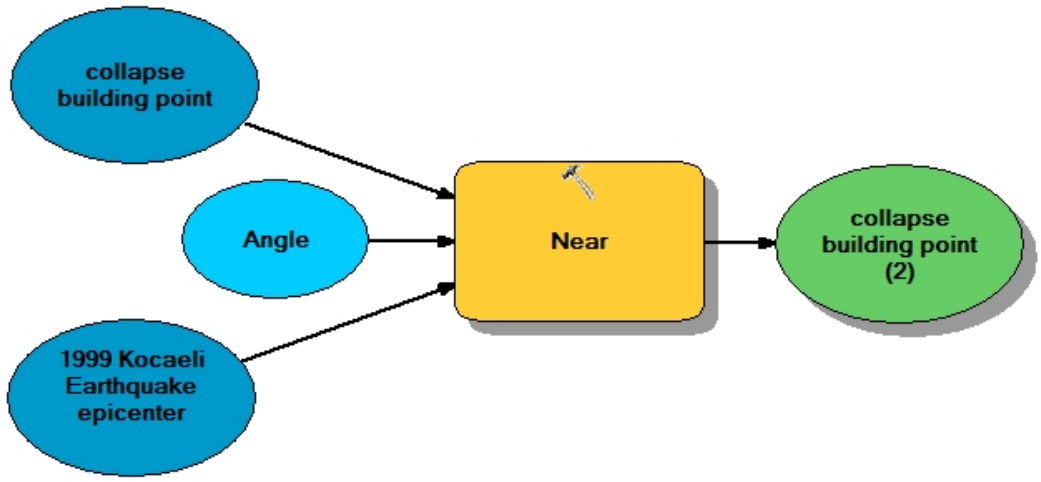


Figure 7.9 : The second model builder for near analysis.

As a result of the analyses, the azimuth angles and horizontal distances of each collapsed building in Gölcük from the epicenter of the 1999 Kocaeli Earthquake, were revealed and the main collapse directions and distances were determined.

The Near angle of the related direction was calculated in any direction according to the nearest coordinate axis in the Near Analysis on ArcGIS. To make a common classification of the collapsed buildings' directions, a reference direction was required for the unique calculation of the spreading angles. That is why it is not possible to use the Near angle values in classifications that were calculated in this way. For this reason, the Near angles obtained from the Near analysis were transformed to Azimuth Angles, which moves in a clockwise direction on a north axis by using the method that is shown in Figure 7.10. Thus, the Azimuth value of the angle between the collapsed building and the 1999 fault point was determined, according to common references and then it was classified. The same process was performed for the angle between the collapsed building and the spreading angle.

In order to calculate the Azimuth angle (t) of the Near analysis angle values (α), the following calculations, were made. If the angle value was higher than 90°, the angle value was subtracted from 450°. If the angle value was between 0 and 90°, the angle value was subtracted from 90°. If the angle value was (-), the angle value was subtracted from 90° (Figure 7.10).

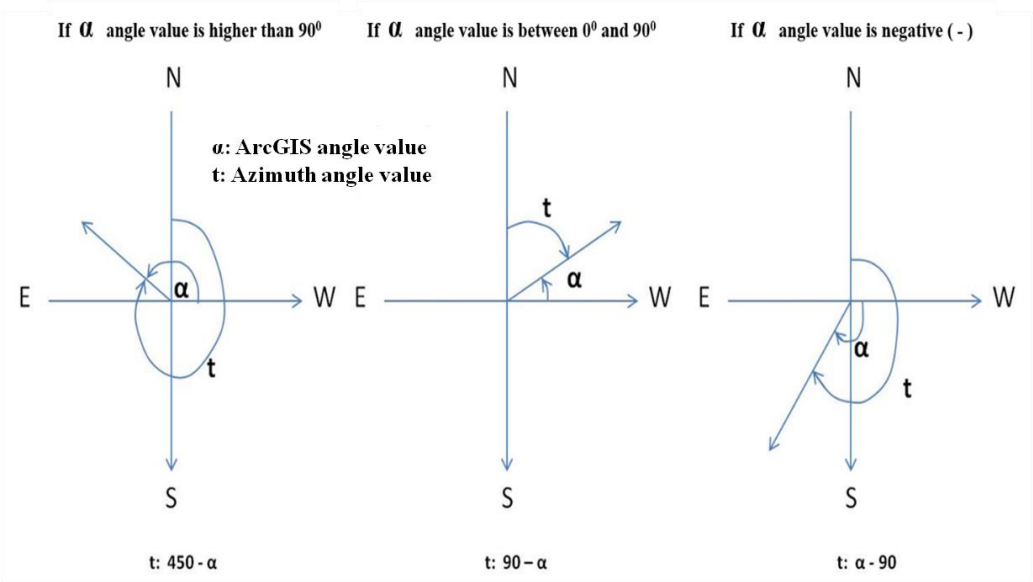


Figure 7.10 : How to obtain azimuth angle value from near analysis angle value.

The calculated Azimuth angle values were added to the fields of every single collapsed building in related tables. The sample table is given in Table 7.1.

Table 7.1 : Sample of near analysis results.

Id	S_Y	N_1	S_F	N_2	T_{1t}	T_{2t}
1	17.34	-173.18	4217.15	31.27	263.18	58.73
2	22.46	-175.32	4250.05	31.44	265.32	58.56
3	17.19	-152.55	4201.43	31.46	242.55	58.54
4	17.21	-98.53	4214.99	32.20	188.53	57.80
5	11.94	-103.25	4184.30	32.03	193.25	57.97

N_1= Collapse direction (Near angle as α between the collapsed building point and the debris spreading point).

S_S = Collapse distance (Near distance between the collapsed building point and the debris spreading point).

N_2= Fault direction (Near angle as α between the collapsed building point and 1999 Fault epicenter point).

S_F = Fault distance (Near distance between the collapsed building point and 1999 Fault epicenter point).

T_{1t} = Azimuth of the collapse direction (as t)

T_{2t} = Azimuth of the fault direction (as t)

Before applying the estimation model to Istanbul, it was necessary to reveal the relationship between the values. For this reason, a correlation analysis was compiled by using the Azimuth angle values. Correlation analysis is the statistical method which is used in order to be able to indicate a predictable linear relationship between two or more random variables by using Pearson's Correlation Coefficient (Table 7.2).

Table 7.2 : Pearson correlation coefficient explanation.

r	Relationship
0,00 – 0,25	Very Weak
0,26 – 0,49	Weak
0,50 – 0,69	Moderate
0,70 – 0,89	Strong
0,90 – 1,00	Very Strong

First step of the correlation analysis, was to sort the buildings according to S_F (fault distance) from the farthest to the nearest point. The second step was to make another correlation analysis between T_{1t} and T_{2t} values (Table 7.3).

Table 7.3 : Correlation analysis results.

Building Number	S_F (meter)	T_{1t}	T_{2t}	Pearson Coefficient	Correlation Relationship
25	4351 - 4499	210.66 - 359.07	53.97 - 57.66	0.72	Strong
51	3806 - 4250	36.66 - 265.82	49.59 - 52.15	0.35	Weak
80	3553 - 3679	102.88 - 203.12	39.61 - 52.31	0.73	Strong
61	3186 - 3395	88.25 - 336.95	38.11 - 47.16	0.66	Moderate
23	2920 - 3089	156.47 - 281.63	36.58 - 43.53	0.46	Weak
14	2671 - 2828	294.46 - 322.56	34.18 - 44.18	0.56	Moderate

Regarding the correlation analyses, the strong and moderately correleted results were chosen to create a model for the building collapse direction estimation.

To determine the average spreading direction of the collapsed building in Gölcük, a LDM Analysis (Linear Directional Mean) on ArcGIS was used (Figure 7.11). In this analysis, the collapse direction was used as an input variable. At the end of the analysis, the average spreading direction of the collapsed building was achieved.

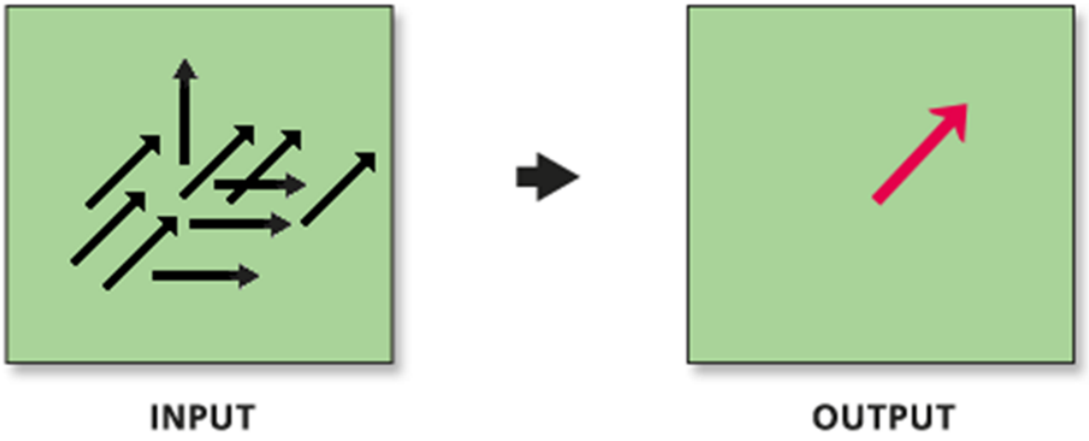


Figure 7.11 : LDM analysis illustration on ArcGIS (ArcGIS Help File).

When LDM analysis was performed for first time, the case field was not filled in. Regarding this analysis, it is determined that the average direction of collapsed building spreading in Gölcük is approximately south (Figure 7.12).



Figure 7.12 : LDM analysis (field case: empty).

When the LDM analysis was repeated for a second time and T_{1t} was chosen as the case field. The spreading direction of the collapsed buildings was distributed in five directions. The spreading direction was classified as: approximately north east as LDM1; approximately north west as LDM2; approximately south LDM3; approximately south east LDM4; and approximately west as LDM5 (Figure 7.13). The

appropriate direction from this classification was defined for every collapsed building in Gölcük by using the collapsed direction.



Figure 7.13 : LDM analysis (field case: $T_{1\text{-}A}$).

7.1.3 The classification of the spreading of the collapsed building in Gölcük

As seen in Figure 2.5, the 1999 Kocaeli Earthquake Epicenter was located in the north east part of Gölcük. However, the location of a potential Istanbul earthquake epicenter is estimated to be in the southern part of the city. To make an affinity between Gölcük and Istanbul, there should be a spatial conformity between the epicenter location and the building inventory belonging to both samples. In the circumstances, it was approved for us to use the Near angle references, which was the nearest axis, instead of the azimuth angle referencing fixed north axis during the affinity. For this reason, the process of transformation from the Near angle to azimuth angle mentioned in previous section was used here.

By using the values of 76 collapsed buildings in Gölcük, 11 classes were created considering the N_2 angle as shown at Table 7.4.

Table 7.4 : Classification of near analysis results of collapsed building in Gölcük based on T_2t azimuth directions.

CLASS	Id	$N_2(^0)$	$N_1(^0)$	S_F (m)	S_S (m)
CLS01	1	31.270	-173.180	4217.146	17.338
CLS01	2	31.436	-175.322	4250.049	22.460
CLS01	3	31.464	-152.554	4201.426	17.194
CLS02	20	31.469	112.253	4033.404	16.008
CLS02	17	31.592	104.689	3970.481	12.300
CLS02	18	31.751	87.231	3962.794	13.832
CLS02	21	31.920	98.713	4037.014	12.960
CLS02	19	31.932	83.102	3952.983	13.681
CLS03	5	32.032	-103.245	4184.300	11.945
CLS03	4	32.202	-98.531	4214.989	17.213
CLS03	25	32.471	-105.535	4083.368	14.555
CLS04	38	34.465	104.902	3926.233	11.643
CLS04	37	34.740	87.367	3952.922	16.609
CLS04	36	35.069	90.566	3951.643	15.290
CLS05	92	37.552	-88.522	3753.536	11.819
CLS05	90	38.011	-88.963	3724.207	10.326
CLS05	94	38.136	-90.954	3743.852	15.840
CLS05	91	38.362	-87.156	3725.053	13.296
CLS05	62	38.448	-93.315	3693.795	20.428
CLS05	80	38.767	-91.857	3724.298	15.487
CLS05	81	38.914	-91.473	3763.304	25.545
CLS06	64	39.229	62.497	3626.369	23.398
CLS06	65	39.516	71.434	3613.660	24.626
CLS06	66	39.773	82.970	3599.420	23.205
CLS07	70	40.234	-33.676	3639.981	17.151
CLS07	71	40.758	-12.876	3558.634	20.214
CLS07	96	41.619	-13.378	3534.397	16.876
CLS08	98	42.207	-73.136	3526.948	23.091
CLS08	114	42.279	-60.968	3441.429	19.805
CLS08	115	42.340	-50.263	3411.456	20.491
CLS08	116	42.344	-40.749	3352.575	18.697
CLS08	102	42.365	-55.798	3563.260	9.980
CLS08	100	42.722	-57.511	3593.598	10.925
CLS08	208	42.838	-68.143	3135.133	27.105
CLS08	104	44.059	-48.161	3679.638	23.765
CLS08	119	44.108	-56.554	3604.337	17.741
CLS08	107	44.258	-45.616	3709.398	20.699
CLS08	110	44.429	-59.834	3430.440	21.363

Table 7.4 (continued) : Classification of near analysis results of collapsed building in Gölcük based on T_2t azimuth directions.

CLASS	Id	$N_2(^0)$	$N_1(^0)$	S_F (m)	S_S (m)
CLS09	189	45.043	-85.287	3342.133	28.345
CLS09	199	45.073	-81.935	3264.924	14.081
CLS09	193	45.185	-75.159	3395.152	11.639
CLS09	123	45.287	-83.984	3715.700	30.253
CLS09	198	45.403	-77.940	3237.441	19.768
CLS09	125	45.489	-80.946	3644.056	20.155
CLS09	201	45.506	-86.948	3268.609	17.491
CLS09	124	46.018	-95.168	3656.907	22.531
CLS09	178	46.148	-83.705	3401.588	31.396
CLS09	120	46.179	-79.487	3687.097	31.468
CLS09	210	46.336	-66.468	3089.287	22.369
CLS09	143	46.345	-95.019	3558.457	27.400
CLS09	206	46.366	-97.342	3288.225	22.958
CLS09	184	46.458	-85.986	3326.031	21.035
CLS09	209	46.671	-68.375	3172.181	14.373
CLS09	205	46.789	-93.968	3284.766	25.346
CLS09	181	46.887	-70.579	3351.046	12.856
CLS09	131	46.898	-77.381	3774.794	30.922
CLS09	130	46.942	-83.967	3752.975	20.833
CLS09	129	46.977	-84.383	3724.321	27.721
CLS10	155	48.068	-111.538	3596.019	17.311
CLS10	138	48.250	-112.868	3632.748	29.140
CLS10	175	48.346	-117.468	3489.442	12.407
CLS10	153	48.578	-113.117	3565.719	28.838
CLS10	134	48.718	-131.848	3685.208	29.857
CLS10	151	48.938	-110.549	3553.648	26.866
CLS11	243	50.853	177.734	3031.195	16.538
CLS11	225	50.913	151.014	2825.179	33.247
CLS11	247	51.016	117.750	3119.245	14.029
CLS11	248	51.587	157.603	3186.402	32.239
CLS11	249	51.599	143.560	3218.696	12.659
CLS11	250	51.888	113.049	3206.826	12.381
CLS11	238	52.131	148.699	2976.391	14.392
CLS11	237	52.373	138.757	2988.570	14.462
CLS11	223	52.718	142.446	2804.747	21.404
CLS11	239	53.421	170.596	3025.384	18.884
CLS11	236	55.083	127.741	2671.752	22.004
CLS11	235	55.816	118.293	2785.006	24.284

The average angle and distance for each of the 11 classes were determined by judging the 11 classes on their own merit.

The collapsed building in Gölcük belonging to Class 1 (CLS 01), in which the the N_2 angles were changed between 31.2700 – 31.4640, were demolished with an average spreading angle of -167.0190. These types of collapsed buildings created an average distance debris of 18.998 m. The collapse direction of this type of building was LDM 5 and the direction of the debris was concentrated approximately to the east . The collapsed buildings in Gölcük belonging to Class 2 (CLS 02), in which the N_2 angles were changed between 31.4690 – 31.9320, were demolished with an average spreading angle of 97.1980. These types of collapsed buildings created an average distance of debris of 13.756 m. The collapse direction of this type of building was LDM 1 and the direction of the debris was concentrated approximately to the north east. The collapsed buildings in Gölcük belonging to Class 3 (CLS 03), in which the N_2 angles were changed between 32.0320 – 32.4710, were demolished with an average spreading angle of -102.4370. These types of collapsed buildings created an average distance of debris of .14.571 m The collapse direction of this type of building was LDM 3 and the direction of the debris concentrated approximately to the south. The collapsed buildings in Gölcük belonging to Class 4 (CLS 04), in which the N_2 angles were changed between 34.4650 – 35.0690, were demolished with an average spreading angle of 94.2780. These types of collapsed buildings created an average distance of debris of 14.514 m. The collapse direction of this type of building was LDM 1 and the direction of the debris concentrated approximately to the north east. The collapsed buildings in Gölcük belonging to Class 5 (CLS 05), in which the N_2 angles were varied between 37.5520 – 38.9140, were demolished with an average spreading angle of -90.3200. These types of collapsed buildings created an average distance of debris of 16.106 m. The collapse direction of this type of building was LDM 3 and the direction of the debris concentrated approximately to the south. The collapsed buildings in Gölcük belonging to Class 6 (CLS 06), in which the N_2 angles were changed between 39.2290 – 39.7730, were demolished with an average spreading angle of 72.3000. These types of collapsed buildings created an average distance of debris of 23.743 m. The collapse direction of this type of building was LDM 1 and the direction of the debris concentrated approximately to the north east. The collapsed buildings in Gölcük belonging to Class 7 (CLS 07), in which the N_2 angles were changed between 40.2340

– 41.6190 were demolished with an average spreading angle of -19.9770. These types of collapsed buildings created an average distance of debris of 18.081 m. The collapse direction of this type of building was LDM4 and the direction of the debris concentrated approximately to the south east . The collapsed buildings in Gölcük belonging to Class 8 (CLS 08), in which the N_2 angles were changing between 42.2070 – 44.4290, were demolished with an average spreading angle of -56.0670. These types of collapsed buildings created an average distance of debris of 19.424 m. The collapse direction of this type of building was LDM 4 and the direction of debris concentrated approximately to the south east . The collapsed buildings in Gölcük belonging to Class 9 (CLS 09), in which the N_2 angles were changed between 45.0430 – 46.977, were demolished with an average spreading angle of -82.7010. These types of collapsed buildings created an average distance of the debris of 22.647 m. The collapse direction of this type of building was LDM 3 and the direction of debris concentrated approximately to the south . The collapsed buildings in Gölcük belonging to Class 10 (CLS 10), in which the N_2 angles were changed between 48.0680 – 48.9380, were demolished with an average spreading angle of -116.2310. These types of collapsed buildings created an average distance of debris of 24.070 m. The collapse direction of this type of building was LDM 3 and the direction of debris concentrated approximately to the south . The collapsed buildings in Gölcük belonging to Class 11 (CLS 11), in which the N_2 angles were changed between 50.8530 – 55.8160, were demolished with an average spreading angle of 142.2700. These types of collapsed buildings created an average distance of debris of 19.710 m. The collapse direction of this type of building was LDM 2 and the direction of the debris concentrated approximately to the north west. The average of these values is given in Table 7.5; these values will be applied to Istanbul in order to reveal the road functionality in Istanbul.

Table 7.5 : The average N_1 and S_S according to classification of spreading direction of the collapsed building in Gölcük.

CLASS	N_1 (^{0}) (Average)	S_S (m) (Average)	LDM _CLASS	Spreading direction
CLS01	-167.0185418	18.99756461	LDM 5	approximately to the east
CLS02	97.19761347	13.75613674	LDM 1	north east
CLS03	-102.4370561	14.57107244	LDM 3	approximately to the south
CLS04	94.27849198	14.51383269	LDM 1	north east
CLS05	-90.32007257	16.10592112	LDM 3	approximately to the south
CLS06	72.30034224	23.74302077	LDM 1	north east
CLS07	-19.97654196	18.08067693	LDM 4	south east
CLS08	-56.06655713	19.42388347	LDM 4	south east
CLS09	-82.70132102	22.64697342	LDM 3	approximately to the south
CLS10	-116.2311189	24.06986405	LDM 3	approximately to the south
CLS11	142.2701782	19.71037329	LDM 2	north west

When all the collapsed buildings in Gölcük were assessed according to N_2 (x) and N_1 (y), in order to reveal relationship between them, the formula given in the Figure 5.23 was obtained. The horizontal axis shows the N_2 angle and vertical axis shows the N_1 angle. In order to obtain from N_2 to N_1, we tried to find a formula by formatting the trendline option on Excel. Trendlines are used to graphically display trends in data and to help analyze problems of prediction. When a chart is added, a trendline can be generated in Microsoft Office Excel. Polynomial trendlines were choosen in this study. A trendline is most accurate when its R-squared value is at, or near, 1. Excel automatically calculates its R-squared value. Within the context of this study, five formulas were obtained, in order to apply the test to Istanbul. But because R-squared value was not near 1, these formulas were not used for Istanbul's buildings (Figure 7.14, Figure 7.15, Figure 7.16, Figure 7.17).

When all the collapsed buildings in Gölcük were assessed according to N_2 (x) and N_1 (y), in order to reveal the relationship between them, the formula given in Figure 7.14 was obtained. The horizontal axis show the N_2 angle and the vertical axis shows the N_1 angle.

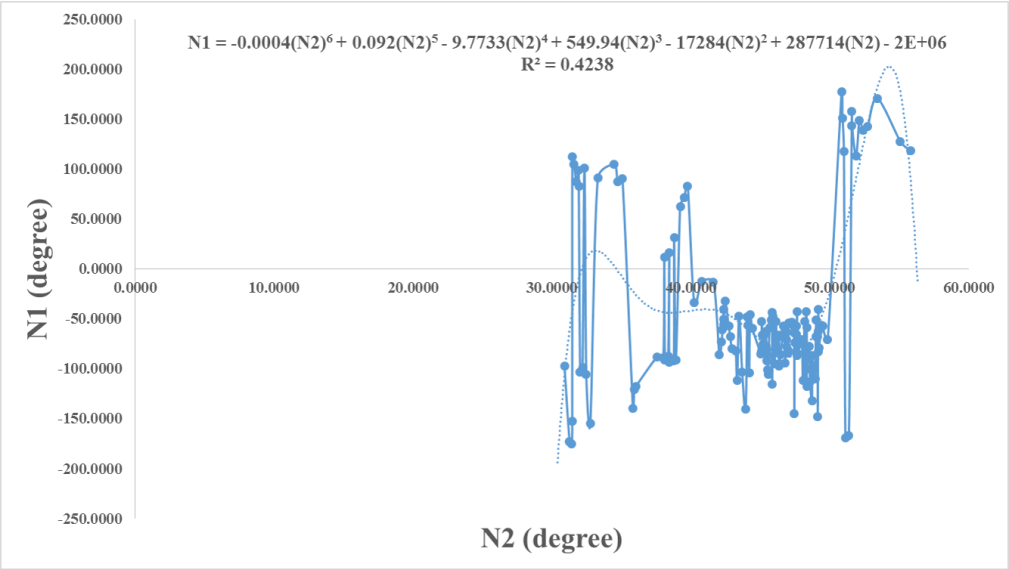


Figure 7.14 : The formula between N_2 and N_1 obtained from collapsed buildings in Gölcük.

When all the collapsed buildings in Gölcük were assessed according to N_2 (x) and T_{1t} (y), in order to reveal the relationship between them, the formula given in Figure 7.15 was obtained. The horizontal axis shows the N_2 angle and the vertical axis shows the T_{1t} angle.

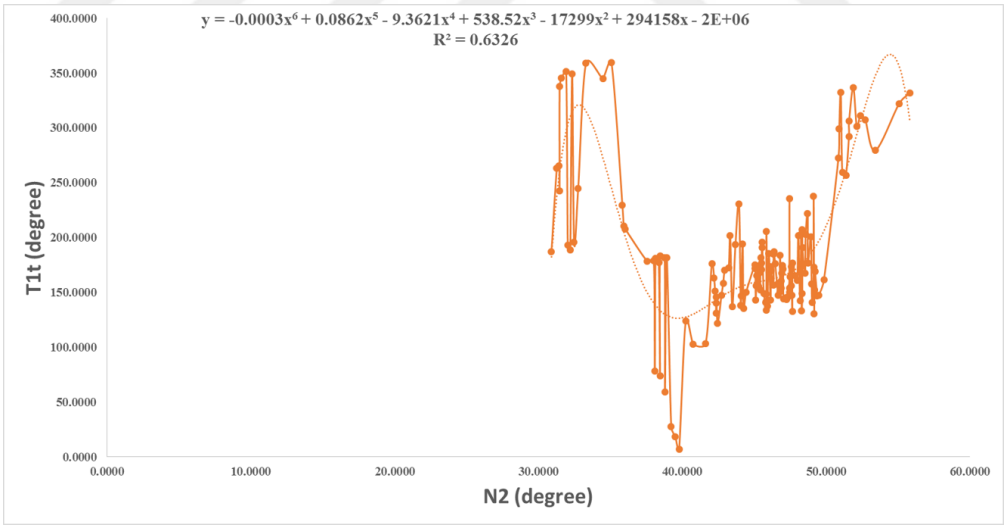


Figure 7.15 : The formula between N_2 and T_{1t} obtained from collapsed buildings in Gölcük.

When the building classes in Gölcük were assessed according to N_2 (x) and N_1 (y) in order to reveal the relationship between them, the formula given in Figure 7.16 was obtained. The horizontal axis shows the N_2 angle and the vertical axis shows theN_1 angle.

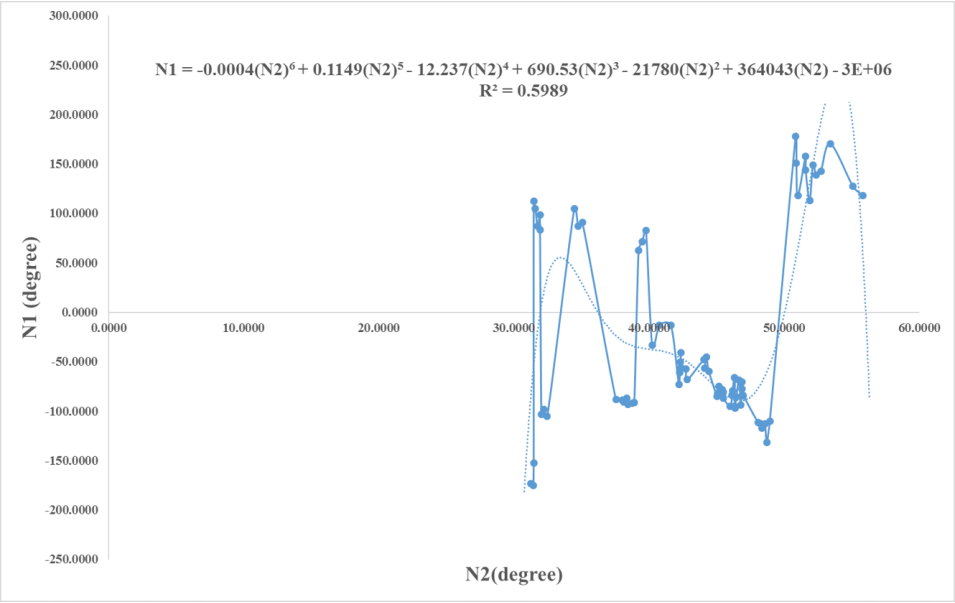


Figure 7.16 : The formula between N_2 and N_1 obtained from building classes in Gölcük.

When the building classes in Gölcük were assessed according to N_2 (x) and T_{1t} (y) in order to reveal the relationship between them, the formula given in Figure 7.17 was obtained. The horizontal axis shows the N_2 angle and the ertical axis shows the T_{1t} angle.

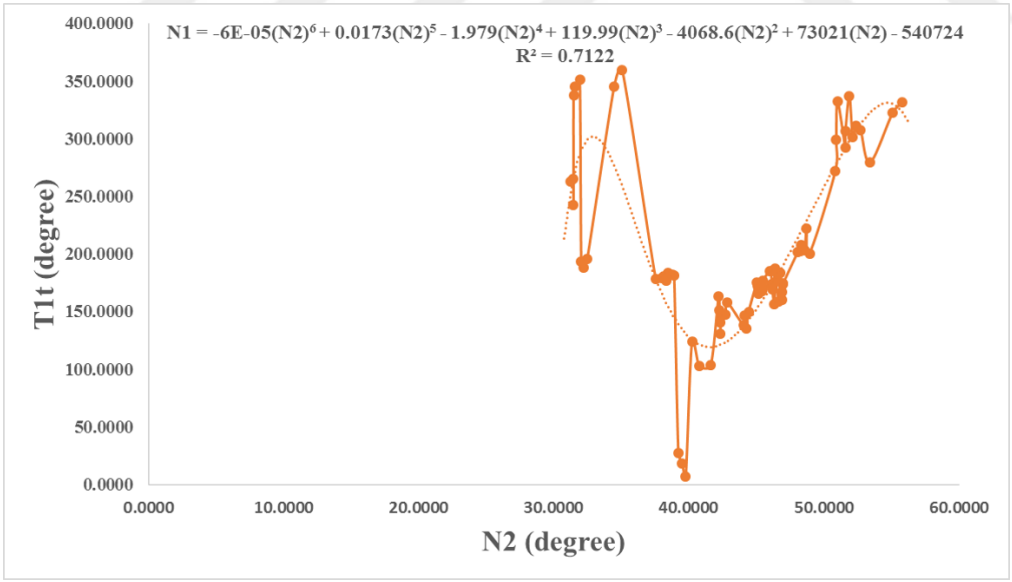


Figure 7.17 : The formula between N_2 and T_{1t} obtained from building classes in Gölcük.

7.1.4 Average collapsed distance determination

The method (classification) that was obtained in the previous section was applicable only to angles between 31.270º and 55.816 º. In order to be applicable to all buildings in Istanbul with a buffer analysis, the second method was formed by using the avearage distance. The average distance was determined by following the steps below.

The collapsed buildings in Gölcük caused debris around the buildings. In order to find the minimum, maximum and average spreading of the collapsed buildings, 80 collapsed buildings from the 254 collapsed buildings were chosen. Adding to the collapse direction, building debris spreading lines were drawn in all directions around the collapsed buildings. As a result, 317 debris spreading vectors in every direction were obtained (Figure 7.18).



Figure 7.18 : Debris spreading vectors around the collapsed buildings in Gölcük.

According to the statistical process between 317 debris spreading vectors in every direction, the maximum distance of the debris of the collapsed buildings in Gölcük was 37.18m, the average distance of the debris of the collapsed buildings in Gölcük was 17.45m and the least distance of the debris of the collapsed buildings in Gölcük is 4.81m (Figure 7.19).

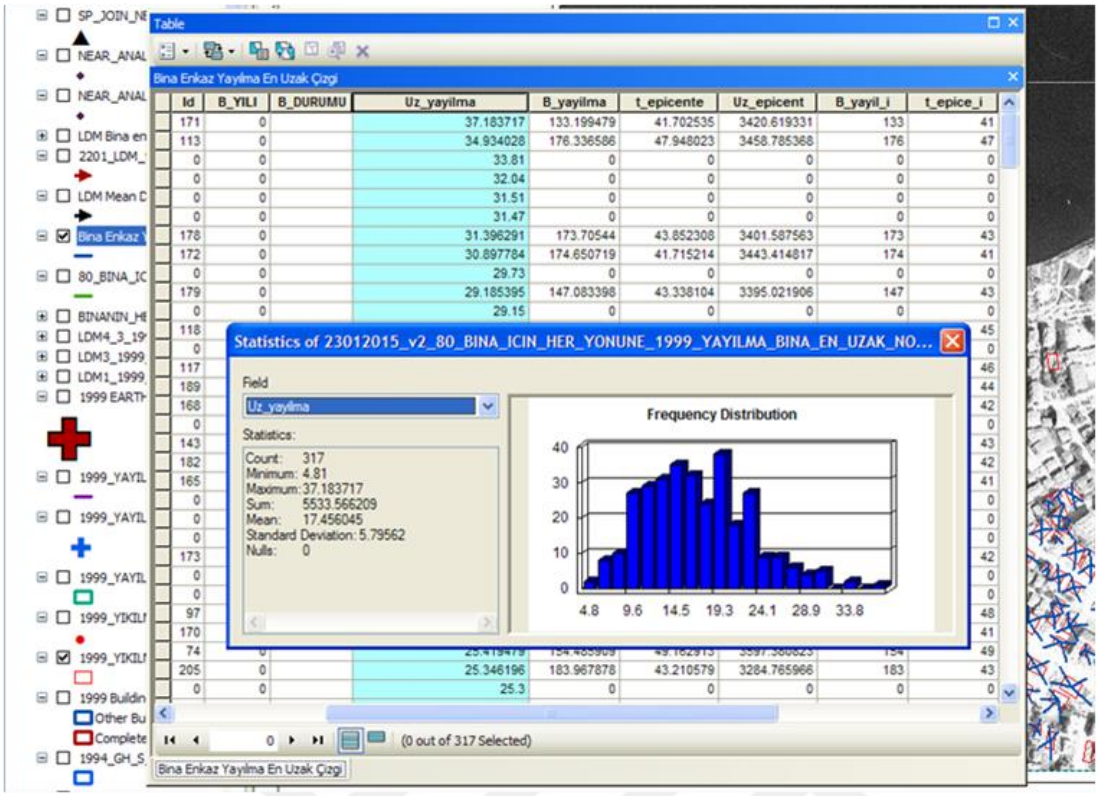


Figure 7.19 : Determination of average collapsed building spreading.

7.2 Building Collapse Direction Analysis in Istanbul

7.2.1 Building collapse direction classification method

It was determined that there were 990584 buildings in Istanbul in 2013 (Figure 4.1). In order to determine the potential collapsed building spreading direction and distance, it was necessary to calculate the building damage possibility for every single building in Istanbul against the anticipated Istanbul earthquake risk.

According to building damage analysis using HAZTURK software, there are 680817 buildings in Istanbul that have the possibility for mean damage of more than 30% against to Sa (Figure 7.20).

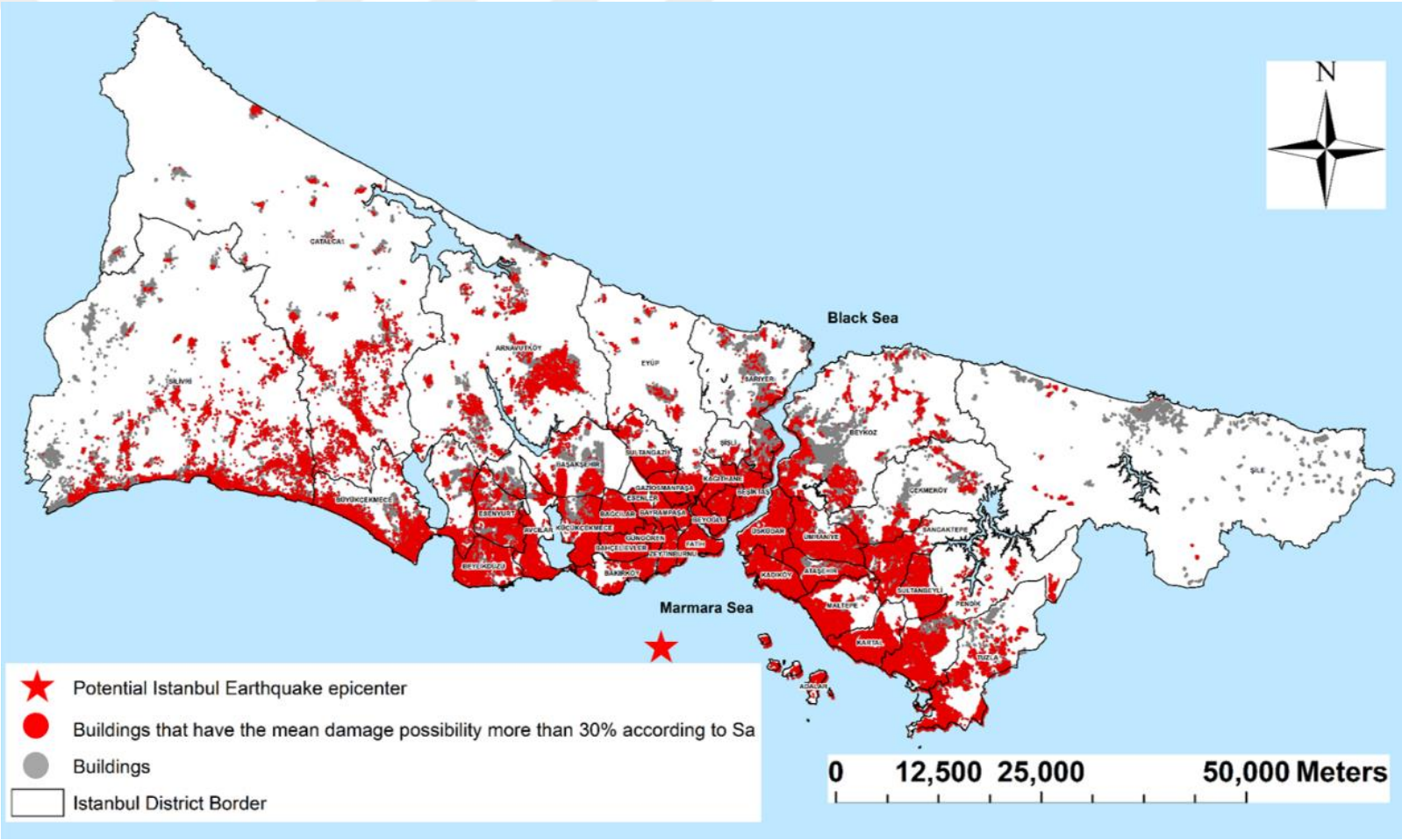


Figure 7.20 : The buildings in Istanbul that have the mean damage possibility more than 30% .

To determine the N_1 angle, S_S distance and LDM direction of the buildings that have the mean damage possibility of more than 30% in Istanbul, it was necessary to calculate the N_2 angle, which is the near angle between these building points and the anticipated Istanbul Earthquake epicenter point by making a Near analysis. After performing the Near analysis, N_1 and S_S values were defined for the buildings that have the possibility of more than 30% mean damage in Istanbul.

In this step, the N_1 angles of buildings in Istanbul were assigned by using N_2. In Gölcük, the N_2 angle values changed between 31.2700 and 55.8160. So the classification tables were created between these values. For this reason, the buildings whose Near angle values in Istanbul lay outside of the range 31.2700 and 55.8160 were deleted. After deleting buildings that have the inappropriate N_2 values, there were 44642 buildings in Istanbul whose Near angles were between 31.2700 and 55.8160 (Figure 7.21).

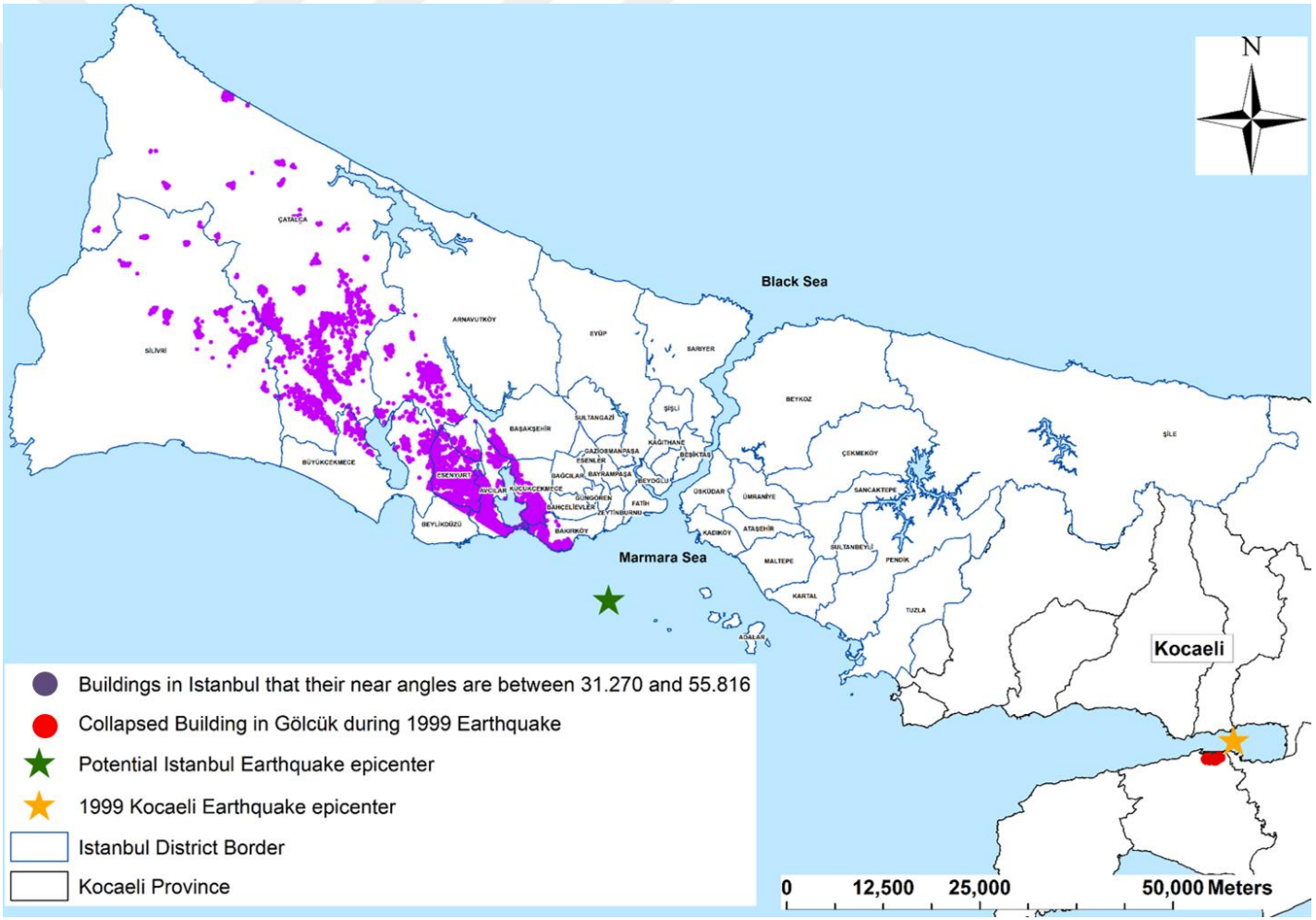


Figure 7.21 : The buildings in Istanbul that their near angles are between 31.2700 – 55.8160.

Regarding classification of the spreading direction of the collapsed building tables in Istanbul, there were 630 buildings belonging to CLS01, 1214 buildings belonging to CLS02, 1208 buildings belonging to CLS03, 2267 buildings belonging to CLS04, 6513 buildings belonging to CLS05, 2011 buildings belonging to CLS06, 5381 buildings belonging to CLS07, 7098 buildings belonging to CLS08, 2929 buildings belonging to CLS09, 1421 buildings belonging to CLS10, and 13970 buildings belonging to CLS11. It is expected that the collapse direction of CLS01 buildings would be LDM5 (approximately east), the collapse direction of CLS02, CLS04, CLS06 buildings would be LDM1 (north east), the collapse direction of CLS03, CLS05, CLS09, CLS10 buildings would be LDM3 (south), the collapse direction of CLS07, CLS08 buildings would be LDM4 (south east), the collapse direction of CLS11 buildings would be LDM2 (north west) (Figure 7.22).

By using the average S_S for every class value given in Table 4 and taking into account the LDM class (collapsed buildings spreading direction), the possible road blockages were determined for these areas in Istanbul. The current road network in Istanbul is approximately 30325 km, of which, according to the road blockage analysis, approximately 888 kms of road could decrease its functionality (Figure 7.23). As seen in Figure 7.24, possible non-functional roads in Istanbul are located in the most populated area in Istanbul.

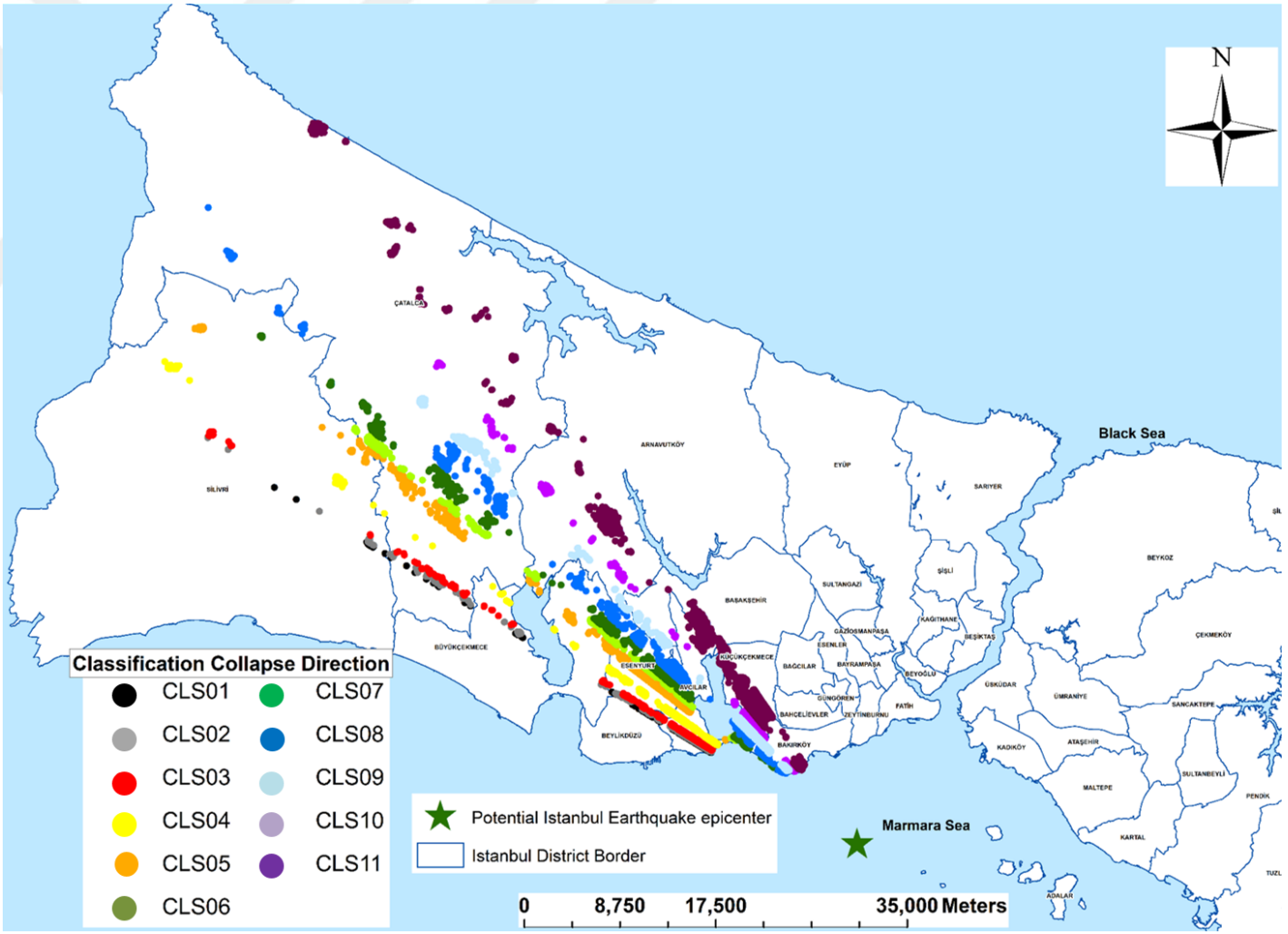


Figure 7.22 : The distribution of collapse direction classification in Istanbul.

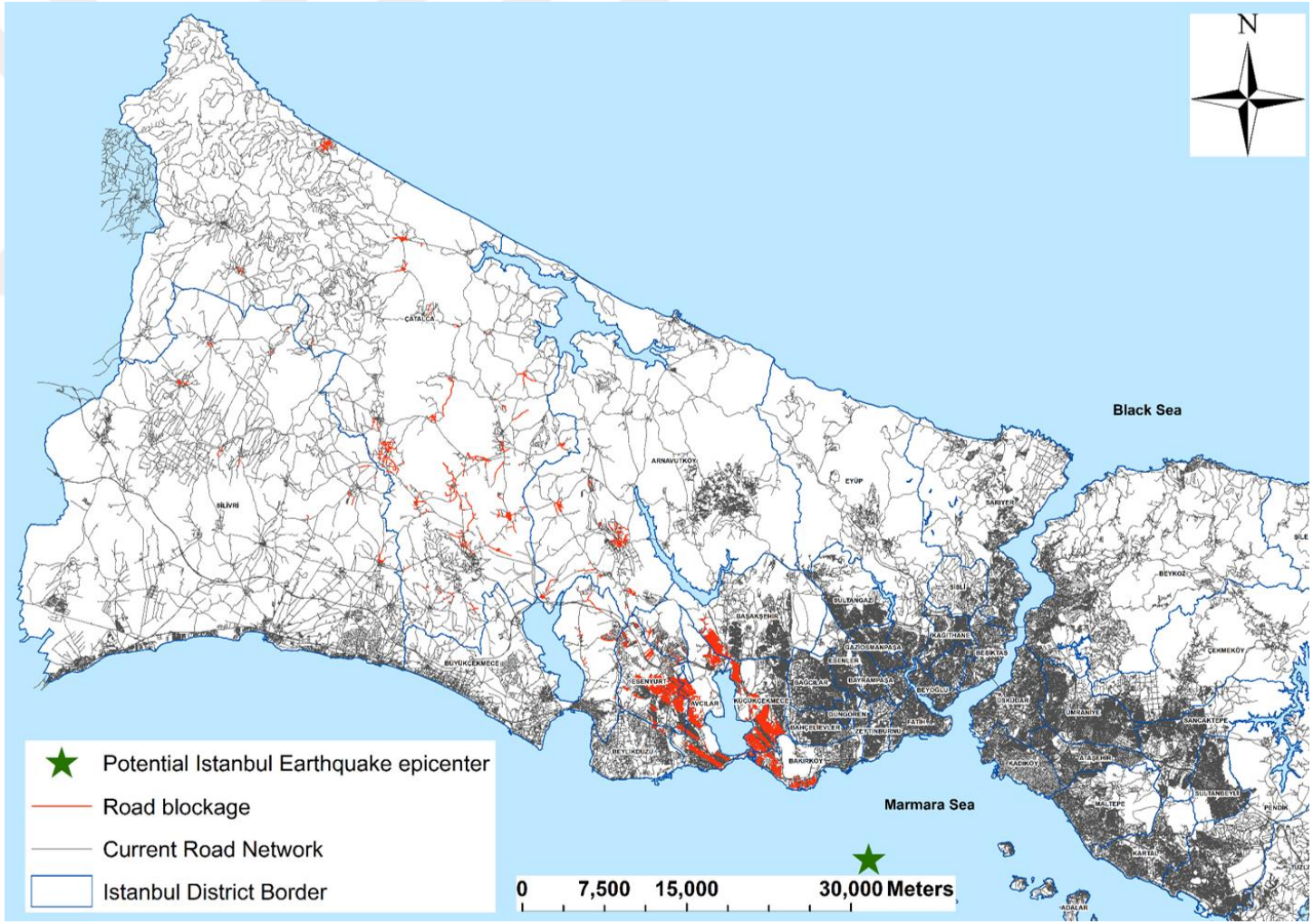


Figure 7.23 : Road blockage in Istanbul because of the building collapse direction.

7.2.2 Building collapse direction in Küçükçekmece

The Küçükçekmece district was selected for the next step of this study in order to examine possible road blockages in detail. This was because most of the buildings in Istanbul which had N_2 angles which were suitable for the classification tables were located in Küçükçekmece. There were 35589 buildings in Küçükçekmece in 2013 (Figure 7.24).

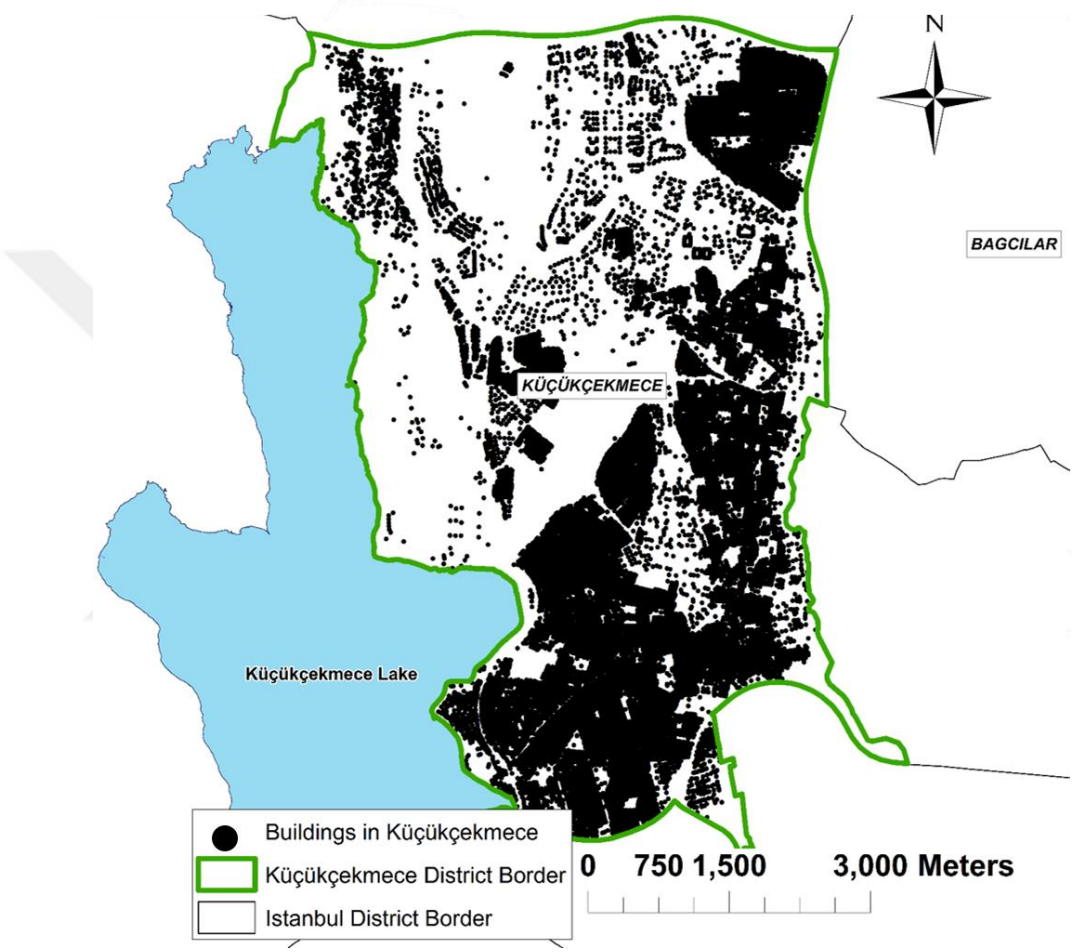


Figure 7.24 : Buildings in Küçükçekmece.

According to building damage analysis calculated by using HAZTURK software, there are 31061 buildings that have the possibility of more than 30% mean damage (Figure 7.25).

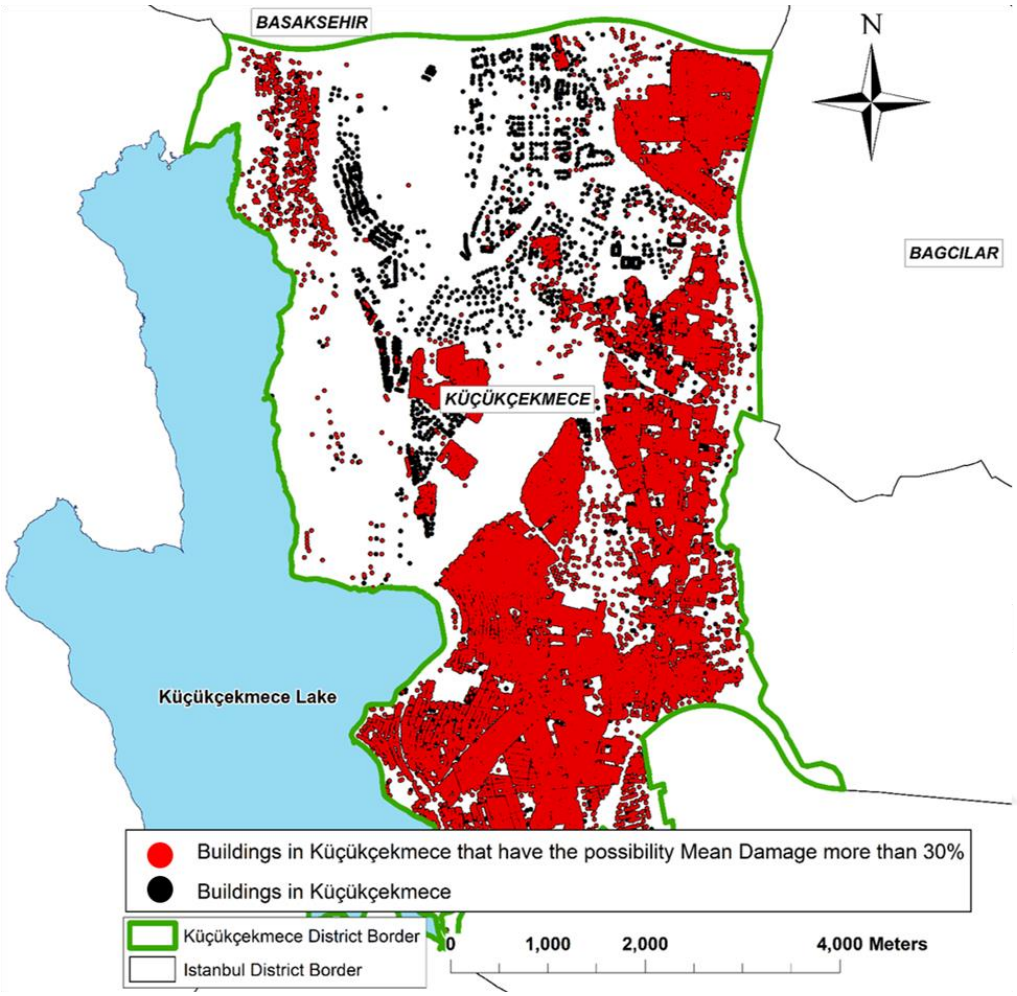


Figure 7.25 : Buildings in Küçükçekmece with more than 30% mean damage possibility.

When the buildings were deleted which had the N_2 angles which were not between 31.2700 - 55.8160, there were 12292 buildings in Küçükçekmece that were suitable for classification of possible spreading direction and distance of collapsed buildings as obtained from the Gölcük study. Regarding this classification, there were 10 buildings belonging to CLS06, 91 buildings belonging to CLS07, 439 buildings belonging to CLS08, 1346 buildings belonging to CLS09, 955 buildings belonging to CLS10, 9451 buildings belonging to CLS11 in Küçükçekmece. These buildings will cause debris in directions LDM1, LDM4, LDM3 and LDM2 (Figure 7.26).

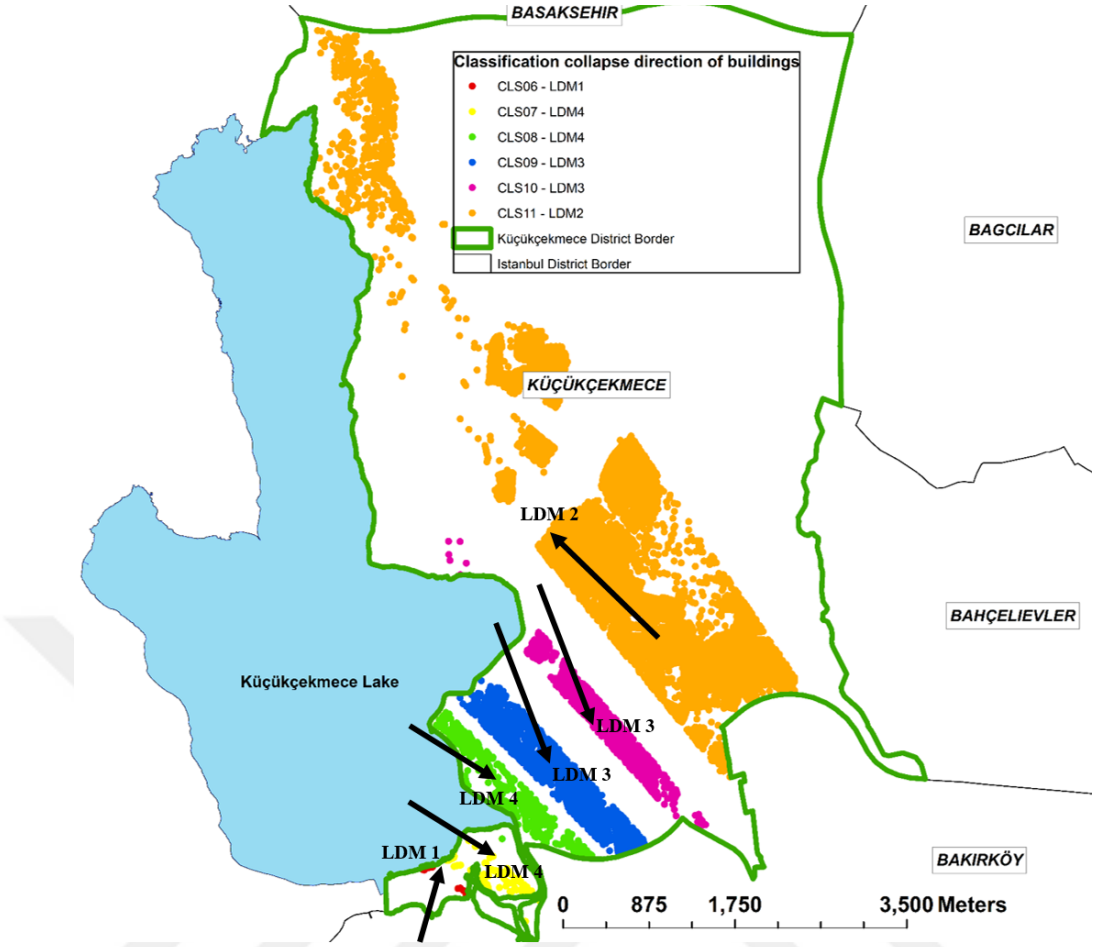


Figure 7.26 : Classification of spreading direction of collapsed buildings in Küçükçekmece.

Regarding the spreading direction and spreading distance of collapsed buildings, the estimation of possible road blockages in Küçükçekmece is given in Figure 6.26. The current road network in Küçükçekmece is approximately 624 km; according to road blockage analysis, approximately 210 km of these roads could decrease in functionality (Figure 7.27).

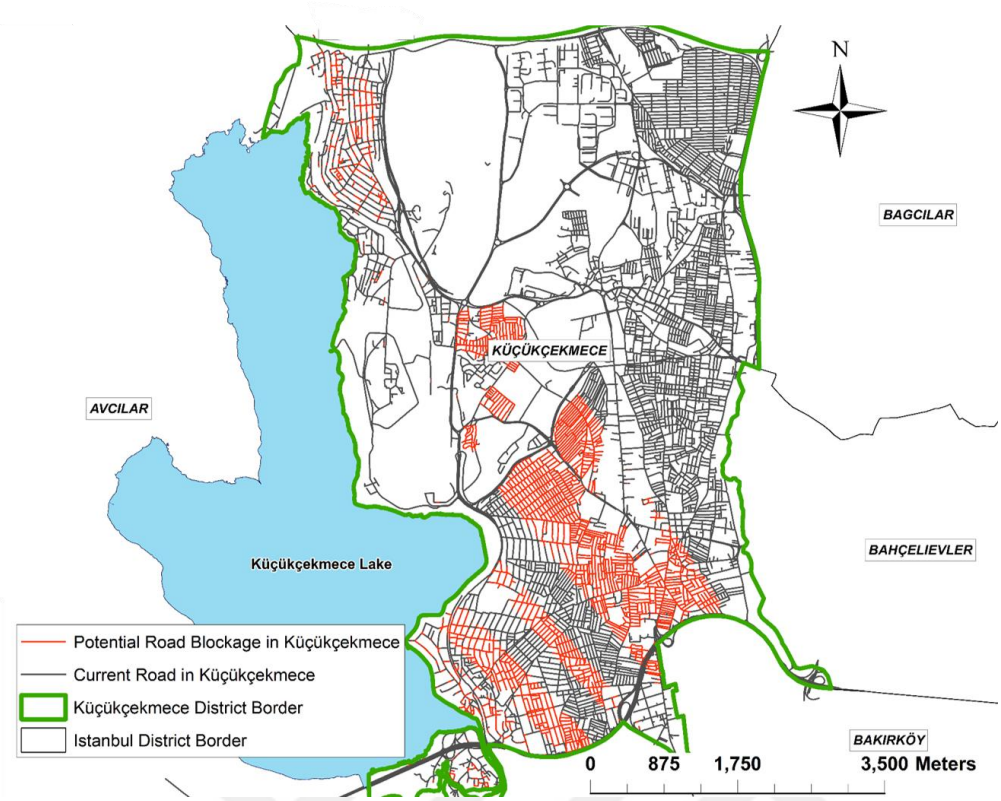


Figure 7.27 : Road blockage in Küçükçekçemece because of the building collapse direction.

7.2.3 Building collapse direction in Fevzi Çakmak

Fevzi Çakmak, which is the sub-district of Küçükçekmece, was studied to examine possible road blockages in more detail (Figure 7.28).

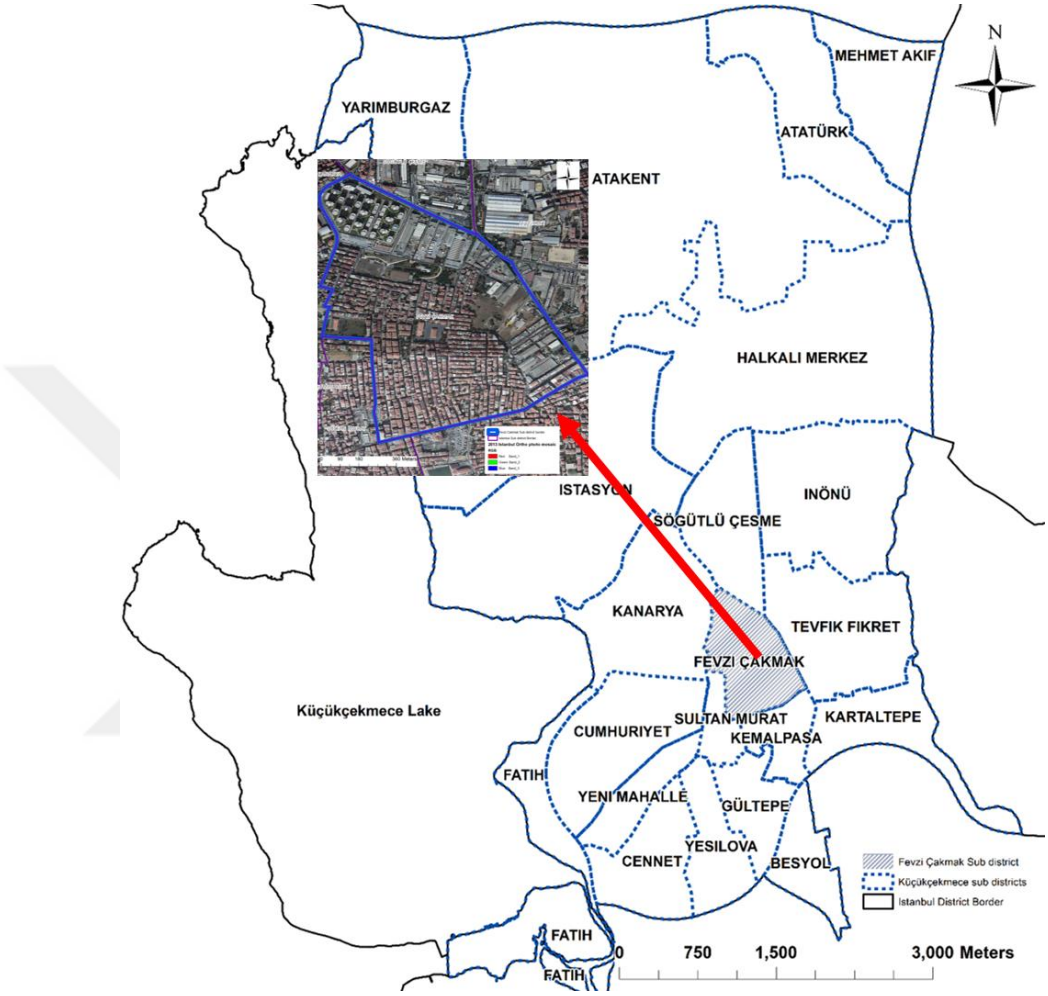


Figure 7.28 : Location of Fevzi Çakmak sub district of Küçükçekmece district.

There were 1418 buildings in the Fevzi Çakmak sub-district in Küçükçekmece in 2013 (Figure 7.29).

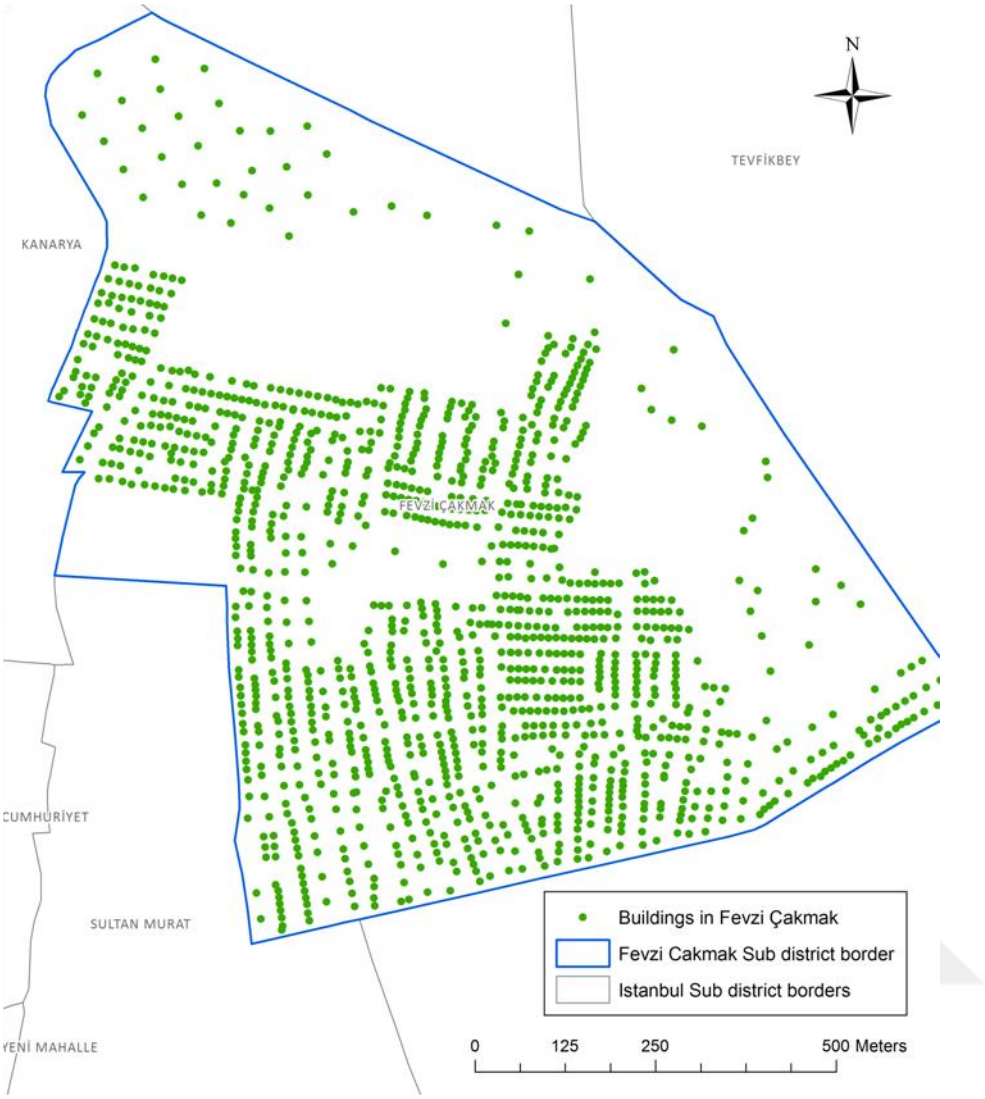


Figure 7.29 : Buildings in Fevzi Çakmak sub district.

Of these, 1354 had the possibility of mean damage of more than 30% in a potential Istanbul earthquake (Figure 7.30).



Figure 7.30 : Buildings in Fevzi Çakmak sub district that mean damage possibility more than 30%.

The collapse classification of these 1354 buildings was CLS11 and it is expected that these buildings will collapse in the direction of LDM2 (approximately north east) with an average debris spreading distance of 19.710m (Figure 7.31).

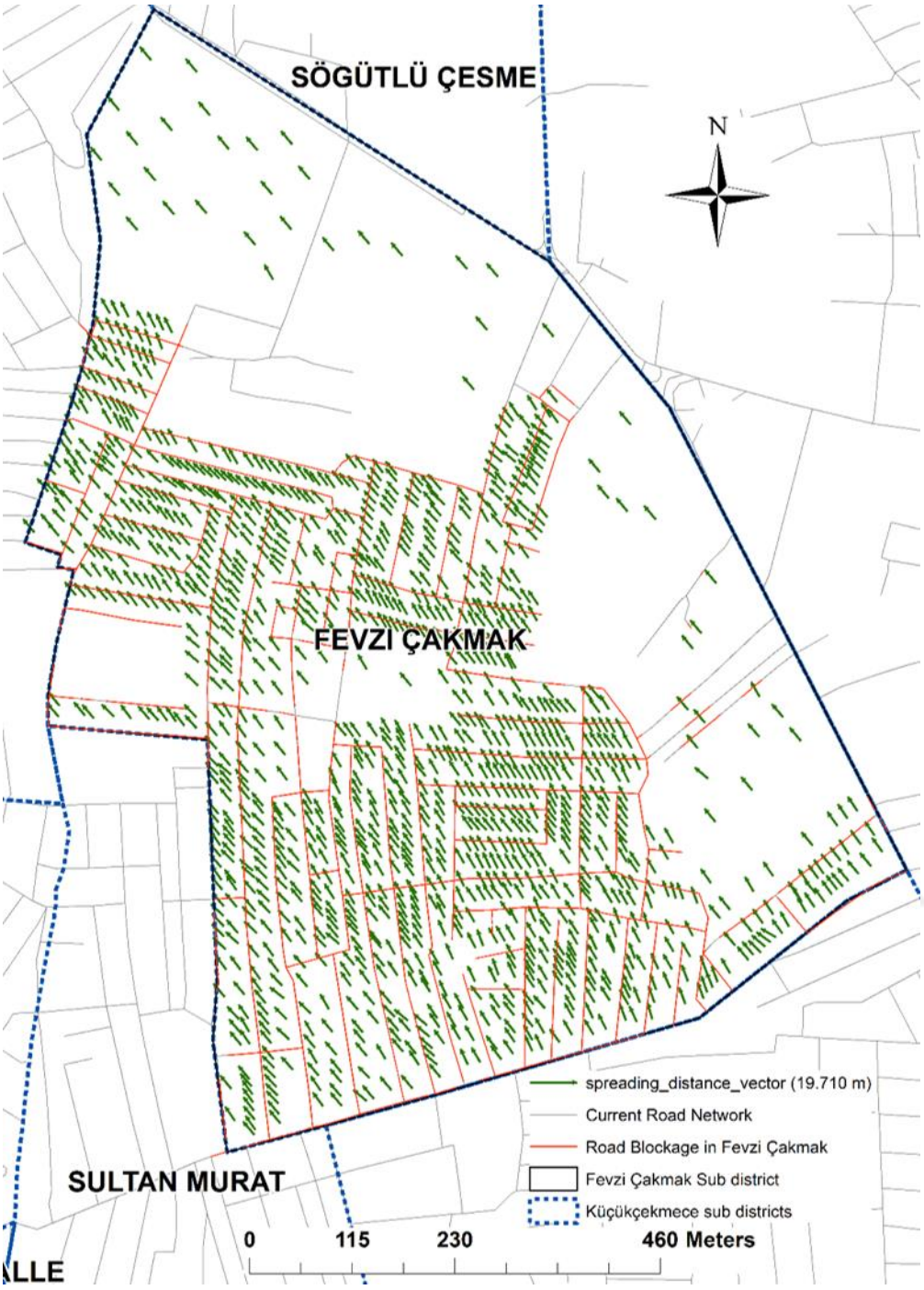


Figure 7.31 : Classification of spreading direction of collapsed buildings in Fevzi Çakmak.

In considering the LMD 2 spreading direction, a buffer analysis was made according to average debris spreading distance of 19.710m of LDM 2 and it was seen that nearly all the sub-districts will be covered with debris (Figure 7.32).

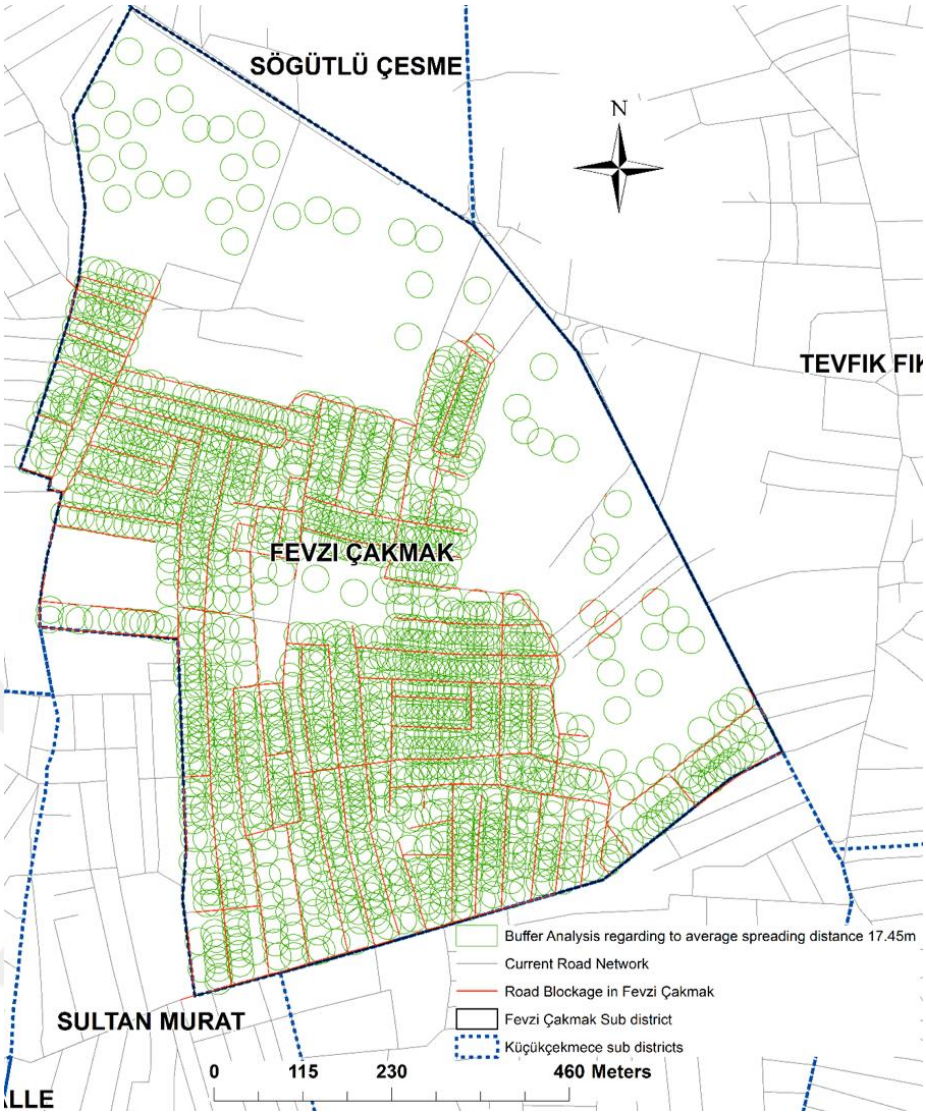


Figure 7.32 : Buffer analysis according to the average debris spreading of LDM2 classification in Fevzi Çakmak sub district.

Possible road blockages due to the debris of collapsed buildings in Fevzi Çakmak is shown in Figure 31. Road blockages do cause the loss of road functionality. Currently, the sub-district of Fevzi Çakmak has, 18745m of roads. If the potential earthquake in Istanbul occurs, it is estimated that the functional road length will decrease to 7004 m (Figure 7.33). If the anticipated earthquake occurs in Istanbul, most of the roads in Fevzi Çakmak will lose their functionality.

As seen in Figure 34, if it is accepted that the estimated debris spreading distance would be 19.710 m regarding Near and LDM analysis, then Ahmet Kocabıyık street will be closed, but if it is accepted that the average debris spread would be 17.40 m, then it is thought that Ahmet Kocabıyık street will not be closed (Figure 7.34). When we look at Sultan Murat Street, if it is accepted that the spread of debris would be

17.40 m, then this road could be closed. But regarding the collapse direction, it may not be closed.

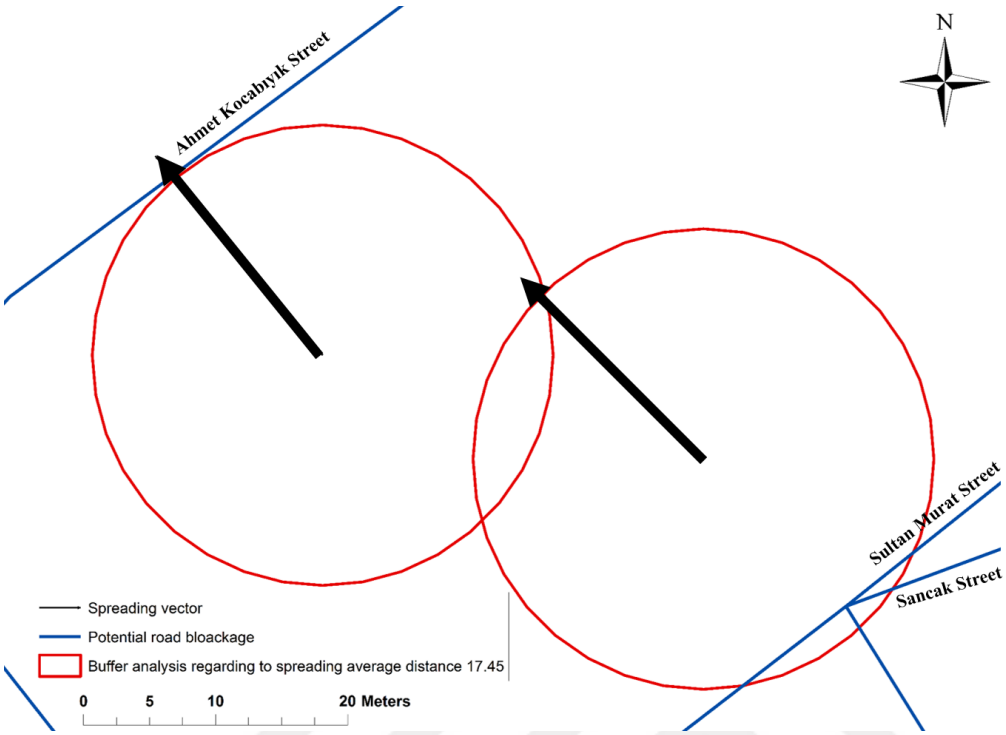


Figure 7.33 : Road blockage in Fevzi Çakmak because of the building collapse direction.

If the road functionality length decreases, the accessibility to critical facilities from Fevzi Çakmak district decreases, making the response stage difficult (Figure 7.34).

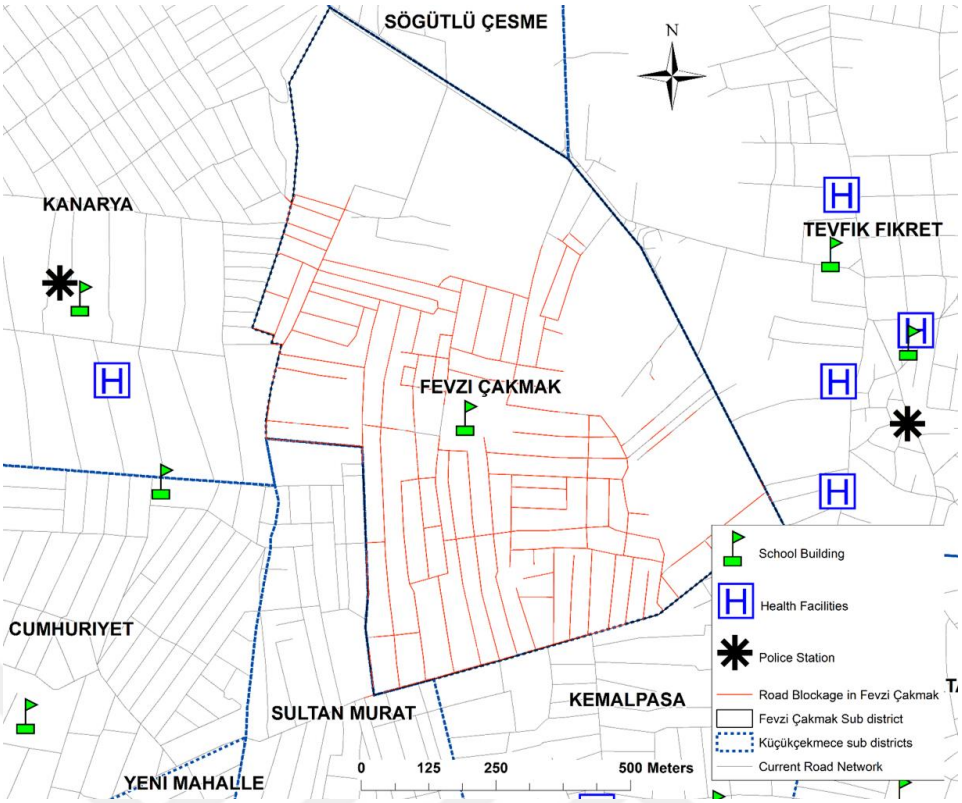


Figure 7.34 : Accessibility of critical facilities around Fevzi Çakmak sub district.

7.2.4 Average spreading distance application to Istanbul

During the 1999 Kocaeli Earthquake, the collapsed buildings in Gölcük caused debris to be scattered across an average distance of 17.45 m. In this part of the study, this value was applied to Istanbul's buildings that have the possibility of collapse of more than 30 %, according to Sa.

There are 3646 buildings that have the possibility of complete damage of more than 50%, while there are 15863 buildings that have the possibility of complete damage of between 40% and 50%, and 53999 buildings that have the possibility of complete damage of between 30% and 40% (Figure 7.35).

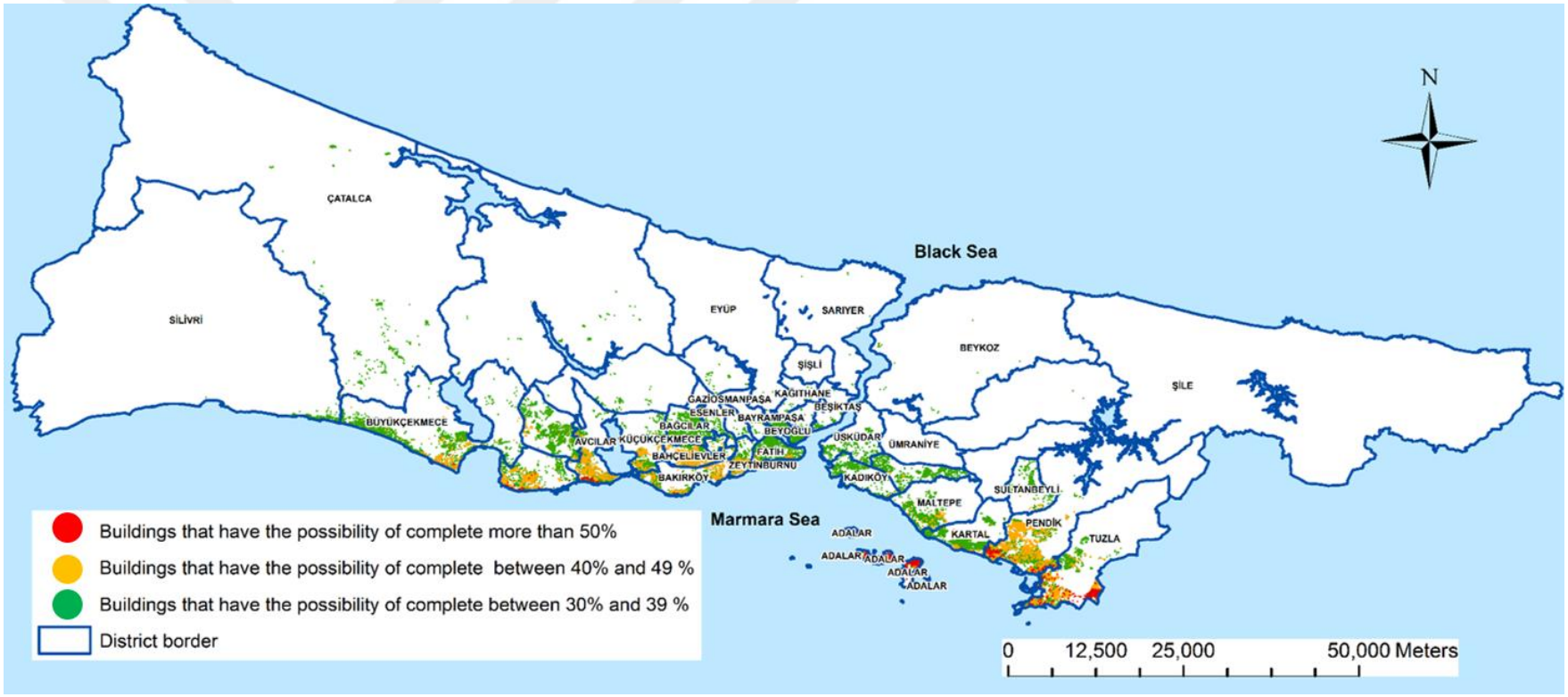


Figure 7.35 : Buildings that have the complete possibility more than 30%.

According to the building damage analysis performed by calculating HAZTURK software, there are 73508 buildings that have a collapse possibility of more than 30%. The buffer analysis was made by using these buildings and it was accepted that these collapsed buildings would create a 17.45 m debris site around them.

The model builder was created for this process from damage possibility to road blockage, as seen in Figure 7.36.

The current road network in Istanbul is approximately 30325 km, according to the road blockage analysis, approximately 3000 km of roads could decrease in functionality (Figure 7.37).

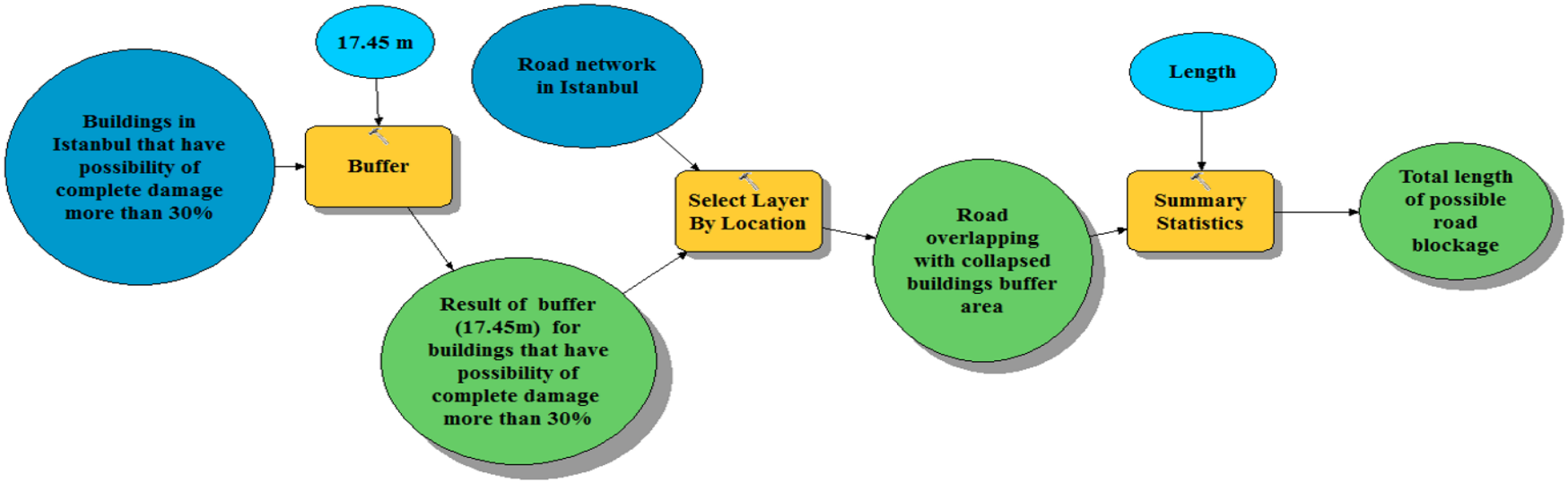


Figure 7.36 : Model builder for defining road blockage in Istanbul by using average debris value (17.45 m).

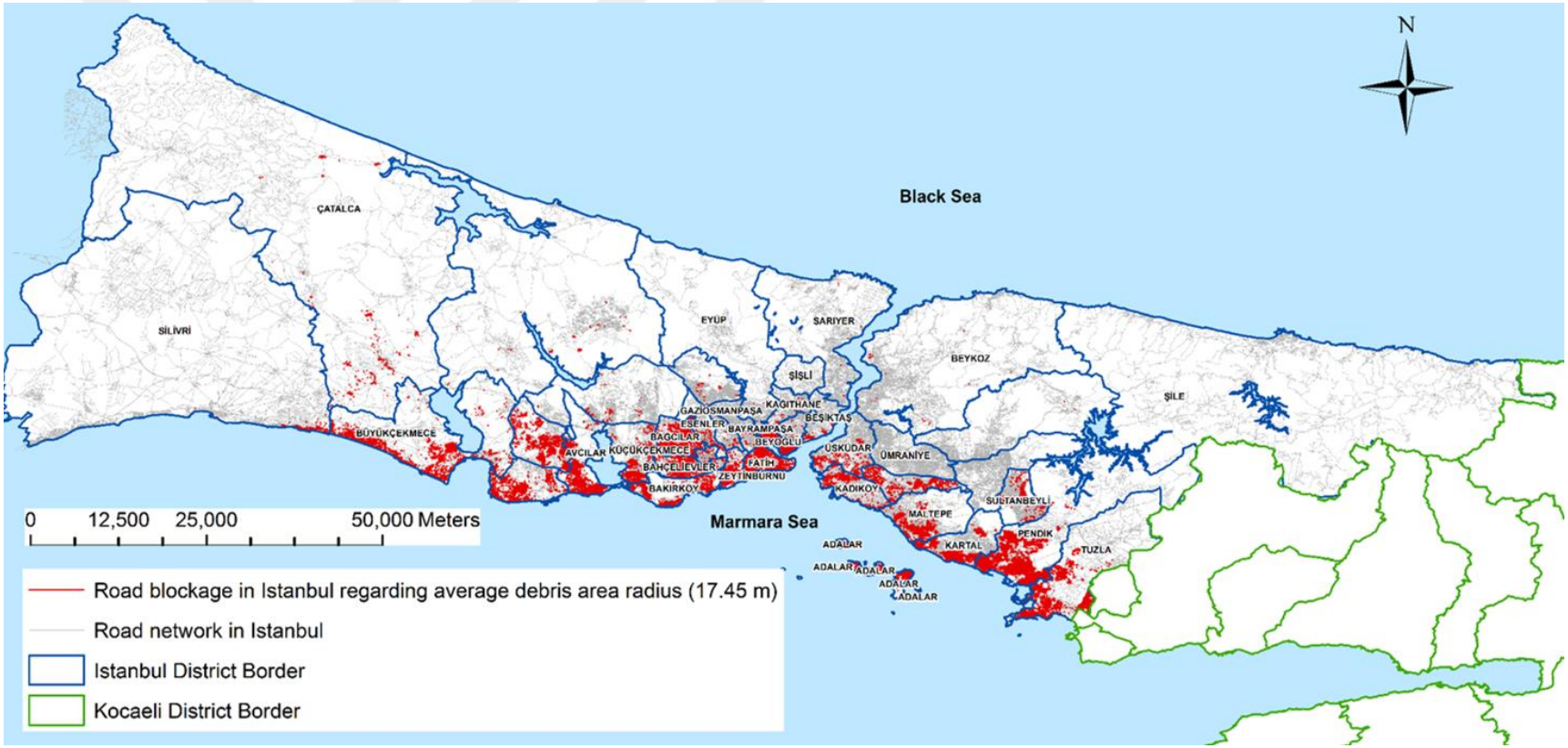


Figure 7.37 : Road blockage in Istanbul.

In the event of a potential Istanbul earthquake, it is estimated that many buildings in Istanbul have the possibility of damage. Because of the potential for collapsed buildings, a great number of roads will be blocked. Accessibility between critical facilities and the disaster area during a disaster situation is very important because road networks play a critical role for the evacuation, logistics, response and recovery process.

In this part, the possible road blockages that will be caused because of the debris of fallen buildings that have the possibility of collapse of more than 30 % (according to Sa) was used to determine the accessibility of critical facilities.

One of the most important critical facilities in a disaster is the fire service. Figure 7.38 shows the location of the fire station and their accessibility after a potential earthquake. It is seen that the accessibility of the fire station,which is located in the northern part of Istanbul is very high. In contrast to the northern part, the accessibility of the fire station, which is located in the south is very low. This shows that if there was a fire in the southern part of Istanbul during or after an earthquake, it would be impossible for them to respond to the fire. Therefore, the secondary disaster may occur.

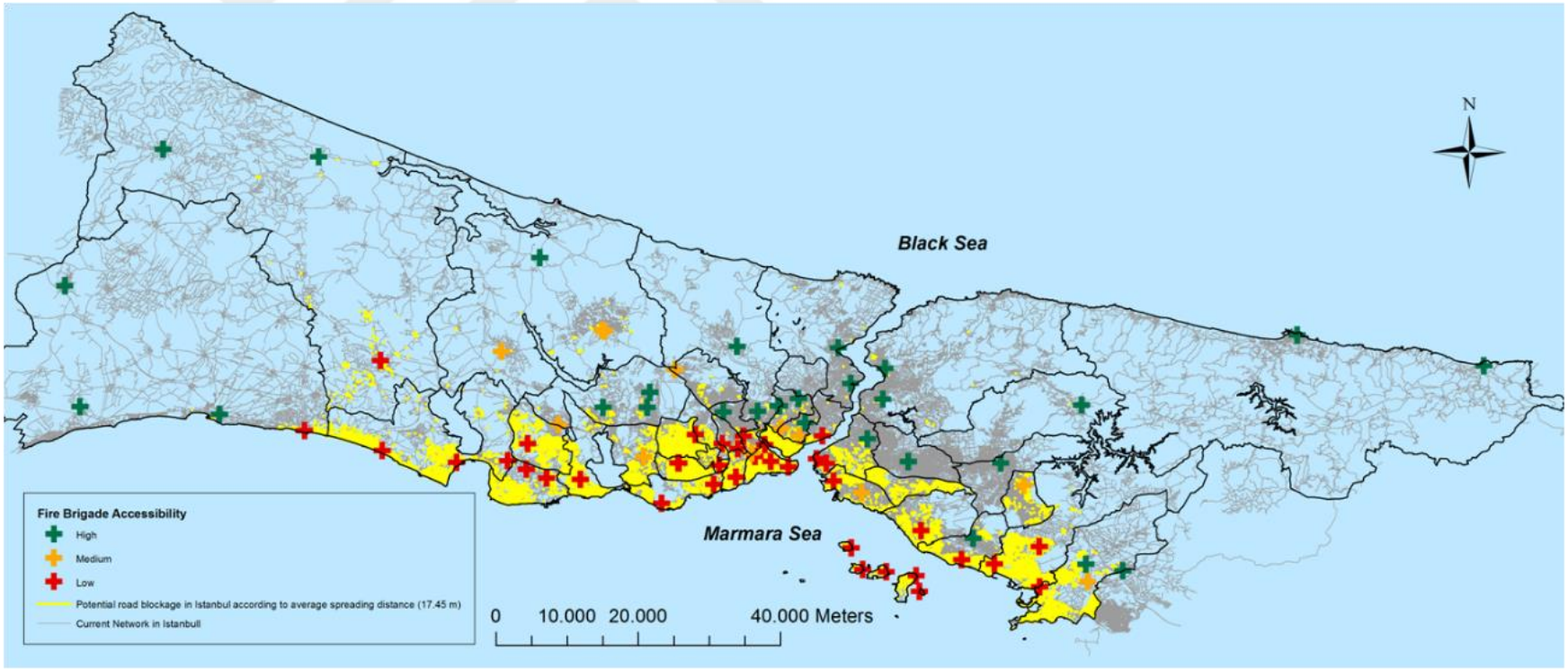


Figure 7.38 : Accessibility of fire stations in Istanbul

8. BRIDGE DAMAGE AND FUNCTIONALITY

8.1 Method of Bridge Functionality

The seismic risk to bridges in Istanbul was evaluated with the seismic risk assessment metholology, as given in Figure 8.1. These inputs were integrated to loss assessment software called HAZTURK, which was developed by İstanbul Technical University and Illinois University.

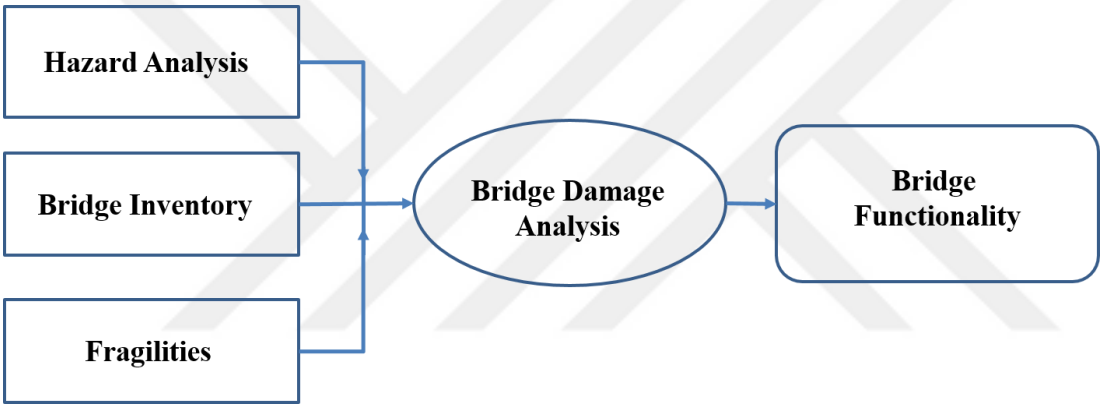


Figure 8.1 : Methodology of bridge functionality.

HAZTURK estimates the damage to transportation structures based on a particular hazard. Vulnerability is a function of the type of bearing, skew angle of the superstructure, minimum support length, height of the middle bents, height of the abutments, seating at the abutments due to landfill (HAZTURK Help File, 2015)

8.1.1 Hazard analysis of bridges

Peak ground acceleration (PGA) for each transportation structure was used for this calculation by using fragility curves and the hazard definition (Figure 8.2). By using PGA with the related fragility curves, the damage, retrofitting cost and the functionality analysis were obtained for each of the transportation structures.

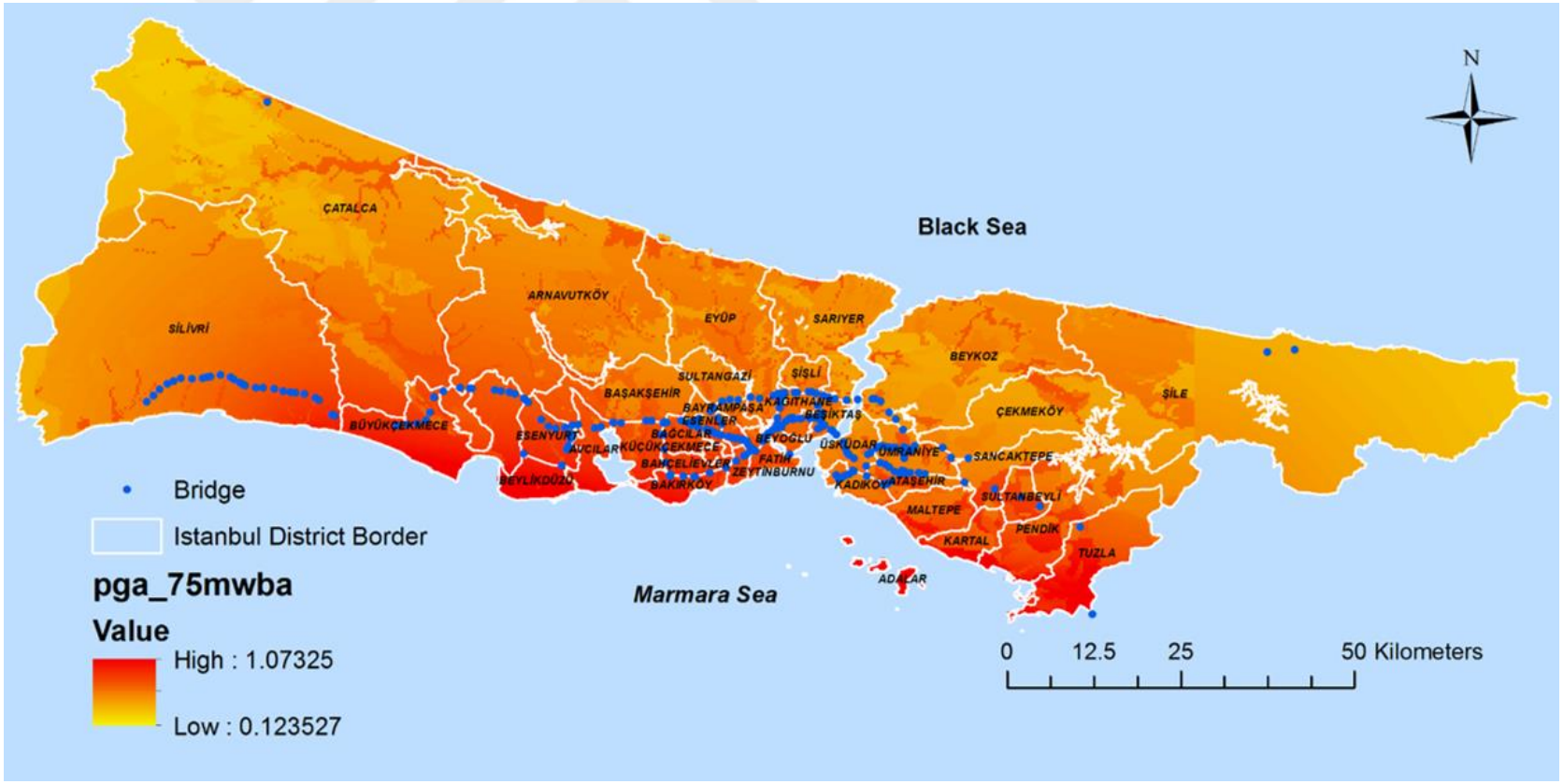


Figure 8.2 : Distribution of bridge locations on Istanbul Earthquake Hazard Map according to Boore & Atkinson (2008) PGA.

A deterministic hazard map was used in the seismic risk analyses. For the deterministic hazard, Model A of the JICA and IMM (2002) was used with an epicenter of 28.9 N, 40.9 W, which is approximately in the south eastern part of Istanbul.

8.1.2 Bridge inventory

Within the context of this study underpasss bridges were accepted to be classified as a Tunnel/Culvert; there were 16 MSC_Conc Box, 96 MSC_Concrete,32 MSC_Slab, 5 MSC_Steel, 9 SS_Concrete and 89 Tunnel/Culvert studied in order to calculate their risk of damage. (Table 8.1)

Table 8.1 : Distribution of bridge classes within study area.

Bridge Type	Number	%
MSC_Conc Box	16	6.47 %
MSC_Concrete	96	38.86 %
MSC_Slab	32	12.95 %
MSC_Steel	5	2.02 %
SS_Concrete	9	3.64 %
Tunnel/Culvert	89	36.03%

8.1.3 Fragility curves

Fragility curves for highway system components were defined with respect to classification and ground motion parameters and they are an efficient and intutitive tool for evaluating the seismic vulnerability of bridges and viaducts. These curves describe the probability of reaching, or exceeding, each damaged state given the level of ground motion (HAZUS BOOK).

Fragility curves are used to estimate the physical damage, the cost to repair the damage and the post-earthquake functionality to the transportation structure. HAZTURK uses the fragility curves of Nielson and DesRoches (2007a) and Nielson and DesRoches (2007b) to estimate the damage, based on the PGA demand typed earthquake hazard maps. Then each bridge was spatially intersected with the PGA typed earthquake hazard map and the specific g value at that site was attained as the earthquake shaking for that specific bridge. Following this match, the fragility mapping was accomplished by using the attributes of the bridge data given above in Table 4.26.

The key fields used for damage analysis were “Main Structure Type”, which allowed the classification of the transportation structures according to the types for which fragilities had been developed (Reginald DesRoches, Leon, & Dyke, 2003; R

DesRoches, Padgett, Elnashai, Kim, & Reed, 2006) as well as the number of spans, total length, and width.

For transporation structures, fragility curves are defined in terms of PGA (Figure 8.3, Figure 8.4, Figure 8.5, Figure 8.6).

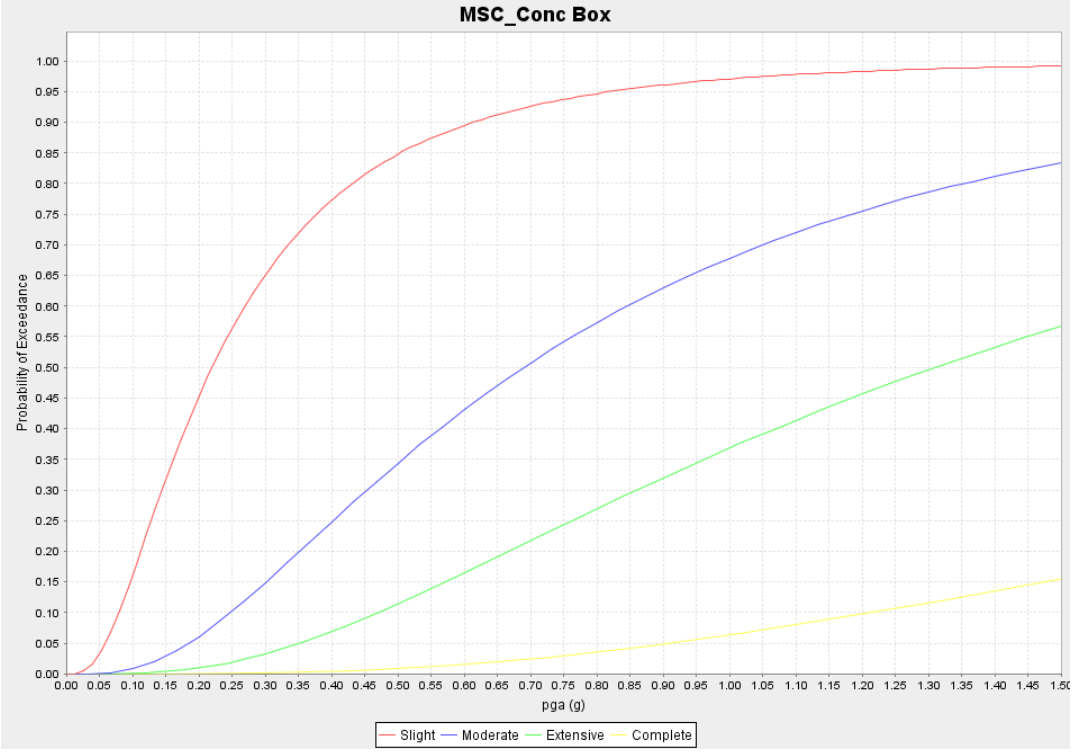


Figure 8.3 : Fragility curves for the continuous bridge classes: MSC_Conc Box.

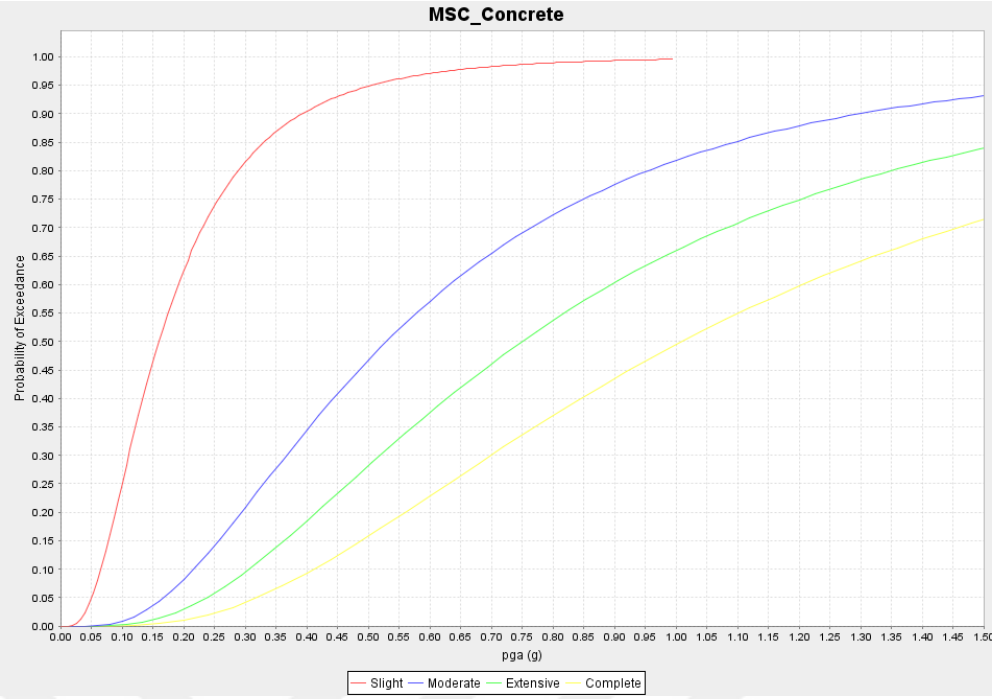


Figure 8.4 : Fragility curves for the continuous bridge classes: MSC_Concrete.

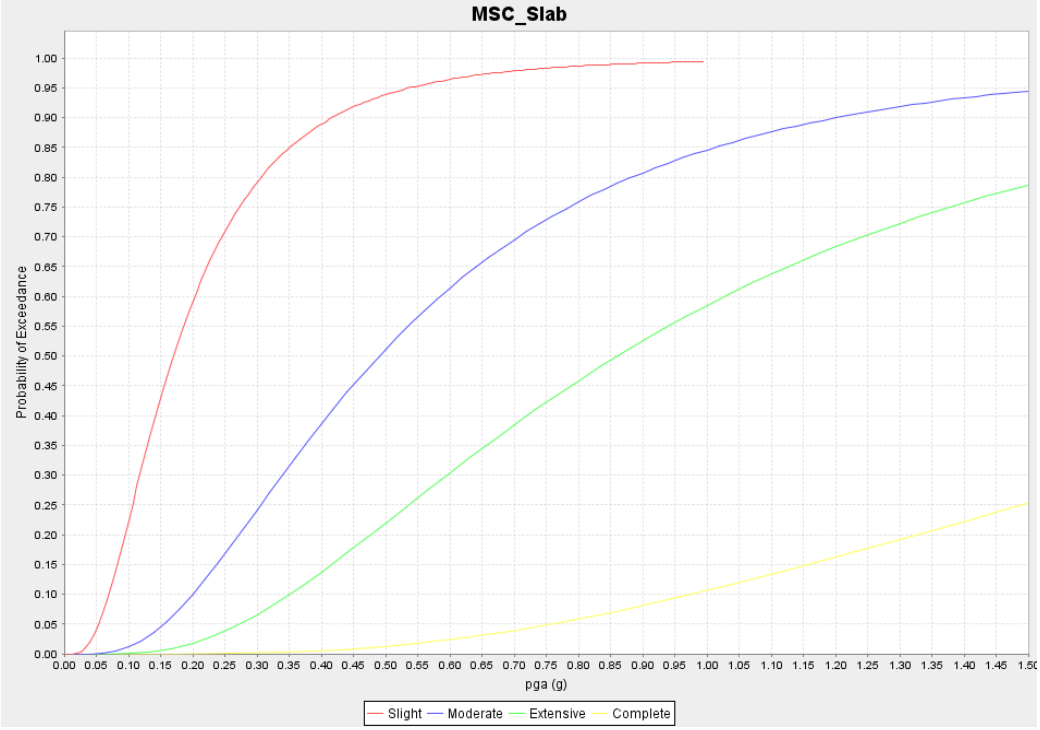


Figure 8.5 : Fragility curves for the continuous bridge classes: MSC_Slab.

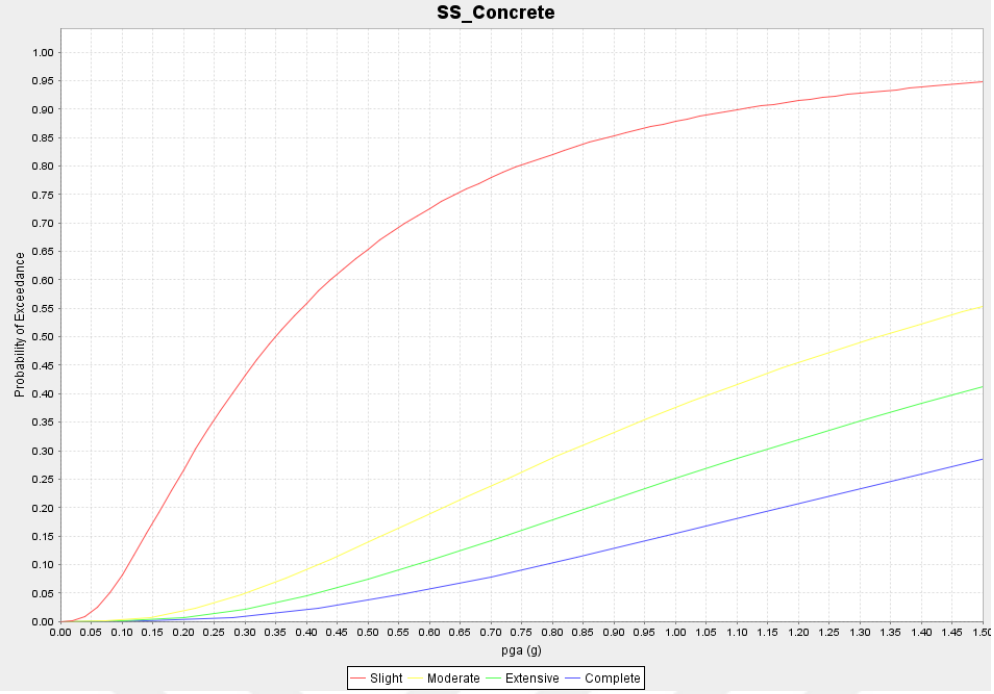


Figure 8.6 : Fragility curves for the single span simply supported bridge classes: SS Steel.

After the incorporation of the fragility data associated with each bridge classification was completed, the seismic risk assessment analyses were run in HAZTURK to assess the performance of the transportation structures in Istanbul against the anticipated Istanbul earthquake. Three main results were obtained from the analysis with HAZTURK software: (1) damage analysis, (2) retrofitting cost, (3) functionality. Using the specific PGA values and the related fragility curves, the damage possibility was calculated for each bridge. Using recently developed bridge fragility curves, and damage-functionality relationships for bridges, an analysis of the 247 transportation structures in the Istanbul was performed. Once the damage states are determined, the expected repair costs can be calculated. Functionality analysis provides the functionality of all of the transportation structures in the transportation network and reveals the anticipated restoration over time. Functionality is described by the probability of the damage state (immediately following the earthquake) and by the associated fractions or percentages of the components that are expected to be functional after a specified period of time. For example: (1) closed immediately, (2) partially open after a 3-day restoration period and (3) fully open after a 1-month restoration period (Nilsson, 2008).

8.2 Transformation Structures (Bridge, Viaduct) Damage Analysis and Results

The relationship between the bridge damage and the resulting loss of functionality of the bridge is critical in assessing the impact of an earthquake event on the performance of the transportation network (Padgett & DesRoches, 2007). This section discusses the possible transportation structure damage and its functionality following an earthquake.

8.2.1 Results of bridge damage analysis

A damage analysis for the bridges in Istanbul was performed by using the fragility curves and the hazard definition, with deterministic scenario. It was estimated that if the potential Istanbul earthquake occured with a M_W 7.5, at least moderate damage would be seen among the 247 Istanbul bridge inventory.

It can be understood from Table 8.2, that MSC_Steel and MSC Concrete classes of bridges are more vulnerable than the others. The detailed table for every class of transportation structure is given in Appendix A Tables.

Table 8.2: Distribution of average damage state of transportation structures based on bridge class.

class	none	slight_mod	mod_extens	ext_comple	complete	meandamage
Tunnel/Culvert	0.85	0.07	0.04	0.03	0.01	0.03
SS_Concrete	0.47	0.44	0.04	0.02	0.02	0.04
MSC_Steel	0.10	0.30	0.19	0.15	0.25	0.16
MSC_Slab	0.10	0.46	0.26	0.17	0.01	0.08
MSC_Conc Box	0.18	0.50	0.21	0.09	0.01	0.06
MSC_Concrete	0.09	0.54	0.16	0.10	0.11	0.13

Complete damage distribution of the transportation structure based on PGA, is represented in Figure 8.7, while the mean damage distribution according to PGA is shown in Figure 8.8.

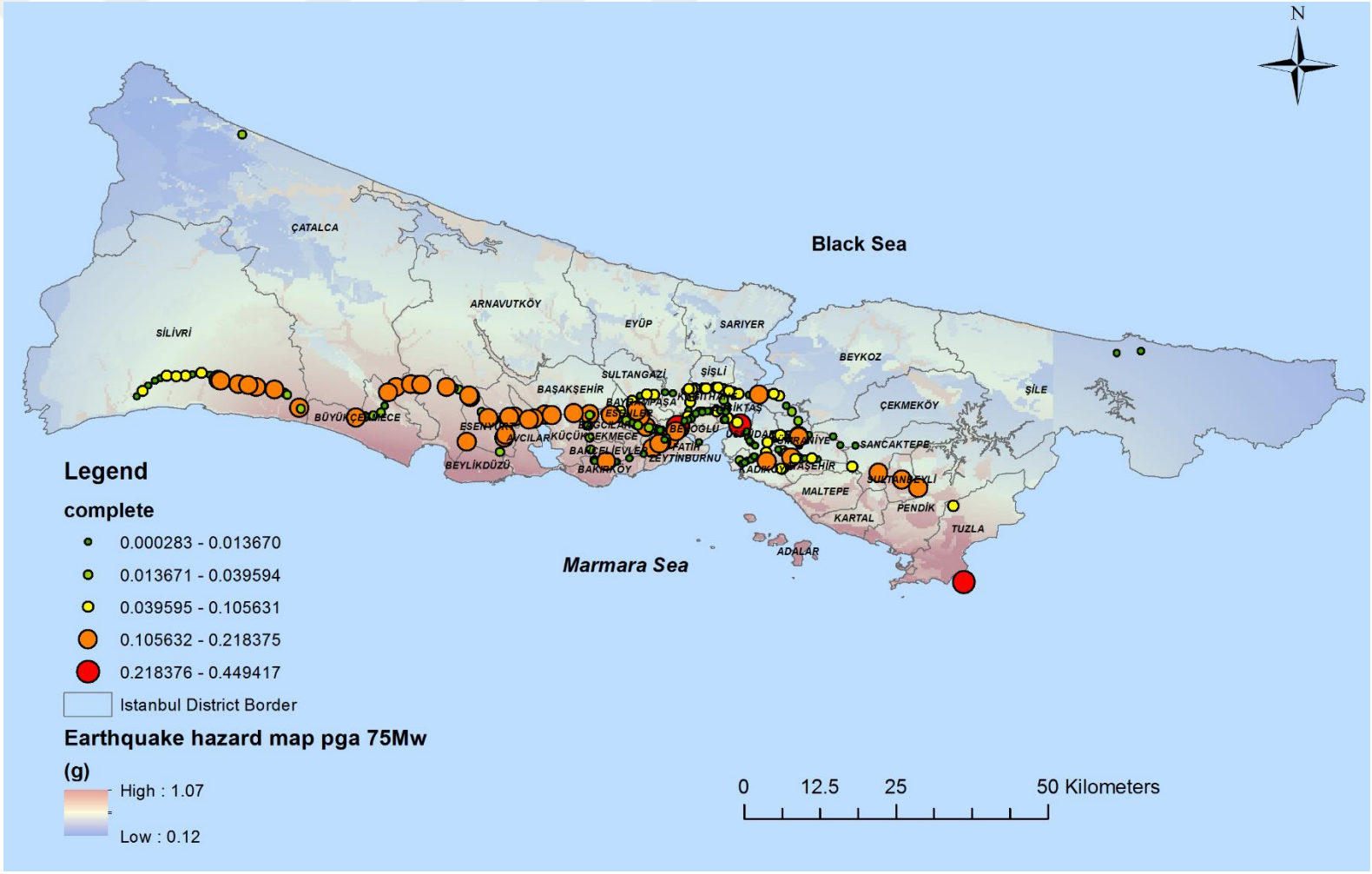


Figure 8.7 : Distribution of complete damage possibility of bridges in Istanbul.

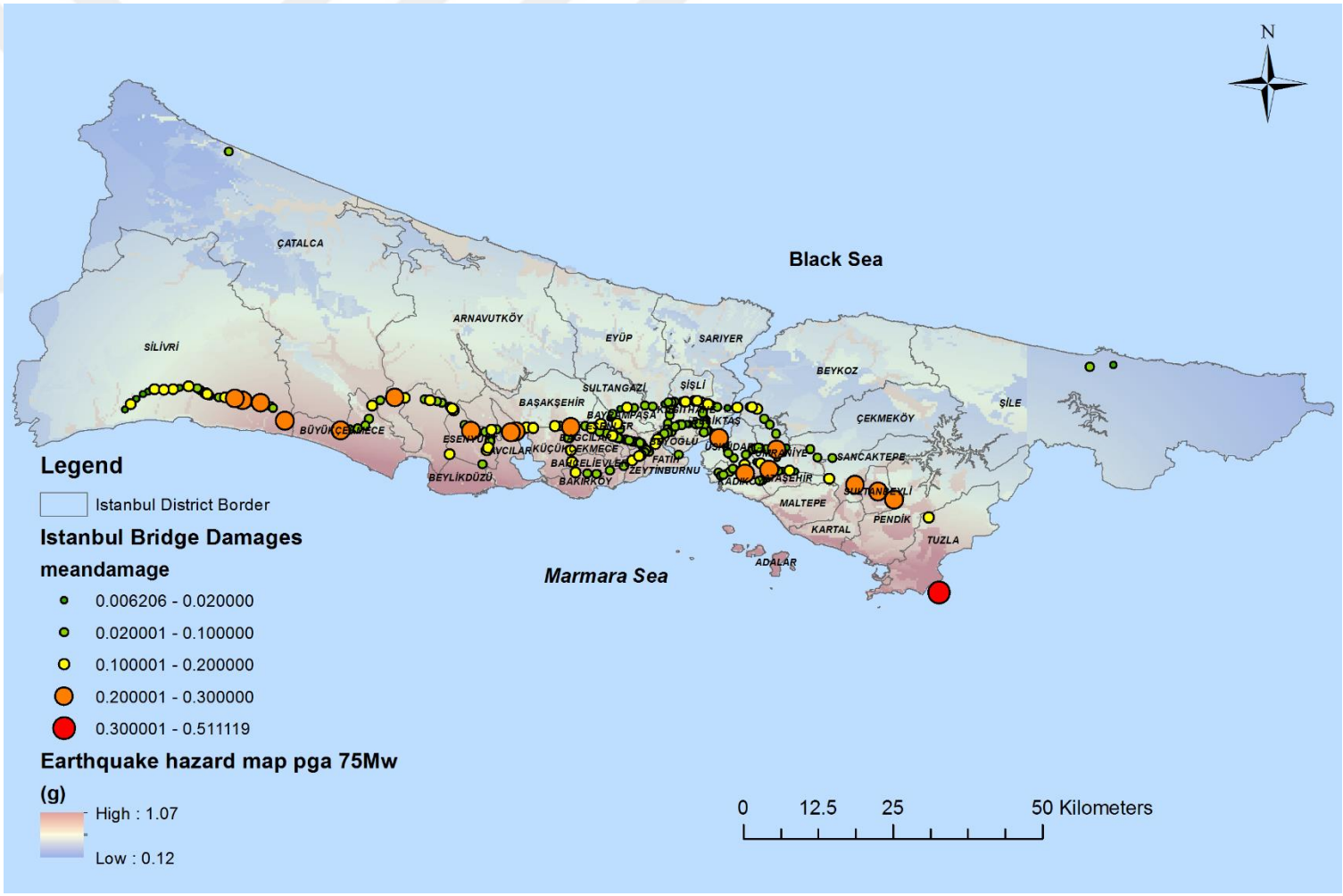


Figure 8.8 : Distribution of mean damage possibility of bridges in Istanbul.

When transportation structures that had the possiblity of mean damage and the potential spreading debris area were assessed together, it was estimated that most of the roads in Istanbul would lose their functionality after a potential Istanbul earthquake (Figure 8.9). As seen in Figure 8.9, this would especially affect the roads that are located in the southern part of Istanbul, which may mean they would not be able to be used after the potential earthquake during the response process.

It is also revealed in Figure 8.10 that it would be almost imposibble to transfer any disaster aid coming via marine transportation to the disaster area, because most of the roads near the Marmara Sea would be blocked due to the debris from the collapse of buildings.

In the regions that were highlighted with the red polygons and with red x marks, the traffic flow would be impossible following an earthquake due to the debris from collapsed buildings and the damage to transportation structures (Figure 8.11).

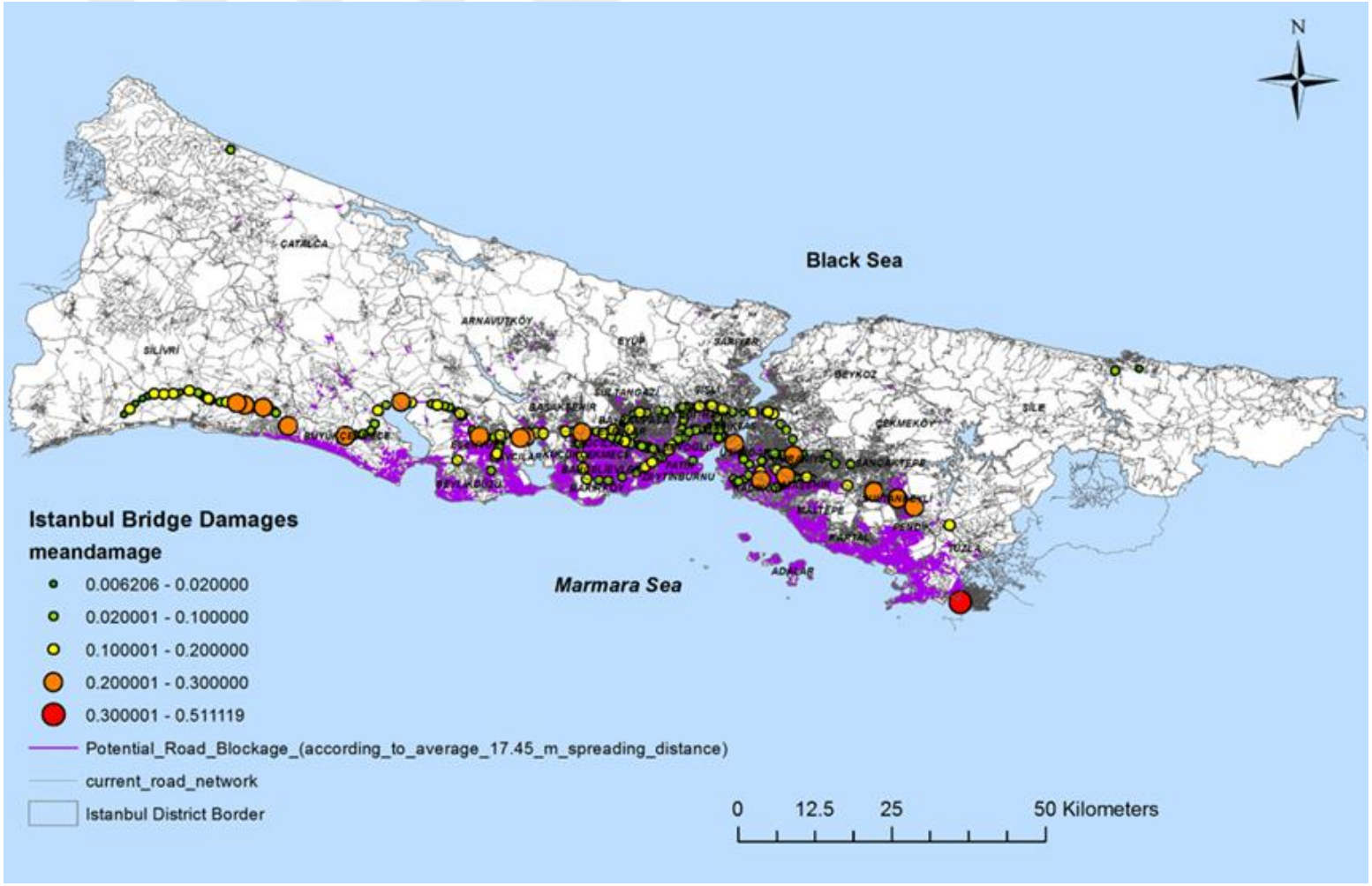


Figure 8.9 : Non functional roads and bridge damage distribution in Istanbul.

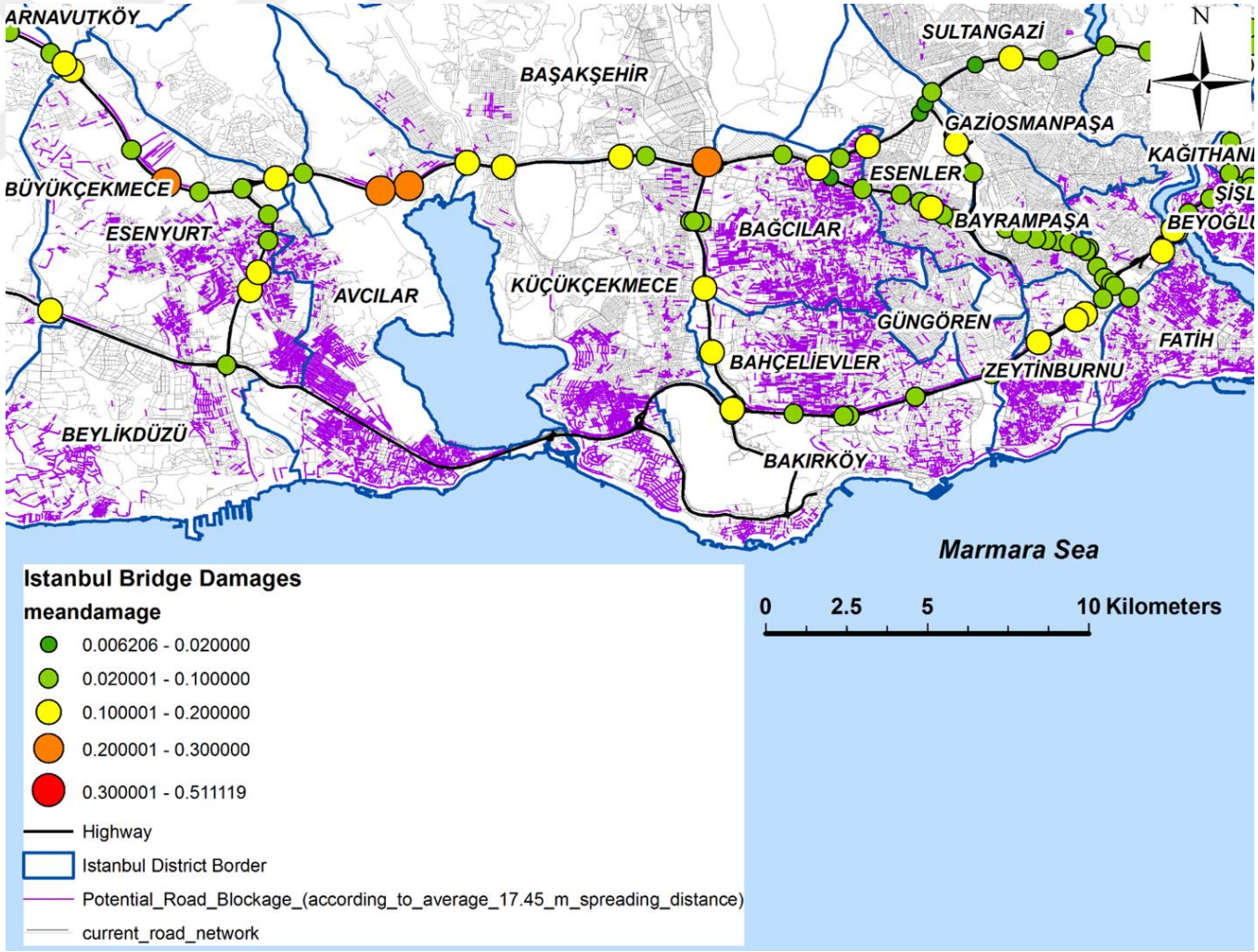


Figure 8.10 : Large scale representation of non functional roads and bridge damage distribution in Europian Side.

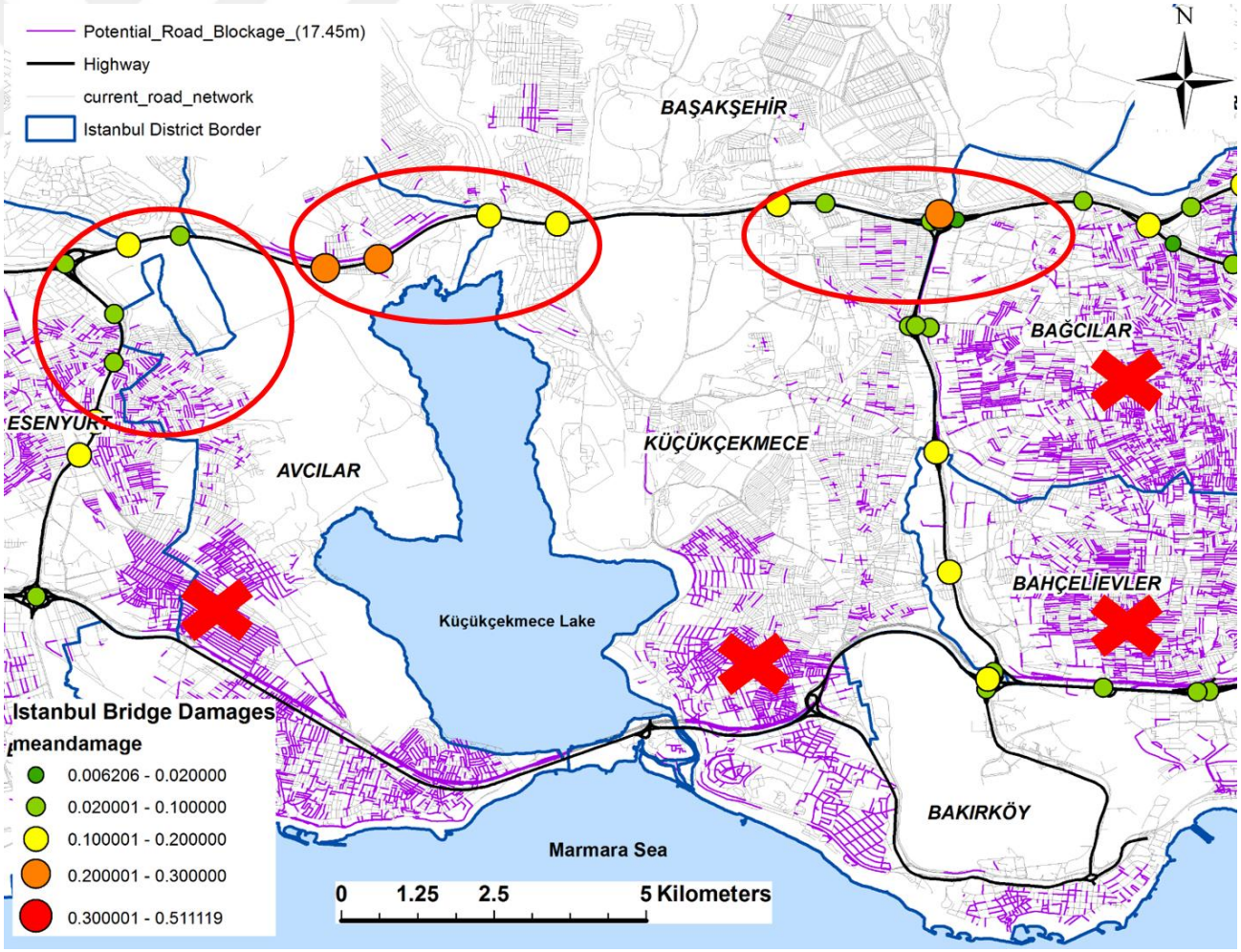


Figure 8.11 : Large scale representation of non functional roads and bridge damage distribution in Küçükçekmece and Avcılar Districts.

8.2.2 Results of the bridge functionality analysis

As was mentioned previously, the results of the functionality analysis were classified as:

(1) closed immediately;

(2) partially open after a 3-day restoration period;

(3) fully open after a 1-month restoration period.

Functionality results were given according to continous and step analysis. Continuous analysis gives results between 0% and 100% and the step analysis gives the results of 0%, 50% and 100%.

Continuous functionality analysis results estimate that 9 bridges would have 1 to 25% functionality , while there would be 134 bridges with 26 to 50% functionality, 14 bridges with 51 to 75% functionality and 90 bridges with 76 to 100% functionality possibilities, as it can be recognized in Figure 8.12.

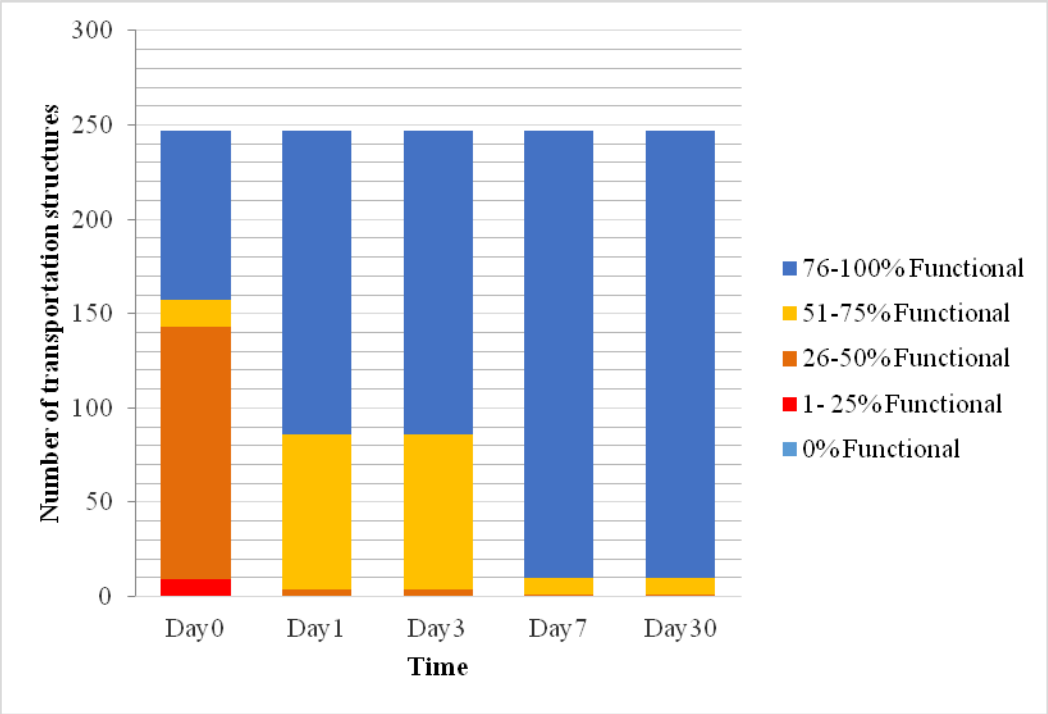


Figure 8.12 : Continuous functionality analysis for bridge in Istanbul.

The functionality analysis results according to the step analysis are given in Figure 8.13. According to step functionality analysis, 194 bridges would have 0 % functionality, 40 bridges would have 50 % functionality and, 13 would have 100 %

functionality immmediately after an earthqauke. It was estimated that 32 bridges would be non-functional 3 days after the earthqauke (Figure 8.13).

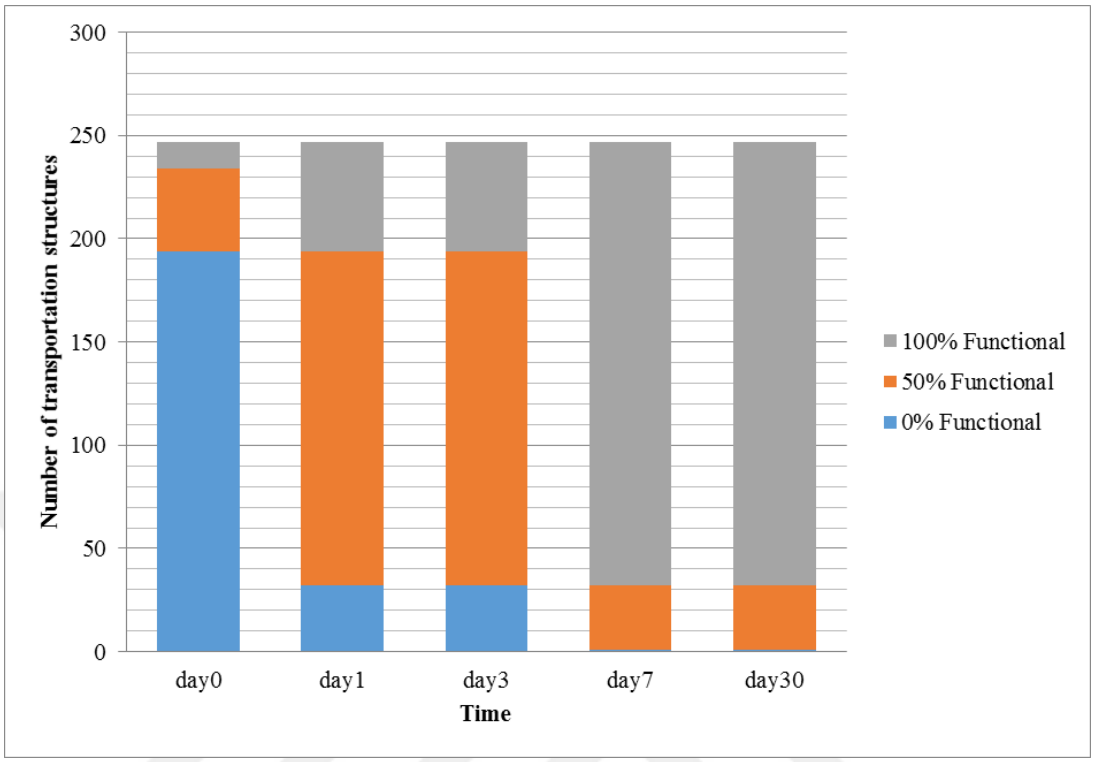


Figure 8.13 : Step functionality analysis for bridge in Istanbul.

The results in Table 8.3 show that most of the non-functional bridges were classified as MSC_Concrete of 194 non-functional bridges on the day of the earthquake, according to the step analysis.

Table 8.3 : Distribution of construction type of bridges counts by step functionality in day 0.

Bridge Classification	0% functionality	50% functionality	100% functionality
MSC_Conc Box	16		
MSC_Concrete	96		
MSC_Slab	31	1	
MSC_Steel	5		
SS_Concrete	7	2	
Tunnel/Culvert	39	37	13

The functionality situation of the bridges would still look the same 3 days after the earthquake, as can be seen in Table 8.4.

Table 8.4 : Distribution of construction type of bridges counts by step functionality in day 3.

costruction type	0% functionality	50% functionality	100% functionality
MSC_Conc Box		16	
MSC_Concrete	30	66	
MSC_Slab		31	1
MSC_Steel	2	3	
SS_Concrete		7	2
Tunnel/Culvert		39	50

After 7 days from the potential Istanbul earthquake, it is estimated that one bridge would be non-functional (day7, 0%) (Table 8.5).

Table 8.5 : Distribution of construction type of bridges counts by step functionality in day 7.

costruction type	0% functionality	50% functionality	100% functionality
MSC_Conc Box		2	14
MSC_Concrete	1	5	90
MSC_Slab		2	30
MSC_Steel		1	4
SS_Concrete		3	6
Tunnel/Culvert		18	72

Figures 8.14 and 8.15 represent the functional and non functional bridges in Istanbul immediatelly following an earthqauke and 3 days after an earthquake, respectively.

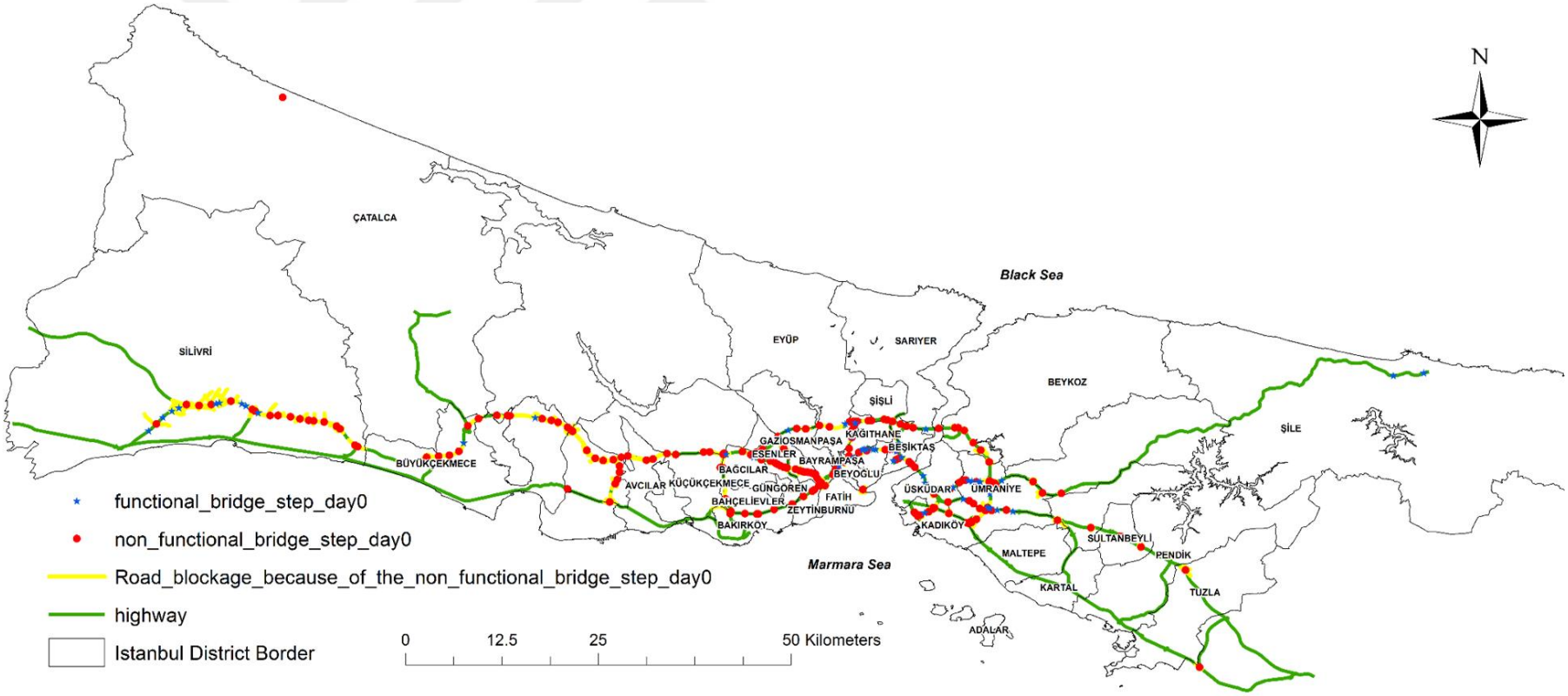


Figure 8.14 : Functional and non functional bridge distribution in Istanbul following potential Istanbul Earthquake (Step Functionality).

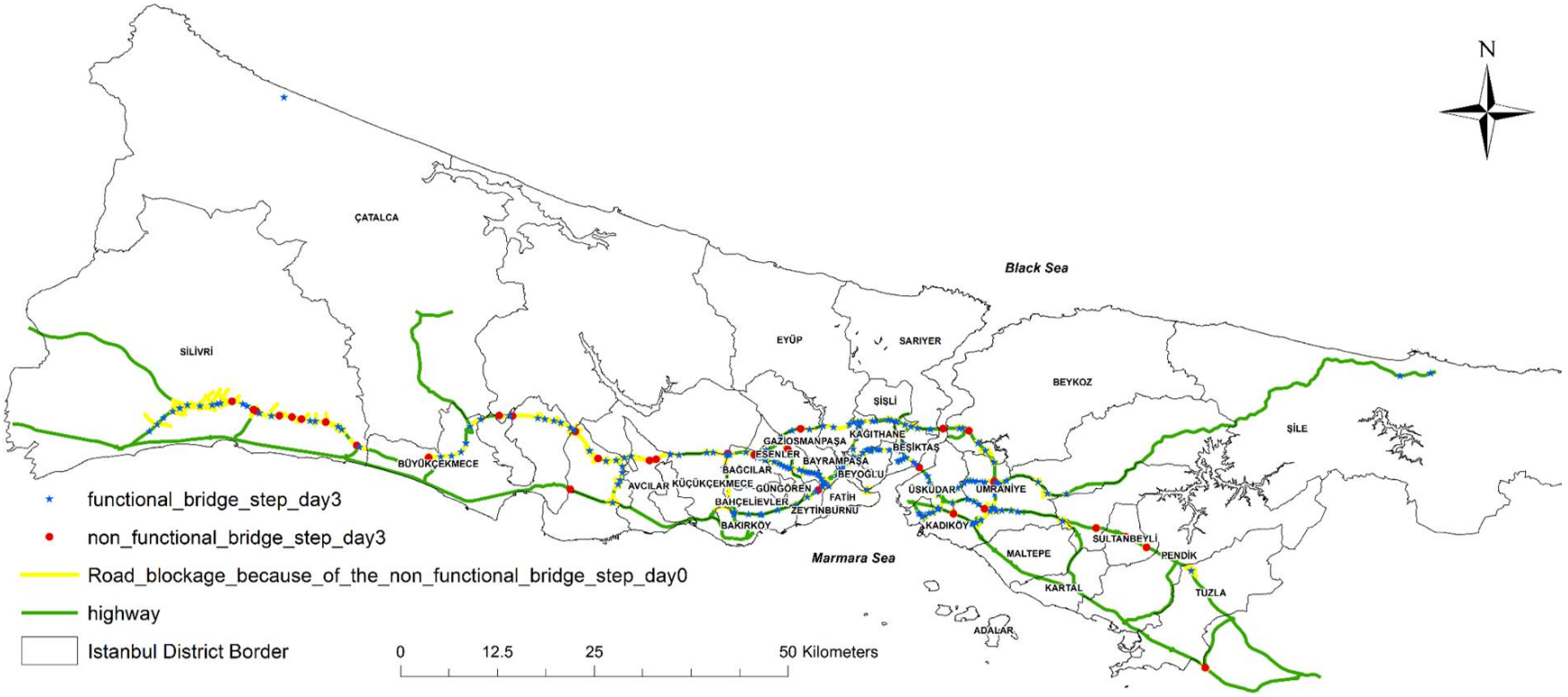


Figure 8.15 : Functional and non functional bridge distribution in Istanbul after 3 days from potential Istanbul Earthquake (Step Functionality).

8.2.3 Results of the bridge retrofitted analysis

Some bridges are retrofitted with in the context of risk mitigations studies in Istanbul. Some of these bridges are shown in Table 8.6.

Table 8.6 : Name of Retrofitting Bridges in Istanbul , Apaydin (2005).

Highway (O-1)	Highway (O-2)	Highway (O-1)
Osmaniye Overpass Bridge	Mahmutbey Vaiaducts	Sağmacılar Viaducts
Yenibosna Overpass Bridge	Gaziosmanpaşa	
	RM01 Overpass Bridge	
	NM01 Overpass Bridge	
	M5 U1 Underpass Bridge	
	K4A Overpass Bridge	
	B3B Underpass Bridge	

The locations and the distributions of the aformentioned bridges can also be seen in Figure 8.16.

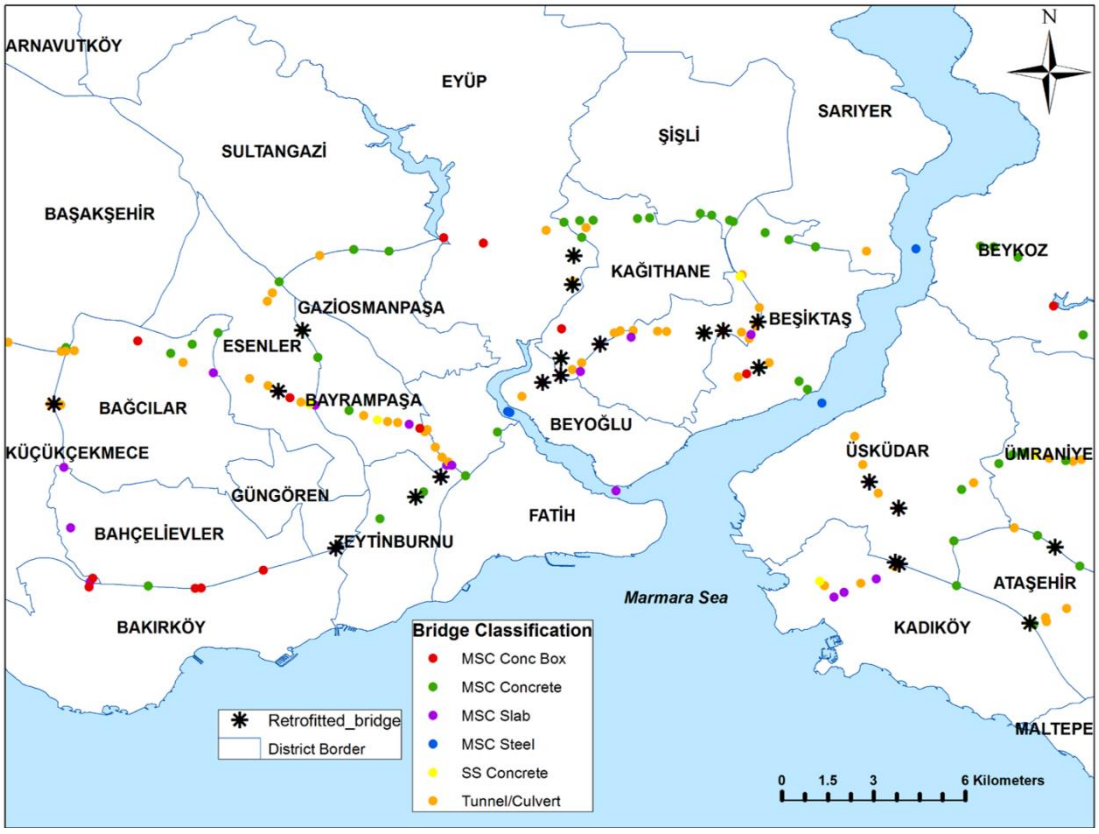


Figure 8.16 : Distribution of Retrofitted bridges in Istanbul.

However, the retrofitting types for the retrofitted bridges can not be acquired either from the Turkish Highway Directorate or from the Istanbul Metropolitan Municipality Transportation Directorate. According to Apaydin (2014) and Dönmez et al. (2014), it was notified that most of the bridges in Turkey are retrofitted either by using steel jacket or elastometric bearing methods. By referring these publications it is accepted

that all of the the bridges were retrofitted either with steel jacket or with elastrometric bearing methods, since the specific retfofit information could not be determined for each structure. When the analysis was made according to this assumption, the tables below were obtained. It can easily be seen that the damage possibility decreased after retrofitting process (Table 8.7, Table 8.8, Table 8.9).

Table 8.7 : Bridge damage distribution without retrofitting process for retrofitted bridges.

class	none	slight_mod	mod_extens	ext_comple	complete	meandamage
MSC_Conc Box	0.24	0.53	0.17	0.06	0.00	0.05
MSC_Concrete	0.10	0.56	0.16	0.09	0.09	0.09
MSC_Slab	0.10	0.48	0.26	0.16	0.01	0.08

Table 8.8 : Bridge damage distribution after elastrometric retrofitting process retrofitted bridges.

class	none	slight_mod	mod_extens	ext_comple	complete	meandamage
MSC_Conc Box	0.73	0.17	0.07	0.03	0.00	0.02
MSC_Concrete	0.60	0.26	0.03	0.01	0.10	0.06
MSC_Slab	0.92	0.32	0.20	0.12	0.01	0.06

Table 8.9 : Bridge damage distribution after steel jacket retrofitting process for retrofitted bridges.

class	none	slight_mod	mod_extens	ext_comple	complete	meandamage
MSC_Conc Box	0.22	0.62	0.12	0.03	0.00	0.04
MSC_Concrete	0.15	0.60	0.13	0.06	0.05	0.07
MSC_Slab	0.08	0.61	0.21	0.09	0.00	0.06

8.2.4 Results of the expected bridge retrofit cost

During the damage analysis proccess, the expected retrofit costs were also calculated by using the HAZTURK software. The mean retrofit costs in dollars per square foot are given for each retrofitted bridge class in Tables 8.10 and Table 8.11. These values were estimated according to the USA retrofitting cost values.

Table 8.10 : Statistical Costing data per Bridge classification according to Elastrometric Bearing Method.

class	retro_cost $	retrofit
MSC_Conc Box	57600.00	Elastomeric Bearing
MSC_Concrete	354566.67	Elastomeric Bearing
MSC_Slab	72971.43	Elastomeric Bearing

Table 8.11 : Statistical Costing data per Bridge classification according to Steel Jacket Method.

class	retro_cost $	retrofit
MSC_Conc Box	32400.00	Steel Jacket
MSC_Concrete	199311.11	Steel Jacket
MSC_Slab	18119.19	Steel Jacket

9. POTENTIAL ROAD BLOCKAGE IN ISTANBUL

The main aim of this study is to determine the number of potentially blocked roads in Istanbul following a possible Istanbul earthquake. Within the context of this study, road blockages were revealed with different analyses.

One of them was by using the building collapse radius. There are 73508 buildings in Istanbul that have a collapse possibility of more than 30%. It was accepted that the collapse radius of those buildings would be 17.45m, based on the average number of floors and the average radius' of collapsed buildings in Gölcük . Based on this assumption, 3000 kms of the road network in Istanbul may loose its functionality.

A further test was by using bridge functionality analysis following the potential earthquake. There are 247 bridges on the highway in Istanbul. According to the step functionality analysis using HAZTURK, 194 bridges could be non-functional immediately following an earthquake. After a restoration period only 32 bridges could be non-functional after 3 days. Because of the non-functional bridges, it is estimated that most parts of the highway could be unavailable for transportation because of the damage.

Figures 9.1 and 9.2 show the potential road blockages according to the assessment of the buildings collapse distance and bridge step functionality immediately after an earthquake and 3 days after an earthquake, respectively.

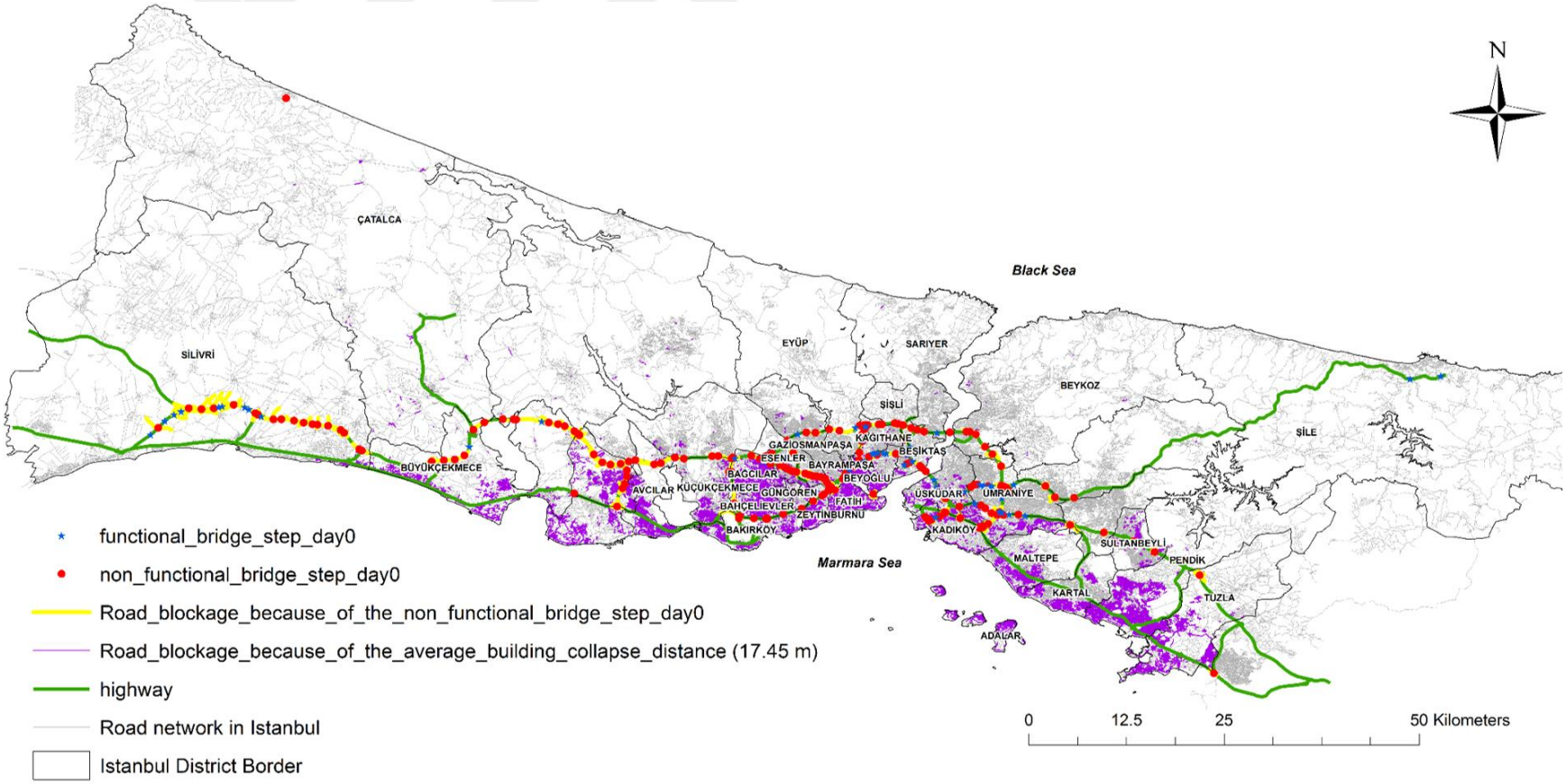


Figure 9.1 : Road blockage in Istanbul immediately after a potential earthquake.

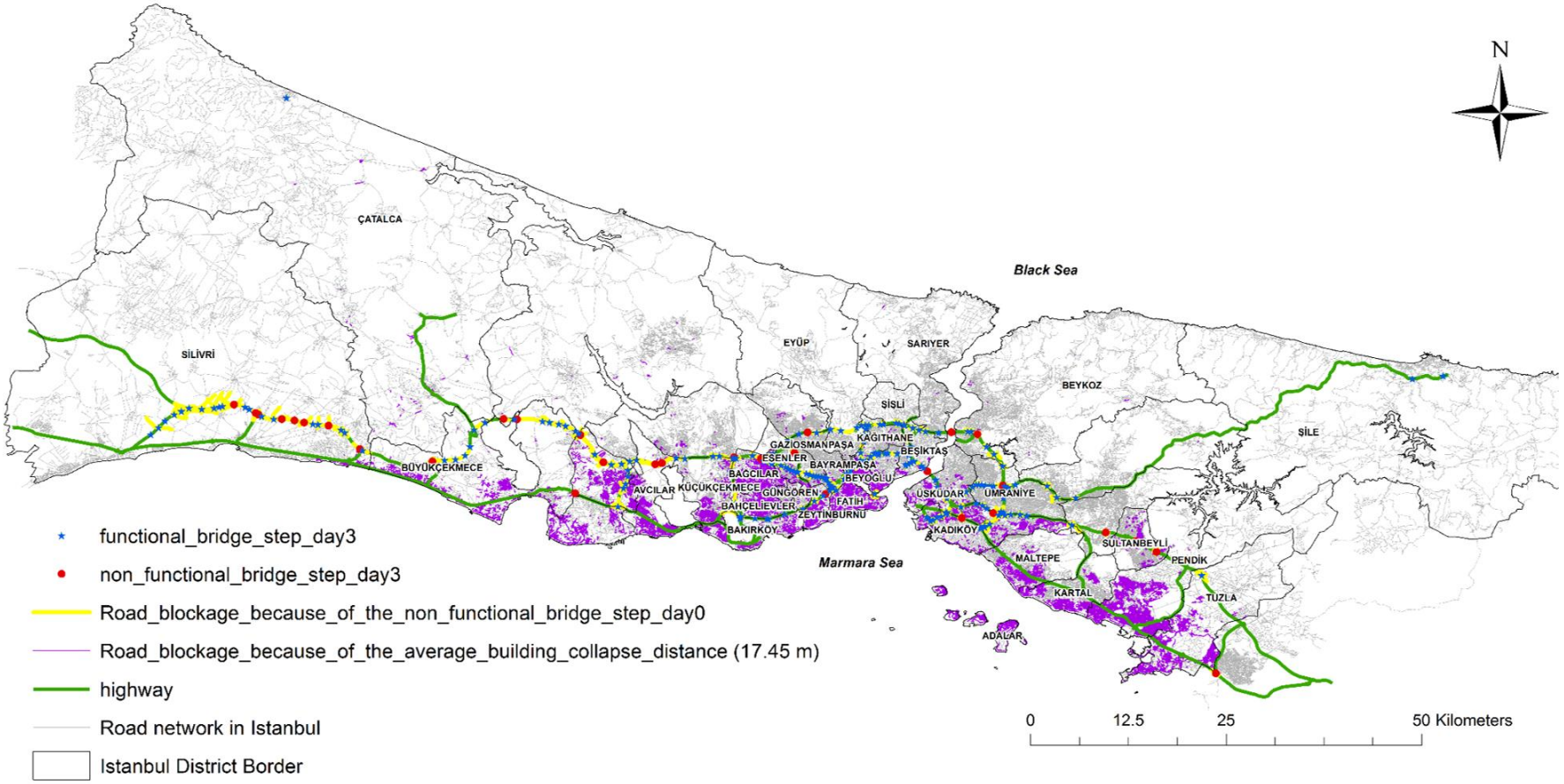


Figure 9.2 : Road blockage in Istanbul immediately after 3 days a potential earthquake.

Figures 9.3 and 9.4 show the results on a larger scale with a randomly selected region. Figure 9.3 displays the road and bridge functionality on the day of the earthquake and Figure 9.4 shows the same situation 3 days after the earthquake.

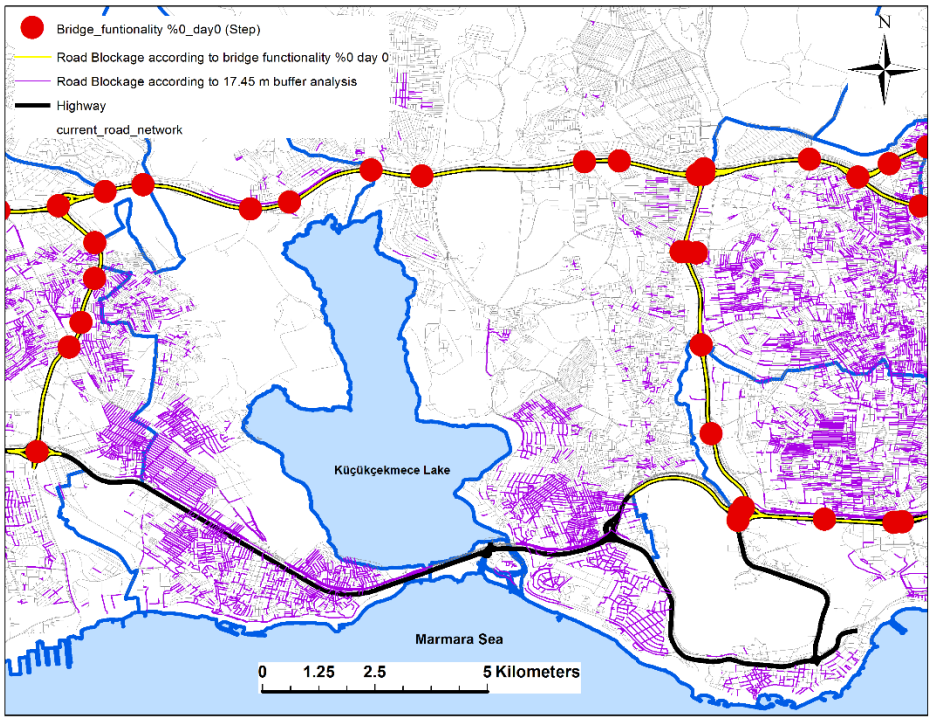


Figure 9.3 : Large scale representation of road blockage for day 0.

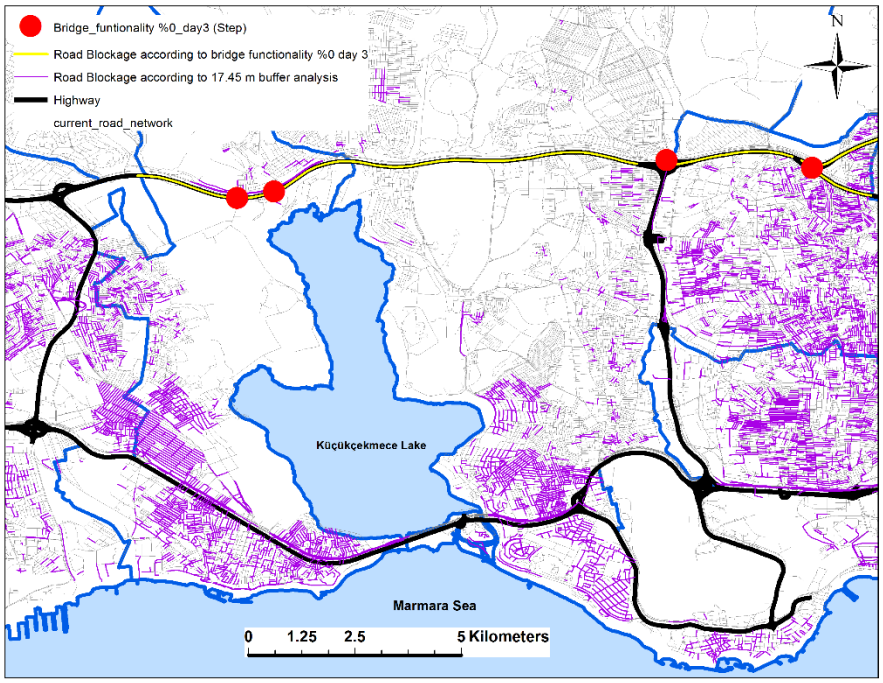


Figure 9.4 : Large scale representation of road blockage for day 3.

Figures 9.5 and 9.6 represent population in Istanbul that would be affected by the road blockages based on the sub-district border. As can be seen from the aformentioned figures, mostly populated areas would be affected by road blockage during the response time. Regarding these figures, it is estimated that these road blockages would affect 8,308,190 people around non-functional roads after an earthquake in Istanbul. This situation could cause an increase in the number of deaths or injuries in people because of a lack of access treatment.

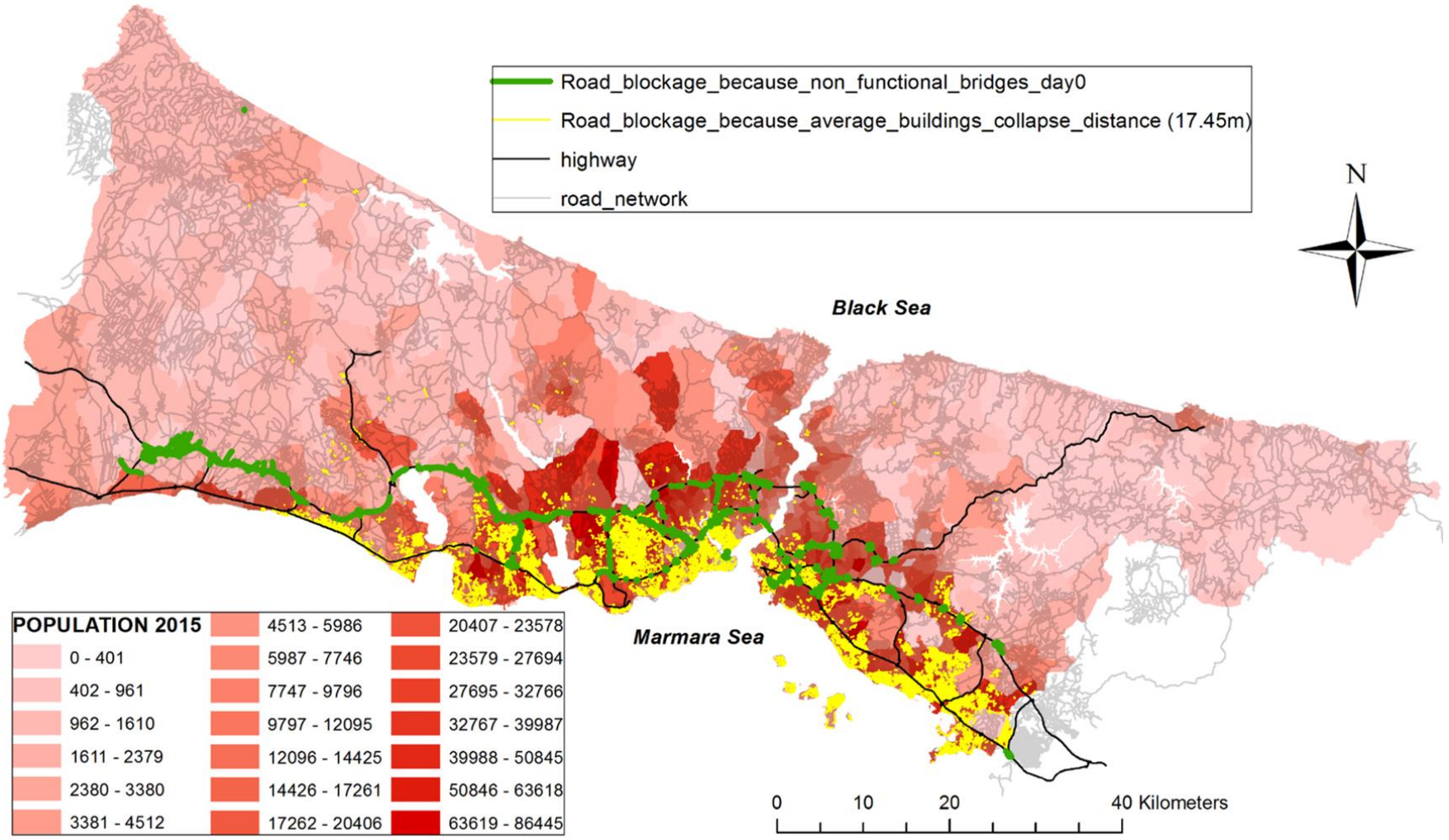


Figure 9.5 : Representation of road blockage in Istanbul with population distribution based on sub district.

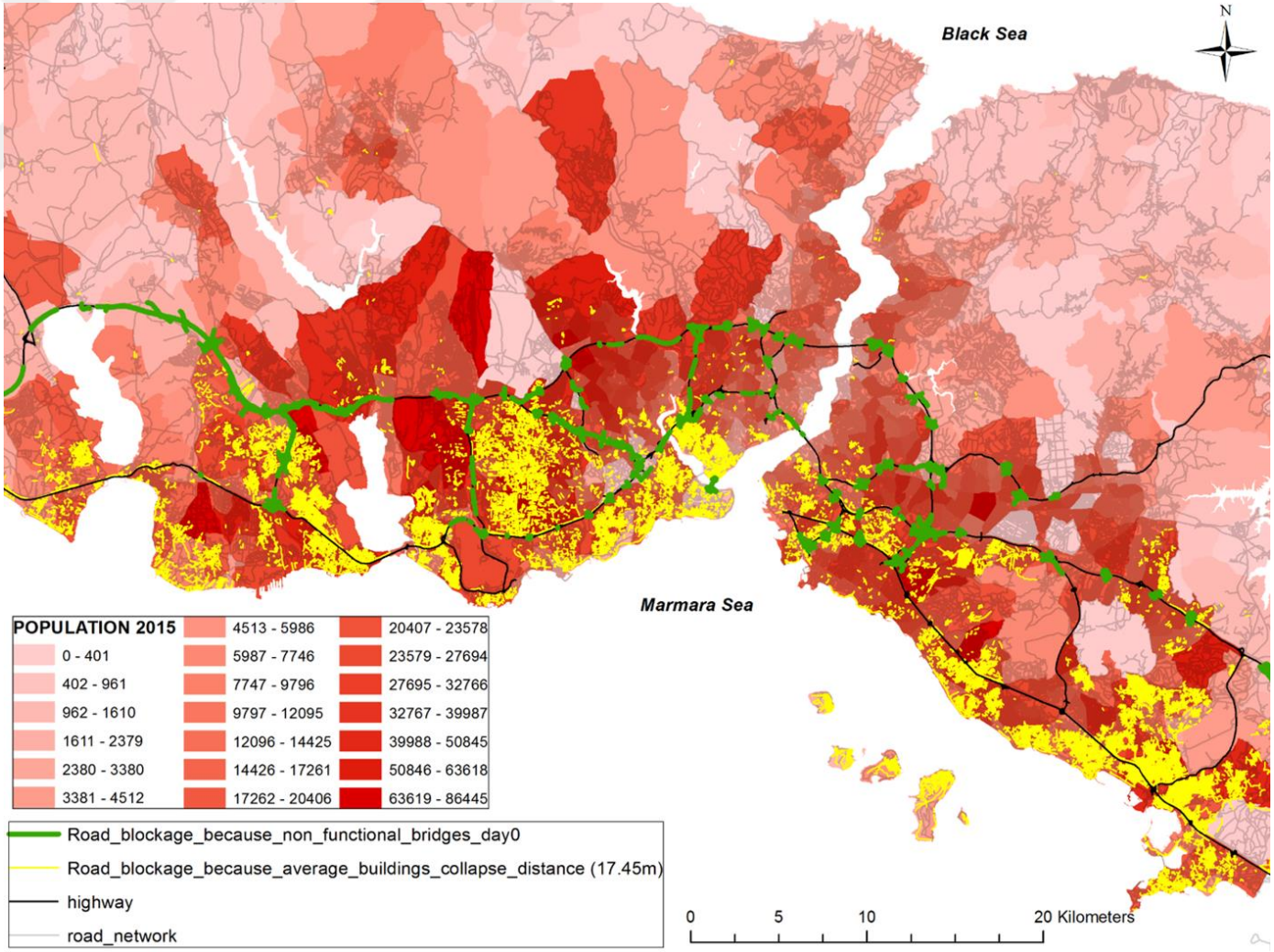


Figure 9.6 : Large scale representation of road blockage in Istanbul with population distribution based on sub district.

10. VALIDATION WITH OTHER STUDIES

10.1 Validation of the Building Age Study

10.1.1 Validation with the Küçükçekmece study

It was also important to validate the study with the data where the age information of the buildings was known. The Küçükçekmece district of Istanbul was an important sample to identify the ages of buildings where both empty lands, collapsed buildings and urban transformation projects existed (Figure 10.1).



Figure 10.1 : Change of buildings at Küçükçekmece district between 2004 and 2013.

The Urban Transformation Project in Küçükçekmece (KDMP) was completed in 2009 by the Istanbul Metropolitan Municipality, The Directory of Urban Transformation. The building age data for every building in the Küçükçekmece district were produced in GIS in the KDMP study. In order to validate the results, both KDMP and this study's results were compared.

KDMP data contained 32,965 items as polygon data. First, the structures in Küçükçekmece that did not match the building definitions like transform and bus stop were deleted from the KDMP data and 25,649 buildings remained to be compared. According to the KDMP, the oldest building was built in 1939 and the newest one in 2007. In order to compare two data sets, the building age of the KDMP data was

reclassified with regard to this study's building age classification. According to this study, 32,968 buildings were located in the Küçükçekmece district until the year 2013. According to Table 10.1, there is a difference between the total number of buildings, because of the latest recorded buildings inside the KDMP study does not contain the buildings constructed after 2007.

Table 10.1 : Comparison of building age classification between KDMP and this study.

Building Age Distribution	***KDMP***	***This Study***
Pre 1968	563	417
Between 1969 - 1982	9973	13002
Between 1983 - 1996	11879	14465
Between 1997- 2004	2292	3058
Between 2005 - 2007	762	1301
Between 2008 - 2013		725
Total	***25649***	***32968***

It can be seen from Figure 10.2 that the rate of increase and the difference in the number of buildings were directly proportional in both studies.

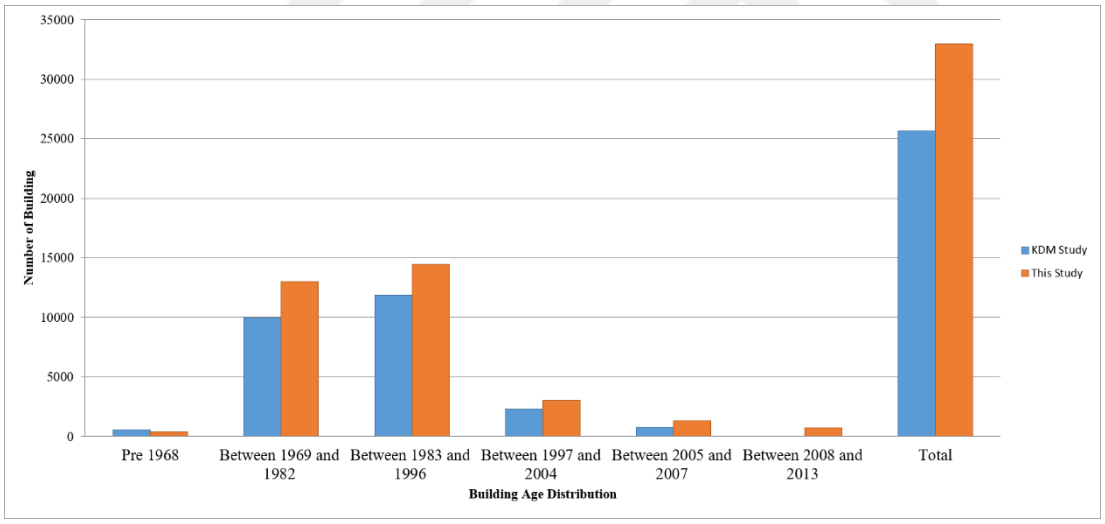


Figure 10.2 : Building age comparison of KDMP and this study in Küçükçekmece district.

In order to measure the concordance between the two studies for Küçükçekmece, the correlation between the two datasets was run and a value close to 1 was obtained (Table 10.2), which shows a very good linear association between these two datasets.

Table 10.2 : Correlation of KDMP and this study.

	Correlation Coefficient
Correlation between KDMP and This Study	0.9982

10.1.2 Validation with the TUIK study

Another validation was constituted with the Building Census work. The most recent officially registered study for buildings in Istanbul was completed in 2000 by theTurkish Statistical Institute (TUIK, 2014), what was then known as DIE (State Institute of Statistics). The Building Census was conducted between April and September 2000 on a national scale in Turkey. Previous studies about the building census were carried out by DIE in 1965, 1970 and 1984. The TUIK 2000 report also represents the result for the 1984 building census results (TUIK, 2014). Since 2000, TUIK has not published any data about the ages of the buildings. This also shows the importance of this study for Turkey and Istanbul. According to TUIK 2000, the Istanbul's building stock increased at a rate of 72% from 505,224 in 1984 to 869,444 buildings in 2000 (Table 10.3).

Table 10.3 : Result of TUIK building census of 1984 and 2000 (TUIK, 2014).

	1984 Building Census Study	***2000 Building Census Study***	***Year 2000 Estimated Building Count of This Study***
The number of buildings	505224	869444	851564

According to TUIK 2000, the number of buildings that were constructed between 1919 and 1969 was 132,461. This study shows that the number of buildings that were digitized from the 1966 Air Photo was 98,656. It can be easily estimated that, some of the structures that were not buildings could be counted as buildings today and some of the buildings may have collapsed before 1966. The difference between the second columns comparison in Figure 10.3, could have arisen due to the year intervals not matching each other with 4 years at the beginning and 3 years at the end, which was the highest number of constructions that occurred in Istanbul.

DIE 1984 counted the building stock in Istanbul in 1984 as 505,224, while this study digitized 432,150 buildings on the 1982 aerial image. TUIK 2000 study declared that the number of buildings in Istanbul in 2000 was 869,444, this study determined that the number of buildings in Istanbul in 1996 was 794,324 and in 2004 was 908,805. When the yearly increase ratio was considered, the estimated buildings count in 2000 from this study's values was estimated to be 851,564.

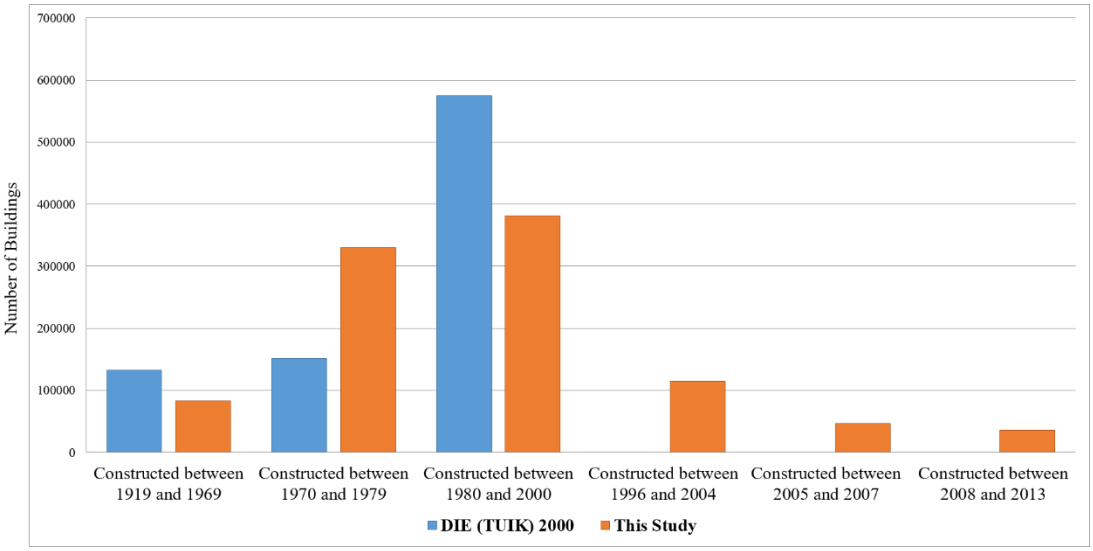


Figure 10.3 : Building age comparison of TUIK 2000 and this study.

10.2 Validation of the Building Damage Analysis Results

Evaluation of the HAZTURK software assessment results was published by H. Karaman et al. (2008). Based on the evaluation, it can be accepted that the software represents valuable results for earthquake loss assessment. Now, it is important to compare the results of the earthquake damage to buildings based on the new data and mappings for them. Table 10.4 shows the damage estimation results of several studies on the Istanbul building inventory including this study results (Bal, Crowley, & Pinho, 2008; BU-ARC, 2002; BU, ITU, METU, & YTU, 2003; Di Pasquale et al., 2004; Erdik et al., 2008; JICA & IMM, 2002; H. Karaman et al., 2008; Strasser et al., 2008; Yakut, Ozcebe, & Yucemen, 2006). Based on the refined building inventory it can be clearly noticed that the number of buildings at risk are increased during the 7 years. It is also important to declare that this study did not includes the recently constructed buildings based on the urban renovation law. Another important fact in Table 7.4 is that, most of the results that were compared in this study were based on the 7.5 Mw earthquake of JICA and IMM (2002) Model A scenario.

Table 10.4 : Comparison of Istanbul building damage estimation results based on Mw 7.5 earthquake scenario.

SIGE-DPC in 2008 (Di Pasquale et al., 2004) (Strasser et al., 2008)	***D0+D1***	***D2***	***D3*** 40.00	***D4+D5*** 3.64
ESCENARIS in 2008			***Heavy***	***Beyond Repair***
Level 0 (Strasser et al., 2008)			13.80	7.80
Level 1 (Strasser et al., 2008)			9.09	4.36
DBELA in 2008		***Moderate***	***Extensive***	***Collapse***
(Bal et al., 2008)		27.24	11.05	6.37
HAZTURK in 2008 (H. Karaman et al., 2008)	***Insignificant***	***Moderate***	***Heavy***	***Complete***
Boore and Atkinson (2006)	43.78	35.60	16.40	4.22
Ozbey et al., (2004)	43.69	35.02	16.63	4.66
Boore et al., (1997)	36.12	36.99	20.14	6.75
Kalkan & Gulkan (2004)	30.91	37.69	22.74	8.66
JICA in 2002	***H+M+P***	***H+M***	***Heavily***	
(JICA & IMM, 2002) *Boore et al., (1997)*	61.2	34.0	16.6	
KOERI in 2002		***Moderately***	***Extensive***	***Complete***
(BU-ARC, 2002)		26.45	9.14	4.72
Spectral Displacement Ba (Bal et al., 2008)sed			***Heavy***	***Damage Beyond Repair***
Intensity Based			10.43	5.5
(Yakut et al., 2006)	***Low Risk***	***Moderate Risk***	***High Risk***	
	10	21	69	
EMPI in 2003 (BU et al., 2003)			***Heavily Damaged Building Ratio***	
			13.22	
IMM *w ELER* in 2009 (IMM, 2009)	***Insignificant***	***Moderate***	***Heavy***	***Extensive***
Coefficient Method ASCE %	30.87	13.78	3.08	0.91
	Insignificant	***Moderate***	***Heavy***	***Extensive***
Mean Damage Building %	27.29	10.01	1.82	0.46
HAZTURK in 2015	***Insignificant***	***Moderate***	***Heavy***	***Complete***
Boore and Atkinson (2008) Sa	21.52	35.55	28.21	14.68
Boore and Atkinson (2008) PGA	50.37	31.85	13.99	3.80

It must also be taken into consideration that most of the studies that were compared in Table 7.4 used different attenuation relations, vulnerability functions; and the most important difference was in the focused building data as the format, date, attributes and specifications. As can be seen from H. Karaman et al. (2008), the methodology of the HAZTURK loss assessment and damage estimation analyses were validated. This study focused the study from a new perspective by taking into account the changes in the inventory which were at risk. So, the differences should be taken into account by noticing the changes in the actual inventory.

11. DISCUSSION AND CONCLUSIONS

Here is a brief outline of the main steps taken and facts about this study.

- The building ages were determined for every single building in Istanbul based on GIS for the first time in this study.
- A building damage analysis for every single building in Istanbul was made by using recent and current building datasets.
- The building collapse direction was studied for the first time on a national and international scale.
- A bridge damage analysis was made for 247 bridges on the highway in Istanbul.
- There were 990,584 buildings in Istanbul at the end of 2013.
- 794,325 buildings in Istanbul were constructed before 1996.
- The increase in the building stock between 1996 and 2013 was 24.71% from 794,325 to 990,584.
- 80% of the buildings in Istanbul are occupied as multi family dwellings.
- Approximately 5000 of the buildings in Istanbul are used as Educational Facilities.
- About 1500 buildings in Istanbul are used as health facilities.; 721 of them are hospitals.
- The oldest buildings are located in the Fatih district of the European side of th city.
- An increase in the number of buildings between 1969 and 1982 was seen mostly in the Sarıyer, Kağıthane, Gaziosmanpaşa, Bayrampaşa and Bağcılar districts in the European side of Istanbul.

- Between 1983 and 1996 the Silivri, Sultangazi, Bağcılar, Avcılar and Esenyurt distircts have had the highest increases in the number of buildings in the European side of Istanbul.
- The districts with the highest increase rate from 1997 to 2004 were Esenyurt, Silivri, Büyükçekmece, Avcılar and Başakşehir on the European side of Istanbul.
- The highest rate of increase occurred in Büyükçekmece, Esenyurt, Arnavutköy, Avcılar and Silivri between 2005 and 2007, while in Esenyurt, Büyükçekmece, Arnavutköy, Sarıyer and Zeytinburnu districts the increase rate maximized between 2008 and 2013 on the European side of Istanbul.
- Most of the buildings that were constructed before 1969 are mostly located in the Kadiköy and Üsküdar districts in the Anatolian side of Istanbul.
- Between 1969 and 1982, the number of buildings were mostly increased in the Üsküdar, Beykoz, Ümraniye, Kartal and Maltepe districts in Anatolian side of Istanbul.
- Pendik, Sultanbeyli, Ümraniye, Sancaktepe and Beykoz were the top five districts where the most increase occured between the years 1983 and 1996 in the Anatolian side of Istanbul.
- Between 1997 and 2004, the Beykoz, Ataşehir, Ümraniye, Pendik, Çekmeköy districts saw the highest increase in the number of buildings in the Anatolian side of Istanbul.
- The increase in the number of buildings between 2005 and 2007 occurred mostly in Çekmeköy, Ümraniye, Sancaktepe, Pendik and Maltepe districts in the Anatolian side of Istanbul.
- Between 2008 and 2013, the Tuzla, Sancaktepe, Pendik, Ataşehir ve Çekmeköy districts saw the highest increase in buildings in the Anatolian side of Istanbul.
- When the increases in the number of buildings were analyzed between 1982 and 2013 on a district basis, the highest increase in the number of buildings was seen in the Silivri district, with 33,688 buildings. This was closely followed by the districts of Pendik, Ümraniye, Esenyurt and Sancaktepe.

- The lowest increase rate was observed in Bakırköy district with 29,14 buildings built between 1982 and 2013.
- With 46,347 buildings, the highest number of buildings were located in the Ümraniye district on the Anatolian side of the city, while the smallest number of buildings were located in Adalar district with 5,905 buildings.
- 196,529 buildings were constructed in Istanbul between the years of 1997 and 2013.
- Büyükçekmece, Esenyurt, and Küçükçekmece are the districts where the newest buildings were located, while the oldest buildings were located in Fatih, Beyoğlu, and Beşiktaş.
- According to Sa, the distribution of damage ratio of Istanbul buildings were 21.52% insignificant damage, 35.55% moderate damage, 28.21% heavy damage, 14.68% complete damage, and 35.23% mean damage, respectively.
- According to PGA, the distribution of damage ratio of Istanbul's buildings were 50.37% insignificant damage, 31.85% moderate damage, 13.99% heavy damage, 3.80% complete damage, and 15.6% mean damage, respectively.
- There are 19,679 buildings in Istanbul that may have complete and heavy damage, with a possibility greater than 40% according to 0.2 sec Sa.
- There are 14,066 buildings that have the possibility of complete and heavy damage of more than 30%, due to PGA.
- There are 680,817 buildings in Istanbul that have the possibility of mean damage of more than 30% according to Sa.
- There are 44,642 buildings in Istanbul with Near angles between 31.2700 and 55.8160.
- According to the statistical process between 317 debris spreading vectors in every direction, the maximum distance of the debris of the collapsed buildings in Gölcük was 37.18m, the average distance of the debris of the collapsed buildings in Gölcük was 17.45m and the least distance of the debris of the collapsed buildings in Gölcük is 4.81mThe current road network in Istanbul is approximately 30325 km in length.

- Regarding the road blockage analysis (debris area), approximately 3000 km of the road network could lose its functionality. This results show that 10% of the Istanbul road network could lose its functionality.
- Mostly potentially non-functional roads would be located in the southern part of the city. In these locations, the level of urbanization is very high. For this reason, it can be understood that the process of response and recovery operations following the earthquake may not be possible for many locations due to the non-functionality of the road network.
- According to the step functionality analysis, 194 bridges are estimated to be non-functional immediatelly following an earthqauke.
- After 3 days from the earthquake, 33 bridges are estimated to be non-functional.
- The highway in Istanbul is approximately 700 km in length
- Because of the non-functional bridges, approximately 500km of roads will loose their functionality immediately after a potential earthqauke.
- 3500 kms of roads will lose their functionality after an earthquake by assessment of the building collapse direction and bridge functionality together.
- The results and the proposed methods in this study represent important contributions that can be used as a database for decision makers to develop important strategies for risk reduction, to prevent a hazard from becoming a disaster and to transform the urban areas based on the earthquake risk. Another important outcome of this study is to enable the decision makers to optimize the resources that will be used in the response and recovery phases of the integrated disaster management cycle.
- Within the context of this study, the methods, used to determine "Building Collapse Direction and Angles" for the buildings in Istanbul, were produced by using the data from the collapsed buildings in Gölcük during the 1999 Kocaeli Earthquake. However, the direction and the angles obtained had limitations because the collapsed buildings in Gölcük were located approximately in the southern part of the 1999 Kocaeli Earthquake epicenter. If it was possible to obtain the pre and post-earthquake remote sensing for the

areas where the damaged buildings were located around the earthquake epicenter, this would supply us with a wide-spectrum of data.

- If it was possible to obtain number of floors, construction type and even load-bearing columns or weak columns, it would supply us with more accurate and reliable results for the building collapse direction. By using these data, the building collapse direction model would be further developed.
- One of the most important limitations of this study is to determine the buildings from remote sensing data by using the digitisation process as it takes a long time. In order to decrease the processing time, a new programme should be developed for detecting buildings according to their roof type and colour and shape. If this programme could be developed, it would be more possible to detect buildings in Istanbul.

REFERENCES

Alyamac, K. E. & Erdogan, A. S. (2005). Geçmişten Günümüze Afet Yönetmelikleri ve Uygulamada Karşılaşılan Hataları. *Deprem Sempozyumu*, Kocaeli, Türkiye: March 23-25.

Ambraseys, N. (2002). The seismic activity of the Marmara Sea region over the last 2000 years. *Bulletin of the Seismological Society of America, 92*(1), 1-18.

Ambraseys, N. & Finkel, C. (1991). Long-term seismicity of Istanbul and of the Marmara Sea region. *Terra Nova, 3*(5), 527-539.

Apaydin, N. (2005). İstanbul'daki Köprülerin Değerlendirilmesi. *3. İstanbul Deprem Sempozyumu*, İstanbul, Türkiye: June 8-9.

Apaydin, N. (2014). Seismic retrofit of large scale bridges in Istanbul. *Istanbul Bridge Conference,* Istanbul, Turkey: August 11-13.

Apaydın, N. M. (2010). Earthquake performance assessment and retrofit investigations of two suspension bridges in Istanbul. *Soil Dynamics and Earthquake Engineering, 30*(8), 702-710.

Armijo, R., Meyer, B., Navarro, S., King, G., & Barka, A. (2002). Asymmetric slip partitioning in the Sea of Marmara pull-apart: a clue to propagation processes of the North Anatolian Faul. *Terra Nova, 14*(2), 80-86.

Armijo, R., Pondard, N., Meyer, B., Uçarkus, G., De Lépinay, B. M., Malavieille, J., & Beck, C. (2005). Submarine fault scarps in the Sea of Marmara pull-apart (North Anatolian Fault): Implications for seismic hazard in Istanbul. *Geochemistry, Geophysics, Geosystems, 6*(6).

Awrangjeb, M. (2015). Effective Generation and Update of a Building Map Database Through Automatic Building Change Detection from LiDAR Point Cloud Data. *Remote Sensing, 7*(10), 14119. Retrieved from http://www.mdpi.com/2072-4292/7/10/14119.

Aytekin, Ö., Erener, A., Ulusoy, İ., & Düzgün, Ş. (2012). Unsupervised building detection in complex urban environments from multispectral satellite imagery. *International Journal of Remote Sensing, 33*(7), 2152-2177. doi:10.1080/01431161.2011.606852.

Bal, I., Crowley, H., & Pinho, R. (2008). Displacement-based earthquake loss assessment for an earthquake scenario in Istanbul. *Journal of Earthquake Engineering, 12*(S2), 12-22.

Başöz, N., & Kiremidjian, A. S. (1996). Risk assessment for highway transportation systems. John A. Blume Earthquake Engineering Center.

Benedek, C., Descombes, X., & Zerubia, J. (2012). Building Development Monitoring in Multitemporal Remotely Sensed Image Pairs with Stochastic Birth-Death Dynamics. *IEEE Transactions on Pattern Analysis and Machine Intelligence, 34*(1), 33-50. doi:10.1109/TPAMI.2011.94.

Bibbee, A., Gönenç, R., Jacobs, S., Konvitz, J., & Price, R. W. (2000). *Economic Effects of the 1999 Turkish Earthquakes: An Interim Report, Organisation for Economic Co-operation and Development, Economics Department Working Papers* (Report No: 247). June 26, 2000, Paris. Retrieved from http://dx.doi.org/10.1787/233456804045.

Boore, D. M., & Atkinson, G. M. (2008). Ground-Motion Prediction Equations for the Average Horizontal Component of PGA, PGV, and 5%-Damped PSA at Spectral Periods between 0.01 and 10.0. *Earthquake Spectra, 24*(1), 99-138. doi:10.1193/1.2830434.

BU-ARC. (2002). *Earthquake risk assessment for the Istanbul metropolitan area*. Istanbul: Boğaziçi University, Kandilli Observatory and Earthquake Research Institute.

BU, ITU, METU, & YTU. (2003). *Earthquake master plan for Istanbul*.Istanbul: Istanbul Metropolitan Municipality.

Catal, H., Yazıcı, H., & Tüzün, C. (1999, 24.11.1999). Comparison of Earthquake Codes. Türkiye İnşaat Mühendisliği XV. Teknik Kongresi, Ankara, Turkey: November 24-26. http://www.imo.org.tr/resimler/ekutuphane/pdf/12931.pdf.

Chang, S., & Nojima, N. (1998). Measuring lifeline system performance: highway transportation systems in recent earthquakes. *The 6 th National Earthquake Conference on Earthquake Engineering*, Seattle, USA.

Crowley, H., Bommer, J. J., Pinho, R., & Bird, J. (2005). The impact of epistemic uncertainty on an earthquake loss model. *Earthquake Engineering & Structural Dynamics, 34*(14), 1653-1685. doi:10.1002/eqe.498.

Crowley, H., Pinho, R., & Bommer, J. (2004). A Probabilistic Displacement-based Vulnerability Assessment Procedure for Earthquake Loss Estimation. *Bulletin of Earthquake Engineering, 2*(2), 173-219. doi:10.1007/s10518-004-2290-8.

DESA, U. (2014). Department of Economic and Social Affairs, Population Division, United Nations (2014). World Urbanization Prospects: The 2014 Revision, CD-ROM Edition. from UN publications, New York, http://esa.un.org/unpd/wup/CD-ROM/

DesRoches, R., Leon, R. T., & Dyke, S. (2003). Response modification of bridges. *Mid-America Earthquake Center CD Release 03-08*.

DesRoches, R., Padgett, J., Elnashai, A., Kim, Y., & Reed, D. (2006). MAE Center transportation test bed. *The 8th US National Conference on Earthquake Engineering*, San Francisco, California: April 18-22.

DesRoches, R., Padgett, J., & Nilsson, E. (2008). Seismic Risk Assessment of the Transportation Network of Charleston, South Carolina. *The Sixth National Seismic Conference on Bridges and Highways*, South Carolina: Jully 27-30.

Di Pasquale, G., Ferlito, R., Orsini, G., Papa, F., Pizza, A., Van Dyck, J., & Veneziano, D. (2004). Seismic scenario tools for emergency planning and management. *Proceedings of the XXIX general assembly of the European Seismological Commission*, Potsdam, Germany.

Dönmez, M. C., Cilingir, İ. N., & Özer, E. (2014). Seismic evaluation and retrofit of an existing bridges by using current codes of practice. *Istanbul Bridge Conference*, Istanbul, Turkey: August 11-13.

Elnashai, A. S., Hampton, S., Karaman, H., Lee, J. S., Mclaren, T., Myers, J., & Tolbert, N. (2008). Overview and applications of Maeviz-Hazturk 2007. *Journal of Earthquake Engineering, 12*(S2), 100-108.

Erdik, M., Cagnan, Z., Zulfikar, C., Sesetyan, K., Demircioglu, M., Durukal, E., & Kariptas, C. (2008). Development of rapid earthquake loss assessment methodologies for Euro-Med region. *14th World Conference on Earthquake Engineering*, Beijing, China: October 12-17.

ERGO. (2015). ERGO Multi-Hazard Assessment, Response, and Planning. Retrieved from http://ergo.ncsa.illinois.edu/

FEMA, H.-M. (2003). MR3 Technical Manual. *Multi-hazard Loss Estimation Methodology Earthquake Model*.

Fraser, C., Baltsavias, E., & Gruen, A. (2002). Processing of Ikonos imagery for submetre 3D positioning and building extraction. *ISPRS Journal of Photogrammetry and Remote Sensing, 56*(3), 177-194.

Gupta, R., Saraf, A., Saxena, P., & Chander, R. (1994). IRS detection of surface effects of the Uttarkashi earthquake of 20 October 1991, Himalaya. *International Journal of Remote Sensing, 15*(11), 2153-2156.

HAZTURK. (2007). *Developing a Loss Estimation Program, HAZTURK Based On HAZUS (Hazards Us) to be Used Before, During and After a Disaster: A Case Study For Istanbul (Report No: 104Y254).*TUBİTAK.

Holmes, W., Kircher, C., Petak, W., & Youssef, N. (2008). Seismic performance objectives for tall buildings: A report for the tall buildings initiative, PEER 2008/101. *Berkeley (CA): Pacific Earthquake Engineering Research Center*.

Hron, V., & Halounova, L. (2015). *Use of Aerial Images for Regular Updates of Buildings in the Fundamental Base of Geographic Data of the Czech Republic*. Paper presented at the Joint ISPRS conference 2015, Munich, Germany. http://www.int-arch-photogramm-remote-sens-spatial-inf-sci.net/XL-3-W2/73/2015/.

Huertas, A., & Nevatia, R. (1988). Detecting buildings in aerial images. *Computer Vision, Graphics, and Image Processing, 41*(2), 131-152. doi:http://dx.doi.org/10.1016/0734-189X(88)90016-3.

IMM. (2009). *İstanbul Olası Deprem Kayıp Tahminleri.* İstanbul: İstanbul Büyükşehir Belediyesi.

Jeong, S.-H., & Elnashai, A. S. (2006). New three-dimensional damage index for RC buildings with planar irregularities. *Journal of Structural Engineering, 132*(9), 1482-1490.

JICA, & IMM. (2002). *The Study on A Disaster Prevention / Mitigation Basic Plan in Istanbul including Seismic Microzonation in the Republic of Turkey*, İstanbul: İstanbul Büyükşehir Belediyesi.

Kameda, H. (2000). Engineering management of lifeline systems under earthquake risk. *Bulletin of the New Zealand Society for Earthquake Engineering, 33*(3), 248-264.

Karaman, H. (2009). Comparison of The Istanbul Earthquake Loss Assessment Studies. *The 16th TIEMS Annual Conference*, Istanbul, Turkey: June 9-11.

Karaman, H., & Erden, T. (2014). Net earthquake hazard and elements at risk (NEaR) map creation for city of Istanbul via spatial multi-criteria decision analysis. *Natural Hazards*, 1-25. doi:10.1007/s11069-014-1099-2

Karaman, H., Şahin, M., & Elnashai, A. S. (2008). Earthquake loss assessment features of maeviz-istanbul (hazturk). *Journal of Earthquake Engineering, 12*(S2), 175-186.

Karaman, H., Sahin, M., Elnashai, A. S., & Pineda, O. (2008). Loss assessment study for the zeytinburnu district of Istanbul using Maeviz-Istanbul (HAZTURK). *Journal of Earthquake Engineering, 12*, 187-198. doi:10.1080/13632460802014030

Karim, K. R., & Yamazaki, F. (2003). A simplified method of constructing fragility curves for highway bridges. *Earthquake Engineering & Structural Dynamics, 32*(10), 1603-1626.

Kaya, Ş., Curran, P., & Llewellyn, G. (2005). Post-earthquake building collapse: a comparison of government statistics and estimates derived from SPOT HRVIR data. *International Journal of Remote Sensing, 26*(13), 2731-2740.

Kiremidjian, A., Moore, J., Basoz, N., Burnell, K., Fan, Y., & Hortacsu, A. (2002). Earthquake risk assessment for transportation systems: Analysis of pre-retrofitted system. *The 7th National Conference on Earthquake Engineering*, Boston, Mass, USA: July 21-25.

Kobe Earthquake, 1995. (2015). *Retrieved November 21, 2015* from http://kids.britannica.com/comptons/art-186771/Kobe-Japan-was-hard-hit-by-an-earthquake-in-January.

Le Pichon, X., Chamot-Rooke, N., Rangin, C., & Sengör, A. (2003). The North Anatolian fault in the Sea of Marmara. *Journal of Geophysical Research: Solid Earth (1978–2012), 108*(B4).

Lee, D. S., Shan, J., & Bethel, J. S. (2003). Class-guided building extraction from Ikonos imagery. *Photogrammetric Engineering & Remote Sensing, 69*(2), 143-150.

Lin, C., & Nevatia, R. (1998). Building Detection and Description from a Single Intensity Image. *Computer Vision and Image Understanding, 72*(2), 101-121. doi:http://dx.doi.org/10.1006/cviu.1998.0724.

Manno-Kovacs, A., & Sziranyi, T. (2015). Orientation-selective building detection in aerial images. *ISPRS Journal of Photogrammetry and Remote Sensing, 108*, 94-112. doi:http://dx.doi.org/10.1016/j.isprsjprs.2015.06.007.

Matikainen, L., Hyyppä, J., Ahokas, E., Markelin, L., & Kaartinen, H. (2010). Automatic detection of buildings and changes in buildings for updating of maps. *Remote Sensing, 2*(5), 1217-1248.

Meacham, B., Bowen, R., Traw, J., & Moore, A. (2005). Performance-based building regulation: current situation and future needs. *Building Research & Information, 33*(2), 91-106. doi:10.1080/0961321042000322780

Molina, S., & Lindholm, C. (2005). A logic tree extension of the capacity spectrum method developped to estimate seismic risk in Oslo, Norway. *Journal of Earthquake Engineering, 09*(06), 877-897. doi:doi:10.1142/S1363246905002201

Namlı, E., Yıldız, D., Erinçer, M., & Özer, E. (2014). *Seismic Retrofit of reinforced Concrete Bridges by using Structural Steel Elements. Istanbul Bridge Conference,* Istanbul, Turkey: August 11-13.

Nielson, B. G. (2005). *Analytical fragility curves for highway bridges in moderate seismic zones* (PhD Thesis). School of Civil and Environmental Engineering, Georgia Institute of Technology, USA.

Nielson, B. G., & DesRoches, R. (2007a). Analytical seismic fragility curves for typical bridges in the central and southeastern United States. *Earthquake Spectra, 23*(3), 615-633.

Nielson, B. G., & DesRoches, R. (2007b). Seismic fragility methodology for highway bridges using a component level approach. *Earthquake Engineering and Structural Dynamics, 36*(6), 823.

Niemeyer, J., Rottensteiner, F., & Soergel, U. (2014). Contextual classification of lidar data and building object detection in urban areas. *ISPRS Journal of Photogrammetry and Remote Sensing, 87*, 152-165. doi:http://dx.doi.org/10.1016/j.isprsjprs.2013.11.001.

Nilsson, E. (2008). *Seismic Risk Assessment of thr Transportation Network in Charleston, SC.* (MSc Thesis). Georgia Institute of Technology, USA.

Ok, A. O., Senaras, C., & Yuksel, B. (2013). Automated Detection of Arbitrarily Shaped Buildings in Complex Environments From Monocular VHR Optical Satellite Imagery. *IEEE Transactions on Geoscience and Remote Sensing, 51*(3), 1701-1717. doi:10.1109/TGRS.2012.2207123.

Özmen, B. (2000). *17 Ağustos 1999 İzmit Körfezi Depremi'nin Hasar Durumu (Rakamsal Verilerle)* (TDV / DR 010-53). Retrieved from: http://deprem.gazi.edu.tr/posts/download?id=43388.

Padgett, J. E., & DesRoches, R. (2007). Bridge functionality relationships for improved seismic risk assessment of transportation networks. *Earthquake Spectra, 23*(1), 115-130.

Parsons, T. (2004). Recalculated probability of M≥ 7 earthquakes beneath the Sea of Marmara, Turkey. *Journal of Geophysical Research: Solid Earth (1978–2012), 109*(B5).

Parsons, T., Toda, S., Stein, R. S., Barka, A., & Dieterich, J. H. (2000). Heightened odds of large earthquakes near Istanbul: An interaction-based probability calculation. *Science, 288*(5466), 661-665.

Rangin, C., Demirbağ, E., Caner, İ., Crusson, A., Le Pichon, X., & Şengör, A. C. (2001). *Marine Atlas of the Sea of Marmara (Turkey): Data Collected on Board RV Le Suroît, September 2000*: Ifremer.

Rojahn, C., Scawthorn, C., & Khater, M. (1992). Transportation lifeline losses in large eastern earthquakes. *In Lifeline earthquake engineering in the Central and Eastern US.* ASCE, *1992.*

Roux, M., & McKeown, D. M. (1994). Feature matching for building extraction from multiple views. *In Computer Vision and Pattern Recognition, 1994. Proceedings CVPR'94., 1994 IEEE Computer Society Conference on*. IEEE, 1994.

Saraf, A., Sinvhal, A., Sinvhal, H., Ghosh, P., & Sarma, B. (2002). Satellite data reveals 26 January 2001 Kutch earthquake-induced ground changes and appearance of water bodies. *International Journal of Remote Sensing, 23*(9), 1749-1756.

Sirmacek, B., & Unsalan, C. (2009). Urban-Area and Building Detection Using SIFT Keypoints and Graph Theory. *IEEE Transactions on Geoscience and Remote Sensing, 47*(4), 1156-1167. doi:10.1109/TGRS.2008.2008440.

Sirmacek, B., & Unsalan, C. (2011). A Probabilistic Framework to Detect Buildings in Aerial and Satellite Images. *IEEE Transactions on Geoscience and Remote Sensing, 49*(1), 211-221. doi:10.1109/TGRS.2010.2053713.

Sohn, G., & Dowman, I. (2001). Extraction of buildings from high resolution satellite data. *Automated Extraction of Man-Made Objects from Aerial and Space Images (III). Balkema Publishers, Lisse*, 345-355.

Strasser, F. O., Bommer, J. J., Şeşetyan, K., Erdik, M., Çağnan, Z., Irizarry, J., Lindholm, C. (2008). A Comparative Study of European Earthquake Loss Estimation Tools for a Scenario in Istanbul. *Journal of Earthquake Engineering, 12*(sup2), 246-256. doi:10.1080/13632460802014188

TUIK. (2014). 2014 Address Based Census System Registration (ADNKS). 2014. Retrieved from http://tuikapp.tuik.gov.tr/adnksdagitapp/adnks.zul

Turker, M., & San, B. (2003). SPOT HRV data analysis for detecting earthquake-induced changes in Izmit, Turkey. *International Journal of Remote Sensing, 24*(12), 2439-2450.

Turker, M., & San, B. (2004). Detection of collapsed buildings caused by the 1999 Izmit, Turkey earthquake through digital analysis of post-event aerial photographs. *International Journal of Remote Sensing, 25*(21), 4701-4714.

Turker, M., & Sumer, E. (2008). Building-based damage detection due to earthquake using the watershed segmentation of the post-event aerial images. *International Journal of Remote Sensing, 29*(11), 3073-3089.

USGS. (2015). Historic Earthquakes. Retrieved from http://earthquake.usgs.gov/earthquakes/eqarchives/year/1999/1999_08_17.php

Utsu, T. (1990). Table of worldwide disastrous earthquakes. University of Tokyo, Tokyo, Japan.

Werner, S. D., Taylor, C., Moore, J.E. II, & Walton, J.S. (2000). *A risk-based methodology for assessing the seismic performance of highway systems.* Report MCEER-00-0014, Multidisciplinary Center for Earthquake Engineering Research, University at Buffalo, (Dec31).

Werner, S. D., Taylor, C. E., Moore, J., Mander, J. B., Jernigan, J. B., & Hwang, H. (2004). New Development in Seismic Risk Analysis for Highway Systems. *In 13th World Conference on Earthquake Engineering*, Vancouver, B.C., Canada .

Werner, S. D., Taylor, C. E., Moore, J. E., & Walton, J. S. (1999). Seismic risk analysis of highway systems: new developments and future directions. *In Optimizing Post-Earthquake Lifeline System Reliability*. ASCE, 1999.

Yakut, A., Ozcebe, G., & Yucemen, M. S. (2006). Seismic vulnerability assessment using regional empirical data. *Earthquake Engineering & Structural Dynamics, 35*(10), 1187-1202. doi:10.1002/eqe.572.

3194 Sayılı İmar Kanunu. (1985). *T.C. Resmi Gazete, 18749*, 09 Mayıs 1985.

APPENDICES

APPENDIX A : Tables
APPENDIX B : Maps

APPENDIX A: Tables

Table A.1 : Classification of building collapse direction, distance and angle in Gölcük according to near and LDM analysis results - CLS01.

CLASS	Id	$N_2(^0)$	S_F (m)	$N_1(^0)$	S_S (m)	LDM_CLASS
CLS01	1	31.270	4217.146	-173.180	17.338	LDM5
CLS01	2	31.436	4250.049	-175.322	22.460	LDM5
CLS01	3	31.464	4201.426	-152.554	17.194	LDM5
Average				-167.019	18.998	

Table A.2 : Classification of building collapse direction, distance and angle in Gölcük according to near and LDM analysis results – CLS02.

CLASS	Id	$N_2(^0)$	S_F (m)	$N_1(^0)$	S_S (m)	LDM_CLASS
CLS02	20	31.469	4033.404	112.253	16.008	LDM1
CLS02	17	31.592	3970.481	104.689	12.300	LDM1
CLS02	18	31.751	3962.794	87.231	13.832	LDM1
CLS02	21	31.920	4037.014	98.713	12.960	LDM1
CLS02	19	31.932	3952.983	83.102	13.681	LDM1
Average				97.198	13.756	

Table A.3 : Classification of building collapse direction, distance and angle in Gölcük according to near and LDM analysis results – CLS03.

CLASS	Id	$N_2(^0)$	S_F (m)	$N_1(^0)$	S_S (m)	LDM_CLASS
CLS03	5	32.032	4184.300	-103.245	11.945	LDM3
CLS03	4	32.202	4214.989	-98.531	17.213	LDM3
CLS03	25	32.471	4083.368	-105.535	14.555	LDM3
Average				-102.437	14.571	

Table A.4 : Classification of building collapse direction, distance and angle in Gölcük according to near and LDM analysis results – CLS04.

CLASS	Id	$N_2(^0)$	S_F (m)	$N_1(^0)$	S_S (m)	LDM_CLASS
CLS04	38	34.465	3926.233	104.902	11.643	LDM1
CLS04	37	34.740	3952.922	87.367	16.609	LDM1
CLS04	36	35.069	3951.643	90.566	15.290	LDM1
Average				94.278	14.514	

Table A.5 : Classification of building collapse direction, distance and angle in Gölcük according to near and LDM analysis results – CLS05.

CLASS	Id	$N_2(^0)$	S_F (m)	$N_1(^0)$	S_S (m)	LDM_CLASS
CLS05	92	37.552	3753.536	-88.522	11.819	LDM3
CLS05	90	38.011	3724.207	-88.963	10.326	LDM3
CLS05	94	38.136	3743.852	-90.954	15.840	LDM3
CLS05	91	38.362	3725.053	-87.156	13.296	LDM3
CLS05	62	38.448	3693.795	-93.315	20.428	LDM3
CLS05	80	38.767	3724.298	-91.857	15.487	LDM3
CLS05	81	38.914	3763.304	-91.473	25.545	LDM3
Average				-90.320	16.106	

Table A.6 : Classification of building collapse direction, distance and angle in Gölcük according to near and LDM analysis results – CLS06.

CLASS	Id	$N_2(^0)$	S_F (m)	$N_1(^0)$	S_S (m)	LDM_CLASS
CLS06	64	39.229	3626.369	62.497	23.398	LDM1
CLS06	65	39.516	3613.660	71.434	24.626	LDM1
CLS06	66	39.773	3599.420	82.970	23.205	LDM1
Average				72.300	23.743	

Table A.7 : Classification of building collapse direction, distance and angle in Gölcük according to near and LDM analysis results – CLS07.

CLASS	Id	$N_2(^0)$	S_F (m)	$N_1(^0)$	S_S (m)	LDM_CLASS
CLS07	70	40.234	3639.981	-33.676	17.151	LDM4
CLS07	71	40.758	3558.634	-12.876	20.214	LDM4
CLS07	96	41.619	3534.397	-13.378	16.876	LDM4
Average				-19.977	18.081	

Table A.8 : Classification of building collapse direction, distance and angle in Gölcük according to near and LDM analysis results – CLS08.

CLASS	Id	$N_2(^0)$	S_F (m)	$N_1(^0)$	S_S (m)	LDM_CLASS
CLS08	98	42.207	3526.948	-73.136	23.091	LDM4
CLS08	114	42.279	3441.429	-60.968	19.805	LDM4
CLS08	115	42.340	3411.456	-50.263	20.491	LDM4
CLS08	116	42.344	3352.575	-40.749	18.697	LDM4
CLS08	102	42.365	3563.260	-55.798	9.980	LDM4
CLS08	100	42.722	3593.598	-57.511	10.925	LDM4
CLS08	208	42.838	3135.133	-68.143	27.105	LDM4
CLS08	104	44.059	3679.638	-48.161	23.765	LDM4
CLS08	119	44.108	3604.337	-56.554	17.741	LDM4
CLS08	107	44.258	3709.398	-45.616	20.699	LDM4
CLS08	110	44.429	3430.440	-59.834	21.363	LDM4
Average				-56.067	19.424	

Table A.9 : Classification of building collapse direction, distance and angle in Gölcük according to near and LDM analysis results – CLS09.

CLASS	Id	$N_2(^0)$	S_F (m)	$N_1(^0)$	S_S(m)	LDM_CLASS
CLS09	189	45.043	3342.133	-85.287	28.345	LDM3
CLS09	199	45.073	3264.924	-81.935	14.081	LDM3
CLS09	193	45.185	3395.152	-75.159	11.639	LDM3
CLS09	123	45.287	3715.700	-83.984	30.253	LDM3
CLS09	198	45.403	3237.441	-77.940	19.768	LDM3
CLS09	125	45.489	3644.056	-80.946	20.155	LDM3
CLS09	201	45.506	3268.609	-86.948	17.491	LDM3
CLS09	124	46.018	3656.907	-95.168	22.531	LDM3
CLS09	178	46.148	3401.588	-83.705	31.396	LDM3
CLS09	120	46.179	3687.097	-79.487	31.468	LDM3
CLS09	210	46.336	3089.287	-66.468	22.369	LDM3
CLS09	143	46.345	3558.457	-95.019	27.400	LDM3
CLS09	206	46.366	3288.225	-97.342	22.958	LDM3
CLS09	184	46.458	3326.031	-85.986	21.035	LDM3
CLS09	209	46.671	3172.181	-68.375	14.373	LDM3
CLS09	205	46.789	3284.766	-93.968	25.346	LDM3
CLS09	181	46.887	3351.046	-70.579	12.856	LDM3
CLS09	131	46.898	3774.794	-77.381	30.922	LDM3
CLS09	130	46.942	3752.975	-83.967	20.833	LDM3
CLS09	129	46.977	3724.321	-84.383	27.721	LDM3
Average				-82.701	22.647	

Table A.10 : Classification of building collapse direction, distance and angle in Gölcük according to near and LDM analysis results – CLS10.

CLASS	Id	$N_2(^0)$	S_F (m)	$N_1(^0)$	S_S (m)	LDM_CLASS
CLS10	155	48.068	3596.019	-111.538	17.311	LDM3
CLS10	138	48.250	3632.748	-112.868	29.140	LDM3
CLS10	175	48.346	3489.442	-117.468	12.407	LDM3
CLS10	153	48.578	3565.719	-113.117	28.838	LDM3
CLS10	134	48.718	3685.208	-131.848	29.857	LDM3
CLS10	151	48.938	3553.648	-110.549	26.866	LDM3
Average				-116.231	24.070	

Table A.11 : Classification of building collapse direction, distance and angle in Gölcük according to near and LDM analysis results – CLS11.

CLASS	Id	$N_2(^0)$	S_F (m)	$N_1(^0)$	S_S (m)	LDM_CLASS
CLS11	243	50.853	3031.195	177.734	16.538	LDM2
CLS11	225	50.913	2825.179	151.014	33.247	LDM2
CLS11	247	51.016	3119.245	117.750	14.029	LDM2
CLS11	248	51.587	3186.402	157.603	32.239	LDM2
CLS11	249	51.599	3218.696	143.560	12.659	LDM2
CLS11	250	51.888	3206.826	113.049	12.381	LDM2
CLS11	238	52.131	2976.391	148.699	14.392	LDM2
CLS11	237	52.373	2988.570	138.757	14.462	LDM2
CLS11	223	52.718	2804.747	142.446	21.404	LDM2
CLS11	239	53.421	3025.384	170.596	18.884	LDM2
CLS11	236	55.083	2671.752	127.741	22.004	LDM2
CLS11	235	55.816	2785.006	118.293	24.284	LDM2
Average				142.270	19.710	

Table A.12 : Damage state distribution of MSC Conc Box bridges.

class	name	none	slight_mod	mod_extens	ext_comple	complete	meandamage
MSC_Conc Box	Akşemsettin (v6)	0.16	0.51	0.22	0.10	0.01	0.06
MSC_Conc Box	Ataköy-1	0.16	0.51	0.23	0.10	0.01	0.06
MSC_Conc Box	Mollagürani (m3 v1)	0.38	0.49	0.10	0.03	0.00	0.03
MSC_Conc Box	Hasdal (v5)	0.16	0.51	0.22	0.10	0.01	0.06
MSC_Conc Box	Ataköy 2	0.16	0.51	0.23	0.10	0.01	0.06
MSC_Conc Box	Sadabat-1 (v3)	0.23	0.52	0.18	0.07	0.00	0.05
MSC_Conc Box	Esenler-3	0.15	0.50	0.23	0.11	0.01	0.07
MSC_Conc Box	Haramidere	0.10	0.46	0.27	0.16	0.02	0.09
MSC_Conc Box	İncirli	0.13	0.49	0.25	0.13	0.01	0.07
MSC_Conc Box	K-305 (Zincirlikuyu)	0.24	0.53	0.17	0.06	0.00	0.05
MSC_Conc Box	Mahmutbey	0.19	0.52	0.20	0.08	0.01	0.05
MSC_Conc Box	K-303	0.23	0.53	0.17	0.06	0.00	0.05
MSC_Conc Box	Çobançeşme a-b kolu	0.16	0.51	0.23	0.10	0.01	0.06
MSC_Conc Box	Çobançeşme c-d kolu	0.12	0.48	0.26	0.14	0.01	0.08
MSC_Conc Box	K-414	0.22	0.52	0.18	0.07	0.00	0.05
MSC_Conc Box	Bayrampaşa	0.15	0.50	0.23	0.11	0.01	0.07

Table A.13 : Damage state distribution of MSC Concrete bridges.

name	class	none	slight_mod	mod_extens	ext_comple	complete	meandamage
OP-703	MSC_Concrete	0.01	0.21	0.17	0.17	0.45	0.51
Gürpınar	MSC_Concrete	0.03	0.41	0.19	0.14	0.22	0.17
YUK-4	MSC_Concrete	0.03	0.42	0.19	0.14	0.21	0.27
UK-80	MSC_Concrete	0.03	0.42	0.19	0.14	0.21	0.27
Esenyurt	MSC_Concrete	0.04	0.43	0.19	0.14	0.20	0.13
Esenyurt	MSC_Concrete	0.04	0.45	0.19	0.13	0.18	0.12
MC3G - OP307	MSC_Concrete	0.04	0.45	0.19	0.13	0.18	0.24
MC3F - OP306	MSC_Concrete	0.04	0.46	0.19	0.13	0.18	0.24
O 207 2C 02	MSC_Concrete	0.05	0.47	0.19	0.13	0.17	0.23
MC3D - OP304	MSC_Concrete	0.05	0.47	0.19	0.13	0.17	0.23
UK-115	MSC_Concrete	0.05	0.47	0.19	0.13	0.17	0.23
UK-36	MSC_Concrete	0.05	0.47	0.19	0.13	0.17	0.23
UK-63	MSC_Concrete	0.05	0.47	0.19	0.13	0.16	0.14
Osmaniye	MSC_Concrete	0.05	0.48	0.19	0.12	0.16	0.14
UK-21	MSC_Concrete	0.05	0.48	0.19	0.12	0.16	0.22
YUK-2	MSC_Concrete	0.05	0.48	0.18	0.12	0.15	0.14
UK-119	MSC_Concrete	0.05	0.49	0.18	0.12	0.15	0.21
Y■-2	MSC_Concrete	0.05	0.49	0.18	0.12	0.15	0.21
Yenibosna	MSC_Concrete	0.05	0.49	0.18	0.12	0.15	0.10
Ulubatlı Hasan	MSC_Concrete	0.06	0.49	0.18	0.12	0.15	0.09
K-101 (Cevizlibağ)	MSC_Concrete	0.06	0.49	0.18	0.12	0.15	0.13
Ispartakule (V-3)	MSC_Concrete	0.06	0.49	0.18	0.12	0.15	0.09

Table A.13 (continued) : Damage state distribution of MSC Concrete bridges.

name	class	none	slight_mod	mod_extens	ext_comple	complete	meandamage
x	MSC_Concrete	0.06	0.49	0.18	0.12	0.15	0.21
K-108	MSC_Concrete	0.06	0.49	0.18	0.12	0.15	0.16
Karasu (V-1)	MSC_Concrete	0.06	0.49	0.18	0.12	0.15	0.09
Yarımburgaz(V-4)	MSC_Concrete	0.06	0.49	0.18	0.12	0.15	0.11
UK-60	MSC_Concrete	0.06	0.49	0.18	0.12	0.15	0.21
Beylikçayır (V-2)	MSC_Concrete	0.06	0.49	0.18	0.12	0.15	0.09
K4A	MSC_Concrete	0.06	0.49	0.18	0.12	0.15	0.21
UK-58	MSC_Concrete	0.06	0.49	0.18	0.12	0.15	0.16
UK-17	MSC_Concrete	0.06	0.50	0.18	0.12	0.15	0.13
UK-120	MSC_Concrete	0.06	0.50	0.18	0.12	0.14	0.20
RMO2	MSC_Concrete	0.06	0.50	0.18	0.12	0.14	0.20
RMO1	MSC_Concrete	0.06	0.50	0.18	0.12	0.14	0.20
UK-44	MSC_Concrete	0.06	0.51	0.18	0.12	0.14	0.20
UK-45	MSC_Concrete	0.06	0.51	0.18	0.12	0.14	0.13
UK-121	MSC_Concrete	0.06	0.51	0.18	0.12	0.14	0.20
Sağmacılar	MSC_Concrete	0.06	0.51	0.18	0.11	0.14	0.09
UK-12	MSC_Concrete	0.06	0.51	0.18	0.11	0.14	0.13
S-4	MSC_Concrete	0.06	0.51	0.18	0.11	0.14	0.10
B-1	MSC_Concrete	0.07	0.51	0.18	0.11	0.13	0.19
YUK-1	MSC_Concrete	0.07	0.52	0.18	0.11	0.13	0.12
İmar yolu	MSC_Concrete	0.07	0.52	0.18	0.11	0.12	0.09

Table A.13 (continued) : Damage state distribution of MSC Concrete bridges.

name	class	none	slight_mod	mod_extens	ext_comple	complete	meandamage
Ulaştırma	MSC_Concrete	0.07	0.53	0.17	0.11	0.12	0.18
K-5	MSC_Concrete	0.07	0.53	0.17	0.11	0.12	0.17
UK-126	MSC_Concrete	0.08	0.53	0.17	0.10	0.11	0.17
VMO1	MSC_Concrete	0.08	0.55	0.17	0.10	0.11	0.16
M 301	MSC_Concrete	0.08	0.55	0.17	0.10	0.10	0.11
B-6	MSC_Concrete	0.09	0.55	0.16	0.10	0.10	0.15
Okmeydanı (V4)	MSC_Concrete	0.09	0.56	0.16	0.09	0.10	0.09
YUK-3	MSC_Concrete	0.09	0.56	0.16	0.09	0.10	0.15
Ortaköy (V 411)	MSC_Concrete	0.10	0.56	0.16	0.09	0.09	0.08
UK-135	MSC_Concrete	0.10	0.56	0.16	0.09	0.09	0.14
V 302	MSC_Concrete	0.10	0.57	0.16	0.09	0.09	0.07
MC4C	MSC_Concrete	0.10	0.57	0.15	0.09	0.08	0.14
Rıdvan Dedeoğşu	MSC_Concrete	0.10	0.57	0.15	0.09	0.08	0.07
UK-139	MSC_Concrete	0.10	0.57	0.15	0.09	0.08	0.14
KMW1	MSC_Concrete	0.11	0.57	0.15	0.09	0.08	0.08
KMO1	MSC_Concrete	0.11	0.57	0.15	0.09	0.08	0.09
Mahmutbey (V-1)	MSC_Concrete	0.11	0.57	0.15	0.08	0.08	0.07
B2 2A	MSC_Concrete	0.11	0.58	0.15	0.08	0.08	0.13
K-6	MSC_Concrete	0.11	0.58	0.15	0.08	0.08	0.10
Sadabat -2 (V1)	MSC_Concrete	0.12	0.58	0.15	0.08	0.07	0.06
M 102	MSC_Concrete	0.12	0.58	0.14	0.08	0.07	0.12
BF-2	MSC_Concrete	0.12	0.59	0.14	0.08	0.07	0.07

Table A.13 (continued) : Damage state distribution of MSC Concrete bridges.

name	class	none	slight_mod	mod_extens	ext_comple	complete	meandamage
BRO	MSC_Concrete	0.12	0.59	0.14	0.08	0.07	0.12
B 13	MSC_Concrete	0.12	0.59	0.14	0.08	0.07	0.12
Levent	MSC_Concrete	0.12	0.59	0.14	0.08	0.07	0.06
B 14	MSC_Concrete	0.12	0.59	0.14	0.08	0.07	0.12
?ÇO	MSC_Concrete	0.12	0.59	0.14	0.08	0.07	0.12
Ortaköy (V 408)	MSC_Concrete	0.12	0.59	0.14	0.08	0.07	0.06
Ortaköy (V 409)	MSC_Concrete	0.13	0.59	0.14	0.08	0.07	0.07
UK-147	MSC_Concrete	0.13	0.59	0.14	0.08	0.07	0.12
K-3	MSC_Concrete	0.13	0.59	0.14	0.07	0.07	0.06
MC3A -OP 301	MSC_Concrete	0.13	0.59	0.14	0.07	0.07	0.11
B-3	MSC_Concrete	0.13	0.59	0.14	0.07	0.07	0.09
NMO1	MSC_Concrete	0.14	0.59	0.14	0.07	0.06	0.11
Gaziosmanpaşa	MSC_Concrete	0.14	0.60	0.13	0.07	0.06	0.09
OP 201 MC2A	MSC_Concrete	0.14	0.60	0.13	0.07	0.06	0.11
Nurtepe (V2)	MSC_Concrete	0.14	0.60	0.13	0.07	0.06	0.06
OP 209 MC 2G	MSC_Concrete	0.14	0.60	0.13	0.07	0.06	0.11
MC2E - OP205	MSC_Concrete	0.14	0.60	0.13	0.07	0.06	0.10
K-1	MSC_Concrete	0.15	0.60	0.13	0.07	0.06	0.06
Gedikpaşa (V2A)	MSC_Concrete	0.15	0.60	0.13	0.07	0.06	0.06
B 16	MSC_Concrete	0.15	0.60	0.13	0.06	0.05	0.10

Table A.13 (continued) **:** Damage state distribution of MSC Concrete bridges

name	class	none	slight_mod	mod_extens	ext_comple	complete	meandamage
UMO5	MSC_Concrete	0.15	0.60	0.13	0.06	0.05	0.10
B-10 (Kemerburgaz)	MSC_Concrete	0.16	0.60	0.13	0.06	0.05	0.07
B-11	MSC_Concrete	0.16	0.60	0.13	0.06	0.05	0.10
B-12	MSC_Concrete	0.16	0.60	0.13	0.06	0.05	0.10
UMO6	MSC_Concrete	0.16	0.60	0.12	0.06	0.05	0.09
K2	MSC_Concrete	0.16	0.60	0.12	0.06	0.05	0.06
M 101	MSC_Concrete	0.16	0.60	0.12	0.06	0.05	0.09
M 501	MSC_Concrete	0.17	0.60	0.12	0.06	0.05	0.07
M 401	MSC_Concrete	0.20	0.61	0.11	0.05	0.04	0.08
M 402	MSC_Concrete	0.20	0.61	0.11	0.05	0.04	0.08
M 302	MSC_Concrete	0.22	0.61	0.10	0.04	0.03	0.07

Table A.14 : Damage state distribution of MSC Slab bridges.

name	class	none	slight_mod	mod_extens	ext_comple	complete	meandamage
Yeni Galata	MSC_Slab	0.11	0.50	0.25	0.14	0.01	0.07
Kemerdere	MSC_Slab	0.07	0.44	0.29	0.19	0.01	0.10
Sarıgazi	MSC_Slab	0.19	0.55	0.19	0.08	0.00	0.05
Çekmeköy	MSC_Slab	0.07	0.44	0.29	0.19	0.01	0.10
Olimpiyat	MSC_Slab	0.05	0.40	0.30	0.23	0.02	0.10
Potdere	MSC_Slab	0.37	0.51	0.09	0.02	0.00	0.03
K-103	MSC_Slab	0.05	0.41	0.30	0.22	0.01	0.10
K-103	MSC_Slab	0.04	0.36	0.31	0.27	0.02	0.11
Atış Alanı	MSC_Slab	0.06	0.42	0.29	0.21	0.01	0.10
İkitelli	MSC_Slab	0.07	0.44	0.29	0.20	0.01	0.09
100.YIL	MSC_Slab	0.07	0.45	0.28	0.18	0.01	0.09
K-512	MSC_Slab	0.17	0.54	0.21	0.09	0.00	0.06
Çobançeşme	MSC_Slab	0.04	0.37	0.31	0.26	0.02	0.11
K-505	MSC_Slab	0.14	0.53	0.22	0.10	0.00	0.06
K-212	MSC_Slab	0.10	0.49	0.26	0.14	0.01	0.07
K-404	MSC_Slab	0.12	0.51	0.24	0.13	0.00	0.07
Esenler 1	MSC_Slab	0.06	0.42	0.30	0.21	0.01	0.10
Güneşli	MSC_Slab	0.05	0.38	0.30	0.25	0.02	0.11
K-517	MSC_Slab	0.16	0.54	0.21	0.09	0.00	0.06
Sefaköy	MSC_Slab	0.04	0.36	0.31	0.27	0.02	0.11
K-515	MSC_Slab	0.16	0.54	0.21	0.09	0.00	0.06
K-509	MSC_Slab	0.13	0.52	0.24	0.12	0.00	0.07

Table A.14 (continued) : Damage state distribution of MSC Slab bridges.

name	class	none	slight_mod	mod_extens	ext_comple	complete	meandamage
K-503	MSC_Slab	0.15	0.53	0.22	0.10	0.00	0.06
PTT	MSC_Slab	0.06	0.42	0.29	0.21	0.01	0.10
K-510	MSC_Slab	0.07	0.44	0.29	0.20	0.01	0.09
K-206	MSC_Slab	0.11	0.51	0.25	0.13	0.01	0.07
K-207	MSC_Slab	0.10	0.49	0.26	0.14	0.01	0.07
K-202	MSC_Slab	0.10	0.49	0.26	0.15	0.01	0.08
K-204	MSC_Slab	0.11	0.50	0.25	0.13	0.01	0.07
Merter	MSC_Slab	0.07	0.44	0.29	0.20	0.01	0.09
K-106	MSC_Slab	0.07	0.44	0.29	0.19	0.01	0.09
K-102	MSC_Slab	0.07	0.45	0.28	0.19	0.01	0.09

Table A.15 : Damage state distribution of MSC Steel bridges.

name	class	none	slight_mod	mod_extens	ext_comple	complete	meandamage
1.Boğaziçi Bridge	MSC_Steel	0.10	0.31	0.20	0.15	0.24	0.23
F.S.MEHMET	MSC_Steel	0.16	0.36	0.19	0.13	0.17	0.17
HALİÇ (ESKİ)	MSC_Steel	0.08	0.28	0.19	0.16	0.28	0.14
HALİÇ B (YENİ)	MSC_Steel	0.08	0.28	0.19	0.16	0.28	0.14
HALİÇ A (YENİ)	MSC_Steel	0.08	0.28	0.19	0.16	0.28	0.14

Table A.16 : Damage state distribution of SS Concrete bridges.

name	class	none	slight_mod	mod_extens	ext_comple	complete	meandamage
Yalıköy	SS_Concrete	0.44	0.47	0.05	0.03	0.02	0.05
Yeniköy	SS_Concrete	0.72	0.26	0.01	0.00	0.00	0.01
Cezaevi	SS_Concrete	0.37	0.50	0.06	0.03	0.03	0.06
NMU 2	SS_Concrete	0.51	0.42	0.03	0.02	0.01	0.03
UMU5	SS_Concrete	0.54	0.40	0.03	0.02	0.01	0.03
K-521 Demiryolu	SS_Concrete	0.48	0.44	0.04	0.02	0.02	0.04
UK-34	SS_Concrete	0.33	0.52	0.07	0.04	0.04	0.07
Esenler-2	SS_Concrete	0.34	0.52	0.07	0.04	0.04	0.07
Büyükdere (BF-1)	SS_Concrete	0.47	0.45	0.04	0.02	0.02	0.04

Table A.17 : Damage state distribution of Tunnel /Culvert bridges.

name	class	none	slight_mod	mod_extens	ext_comple	complete	meandamage
K-205	Tunnel/Culvert	0.88	0.06	0.03	0.02	0.01	0.01
AK-150	Tunnel/Culvert	0.91	0.04	0.02	0.02	0.00	0.01
M2 U2	Tunnel/Culvert	0.91	0.05	0.02	0.02	0.01	0.01
M5 U1	Tunnel/Culvert	0.75	0.10	0.06	0.06	0.03	0.04
AK-31	Tunnel/Culvert	0.78	0.09	0.05	0.05	0.02	0.04
Altıntepsi	Tunnel/Culvert	0.78	0.10	0.05	0.05	0.02	0.04
Gazeteciler	Tunnel/Culvert	0.88	0.06	0.03	0.02	0.01	0.02
Bayrampaşa-1	Tunnel/Culvert	0.77	0.10	0.05	0.05	0.02	0.04
AK-68	Tunnel/Culvert	0.86	0.07	0.03	0.03	0.01	0.02
UM.U3A	Tunnel/Culvert	0.93	0.04	0.02	0.01	0.00	0.01
AK-134	Tunnel/Culvert	0.88	0.06	0.03	0.03	0.01	0.02
AK-55	Tunnel/Culvert	0.83	0.08	0.04	0.04	0.01	0.03
UM.U7	Tunnel/Culvert	0.91	0.05	0.02	0.02	0.00	0.01
K-201	Tunnel/Culvert	0.85	0.07	0.04	0.03	0.01	0.02
B 5	Tunnel/Culvert	0.92	0.04	0.02	0.02	0.00	0.01
Bahçeşehir	Tunnel/Culvert	0.76	0.10	0.06	0.06	0.02	0.05
K-407	Tunnel/Culvert	0.88	0.06	0.03	0.03	0.01	0.02
ALBA SANAYİ	Tunnel/Culvert	0.77	0.10	0.06	0.06	0.02	0.04
NMU 4	Tunnel/Culvert	0.76	0.10	0.06	0.06	0.02	0.05
K-402	Tunnel/Culvert	0.89	0.06	0.03	0.02	0.01	0.01
Atışalanı-2	Tunnel/Culvert	0.78	0.09	0.05	0.05	0.02	0.04
Atışalanı-1	Tunnel/Culvert	0.82	0.08	0.04	0.04	0.02	0.03
K-401	Tunnel/Culvert	0.88	0.06	0.03	0.02	0.01	0.02
AK-51	Tunnel/Culvert	0.78	0.09	0.05	0.05	0.02	0.04

Table A.17 (continued) : Damage state distribution of Tunnel /Culvert bridges.

name	class	none	slight_mod	mod_extens	ext_comple	complete	meandamage
K-518	Tunnel/Culvert	0.79	0.09	0.05	0.05	0.02	0.03
K-504	Tunnel/Culvert	0.91	0.05	0.02	0.02	0.00	0.01
AK-39	Tunnel/Culvert	0.79	0.09	0.05	0.05	0.02	0.04
NMU 1	Tunnel/Culvert	0.92	0.04	0.02	0.01	0.00	0.01
K-513	Tunnel/Culvert	0.93	0.04	0.02	0.01	0.00	0.01
RMU 4	Tunnel/Culvert	0.95	0.03	0.01	0.01	0.00	0.01
B 9 LOT 2A	Tunnel/Culvert	0.93	0.04	0.02	0.01	0.00	0.01
K-301	Tunnel/Culvert	0.88	0.06	0.03	0.02	0.01	0.02
K-300	Tunnel/Culvert	0.88	0.06	0.03	0.02	0.01	0.02
AK-145	Tunnel/Culvert	0.91	0.05	0.02	0.02	0.00	0.01
B3 C	Tunnel/Culvert	0.91	0.05	0.02	0.02	0.00	0.01
AK-141	Tunnel/Culvert	0.90	0.05	0.02	0.02	0.01	0.01
AK-74	Tunnel/Culvert	0.73	0.11	0.06	0.07	0.03	0.06
K-501	Tunnel/Culvert	0.93	0.04	0.02	0.01	0.00	0.01
AK-71	Tunnel/Culvert	0.74	0.11	0.06	0.07	0.03	0.05
RMU 1	Tunnel/Culvert	0.81	0.09	0.05	0.04	0.02	0.03
B 15	Tunnel/Culvert	0.93	0.04	0.02	0.01	0.00	0.01
AK-144	Tunnel/Culvert	0.90	0.05	0.02	0.02	0.01	0.01
K-304	Tunnel/Culvert	0.89	0.06	0.03	0.02	0.01	0.02
Esenler	Tunnel/Culvert	0.78	0.09	0.05	0.05	0.02	0.04
K-203	Tunnel/Culvert	0.87	0.06	0.03	0.03	0.01	0.02
K-211	Tunnel/Culvert	0.88	0.06	0.03	0.03	0.01	0.02

Table A.17 (continued) : Damage state distribution of Tunnel /Culvert bridges.

name	class	none	slight_mod	mod_extens	ext_comple	complete	meandamage
AK-122	Tunnel/Culvert	0.82	0.08	0.04	0.04	0.02	0.03
İkitelli -2	Tunnel/Culvert	0.80	0.09	0.05	0.05	0.02	0.04
RMU3	Tunnel/Culvert	0.80	0.09	0.05	0.05	0.02	0.04
Bayrampaşa-3	Tunnel/Culvert	0.81	0.08	0.05	0.04	0.02	0.03
U 208A	Tunnel/Culvert	0.92	0.04	0.02	0.01	0.00	0.01
Bayrampaşa-2	Tunnel/Culvert	0.77	0.10	0.05	0.05	0.02	0.04
K-502	Tunnel/Culvert	0.92	0.04	0.02	0.01	0.00	0.01
U 210	Tunnel/Culvert	0.92	0.04	0.02	0.01	0.00	0.01
AK-127	Tunnel/Culvert	0.85	0.07	0.04	0.03	0.01	0.02
AK-129	Tunnel/Culvert	0.86	0.07	0.03	0.03	0.01	0.02
K-4	Tunnel/Culvert	0.80	0.09	0.05	0.05	0.02	0.04
NMU 3	Tunnel/Culvert	0.92	0.04	0.02	0.01	0.00	0.01
AK-113	Tunnel/Culvert	0.76	0.10	0.06	0.06	0.03	0.05
K405	Tunnel/Culvert	0.88	0.06	0.03	0.02	0.01	0.02
M5 U2	Tunnel/Culvert	0.94	0.04	0.02	0.01	0.00	0.01
AK-10	Tunnel/Culvert	0.82	0.08	0.04	0.04	0.02	0.03
AK-133	Tunnel/Culvert	0.88	0.06	0.03	0.03	0.01	0.02
AK-116	Tunnel/Culvert	0.77	0.10	0.05	0.05	0.02	0.04
K-105	Tunnel/Culvert	0.80	0.09	0.05	0.05	0.02	0.04
RMU 2	Tunnel/Culvert	0.81	0.09	0.05	0.04	0.02	0.03
B 17	Tunnel/Culvert	0.92	0.04	0.02	0.01	0.00	0.01
AK-124	Tunnel/Culvert	0.83	0.08	0.04	0.04	0.01	0.03
KM U3	Tunnel/Culvert	0.74	0.11	0.06	0.06	0.03	0.05

Table A.17 (continued) : Damage state distribution of Tunnel /Culvert bridges.

name	class	none	slight_mod	mod_extens	ext_comple	complete	meandamage
AK-118	Tunnel/Culvert	0.78	0.09	0.05	0.05	0.02	0.04
BLU 1	Tunnel/Culvert	0.90	0.05	0.02	0.02	0.01	0.01
AK-49	Tunnel/Culvert	0.81	0.08	0.04	0.04	0.02	0.03
UMU8	Tunnel/Culvert	0.91	0.05	0.02	0.02	0.00	0.01
AK-53	Tunnel/Culvert	0.82	0.08	0.04	0.04	0.01	0.03
K-104	Tunnel/Culvert	0.76	0.10	0.06	0.06	0.02	0.03
KM U4	Tunnel/Culvert	0.74	0.11	0.06	0.06	0.03	0.05
UM07	Tunnel/Culvert	0.94	0.03	0.01	0.01	0.00	0.01
K-412	Tunnel/Culvert	0.87	0.06	0.03	0.03	0.01	0.02
B3 B	Tunnel/Culvert	0.91	0.05	0.02	0.02	0.00	0.01
İkitelli-1	Tunnel/Culvert	0.79	0.09	0.05	0.05	0.02	0.04
AK-103	Tunnel/Culvert	0.92	0.04	0.02	0.01	0.00	0.01
K-208	Tunnel/Culvert	0.87	0.06	0.03	0.03	0.01	0.02
AK-110	Tunnel/Culvert	0.75	0.10	0.06	0.06	0.03	0.05
K-511	Tunnel/Culvert	0.80	0.09	0.05	0.05	0.02	0.04
MC2D - U 204	Tunnel/Culvert	0.93	0.04	0.02	0.01	0.00	0.01
K-210	Tunnel/Culvert	0.88	0.06	0.03	0.03	0.01	0.02
K-3	Tunnel/Culvert	0.80	0.09	0.05	0.05	0.02	0.04
AK-76	Tunnel/Culvert	0.72	0.11	0.07	0.07	0.03	0.06
Sağmacılar	Tunnel/Culvert	0.81	0.08	0.05	0.04	0.02	0.03

Table A.18 : Damage distribution of retrofitted bridge in Istanbul according to bridge classification.

id	class	none	slight_mod	mod_extens	ext_comple	complete	meandamage
6	MSC_Slab	0.07	0.45	0.28	0.19	0.01	0.09
7	MSC_Concrete	0.06	0.49	0.18	0.12	0.15	0.13
10	MSC_Slab	0.14	0.53	0.22	0.10	0.00	0.06
11	MSC_Slab	0.15	0.53	0.22	0.10	0.00	0.06
13	MSC_Conc Box	0.23	0.53	0.17	0.06	0.00	0.05
14	MSC_Conc Box	0.24	0.53	0.17	0.06	0.00	0.05
22	MSC_Slab	0.10	0.49	0.26	0.14	0.01	0.07
23	MSC_Slab	0.10	0.49	0.26	0.15	0.01	0.08
34	MSC_Slab	0.11	0.50	0.25	0.13	0.01	0.07
40	MSC_Concrete	0.11	0.57	0.15	0.09	0.08	0.09
41	MSC_Slab	0.07	0.44	0.29	0.20	0.01	0.09
42	MSC_Slab	0.13	0.52	0.24	0.12	0.00	0.07
79	MSC_Slab	0.06	0.42	0.29	0.21	0.01	0.10
94	MSC_Slab	0.07	0.44	0.29	0.20	0.01	0.09
96	MSC_Slab	0.07	0.44	0.29	0.20	0.01	0.09
99	MSC_Concrete	0.07	0.53	0.17	0.11	0.12	0.18
134	MSC_Concrete	0.10	0.56	0.16	0.09	0.09	0.08
135	MSC_Concrete	0.10	0.57	0.16	0.09	0.09	0.07
138	MSC_Concrete	0.15	0.60	0.13	0.07	0.06	0.06
139	MSC_Concrete	0.14	0.60	0.13	0.07	0.06	0.06
141	MSC_Concrete	0.09	0.56	0.16	0.09	0.10	0.09
154	MSC_Concrete	0.10	0.57	0.15	0.09	0.08	0.07

Table A.19: Damage distribution of retrofitted bridge by using elastrometric bear method in Istanbul according to bridge classification.

id	class	none	slight_mod	mod_extens	ext_comple	complete	meandamage
6	MSC_Slab	0.53	0.22	0.15	0.10	0.01	0.05
7	MSC_Concrete	0.48	0.30	0.05	0.02	0.15	0.09
10	MSC_Slab	0.68	0.17	0.09	0.05	0.00	0.03
11	MSC_Slab	0.69	0.17	0.09	0.04	0.00	0.02
13	MSC_Conc Box	0.73	0.17	0.07	0.03	0.00	0.02
14	MSC_Conc Box	0.74	0.16	0.07	0.03	0.00	0.02
22	MSC_Slab	0.60	0.20	0.12	0.07	0.00	0.03
23	MSC_Slab	0.60	0.20	0.12	0.07	0.00	0.04
34	MSC_Slab	0.62	0.20	0.12	0.06	0.00	0.03
40	MSC_Concrete	0.62	0.26	0.03	0.01	0.09	0.06
41	MSC_Slab	0.52	0.22	0.15	0.10	0.01	0.05
42	MSC_Slab	0.66	0.19	0.10	0.05	0.00	0.03
79	MSC_Slab	0.50	0.23	0.16	0.11	0.01	0.06
94	MSC_Slab	0.52	0.22	0.15	0.10	0.01	0.05
96	MSC_Slab	0.51	0.22	0.15	0.10	0.01	0.05
99	MSC_Concrete	0.53	0.29	0.04	0.01	0.13	0.14
134	MSC_Concrete	0.59	0.27	0.03	0.01	0.10	0.05
135	MSC_Concrete	0.60	0.26	0.03	0.01	0.10	0.03
138	MSC_Concrete	0.69	0.22	0.02	0.01	0.07	0.03
139	MSC_Concrete	0.68	0.23	0.02	0.01	0.07	0.02
141	MSC_Concrete	0.58	0.27	0.03	0.01	0.10	0.05
154	MSC_Concrete	0.61	0.26	0.03	0.01	0.09	0.03

Table A.20 : Damage distribution of retrofitted bridge by using steel jacket method in Istanbul according to bridge classification.

id	class	none	slight_mod	mod_extens	ext_comple	complete	meandamage
6	MSC_Slab	0.06	0.59	0.24	0.11	0.00	0.07
7	MSC_Concrete	0.10	0.56	0.16	0.09	0.09	0.10
10	MSC_Slab	0.13	0.66	0.16	0.05	0.00	0.05
11	MSC_Slab	0.13	0.66	0.16	0.05	0.00	0.05
13	MSC_Conc Box	0.22	0.62	0.13	0.03	0.00	0.04
14	MSC_Conc Box	0.22	0.62	0.12	0.03	0.00	0.04
22	MSC_Slab	0.09	0.63	0.20	0.08	0.00	0.06
23	MSC_Slab	0.08	0.63	0.21	0.08	0.00	0.06
34	MSC_Slab	0.09	0.64	0.20	0.07	0.00	0.05
40	MSC_Concrete	0.16	0.61	0.13	0.06	0.05	0.07
41	MSC_Slab	0.06	0.58	0.25	0.12	0.00	0.07
42	MSC_Slab	0.11	0.65	0.18	0.06	0.00	0.05
79	MSC_Slab	0.05	0.57	0.25	0.12	0.00	0.07
94	MSC_Slab	0.06	0.58	0.25	0.12	0.00	0.07
96	MSC_Slab	0.06	0.58	0.25	0.12	0.00	0.07
99	MSC_Concrete	0.12	0.58	0.15	0.08	0.07	0.12
134	MSC_Concrete	0.14	0.60	0.14	0.06	0.05	0.06
135	MSC_Concrete	0.15	0.60	0.13	0.06	0.05	0.05
138	MSC_Concrete	0.20	0.62	0.11	0.04	0.03	0.05
139	MSC_Concrete	0.19	0.62	0.11	0.05	0.04	0.05
141	MSC_Concrete	0.14	0.60	0.14	0.07	0.06	0.06
154	MSC_Concrete	0.15	0.61	0.13	0.06	0.05	0.05

APPENDIX B: Maps

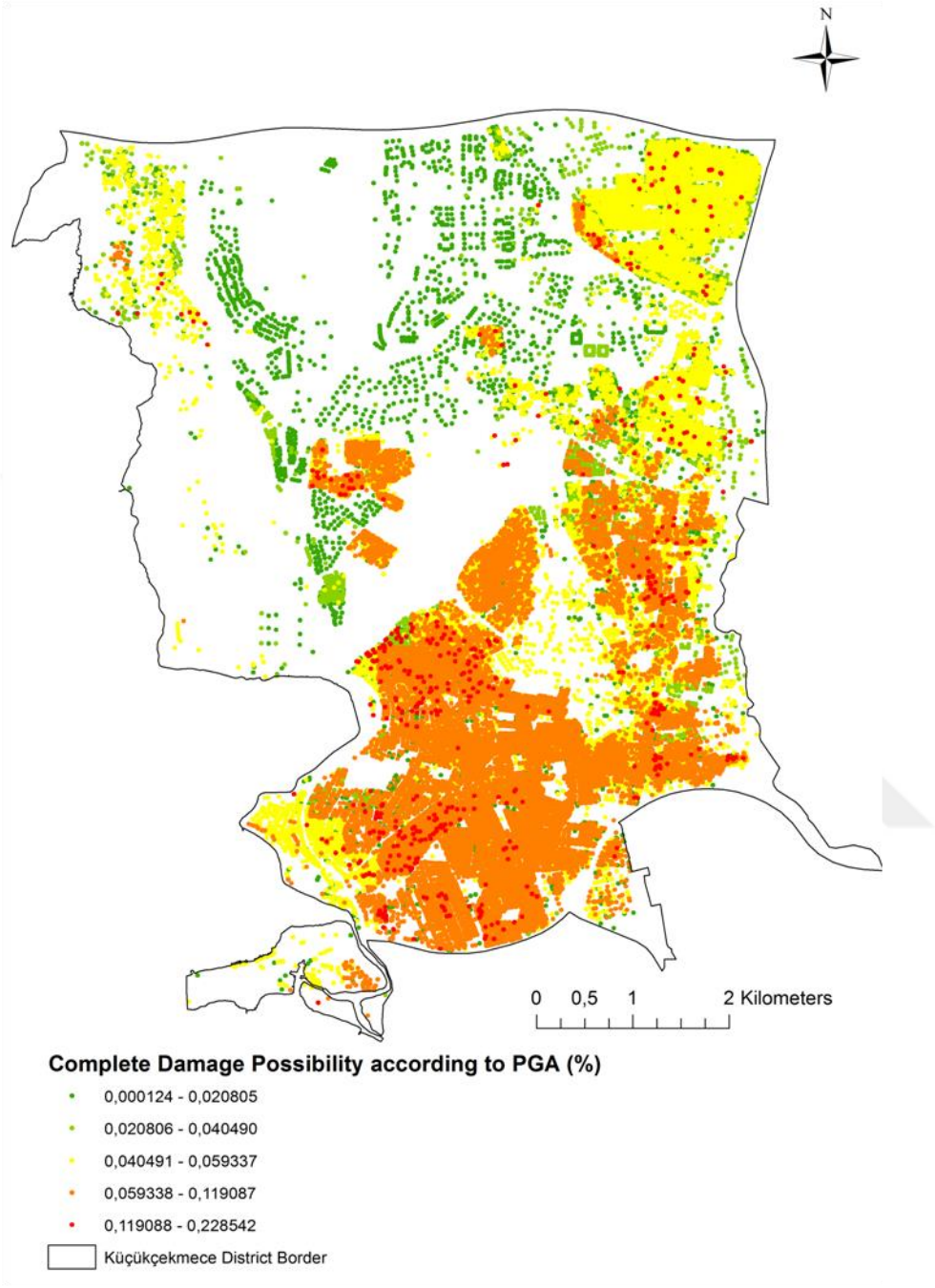


Figure A.1 : Complete damage possibility distribution of Küçükçekmece district according to PGA.

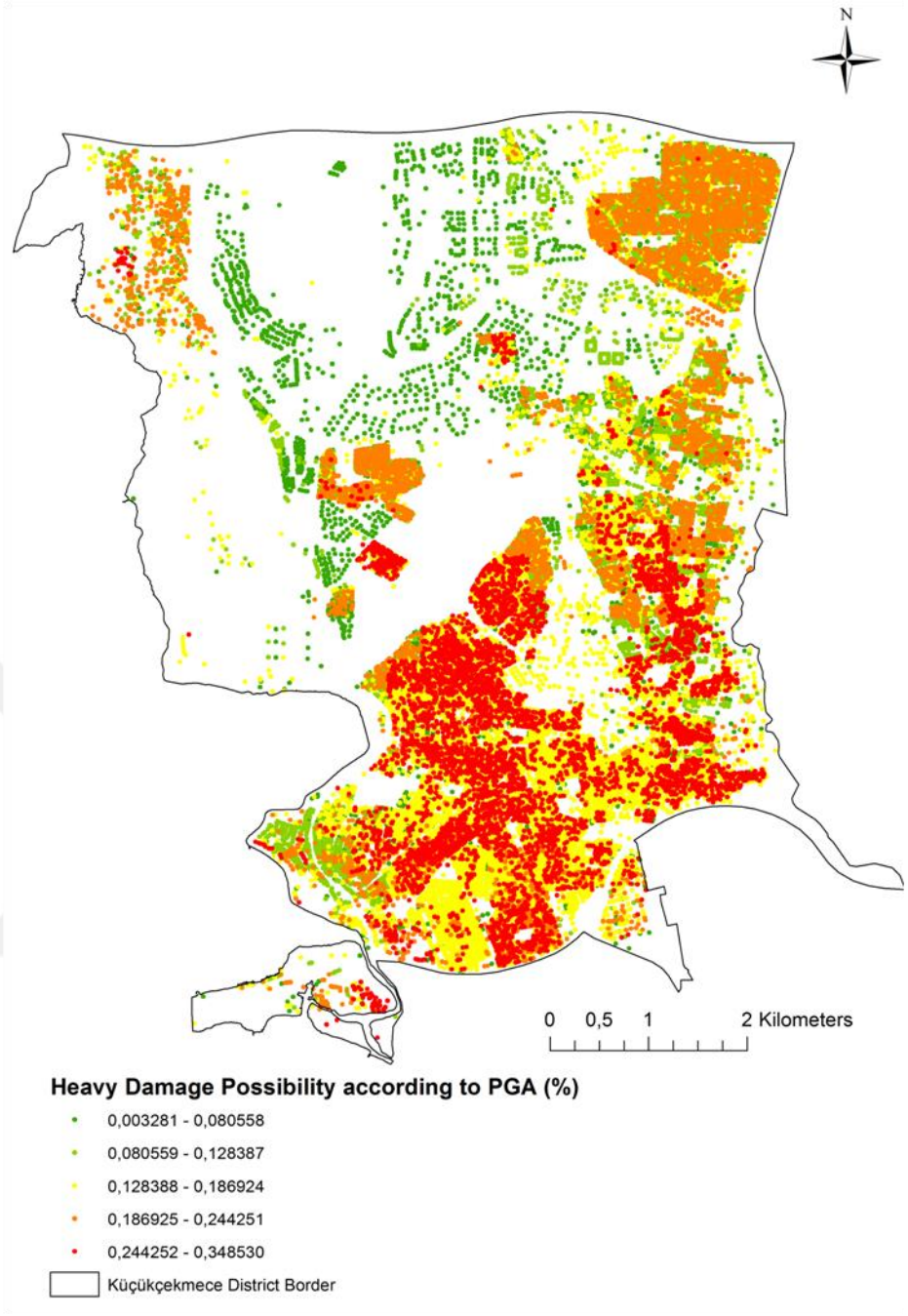


Figure A.2 : Heavy damage possibility distribution of Küçükçekmece district according to PGA.

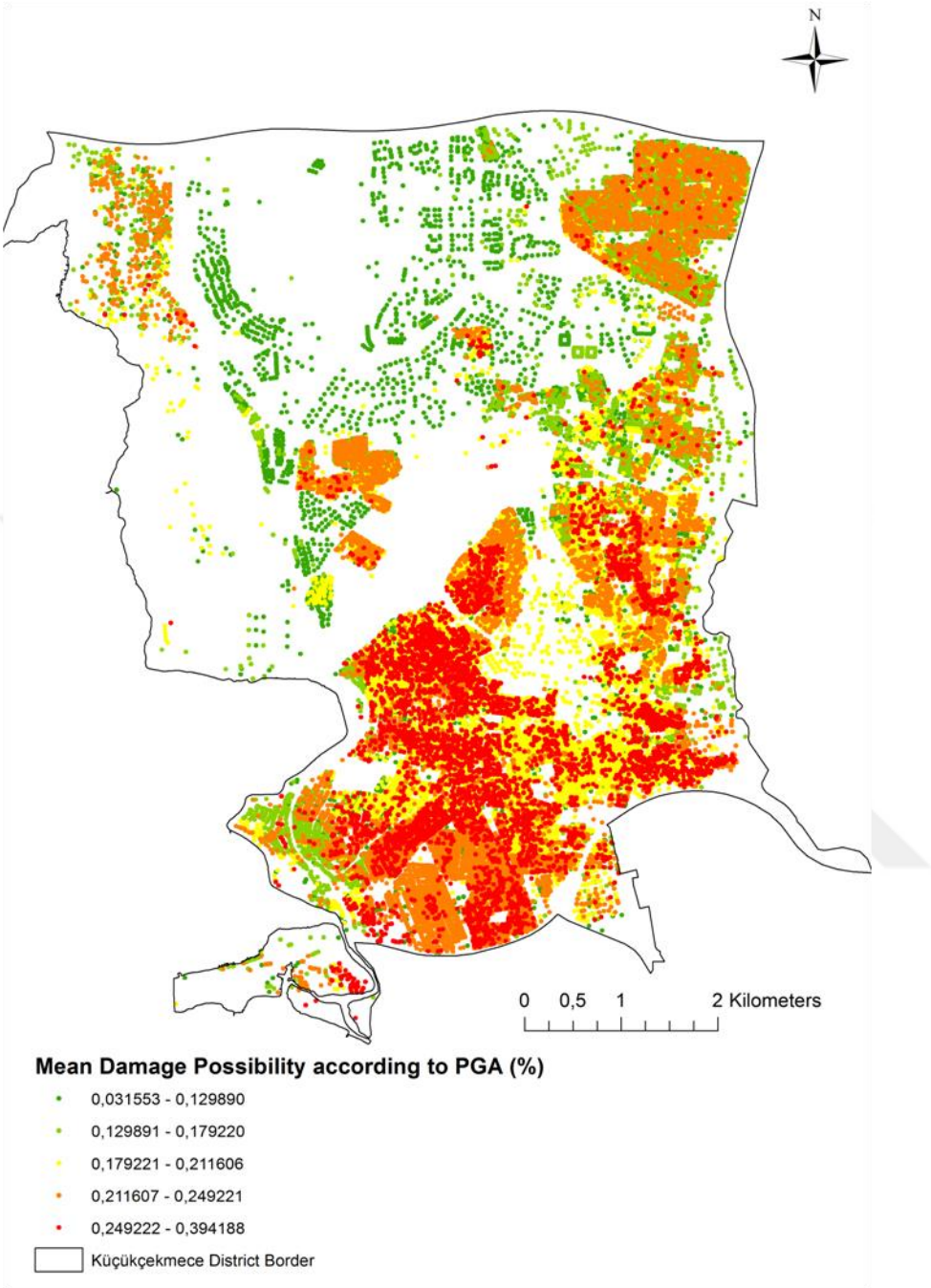


Figure A. 3 : Mean damage possibility distribution of Küçükçekmece district according to PGA.

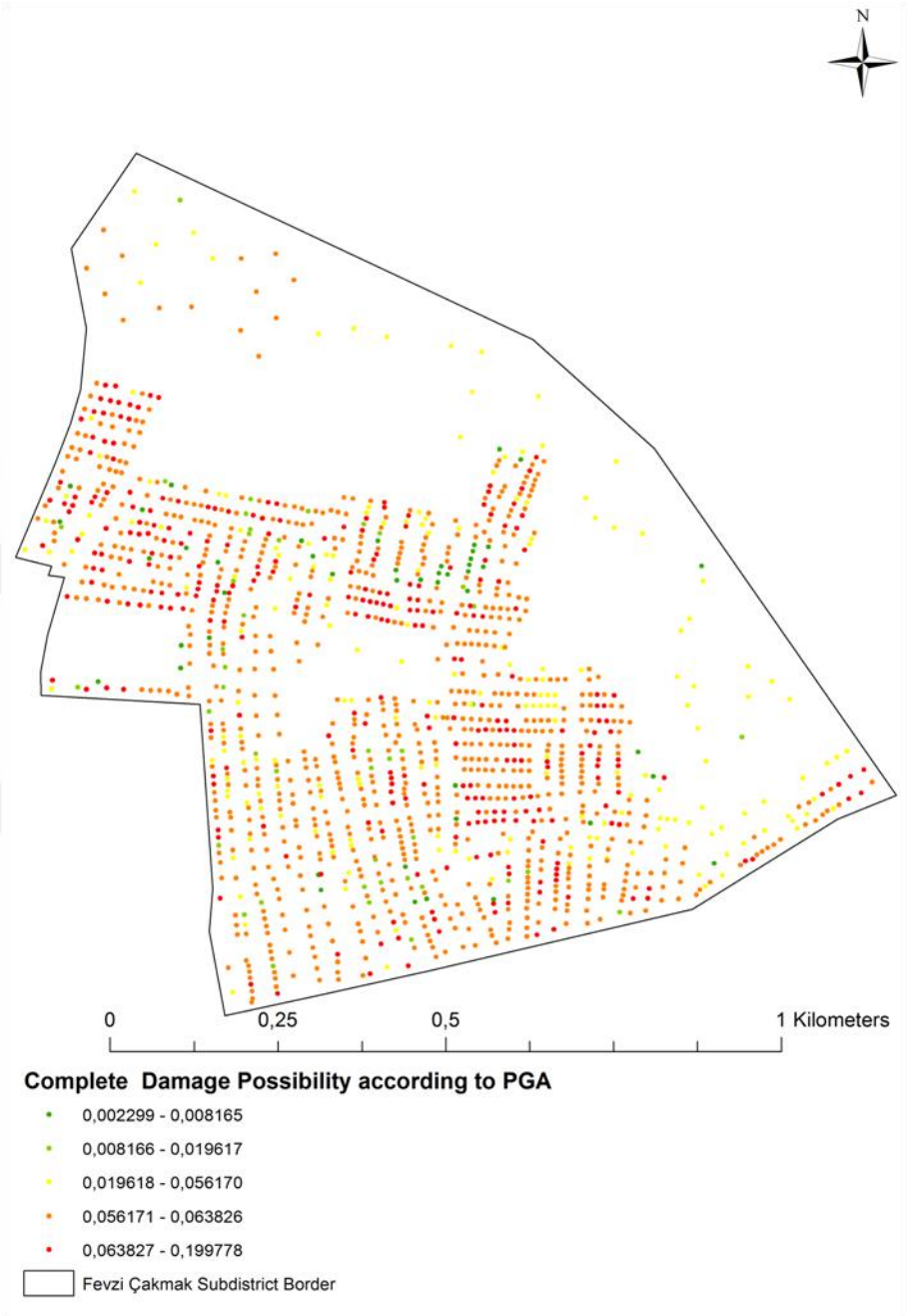


Figure A.4 : Complete damage possibility distribution of Fevzi Çakmak sub district according to PGA.

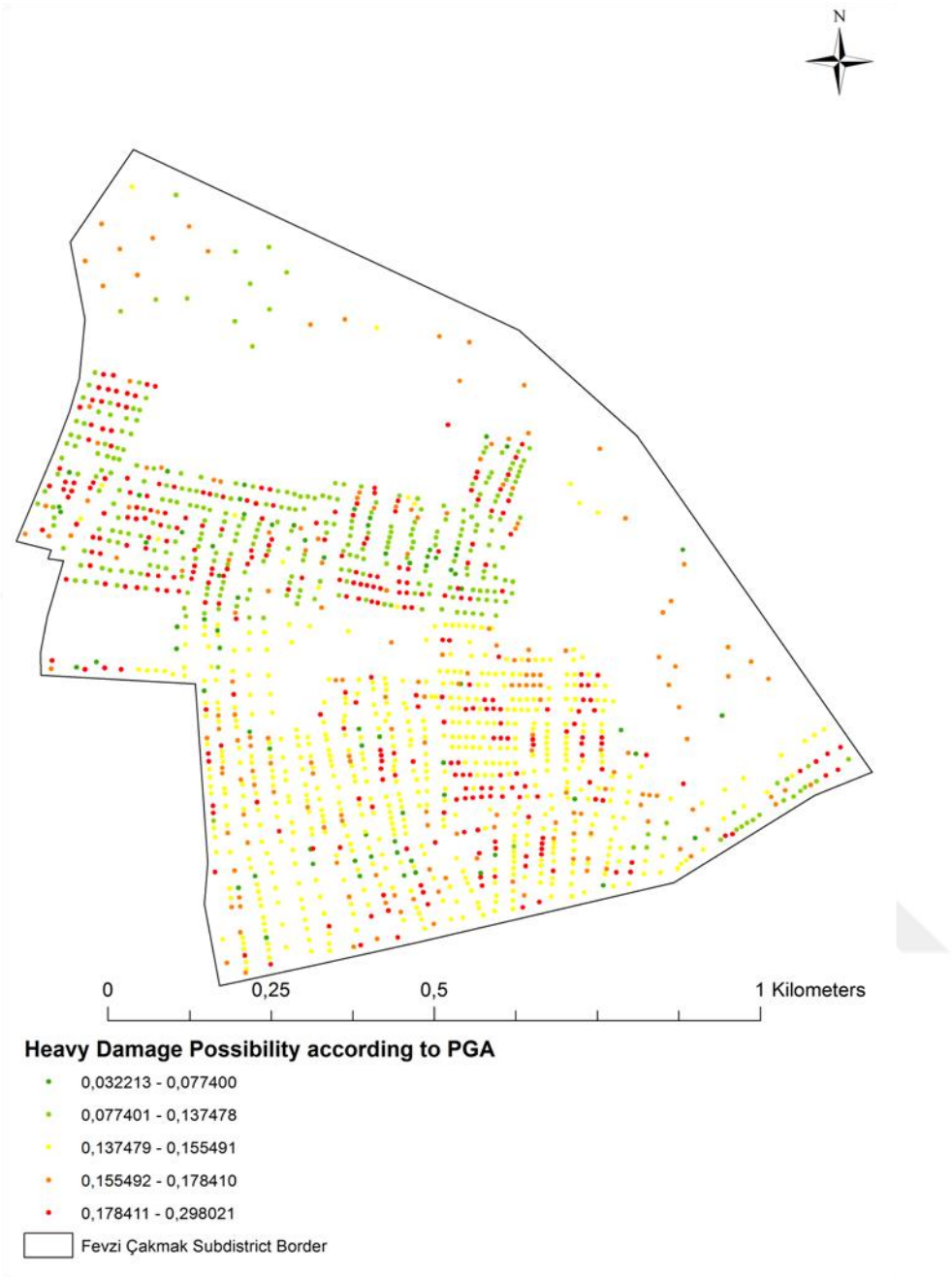


Figure A. 5 : Heavy damage possibility distribution of Fevzi Çakmak sub district according to PGA.

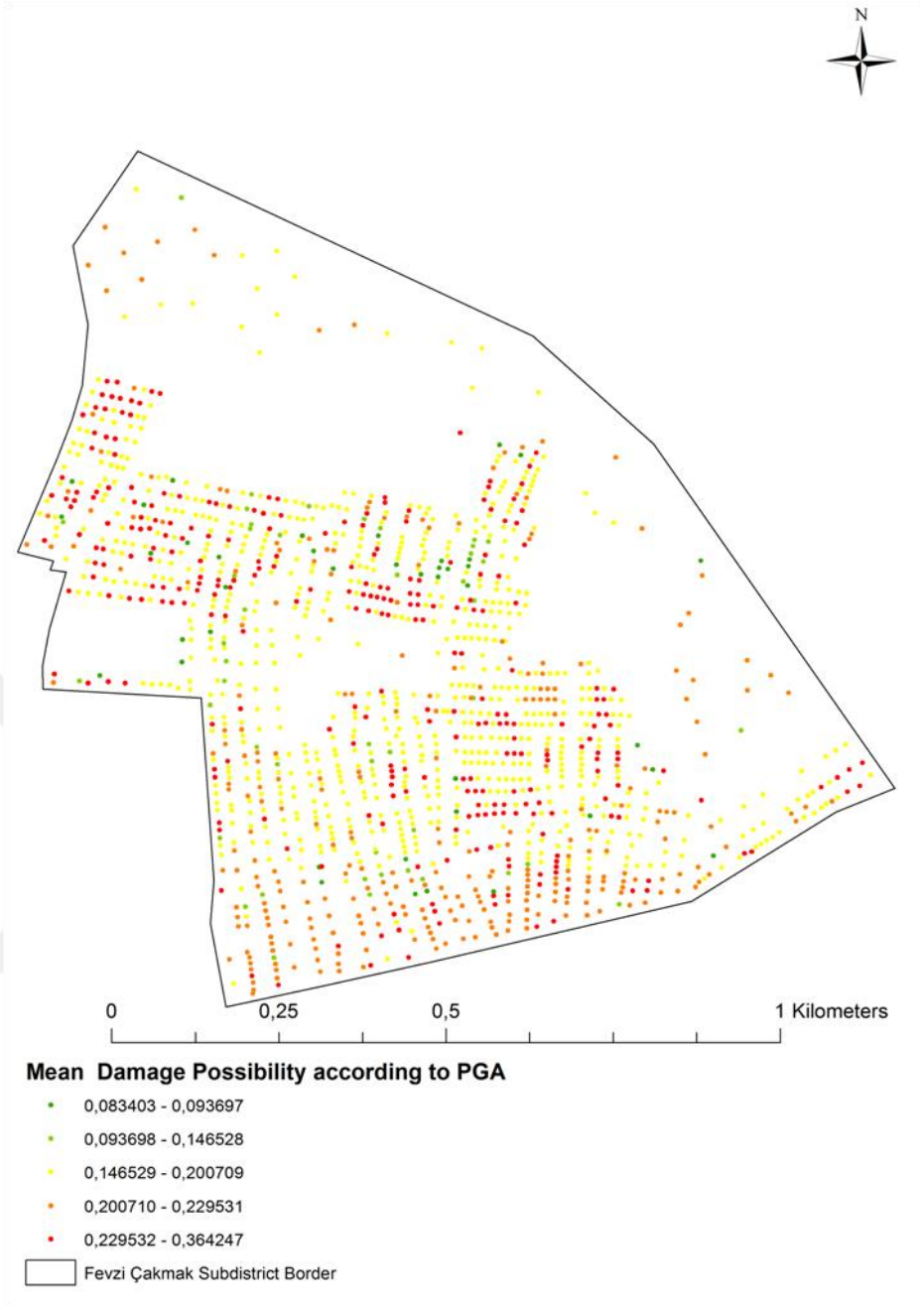


Figure A. 6 : Mean damage possibility distribution of Fevzi Çakmak sub district according to PGA.

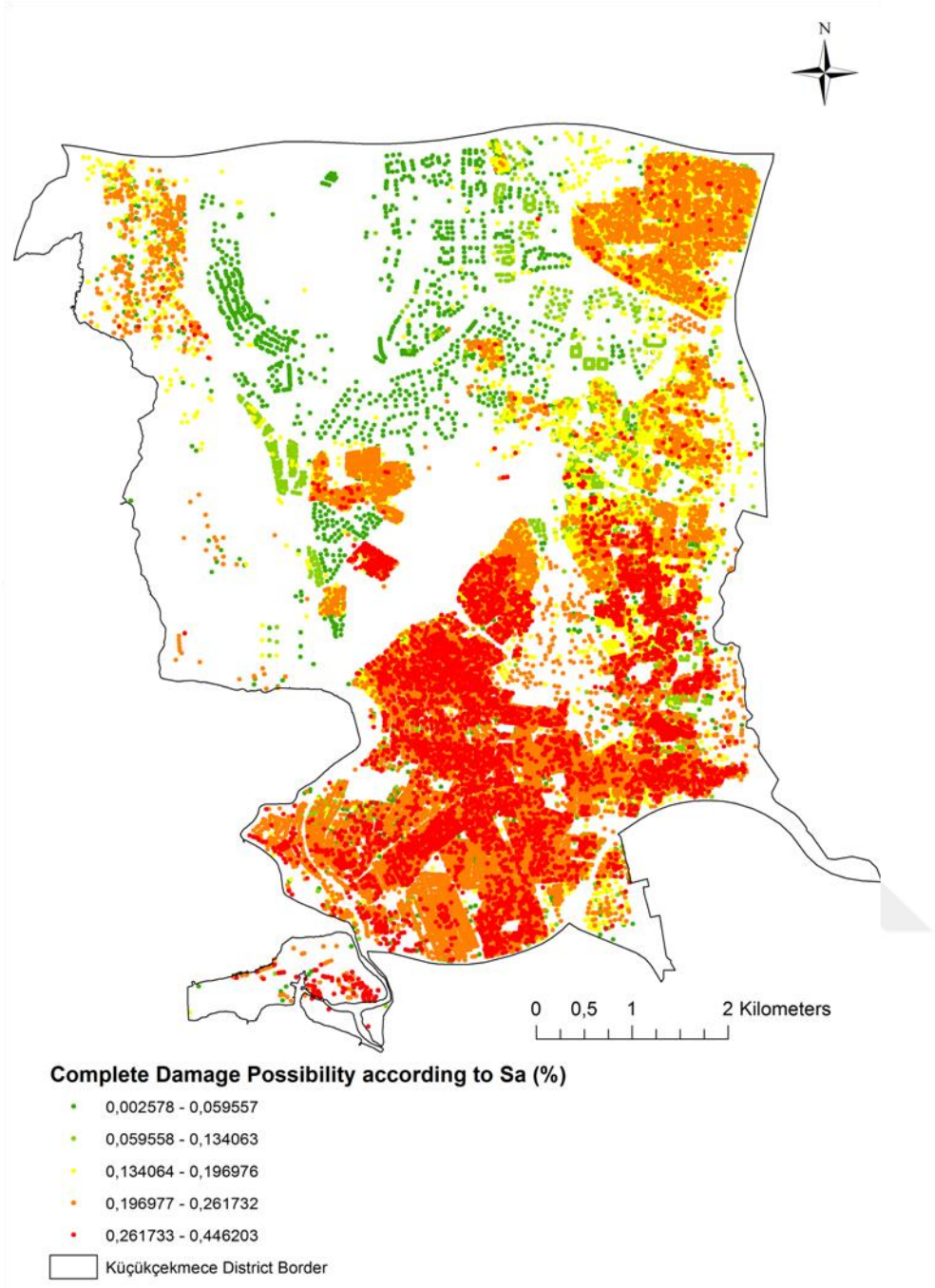


Figure A.7 : Complete damage possibility distribution of Küçükçekmece district according to PGA.

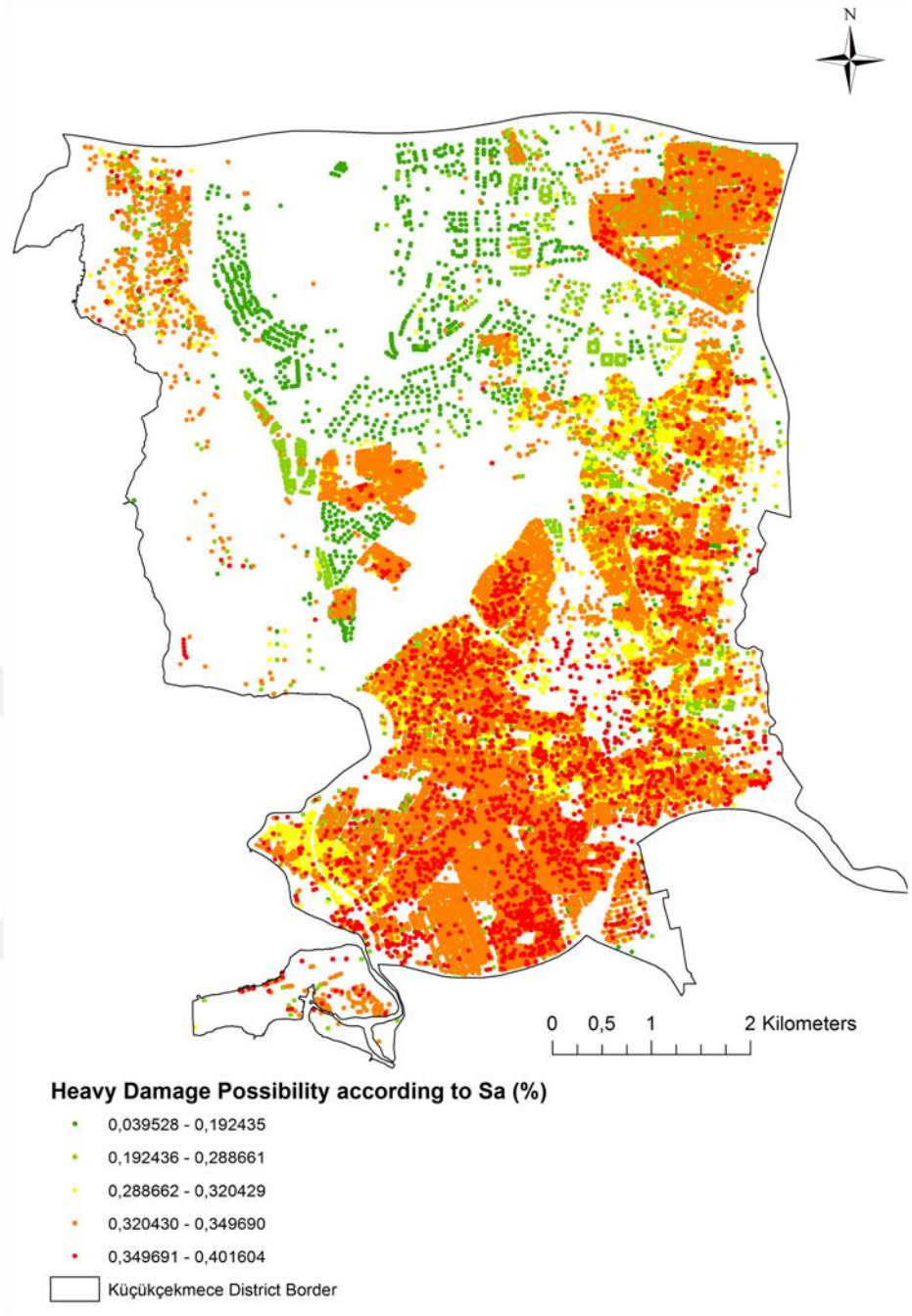


Figure A. 8 : Heavy damage possibility distribution of Küçükçekmece district according to Sa.

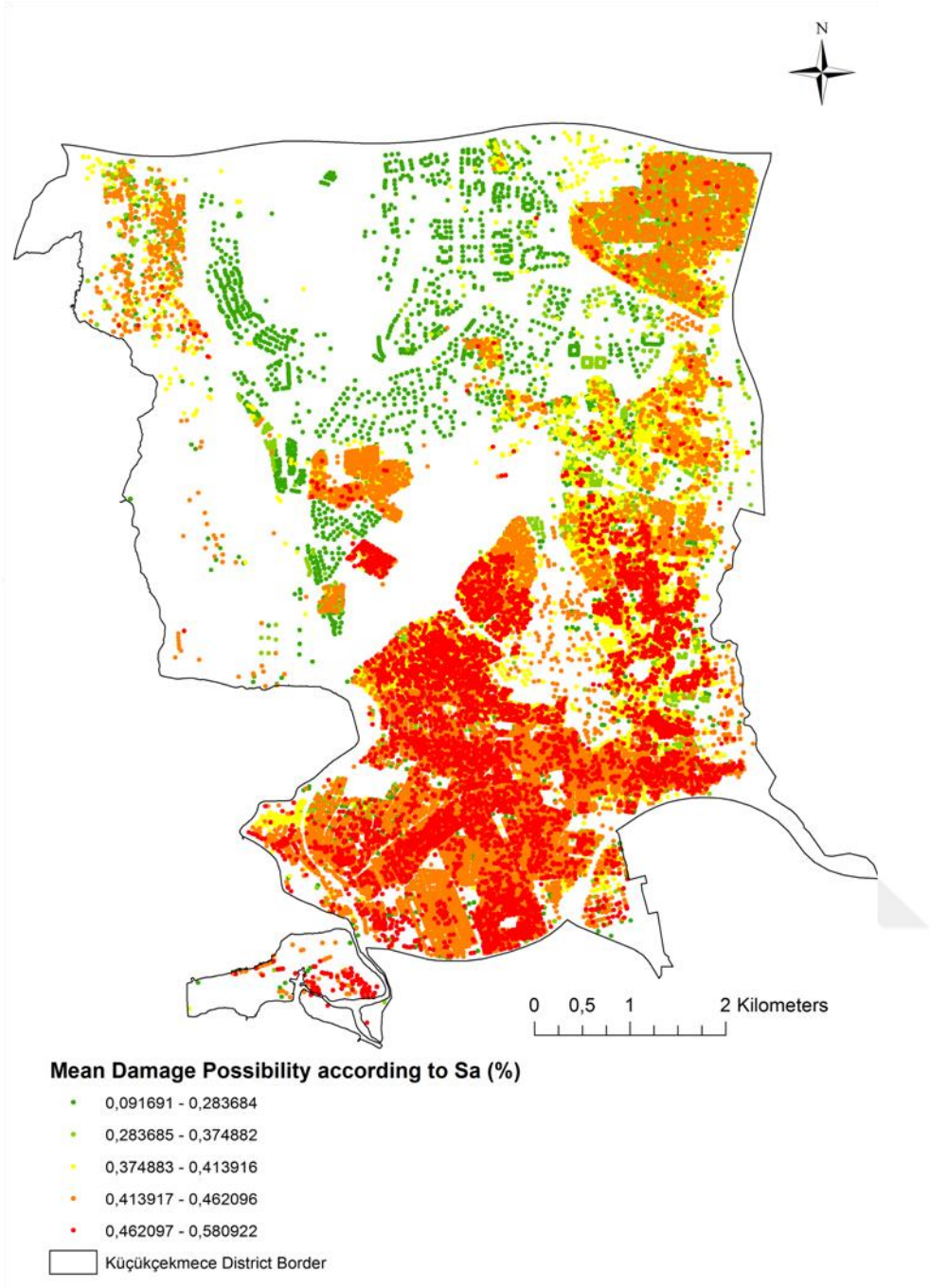


Figure A.9 : Mean damage possibility distribution of Küçükçekmece district according to Sa.

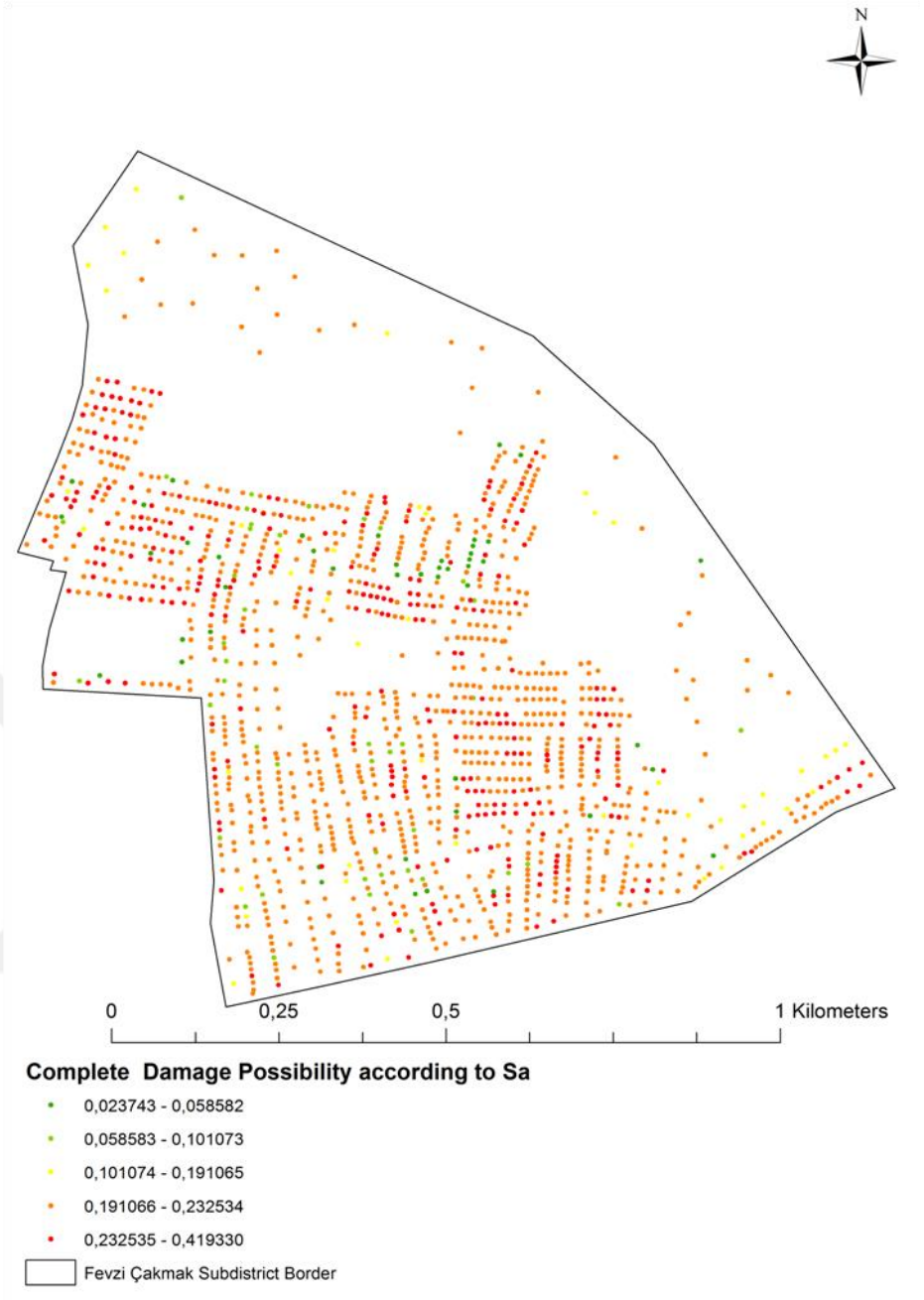


Figure A.10 : Complete damage possibility distribution of Fevzi Çakmak sub district according to Sa.

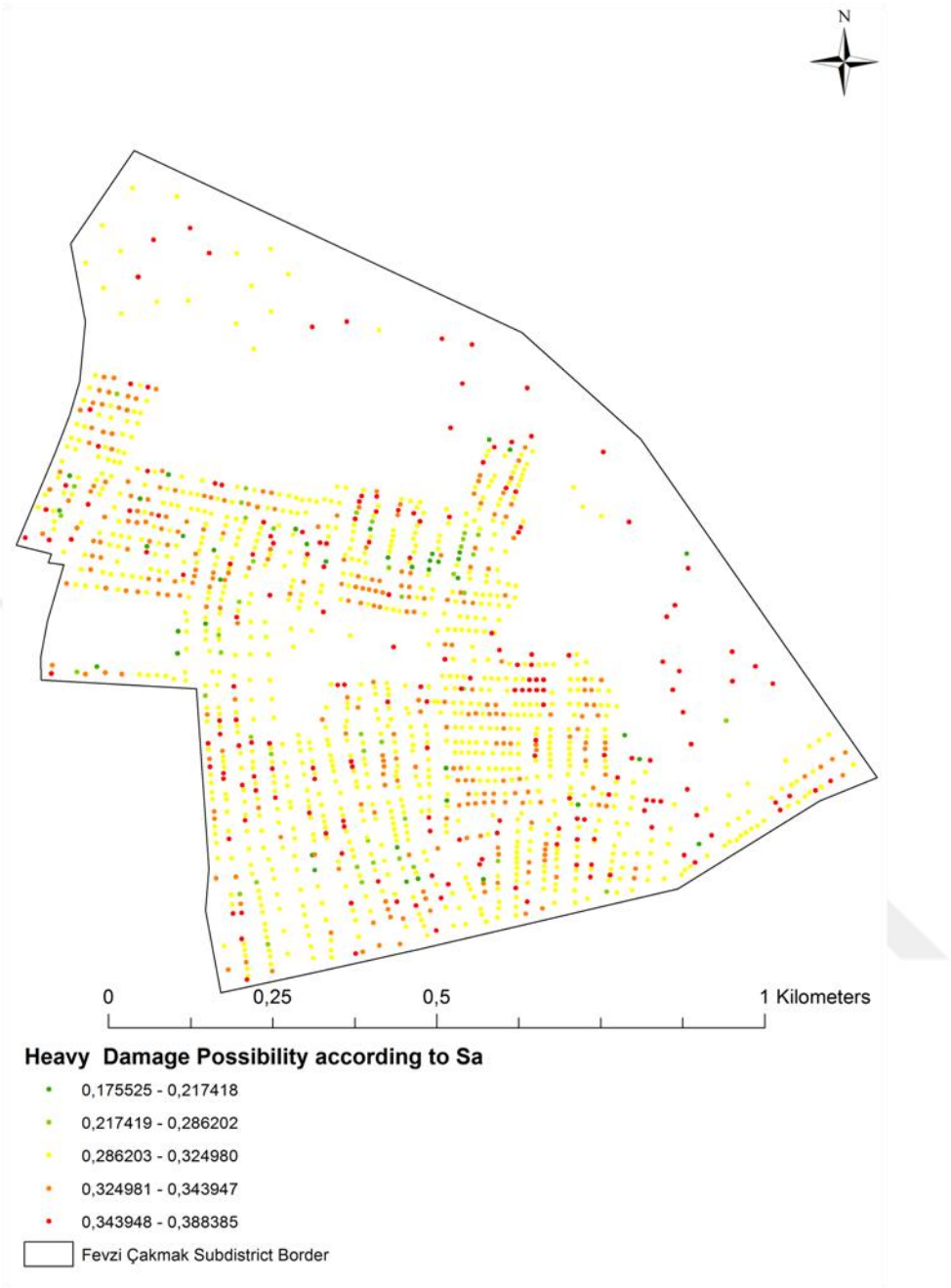


Figure A. 11 : Heavy damage possibility distribution of Fevzi Çakmak sub district according to Sa.

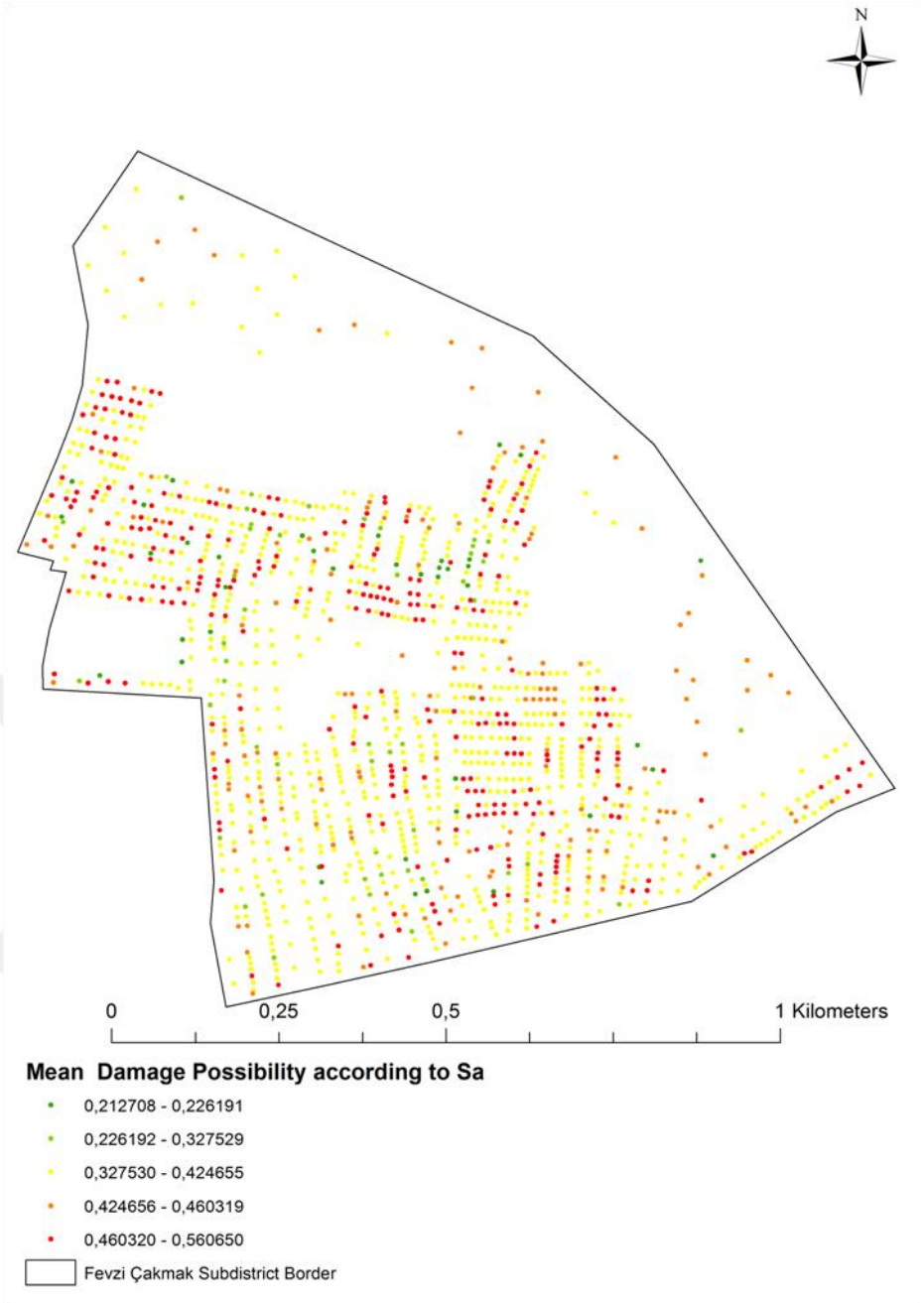


Figure A.12 : Complete damage possibility distribution of Fevzi Çakmak sub district according to Sa.

CURRICULUM VITAE

Name Surname **:** Betül ERGÜN KONUKCU

Place and Date of Birth **:** 29.11.1977

E-Mail **:** betulergun_77@hotmail.com

EDUCATION:

- **School of Foreign Languages :** 1996, Istanbul Technical University
- **B.Sc.** **:** 2000**,** ITU, Department of Geology Engineering
- **M.Sc.** **:** 2003**,** ITU, Eurasia Institute of Earth Sciences

PROFESSIONAL: Istanbul Metropolitan Municipality - Department of Earthquake Risk Management and Urban Development (2005 –)

EXPERIENCE: Preparation of Urban Transformation Master Plan 2015 -2017
Disaster based Social Vulnerability Analysis 2013 – 2015
MegaIST (Indicator System) 2007 – 2012
Urbanization Council (2008 – 2009)
Updating of Probable Earthquake Loses for Istanbul (2007 – 2009)
HAZTURK (Loss Estimation Programme) Project (2006 – 2008)
Microzonation Project (2006 – 2009)

COURSE: JICA, Mitigation Strategies for Mega – Urban Earthquake Disaster, KOBE, JAPAN (2007)

PUBLICATIONS, PRESENTATIONS AND PATENTS ON THE THESIS:

- **Konukcu Ergün, B.**, Karaman, H., Şahin, M., 2016. Building Damage Analysis for the Updated Building Dataset of Istanbul. *Natural Hazards, Review.*

- **Konukcu Ergün, B**., Karaman, H., Şahin, M., 2016. Determination of Building Age for Istanbul Buildings to be used for the Earthquake Damage Analysis According to Structural Codes by Using Aerial and Satellite Images. *Natural Hazards, Review.*

- **Konukcu Ergün, B**., Karaman, H., Şahin, M., 2016. Determination of road functionality for Küçükçekmece district following a scenario earthquake for Istanbul. *International Journal of Environment and Geoinformatics*, 3(1), 24-38.